SPATIAL DISTRIBUTION OF WAVE OVERTOPPING

Dennis van Kester
December 2009

Delft University of Technology
Faculty of Civil Engineering and Geosciences
Department of Hydraulic Engineering

Van Oord
Dredging and Marine Contractors

Delft University of Technology

Van Oord

Colophon

Final report of the master thesis
Title: Spatial distribution of wave overtopping
Delft, 2009

Institute
Delft University of Technology
Faculty of Civil Engineering and Geosciences
Department of Hydraulic Engineering

Master thesis author
D.C.P. van Kester
Student number: 1157469
Email: dennisvankester@hotmail.com

Graduation committee master thesis

prof.dr.ir. M.J.F. Stive	Hydraulic Engineering, TU Delft
ir. H.J. Verhagen	Hydraulic Engineering, TU Delft
prof.dr.ir. W.S.J. Uijttewaal	Environmental Fluid Mechanics, TU Delft
ir. G. Smith	Engineering Department, Van Oord

Preface

This Master Thesis is written as a final part of my master Hydraulic Engineering at the faculty of Civil Engineering at Delft University of Technology.

This report is an overview of an investigation on the thesis subject: spatial distribution of wave overtopping.
The main research objective is to obtain a proper insight in the physics of wave overtopping and to define a method to predict the spatial distribution of wave overtopping discharge over a coastal defence structure.

This study is performed in close collaboration with the engineering department of Van Oord. The experiments were executed in the Laboratory of Fluid Mechanics at Delft University of Technology. I would like to thank both departments for their facilities and support needed to accomplish this study. Special thank to Gerard Spaan, who offered me this opportunity and supported me before he resigned from Van Oord.
I would also like to thank my friends, family and colleagues for their support during this study.
Finally I would like to thank the member of the graduation commission for their supervision and dedication.

Dennis van Kester
Delft, december 2009

Summary

Research objective
The goal of this master thesis is to describe the spatial distribution of the wave overtopping discharge over and behind the crest of a coastal defence structure. The influence of the most relevant parameters on this process is explored. This research has been performed by means of a physical model. Present calculation methods can be verified and expanded or a new valid calculation method will be defined with the results of this research.

Laboratory research
A prototype of a coastal defence structure is assumed to form a basis for the scale model. Hydraulic similitude of the scale model is based on various scaling criterions and similitude requirements. The viscous force associated with flow through the armour layer and core of the structure is also an important scaling criterion. The laboratory equipment consisted of hydraulic instruments (the wave flume and the wave generator) and measurement instruments (wave gauge and the balance). Various influencing parameters were varied to consider their influence on the spatial distribution of the overtopping discharge. Some of them, such as wind and oblique waves, were impossible to investigate in this study, because the wave flume is not suitable to include these parameters. Other parameters, such as a berm, a toe structure or a slope angle, were very difficult and almost unfeasible to vary in sufficient numbers during the experiments. Consequently it was chosen to leave these parameters out of this study and only vary a limited number of practical and relevant parameters. The influences of the following parameters are significant and are investigated: wave height, wave steepness, water depth, crest height and wave spectrum.
Four different types of wave overtopping discharges were measured in this research: total wave overtopping discharge, wave overtopping discharge directly behind the crest, wave overtopping discharge over impermeable backfill and wave overtopping discharge over permeable backfill.

Analysis of results
To determine the reliability of the wave overtopping scale model, it is essential to compare the total wave overtopping experiment results with other overtopping studies and theoretical methods. This is done for the two different wave spectra: irregular waves and regular waves. Based on the equality of this comparison, further experiment results are considered as acceptable and can be used to derive the relation for the spatial distribution of the wave overtopping discharge

Correlation between the wave overtopping discharge and the water depth resulted in variation in the experiment results. A method had to be developed to correct the actual measured overtopping discharge with a varying water depth into the equivalent overtopping discharge with a constant water depth. This is a complex phenomenon and it is difficult to find a universal solution for this problem. Therefore an empirical method is developed that exclusively fits for the specific singular situation in this research.

The total overtopping discharge flows over the crest of the breakwater and is divided in two components: the infiltrated discharge into the crest and the overtopping discharge directly behind the crest. This division has been studied earlier by Steenaard [19]. Steenaard's method is not directly applicable to the experiment results of this thesis. This is caused by the influence of the wave height, wave length and crest height on the division of the overtopping discharge. A variation of Steenaard's method is defined. This new method introduces the influence of the wave height, wave length and crest height.

The spatial distribution of the wave overtopping discharge behind the crest depends on the type of material behind the crest. In case of an impermeable backfill, for example a roadway under a certain slope, the overtopping discharge flows over the roadway and can not infiltrate into the surface material. At every point behind the crest, the overtopping discharge directly behind the crest is separated in two parts: one part flows back to the breakwater over the sloped roadway under the influence of gravity and the other part passes the point and travels further away from the breakwater. In the scale model, the impermeable backfill was imitated by a watertight board, which was placed behind the crest under a slope of 3% towards the crest. The behaviour of this division in relation to the length of the board resulted to the spatial distribution of the overtopping discharge over impermeable backfill.
The final relation between the reduction factor (ratio between the overtopping discharge at a certain distance behind the crest and the overtopping discharge directly behind the crest) and the distance behind the crest was found to depend on a dimensionless presentation of the wave energy flux.

The next part of the research was the investigation of the spatial distribution of the overtopping discharge over permeable backfill. At every point behind the crest, the overtopping discharge directly behind the crest is separated into two parts: one part infiltrates into the backfill and the other part passes the point and travels further away from the breakwater. In the scale model, the permeable backfill was imitated by separation of the collecting tank with a watertight board. The side of the breakwater was filled with rock and the other side of the tank (behind the board) was empty. The two different parts of the tank led to separation of the overtopping discharge directly behind the crest: one part of the discharge flowed over the rock and the board into the empty part of the collecting tank and the other part of the discharge infiltrated into the rock and flowed out of the collecting tank through the wire netting in front of the tank. The behaviour of this division in relation to the length of the rock filled part resulted in the spatial distribution of the overtopping discharge. Again, the relation between the reduction factor and the distance behind the crest was found to depend on a dimensionless presentation of the wave energy flux. The influence of the wave energy flux is smaller for the permeable backfill than for the impermeable backfill.

For the case of irregular waves, the wave overtopping discharge is primary caused by the larger waves in the spectrum. A preliminary method of estimating the overtopping for irregular waves is to replace the spectral wave height by the average wave height of the one-thousandth largest waves. The defined relation for the spatial distribution over impermeable backfill can also be applied for irregular wave spectra in this way.

Table of Contents

List of symbols

a	=wave amplitude	[m]
B	=crest width	[m]
B*	=horizontal distance from intersection of SWL and sea side slope of breakwater to rearmost extend of crest (Jensen, 1984)	[m]
C_r	=reduction factor (Q_{over}/Q_{total})	[-]
$C_{r,m}$	=measured reduction factor C_r with the experiments	[-]
$C_{r,c}$	=calculated reduction factor C_r with the defined relation	[-]
c_{pl}	=coefficient for plunging waves (vd Meer, 1988b)	[-]
c_s	=coefficient for surging waves (vd Meer, 1988b)	[-]
c_g	=group velocity	[m/s]
d	=water depth at toe structure	[m]
D_n	=nominal block diameter	[m]
D_{n50}	=median nominal diameter $\left(=\left(\frac{M_{50}}{\rho_s}\right)^{1/3}\right)$	[m]
D_{50}	=sieve diameter, diameter of stone that exceeds the 50% Value of the sieve curve	[m]
D_{15}	=15% value of sieve curve	[m]
D_{85}	=85% value of sieve curve	[m]
E	=wave induced energy per horizontal unit area	[J/m^2]
f	=wave frequency	[Hz]
f_{peak}	=peak frequency	[Hz]
F	=exceedance probability of travel distance (Lykke Andersen)	[-]
Fr	=Froude number	[-]
g	=acceleration due to gravity (=9,81)	[m/s^2]
G_c	=distance behind the crest (Wallingford, 1999)	[m]
h	=height of structure above the bottom	[m]
$H_{1/3}$	=average of highest 1/3 of wave heights	[m]
$H_{1/1000}$	=average of highest 1/1000 of wave heights	[m]
H_{tr}	=transitional wave	[m]
H_{rms}	=root mean square wave height	[m]
H_{m0}	=significant wave height from spectral analysis $=4\sqrt{m_0}$	[m]
H_s	=significant wave height	[m]
H'_0	=equivalent deep water wave height (SPM, 1984)	[m]
H^*	=dimensionless factor for overtopping discharge directly behind the crest	[-]
H^*_d	=threshold value of H* for overtopping discharge directly behind crest	[-]
H0T0	=dynamic stability number (stability considerations)	[-]
H*T*	=dimensionless presentation of wave energy flux	[-]
I	=pressure gradient	[-]
Ir	=Iribarren number	[-]
L	=wave length measured in direction of wave propagation	[m]
L_0	=deep water wave length (based on $T_{m-1,0}$) = $gT^2_{m-1,0}/2\pi$	[m]
L_{0m}	=mean wave length in deep water = $gT^2_m/2\pi$	[m]
m_n	$=\int_{f_1}^{f_2} f^n S(f)df$ = nth moment of spectral density	[m^2/s^n]
M_n	=mass of particle for which n% of granular material is lighter	[kg]
n	=porosity	[-]

n_v	=volumetric armour layer porosity	[-]
N_{ov}	=number of overtopping waves	[-]
N	=number of incoming waves during storm period	[-]
N_X	=the prototype-to-model scale ratio of the parameter X	[-]
P	=wave energy flux	[W/m]
P	=notional permeability of the structure (vd Meer, 1988b)	[-]
P_{ov}	=probability of overtopping per wave= N_{ov}/N	[-]
P_V	$= P(\underline{V} \geq V)$ = probability of the overtopping volume $\underline{V}$ being larger or equal to V	[-]
Q	=mean overtopping discharge per meter structure width	[m^3/s/m]
Q*	=dimensionless overtopping discharge	[-]
Q^*_0	=empirically determined coefficient that depend on incident wave characteristics and structure geometry (SPM, 1984)	[-]
Q^*_{tot}	=dimensionless total wave overtopping discharge $= \frac{Q}{\sqrt{g \cdot H_s^3}}$	[-]
$Q^*_{tot,S}$	=dimensionless total wave overtopping discharge $= \frac{Q}{\sqrt{g \cdot B^3}}$ (Steenaard, 2002)	[-]
Q^*_{over}	=dimensionless overtopping discharge directly behind crest	[-]
$Q^*_{e,over}$	=dimensionless equivalent overtopping discharge directly behind the crest (same water depth reduction as in the equivalent total overtopping experiment)	[-]
$Q^*_{over,x}$	=dimensionless wave overtopping discharge at a certain distance x behind the crest	[-]
Q_{over}	= overtopping discharge directly behind the crest	[m^3/s/m]
$Q_{e,over}$	=equivalent overtopping discharge directly behind the crest (same water depth reduction as in the equivalent total overtopping experiment)	[m^3/s/m]
Q_{tot}	=total overtopping discharge	[m^3/s/m]
Q^*_d	=threshold value for overtopping discharge directly behind the crest (Steenaard, 2002)	[-]
Q_x	=x^{th} measurement in correlation research	[m^3/s/m]
q(x)	=intensity overtopping discharge at distance x (Jensen, 1984)	[m^3/s/m^2]
q_0	=intensity overtopping discharge at x=0 (Jensen, 1984)	[m^3/s/m^2]
R	=run-up on the structure that would occur if the structure were high enough to prevent overtopping corrected for scale effects	[m]
Re	=Reynolds number	[-]
R_c	=crest freeboard of structure	[m]
R^*	=dimensionless crest height	[-]
s	=wave steepness = H/L	[-]
s_0	=wave steepness with L_0, based on $T_{m-1,0}=H_{m0}/L_0=2\pi H_{m0}/(gT^2_{m-1,0})$	[-]
s_{0m}	=wave steepness with L_0, based on $T_m=H_{m0}/L_{0m}=2\pi H_{m0}/(gT^2_m)$	[-]
s_{0p}	=wave steepness with L_0, based on $T_p=H_{m0}/L_{0p}=2\pi H_{m0}/(gT^2_p)$	[-]
S_d	=characteristic value of damage level (vd Meer, 1988b)	[-]
T_{0m}	=wave period associated with the spectral peak in deep water	[s]
T_m	=average wave period	[s]
$T_{m-1,0}$	=average wave period defined by m_{-1}/m_0	[s]
T_p	=spectral peak wave period	[s]
T_s	=significant wave period	[s]
T_z	=mean zero crossing period	[s]

u_f	=filter velocity	[m/s]
u_p	=velocity in the pores	[m/s]
U	=Ursell number	[-]
V	=wave overtopping volume per wave	[m^3/m]
V_{max}	=maximum overtopping volume per wave per unit crest width	[m^3/m]
x	=distance behind the crest of the breakwater	[m]
x*	=dimensionless distance behind the crest	[-]
$z_{2\%}$	=2% wave run-up level above still water line	[m]
α	=angle between overall structure slope and horizontal	[°]
α	=empirically determined coefficient that depend on incident wave characteristics and structure geometry (SPM, 1984)	[-]
α	=energy scale parameter	[-]
β	=angle of wave attack relative to normal on structure	[°]
β	=a constant, equal to the distance for which the overspill intensity decreases by a factor 10 (Jensen, 1984)	[m]
γ_b	=correction factor for a berm	[-]
γ_f	=correction factor for permeability and roughness of or on the slope	[-]
γ_β	=correction factor for oblique wave attack	[-]
γ_v	=correction factor for a vertical wall on the slope	[-]
γ	=peak-enhancement factor	[-]
ρ	=specific density of water	[kg/m^3]
ρ_r	=specific density of rock (=2650)	[kg/m^3]
μ	=dynamic viscosity	[kg/(sm)]
ξ	=breaker parameter	[-]
ξ_0	=breaker parameter based on s_0 (= $\tan(\alpha/s_0^{1/2})$)	[-]
μ(x)	=mean of measured parameter x with normal distribution	[..]
σ(x)	=standard deviation of measured parameter x with normal distribution	[..]
σ	=peak-width parameter	[-]
σ_a	=peak-width parameter for f<fpeak	[-]
σ_b	=peak-width parameter for f>fpeak	[-]

1. Introduction

1.1.1. Coastal defence structure

Historically, sloping dikes have been the most widely used option for sea defences along the coasts of the Netherlands and other parts of Europe. Dikes or embankment seawalls have been built along many Dutch coastlines protecting the hinterland from flooding, and sometimes providing additional amenity value. Such embankments will need some degree of protection against direct wave erosion, generally using a revetment facing the seaward side.
A second type of coastal structure consists of a mound or layers of quarried rock fill, protected by rock or concrete armour units, also called breakwater. The outer armour layer is designed to resist wave action without significant displacement of armour units. Under-layers of quarry or crushed rock support the armour and separate it from finer material in the embankment or mound. These porous and sloping layers dissipate a proportion of the incident wave energy in breaking and friction.
This second type of coastal structure is used in the research of this thesis.

1.1.2. Wave overtopping

Wave overtopping is water carried over the top of a coastal defence structure as a result of wave run-up or surge action and causes a continuous sheet of water passing over the crest of the structure.
A second form of wave overtopping occurs when waves break on the seaward face of the structure and produce significant volumes of splash. These droplets may then be carried over the wall either under their own momentum or as a consequence of an onshore wind.
Another less important method by which water may be carried over the crest is in the form of spray generated by the action of wind on the wave crests immediately offshore of the wall. Even with strong wind the volume is not large and this spray will not contribute to any significant overtopping volume.
The latest form of wave overtopping (wind) will not be taken into account in this thesis. It is impossible to model the effect of wind on the overtopping discharge. Therefore, only the influence water discharges and splash are recorded during the model tests.

The mean overtopping discharge is the main parameter in the overtopping process and is given in m3/s per m width of the crest. A number of different methods are available to predict overtopping of particular structures (usually simplified sections) under given wave conditions and water levels. With these prediction methods the overtopping discharge at the top of the crest is calculated.

With reclaimed areas, buildings, structures, etc. behind the coastal defence structure, the wave overtopping may be of great inconvenience for the following reasons, which should be taken into account:

1. The water must be drained away. For design of the drainage system the expected intensity of water must be known.
2. If buildings, structures, berths, etc. are located behind the breakwater, the effects of the overtopping water must be taken into consideration in the design in order to avoid damage or unacceptable down-time of operations.
3. In a harbour basin behind the breakwater waves caused by overtopping may inconvenience its use or damage moored vessels and structures etc.

Figure 1 illustrates the damage that overtopping waves can cause to buildings behind the crest.

Figure 1 Damage caused by wave overtopping

1.1.3. Tolerable overtopping discharges

Most coastal defence structures are constructed primarily to limit overtopping volumes that might cause flooding. Over a storm or tide, the overtopping volumes that can be tolerated will be site specific as the volume of water that can be permitted will depend on the size and use of the receiving area, damage versus inundation curves, and return period. The character of the overtopping discharge and the hazards it causes depends on the geometry of the structure and of the immediate hinterland behind the seawall crest, and the form of overtopping discharge.

Guidance on overtopping discharges that can cause damage to buildings or infrastructure, or danger to pedestrians and vehicles have been related to mean overtopping discharges or (less often) to peak volumes. In most instances the tolerable discharges are those at the point of interest, at the roadway or footpath or building.

1.1.4. Problem definition

The available wave overtopping prediction methods lead to the amount of overtopping discharge at the top of the crest of a coastal defence structure. At the same time, the guidelines for the tolerable overtopping discharges are given at the location of interest, which is a certain distance behind the crest. These two procedures do not correspond with each other; the location of the predicted overtopping discharge and the given tolerable overtopping discharge is not the same.

The overtopping discharge reduces with the distance behind the crest by infiltration into the crest, infiltration into the backfill or back flowing over the backfill. The ratio between the overtopping discharge at the top of the crest and at a certain location of interest behind the crest depends on the various hydraulic parameters and physical dimensions. This ratio can be divided in two parts. First the division of the total overtopping discharge in the infiltrating discharge into the crest and the overtopping discharge behind the crest. Second the spatial distribution of the overtopping discharge behind the crest. An appropriate method to calculate these ratios is not available.

1.1.5. Research objective

The goal of this master thesis is a natural consequence of the problem definition: to solve the lack of an appropriate calculation method for the determination of the spatial distribution of the overtopping discharge behind the crest. The intended result of this research will contain a practical method to calculate the overtopping discharge at a certain location behind the crest of a coastal defence structure.
This practical method must help an engineer to design a coastal defence structure with a safe crest height, for which the constructions at a certain distance behind the crest will meet the relevant safety regulations.
To formulate suitable methods and regulations, it is necessary to determine the relations between the several factors of influence. In that manner the influence and significance of the relevant factors will be clarified. This will form an important basis for the final defined calculation method.
Present existing calculation methods can be verified and expanded or a new valid calculation method will be defined with the results of this research.
To reach these objectives, wave overtopping will be investigated with a physical model in a wave flume of the Fluid Mechanics Laboratory of the Delft University of Technology.
The required overtopping discharges to determine the spatial distribution of wave overtopping are illustrated in Figure 2.

Summarized:
"The goal of this master thesis is to describe the spatial distribution of the wave overtopping discharge over and behind the crest of a coastal defence structure. The influence of the most relevant parameters on this process is explored."

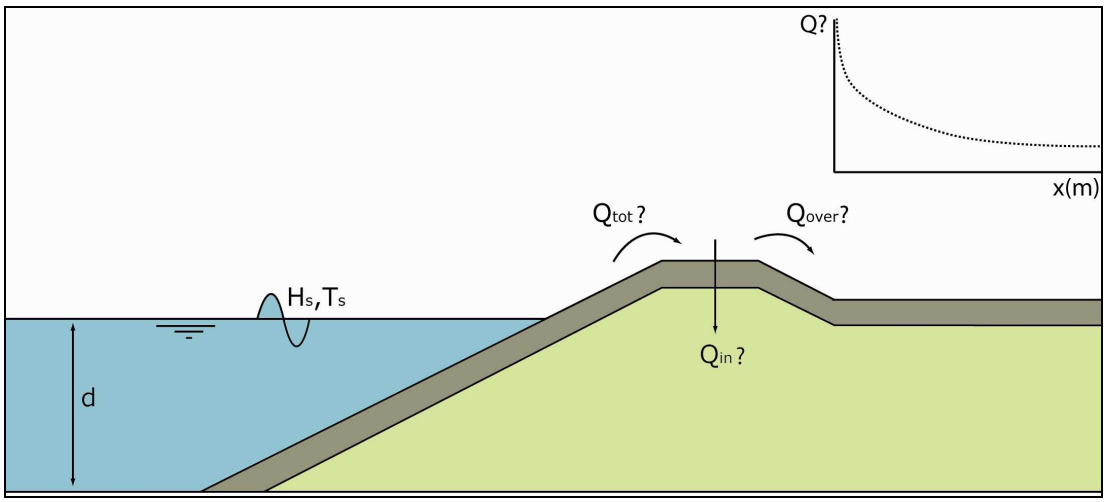

Figure 2 Research objectives

1.1.6. Methodology

For the achievement of the objective the following route has been followed:

- Analyze available relevant theories and studies about wave overtopping and its spatial distribution and understand its physical processes. Be able to apply the existing prediction methods; these methods can form the basis for the objective of this research.
- Define a laboratory plan for the execution of the experiments with the physical model in the laboratory. This plan contains a design for a suitable scale model, which depends on technical requirements, practical requirements, scaling effects and costs. Furthermore, this plan contains an experiment plan, with which the spatial distribution of the wave overtopping and the influence of the several relevant parameters can be investigated.
- Execute the research in the laboratory. This means preparing the wave flume, installing the scale model and finally executing the planned experiments. Evaluation of the experiment results during the research can lead to adjustments of the experiment plan.
- Analyze the experiment results. The large amount of experiment results has to form the basis of the defined calculation method for the spatial distribution of the overtopping discharge and has to be used to determine the influence of the relevant parameters on wave overtopping.

1.1.7. Reader

This report begins in Chapter 2 with a study to relevant existing theories and studies about wave overtopping. Chapter 3 describes the several elements of the laboratory research. In Chapter 4 the analysis of the experiment results is described. This analysis is divided in 5 sections for different overtopping discharges. Chapter 5 shows in which way the conclusions of the analysis are applicable. The final conclusions and recommendations are given in Chapter 6.

2. Literature study

In order to conduct a proper and specific laboratorial project, it is important to be familiar with all the available knowledge about wave overtopping. First of all, the physical process of wave overtopping must be understood. This includes the governing physical dimensions of a coastal defence structure and its materials as well as the relevant hydraulic parameters for wave overtopping.
Furthermore, it is essential to understand the existing wave overtopping calculation methods and be able to apply them. These methods can possibly form the basis for the formulation of the new calculation method.

2.1. Physical dimensions and material

The wave overtopping discharge depends on several physical dimensions, material dimensions and material properties of the coastal defence structure. The relevant dimensions for this research are explained in this chapter. Underlayers, berms and toe structures are not considered.

2.1.1. Physical dimensions

Crest height

The crest height of a structure is defined in terms of the crest freeboard (R_c). The crest freeboard is the vertical distance between the horizontal part of the crest and the SWL (still water level).

Crest width

The crest width has no direct influence on the total wave overtopping, but is important for the behaviour of the total overtopping discharge on top of the crest. In the case of armour stone, the Rock Manual [4] recommends that the crest width should be sufficient to permit at least three to four stones to be placed on the crest. This is a particularly important requirement if significant overtopping is expected to occur. The stones on the crest should be placed with maximum interlocking or packing density to ensure the greatest stability under wave action.

Slope

A slope is defined by TAW [22] as a section of a coastal defence structure of which the slope angle (α) lies between 1:1 and 1:8. The slope angle (α) adopted in design of the front face should ideally be as steep as possible to minimise the volume of the structure, but it depends on hydraulic and geotechnical stability considerations. The slope is generally not steeper than 1:1.5 and may be compared to the natural angle of repose of material dumped under water, which can be as steep as 1:1.2. If seismic activity is to be taken into account, the slopes should generally be gentle, to allow for the expected horizontal accelerations to be absorbed without damage. Foundation stability problems may also be encountered in locations with poor sub-soils, and in such cases gentle slopes should be used.

Figure 3 shows the relevant physical dimensions.

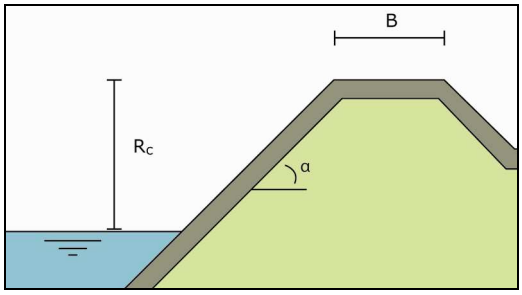

Figure 3 Crest freeboard, crest width and slope

2.1.2. Material dimensions

Armour layer

It is evident that the armour layer is able to withstand the wave attack during design conditions. The severity of the specific conditions follows from economic considerations. D'Angremond [1] states that generally rock armour is placed in a double layer, since this allows a few armour units to be displaced before underlying material is exposed. If the armour layer consists of quarry stone, it is generally the heaviest fraction of the yield curve. This has a narrow grading ($D_{85}/D_{15}<1.5$). If quarry stone is used, it is possible to reduce the slope in order to improve the stability.

Core

In this research, the layer directly under the armour layer is the core (no underlayers between them). It is obvious that the units forming the core are not allowed to pass through the voids in the armour layer. The Shore Protection Manual [20] recommends that the weight ratio of subsequent layers of quarry should be kept between 1/10 and 1/15 (or D_{n50} ratio between 2 and 3)
Terzaghi rules allow a ratio of 4 to 5 in diameter between two subsequent filter layers. However, one must remain a bit on the conservative side because of the consequences of failure of the filter mechanism. The filter is generally designed to be geometrically closed. For the core, quarry run is usually used, indicating that it is meant to represent the finer fractions of the quarry yield curve. Quarry run has generally wide ($1.5<D_{85}/D_{15}<2.5$) to very wide ($2.5<D_{85}/D_{15}$) grading.

2.1.3. Material properties

Permeability and porosity

When a coastal defence structure is constructed, it is important to have an idea of the permeability and the porosity of the used material. They are important because of their determination of at least part of the hydraulic response of the structure and their influence on the stability of the structure.
Void porosity (n_v) is defined as the percentage of voids between units or particles[1]. This parameter mainly depends on the shape, grading and method of placement of the armour stones on the slope.
Loose materials, such as rock, are always porous; the void porosity may range roughly between 30% and 55%. Sand has a comparable void porosity, nevertheless the behaviour of waves on a sandy beach or a rubble mound differs.

[1] The terms 'void ratio' and 'porosity' are well established for granular materials. However, n_v is termed the 'void porosity' of the armour layer, or simply 'volumetric armour layer porosity' to avoid confusion with the term 'porosity' as applied to a specimen of intact rock.

This difference is caused by the difference in permeability. The armour of rubble mound slopes is very permeable and waves will easily penetrate between the armour stoned and dissipate energy.
The permeability of a structure depends on the size of the rock layers. The permeability of a structure is generally given as a notional index that represents the global permeability of the structure, or as the ratio of diameters of core material and armour material. It is an important parameter with respect to the stability of armour layers under wave attack.
A smooth structure, such as a dike, is mostly impermeable for water. In case of a low permeability of the underlayer, the waves are reflected against this underlayer and subsequently increase the lift forces of the armour layers.

Roughness

Roughness on the slope will dissipate wave energy during wave run-up and will therefore reduce wave overtopping. Roughness is created by irregular shaped block revetments, artificial ribs or blocks on a smooth slope. A rubble mound slope with rock or concrete armour is also rough and in general rougher than impermeable dikes or embankments.
Values for roughness reduction factor γ_f can be found in The Rock Manual [4]

2.2. Hydraulic parameters

The wave overtopping discharge depends on several hydraulic parameters. The relevant parameters for this research are explained in this chapter. Oblique waves and wind are not considered.

2.2.1. Wave height and wave period

The wave height is defined as the difference between the maximum and minimum elevations of the sea-surface (peak to trough wave height) over the duration of the wave. This duration is called the wave period in the time domain.

In case of an irregular wave spectrum, breakwaters are commonly not designed with respect to one individual wave (a so-called maximum wave) but are based on the characteristic values of sea-states. Therefore the incident wave height is usually given as the significant wave height. This can be based on a time domain analysis ($H_{1/3}$) or a spectral analysis (H_{m0}). The wave period can be given as either the mean period (T_m), the mean energy period ($T_{m-1,0}$), or the peak period (T_p)
The spectral wave height is defined as $H_{m0} = 4\sqrt{m_0}$, where m_0 (m_n is the n^{th}-moment of the variance spectrum) is obtained by integration of the variance spectrum. The spectral wave period is defined by $T_{m-1,0} = \frac{m_{-1}}{m_0}$. The spectral wave period gives more weight to the longer period in the spectrum than an average period and, independent of the type of spectrum, gives the corresponding wave overtopping for the same values and the same wave heights.

In case of regular waves, it is not very difficult to determine the significant wave height H_s and the significant wave period T_s, because they are the same for all the waves. Consequently, there is just one correct value for both parameters.

The significant wave length (L) in deep water is equal to $\frac{g \cdot T^2}{2\pi}$. The wave flume in this research is assumed as deep water, so this formula for the wave length can also be applied.

2.2.2. Wave steepness and relative wave height

The wave steepness (s=H/L) and relative wave height (H/d) are dimensionless parameters and are measures of non-linearity of a wave. The Rock Manual [4] uses them in particular to quantify the importance of non-linear effects and they appear in the formation of criteria for predicting wave breaking. A specific use of the wave steepness is made if the wave height is taken at the toe of the structure and the wavelength in deep water. In fact this is a fictitious wave steepness $s_0=H/L_0$ and is often used in the design formulae for structures. The main goal in this case is not to describe the wave steepness itself, but to include the effect of the wave period on structure response.
The Ursell number (U) is a combination of the former numbers and is defined in Equation 2.2-1:

$$U = \frac{H \cdot L^2}{d^3} = \left(\frac{H}{d}\right) \Big/ \left(\frac{d}{L}\right)^2 \qquad \textit{Equation 2.2-1}$$

Equation 2.2-1 is used to characterize the degree of non-linearity of the waves.

2.2.3. Breaker parameter

The breaker parameter or surf similarity parameter (ξ), also known as the Iribarren number (Ir), is used for the characterisation of many phenomena related to waves in shallow water, such as wave breaking, wave run-up and wave overtopping. It reflects the ratio of bed slope and wave steepness (s) and is defined in Equation 2.2-2:

$$\xi = \frac{\tan\alpha}{\sqrt{s}} = \frac{\tan\alpha}{\sqrt{H/L}} = \frac{\tan\alpha}{\sqrt{(2\pi \cdot H)/(g \cdot T^2)}} \qquad \textit{Equation 2.2-2}$$

This parameter corresponds with the type of wave breaking and wave load on the structure. Actually, waves can break first on the depth-limited foreshore before reaching the structure and then break once again on to the structure. On the foreshore the breaker type is generally spilling, sometimes plunging. On the structure itself it is never spilling, but plunging (gentle structure slope), surging or collapsing. Figure 4 shows the different types of breaking waves.

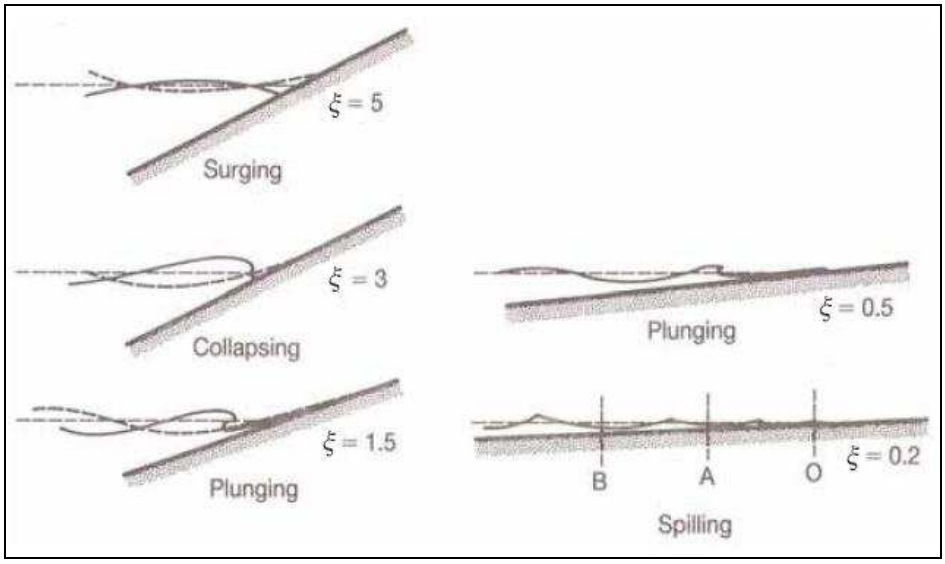

Figure 4 Breaker types as a function of the surf similarity parameter ξ (Battjes, 1972)

2.3. Total wave overtopping

Methods to calculate wave overtopping are generally based on formulae of an exponential form in which the mean specific overtopping discharge, Q (m^3/s per metre length of crest), is given by Equation 2.3-1.

$$Q = Ae^{BR_c} \qquad \textit{Equation 2.3-1}$$

Within Equation 2.3-1, the coefficients A and B are, depending on the method concerned, functions of parameters that describe the wave conditions and the structure dimensions.

Different methods are available to predict overtopping for specific types of hydraulic structures (smooth or rough slopes, permeable or non-permeable structures). Also complicating conditions like oblique waves, shallow foreshores and bermed slopes can be taken into account by using either correction factors or explicit formulae. This chapter describes the most relevant calculation methods.

2.3.1. Owen

To calculate the time-averaged discharge for smooth slopes, the dimensionless freeboard (R*) and the dimensionless discharge (Q*) are defined by Owen [12] with Equation 2.3-2 and Equation 2.3-3. These equations use the mean wave period and the significant wave height at the toe of the structure (H_s).

$$R^* = R_c \Big/ \left(T_m \sqrt{g \cdot H_s}\right) = R_c \Big/ H_s \sqrt{s_{0m}/2\pi} \qquad \textit{Equation 2.3-2}$$

$$Q^* = Q \Big/ \left(T_m \cdot g \cdot H_s\right) \qquad \textit{Equation 2.3-3}$$

Equation 2.3-4 gives the relation between the dimensionless parameters defined in Equation 2.3-2 and Equation 2.3-3.

$$Q^* = a \cdot \exp\left(-b \cdot R^* \Big/ \gamma_f\right) \qquad \textit{Equation 2.3-4}$$

where 'a' and 'b' are empirically derived coefficients that depend on the profile and γ_f is the correction factor for the influence of the slope roughness.

Values for the roughness correction factor, as listed in Table 1, were taken from The Rock Manual [4].

Structure type	γ_f
Concrete, asphalt and grass	1.0
Pitched stone	0.80-0.95
Armourstone – single layer on impermeable base	0.70
Armourstone – two layers on impermeable base	0.55

Table 1 Values for roughness reduction factor, Rock Manual [4]

Introduction of the correction factor, $\gamma_f \leq 1$, practically implies a decrease of the required freeboard (R_c) for the same overtopping rate. For smooth slopes under perpendicular wave attack and a normal deep foreshore, the correction factor is equal to 1.0.

The influence of a berm is not affected through a correction factor, but by means of adapted coefficients 'a' and 'b'. The influence of oblique wave attack is also not effected using a correction factor, but by means of an overtopping ratio. These two methods will not be treated in this section of this report.
For straight smooth slopes the values of 'a' and 'b' to be used in Equation 2.3-4 are given in Table 2.

Slope	**a**	**b**	**Slope**	**a**	**b**
1:1	$7.94*10^{-3}$	20.1	1:4.5	$1.20*10^{-2}$	47.7
1:1.5	$8.84*10^{-3}$	19.9	1:5	$1.31*10^{-2}$	55.6
1:2	$9.39*10^{-3}$	21.6	1:6	$1.00*10^{-2}$	65
1:2.5	$1.03*10^{-2}$	24.5	1:8	$1.00*10^{-2}$	86
1:3	$1.09*10^{-2}$	28.7	1:10	$1.00*10^{-2}$	108
1:3.5	$1.12*10^{-2}$	34.1	1:15	$1.00*10^{-2}$	162

Table 2 Values of the coefficients 'a' and 'b' for straight smooth slopes

2.3.2. TAW2002

According to TAW [22], wave overtopping can be described in two formulae linked to each other: one is for breaking waves ($\gamma_b \cdot \xi_0 \leq 2$), where wave overtopping increases for increasing breaker parameter, and one is for non-breaking waves ($\gamma_b \cdot \xi_0 \geq 2$), where maximum overtopping is achieved.

The wave overtopping formulae are exponential functions with the general form of Equation 2.3-1. The coefficients 'a' and 'b' are functions of wave height, breaker parameter and other influencing factors.

Breaking waves

For breaking waves ($\gamma_b \cdot \xi_0 \leq 2$), the wave overtopping formula is described in Equation 2.3-5.

$$\frac{Q}{\sqrt{g \cdot H_{m0}^3}} = \frac{A}{\sqrt{\tan\alpha}} \gamma_b \cdot \xi_0 \exp\left(-B \frac{R_c}{H_{m0}} \frac{1}{\xi_0 \cdot \gamma_b \cdot \gamma_f \cdot \gamma_\beta \cdot \gamma_v}\right) \qquad \textit{Equation 2.3-5}$$

The dimensionless wave overtopping discharge and dimensionless crest height are related to the breaker parameter. The dimensionless wave overtopping discharge is described in Equation 2.3-6 and the dimensionless crest height is described in Equation 2.3-7.

$$\frac{Q}{\sqrt{g \cdot H_{m0}^3}} \cdot \frac{\sqrt{\tan\alpha}}{\gamma_b \cdot \xi_0}$$ *Equation 2.3-6*

$$\frac{R_c}{H_{m0}} \cdot \frac{1}{\xi_0 \cdot \gamma_b \cdot \gamma_f \cdot \gamma_\beta \cdot \gamma_v}$$ *Equation 2.3-7*

Non-breaking waves

For non-breaking waves, the wave overtopping formula is described in Equation 2.3-8.

$$\frac{Q}{\sqrt{g \cdot H_{m0}^3}} = C \exp\left(-D \frac{R_c}{H_{m0}} \frac{1}{\gamma_f \cdot \gamma_\beta} \right)$$ *Equation 2.3-8*

The dimensionless wave overtopping discharge and dimensionless crest height are not related to the breaker parameter. The dimensionless wave overtopping discharge is described in Equation 2.3-9 and the dimensionless crest height is described in Equation 2.3-10.

$$\frac{Q}{\sqrt{g \cdot H_{m0}^3}}$$ *Equation 2.3-9*

$$\frac{R_c}{H_{m0}} \cdot \frac{1}{\gamma_b \cdot \gamma_f}$$ *Equation 2.3-10*

Coefficients

Values for coefficients A, B, C and D in Equation 2.3-5 and Equation 2.3-8 have been derived representing the average trend through the used dataset for use in probabilistic calculations. Different values (for the parameters B and D), including a safety margin of 1σ, are suggested for deterministic use. These values are presented in Table 3.

Coefficients	Values with safety margin (μ-σ) – deterministic calculations	Values without safety margin/ average trend – probabilistic calculations
A	0.067	0.067
B	4.30	4.75
C	0.20	0.20
D	2.30	2.60

Table 3 Values for coefficients A, B, C and D in Equation 2.3-5 and Equation 2.3-8

2.3.3. Shore Protection Manual 1984 (for regular waves)

The Shore Protection Manual [20] (Department of the Army; Waterways Experiment Station, Corps of Engineers; Coastal Engineering Research Center) developed a calculation method for wave overtopping with regular monochromatic waves.

Incident wave height and wave period are important factors. Wind speed and wave direction with respect to the structure are not taken into account. The volume rate of wave overtopping depends on the structure height, water depth at the structure toe, structure slope and the roughness of the slope. Saville and Caldwell [14] [15] investigated overtopping rates and run-up heights on small-scale laboratory models of structures. Larger scale model tests have also been conducted for Lake Okeechobee levee section by Saville [16]. A reanalysis of Saville's data indicates that the overtopping rate per unit length of the structure can be expressed by Equation 2.3-11.

$$Q = \left(g \cdot Q_0^* \cdot \left(H_0^{'} \right)^3 \right)^{1/2} \cdot e^{-\left[\frac{0.217}{\alpha} \cdot \tanh^{-1}\left(\frac{h-d}{R} \right) \right]} \qquad \textit{Equation 2.3-11}$$

in which $0 \le \frac{h-d}{R} \le 1$

Appendix I-1 can be used to determine the wave run-up R for the conditions in this research.
Appendix I-2 can be used to determine the coefficients Q^*_0 and α for the conditions in this research.

2.3.4. Bradbury

Bradbury [3] completed model tests in which the overtopping discharges in front of vertical faced crown walls mounted on top of straight rock armoured slopes (1:2) were measured. The berm width (G or B) varied from 3 to 6 stone diameters. The attacking waves were irregular and head-on.

This resulted in Equation 2.3-12:

$$\frac{Q}{g \cdot H_s \cdot T_{0m}} = a\left[\left(\frac{R_c}{H_s}\right)^2 \sqrt{\frac{s_{0m}}{2\pi}}\right]^{-b}$$

Equation 2.3-12

The coefficients 'a' and 'b' can be determined with Figure 5.

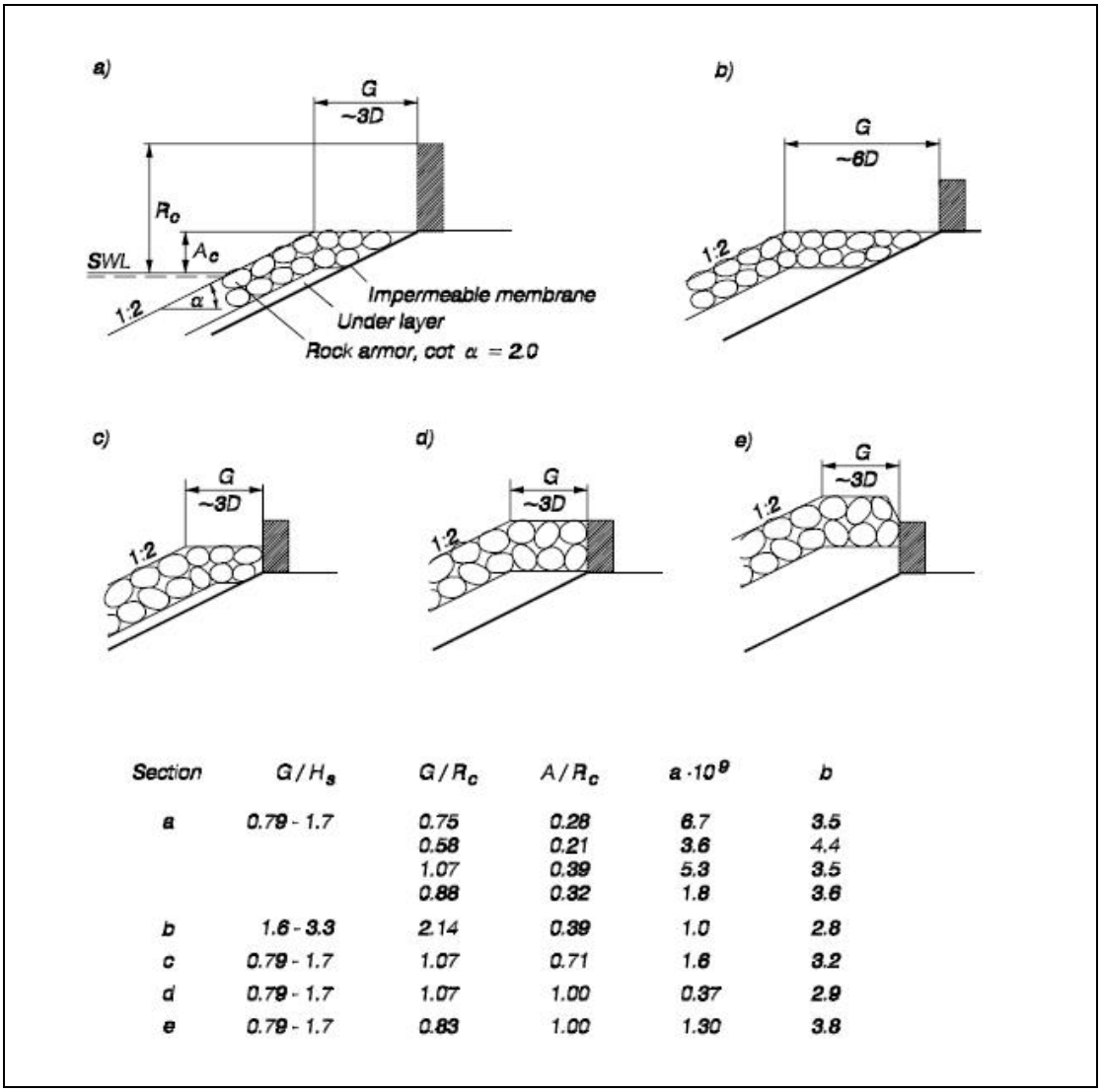

Section	G/H_s	G/R_c	A/R_c	$a \cdot 10^9$	b
a	0.79 - 1.7	0.75	0.28	6.7	3.5
		0.58	0.21	3.6	4.4
		1.07	0.39	5.3	3.5
		0.88	0.32	1.8	3.6
b	1.6 - 3.3	2.14	0.39	1.0	2.8
c	0.79 - 1.7	1.07	0.71	1.6	3.2
d	0.79 - 1.7	1.07	1.00	0.37	2.9
e	0.79 - 1.7	0.83	1.00	1.30	3.8

Figure 5 Coefficients a and b in Equation 2.3-12, Bradbury [3]

2.3.5. Overtopping volume per wave: TAW2002

Often it is sufficient to use the mean overtopping discharge in the design of hydraulic structures. Usually this discharge is expressed as a specific discharge per metre run along the crest, Q in m^3/s per m length or in l/s per m length.

The critical peak volumes, (V_{max}) in m_3 per m length, may be of greater significance than critical discharges in some circumstances. The average wave overtopping discharge does not say much about the amount of water that will flow over the crest for a certain wave. The wave overtopping volumes per wave differ substantially from the average wave overtopping volume.

The probability distribution function for the wave overtopping volume per wave is calculated in TAW [22] by using the average wave overtopping discharge. The probability distribution function is a Weibull distribution with a shape factor b=0.75 and a scale factor 'a', which depends on the average wave overtopping discharge and the probability of overtopping waves. The probability distribution function is given in Equation 2.3-13:

$$P_v = P\left(\underline{V} \le V\right) = 1 - \exp\left[-\left(\frac{V}{a}\right)^b\right] = 1 - \exp\left[-\left(\frac{V}{a}\right)^{0.75}\right] \qquad \textit{Equation 2.3-13}$$

with

$$a = 0.84 \cdot T_m \cdot \frac{q}{P_{ov}} = 0.84 \cdot T_m \cdot q \cdot \frac{N}{N_{ov}} = 0.84 \cdot q \cdot \frac{t}{N_{ov}} \qquad \textit{Equation 2.3-14}$$

The probability of overtopping per wave can be calculated as in Equation 2.3-15.

$$P_{ov} = \exp\left[-\left(\sqrt{-\ln 0.02}\,\frac{R_c}{z_{2\%}}\right)^2\right] \qquad \textit{Equation 2.3-15}$$

Equation 2.3-15 applies to the assumption that the wave run-up distribution conforms to the Rayleigh distribution. The 2% wave run-up can be calculated with Equation 2.3-16 and Equation 2.3-17.

$$\frac{z_{2\%}}{H_{m0}} = 1.75 \cdot \gamma_b \cdot \gamma_f \cdot \gamma_\beta \cdot \xi_0 \qquad \textit{Equation 2.3-16}$$

with a maximum for larger ξ_0 of:

$$\frac{z_{2\%}}{H_{m0}} = \gamma_f \cdot \gamma_\beta \left(4.3 - \frac{1.6}{\sqrt{\xi_0}}\right) \qquad \textit{Equation 2.3-17}$$

in which $z_{2\%}$ is 2% wave run-up level above still water line.
The volume for a certain probability of exceeding P_V follows from Equation 2.3-18:

$$V = a\left[-\ln\left(1 - P_v\right)\right]^{(1/b)} = a\left[-\ln\left(1 - P_v\right)\right]^{(4/3)} \qquad \textit{Equation 2.3-18}$$

A first estimation of the predicted value for the maximum volume of one wave that can be expected in a certain period can be gained by filling in the total number of overtopping waves N_{ov}:

$$V_{\max} = a\left[\ln\left(N_{ov}\right)\right]^{\left(1/b\right)} = a\left[\ln\left(N_{ov}\right)\right]^{\left(4/3\right)}$$ *Equation 2.3-19*

In order to give an idea of the relationship between the average wave overtopping discharge (Q) and the predicted value of the maximum volume in the largest wave overtopping wave (V_{max}), this relationship is shown for two situations in Figure 6. Assumptions are a storm duration of 1 hour, a slope of 1:4 and a wave steepness s_0=0.04 with $T_{m-1,0}/T_m$ relationship of 1.15. Relationships are drawn for wave heights of H_{m0}=1m and H_{m0}=2.5m. For small average wave overtopping discharges (V_{max}) is in the order of q times 1000s and for high average wave overtopping discharges in the order of q times 100s.

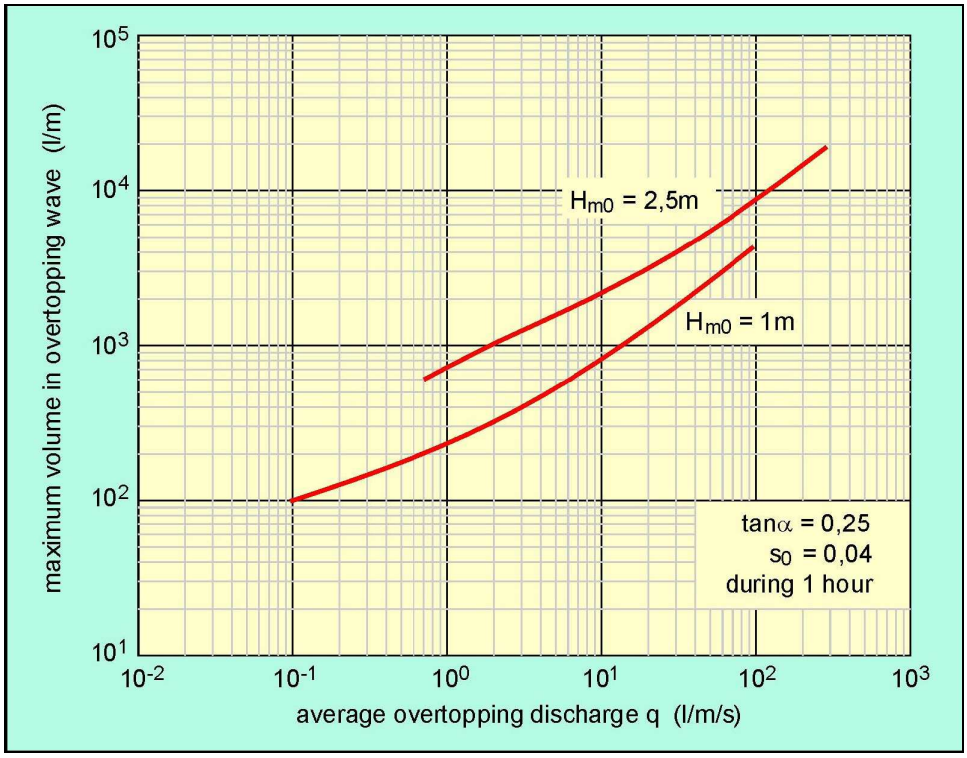

Figure 6 Relationship between average wave overtopping discharge and maximum volume of highest wave overtopping

2.4. Wave overtopping discharge directly behind the crest

The overtopping discharge at the top of the crest is divided in two parts: the overtopping discharge that infiltrates into the crest (infiltrating discharge) and the overtopping discharge that flows over the crest to behind the crest (overtopping discharge directly behind the crest). Steenaard [19] describes this division with Equation 2.4-1.

$$\frac{Q_{over}}{Q_{tot}} = \begin{cases} \dfrac{Q^*_{tot,S} - Q^*_d}{Q^*_{tot,S} + 7.0 \cdot 10^{-2}} & \text{for } Q^*_{tot,S} \geq Q^*_d \\ 0 & \text{for } Q^*_{tot,S} \leq Q^*_d \end{cases} \qquad \textit{Equation 2.4-1}$$

In which
Q^*_d = threshold value for overtopping discharge directly behind the crest ($\approx 8.1*10^{-3}$) (-)

2.5. Distribution wave overtopping discharge

Several methods are known to describe the spatial distribution of wave overtopping discharge behind the crest. This chapter describes the most relevant methods.

2.5.1. Juul Jensen

The intensity of overtopping behind a breakwater decreases with the distance from the breakwater. In all tests performed by Juul Jensen [10] and in the prototype measurements it has been experienced that on average the intensity of overspill decreases exponentially with the distance (x) from the breakwater. This means:

$$q(x) = q_0 \cdot 10^{-(x/\beta)} \qquad \textit{Equation 2.5-1}$$

in which:
q(x) =intensity overtopping discharge at a distance x ($m^3/s/m/m$)[1]

Now the total amount of overtopping (Q) may be calculated by integration:

$$Q = \int_0^{\infty} q_0 \cdot 10^{-(x/\beta)} dx \qquad \textit{Equation 2.5-2}$$

resulting in the following formula:

$$Q = q_0 \cdot \beta / \ln 10 \qquad \textit{Equation 2.5-3}$$

Knowing Q and β, the intensity (q_0) for x=0 may be calculated, and thus the intensity q(x) for any distance x is known.

The breakwater in this thesis can be compared with profile A of Jensen's research: a straight breakwater slope without a crown wall.

[1] Intensity of the overtopping discharge (q(x)) in ($m^3/s/m$ per m), discharge per meter width and per meter length of the crest

The geometry was classified by B* (the horizontal distance from the intersection of the SWL and the sea side slope of the breakwater to the rearmost extend of the crest) and by B (the crest width). Figure 7 illustrates these relevant parameters.

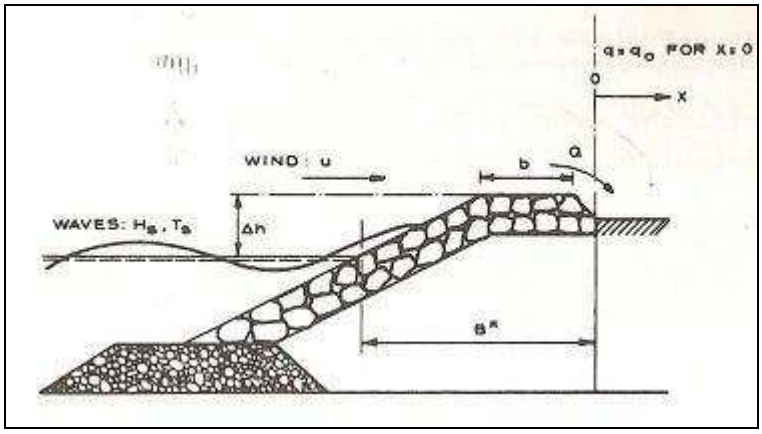

Figure 7 Parameters for method of Juul Jensen

In all tests performed, β has been nearly constant, independent of both wave and wind conditions. For profile A, the breakwater comparable with this research, the approximate value of dimensionless factor β/B* is 0.40-0.55

The results show that the overtopping varies from structure to structure, but some general conclusions may be derived:

- The amount of overtopping increases rapidly with the parameter H_s/R_c. The logarithm of $Q \cdot T_z/(B^*)^2$ is normally a linearly function of H_s/R_c, in which T_z= mean zero crossing period.
- The influence of the wave period differs per structure. However, there is a tendency that longer periods cause greater overtopping.
- No sharp limit exists between wind-carries spray and mass-overtopping where solid masses of water are passing the crest of the breakwater.
- The wind effect is most pronounced for small values of H_s/R_c, while for high sea states and/or high water levels (large values of H_s/R_c) where mass-overtopping occurs the wind has no influence on the amount of overtopping.

2.5.2. Hydraulic Research Wallingford

This method, developed by the Hydraulic Research Wallingford [9], is applicable for breakwaters with simple, straight slopes having an armoured crest. The method computes a reduction factor (C_r) for the overtopping discharge for a wide crested breakwater, see Equation 2.5-4.

Equation 2.5-4

$$C_r = 3.06 \cdot e^{\left(-1.5\frac{G_c}{H_{m0}}\right)} \text{ with } C_r \leq 1$$

2.5.3. Lykke Andersen en Burcharth

Lykke Andersen and Burcharth (Aalborg University) [11] paid attention to the spatial distribution of overtopping water at breakwaters with a crest wall. The spatial distribution was measured by various trays behind the crest wall. The spatial distribution depends on the level with respect to the rear side of the crest wall and the distance from this rear wall, see Figure 8. The coordinate system (x,y) starts at the rear side and at the top of the crest wall, with the positive y-axis downward.

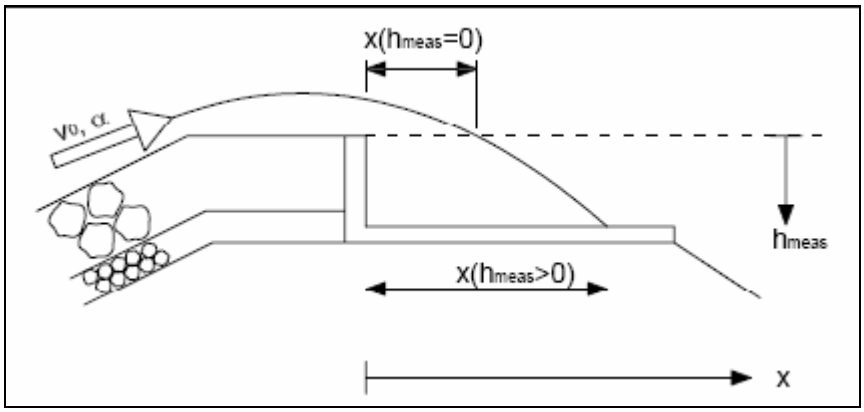

Figure 8 Definition of x- and y-coordinate for spatial distribution

The exceedance probability (F) of the travel distance is defined as the volume of overtopping water passing a given x- and y-coordinate, divided by the total overtopping volume. The probability, therefore, lies between 0 and 1, with 1 at the crest wall. The probability at a certain location can be described with Equation 2.5-5.

$$F(x,y) = \exp\left(\frac{-1.3}{H_{m0}} \cdot \left\{\max\left(\frac{x}{\cos\beta} - 2.7 \cdot y \cdot s_{0p}^{0.15}, 0\right)\right\}\right) \qquad \textit{Equation 2.5-5}$$

which can be rewritten to calculate the travel distance x (at a certain level y) as Equation 2.5-6.

$$\frac{x}{\cos\beta} = -0.77 \cdot H_{m0} \cdot \ln(F) + 2.7 \cdot y \cdot s_{0p}^{0.15} \qquad \textit{Equation 2.5-6}$$

Suppose cosβ=0, then we get:
F=1 x=0
F=0.1 $x=1.77H_s$
F=0.01 $x=3.55H_s$

It means that 10% of the volume of water travels almost two wave heights through the air and 1% of the volume travels more than 3.5 times the wave height. These percentages will be higher if y≠0, which is often the case with a crest unit.
The validity of Equation 2.5-5 and Equation 2.5-6 is for rubble mound slopes of approximately 1:2 and for angles of wave attack between $0^\circ \le |\beta| \le 45^\circ$. It should be noted that the equation is valid for the spatial distribution of the water through the air behind the crest wall. All water falling on the basement of the crest unit will of course travel on and will fall into the water behind and/or on the slope behind.

3. Laboratory research

This chapter describes the physical scale model experiments. First the required prototype for the breakwater is determined. The scaling process is based on this prototype and leads to the scale model. Then the laboratory equipment, experiment set and experiment arrangements are elaborated.

3.1. Prototype

3.1.1. Dimensions and materials

In order to create a representative scale model, it is necessary to assume a prototype of a coastal defence structure. With the help of scale effects and similarity requirements this prototype will form the basis for the design of the scale model.

The prototype is a simplified coastal defence structure, which means that some relevant dimensions and conditions are excluded. The scale model properties do not contain a berm, toe structure or underlayers and the hydraulic conditions do not contain oblique waves and wind. The prototype must represent a common structure, which is used very often in the hydraulic engineering.

This leads to the following dimensions of the prototype coastal defence structure:

Crest freeboard R_c=2m
Slope tan(α)=1:2 (α=tan(1/2)=26.6°)
Material armour layer grading=3-6 T;
M_{15}=3.27 T, M_{50}=4.43 T, M_{85}=6.00 T
D_{n15}=1.07m, D_{n50}=1.19m, D_{n85}=1.31m
D_{15}=1.28m, D_{50}=1.41m, D_{85}=1.56m (foot note[1])

With hydraulic conditions:
Water depth d=13m
Wave height H_s=3.2m ($H_s \approx H_{m0}$)
Wave steepness s=1/30
Wave length L=96m ($L=H_s/s$)
Wave period T_s=7.84s ($L = g \cdot T_s^2 / (2\pi)$)
Breaker parameter ξ=2.74 ($\xi = \frac{\tan\alpha}{\sqrt{s}}$)

A rule of thumb for these hydraulic conditions is:
Waves break for: - s>1/7 or H>0.15L
Spilling if ξ_0<0.5
Plunging if 0.5<ξ_0<3.3
Collapsing or surging if ξ_0>3.3
- H>0.75d

So the waves will not break before the interaction with the coastal defence structure.

[1] Shape parameter=0.84, which means $D_{n50}=0.84 \cdot D_{50}$

3.1.2. Stability armour layer

This research is about the spatial distribution of the wave overtopping discharge and not about the stability of a coastal defence structure. Therefore the used material must be sufficiently strong to resist the attacking waves in all circumstances.

To verify the hydraulic stability of individual stones on the sloping surface of this prototype under wave attack, the method of van der Meer [21] will be used.
Van der Meer [21] derived formulae to predict the stability of armour stones on uniform slopes with a crest above the maximum run-up level. The formulae make a distinction between 'plunging waves' and 'surging waves'.
For plunging waves the formula is given in Equation 3.1-1.

$$\frac{H_s}{\Delta \cdot D_{n50}} = c_{pl} \cdot P^{0.18} \cdot \left(\frac{S_d}{\sqrt{N}}\right)^{0.2} \cdot \xi^{-0.5} \qquad \textit{Equation 3.1-1}$$

For surging waves the formula is given in Equation 3.1-2.

$$\frac{H_s}{\Delta \cdot D_{n50}} = c_s \cdot P^{-0.13} \cdot \left(\frac{S_d}{\sqrt{N}}\right)^{0.2} \cdot \sqrt{\cot \alpha} \cdot \xi^{P} \qquad \textit{Equation 3.1-2}$$

in which:

N	=number of incident waves at the toe, which depends on the duration of the wave conditions (≈100 in the scale model experiments)	(-)
P	=notional permeability of the structure (=0.5 for armour layer with a thickness of 2 stones on top of a core)	(-)
S_d	=characteristic value of the damage level parameter (=2 for start of damage for a slope with cot(α)=2)	(-)
c_{pl}	=coefficient for plunging waves (≈6.2)	(-)
c_s	=coefficient for surging waves (≈1.0)	(-)

In the circumstances of the prototype, the breaker parameter ξ=2.74, so Equation 3.1-1 for plunging waves has to be used. In this prototype, with corresponding hydraulic conditions, this results in the following required D_{n50}:

$$D_{n50} = \frac{H_s}{\Delta \cdot c_{pl} \cdot P^{0.18} \cdot \left(\frac{S_d}{\sqrt{N}}\right)^{0.2} \cdot \xi^{-0.5}} = \frac{3.2}{1.65 \cdot 6.2 \cdot 0.5^{0.18} \cdot \left(\frac{2}{\sqrt{100}}\right)^{0.2} \cdot 2.74^{-0.5}} = 0.81\text{m}$$

The chosen rock diameter D_{n50}=1.187 m is sufficient to meet this requirement, so the stability of the breakwater under the wave attack is guaranteed.

The maximum significant wave height under which the armour layer will meet the stability requirements can also be determined:

$$H_s = \Delta \cdot D_{n50} \cdot c_{pl} \cdot P^{0.18} \cdot \left(\frac{S_d}{\sqrt{N}}\right)^{0.2} \cdot \xi^{-0.5} = 1.65 \cdot 1.187 \cdot 6.2 \cdot 0.5^{0.18} \cdot \left(\frac{2}{\sqrt{100}}\right)^{0.2} \cdot 2.74^{-0.5}$$

$$= 4.69\text{m}$$

3.2. Scaling process

The extensive explanation of the scaling process is described in Appendix II. The most important conclusions and the results of this process are presented in this chapter.

3.2.1. Similitude

Hydraulic similitude of the scale model is based on various scaling criterions and similitude requirements. The most important scaling criterions are the Froude criterion, the Reynolds criterion and the Strouhal criterion. The most important similitude requirements are geometric similarity, kinematic similarity and dynamic similarity.

Froude criterion

The Froude criterion for modelling flows can be described as Equation 3.2-1.

$$\frac{N_V}{\sqrt{N_g \cdot N_L}} = 1 \qquad \textit{Equation 3.2-1}$$

This criterion is valid for flows of which the inertial forces are balanced primarily by the gravitational forces, which is the case in the most flows with a free surface. Consequently, the Froude model law is the most important criterion to be considered when designing a coastal scale model.

Reynolds criterion

The Reynolds criterion for modelling flows can be described as Equation 3.2-2.

$$N_V \cdot N_L = 1 \qquad \textit{Equation 3.2-2}$$

This criterion is important when viscous forces dominate the hydraulic flow. Obviously, the Reynolds criterion does not correspond with the Froude criterion. This means that gravity and viscous forces can not be processed in the same scale model. If gravity is important, viscous forces have to be reduced to a minimum.

Strouhal criterion

The Strouhal criterion for modelling flows can be described as Equation 3.2-3.

$$\frac{N_L}{N_V \cdot N_t} = 1 \qquad \textit{Equation 3.2-3}$$

This criterion simply stated that the velocity scale ratio is equal to the length scale ratio divided by the time scale ratio. This is the same definition for velocity scale that arises from considerations of the fundamental dimensions of velocity.

Geometric similarity

Geometrically similar models are also known as geometrically undistorted models. Geometrically undistorted models are models in which the vertical and horizontal scales are the same, and they represent the true geometric reproduction of the prototype.

Kinematic similarity

Kinematic similarity indicates a similarity of motion between particles in model and prototype. Kinematic similarity is achieved when the ratio between the components of all vectorial motions for the prototype and model is the same for all particles at all times. Kinematic similarity in wave motion requires the Froude criterion.

Dynamic similarity

Dynamic similarity means that there must be constant prototype-to-model ratios of all masses and forces acting on the system. The forces exerted by the wave motion on an object or boundary are similitude when the dynamic similarity is maintained.

Conclusion

According to Warnock [24], the forces associated with surface tension and elastic compression are relatively small for practically all coastal engineering problems, thus can be safely neglected. This leaves selection of an appropriate hydrodynamic scaling law to an evaluation of whether gravity or viscous forces are dominant in the phenomenon. The Froude and Reynolds number are important because similarity of one of these numbers, combined with geometric similarity, provides necessary conditions for hydrodynamic similitude in an overwhelming majority of coastal models.
Gravity forces predominate in free surface flows. Therefore the Froude criterion is used for the design of the scale model in this thesis (as usual in models of coastal processes). Nevertheless, efforts must be made to reduce the effect of viscosity in the model, otherwise the dissimilar viscous effects will constitute a scale effect. Therefore the viscous scale effect (infiltration into the breakwater) is taken into account in the design of the scale model.

3.2.2. Infiltration

A scale effect associated with physical models of rubble mound structures is the viscous force associated with flow through the armour layer, underlayers and core of the structure. Viscous scale effects are often not a problem in the armour layer of the scale model because the Reynolds number based on the characteristic dimension of the armour unit is sufficiently large to insure fully turbulent flow. However, in the core material, there is a possibility that the flow Reynolds number may fall below a value considered critical for avoiding scale effects. In Hughes [8], the defined Reynolds number for which the viscous forces in the pores of a breakwater can be neglected, varies for various studies and definitions of the Reynolds number. The Reynolds number for which similarity of stability number is obtained, is not exactly clear, but most probably it is in order $O(10^4)$.

To investigate the importance of viscous forces during infiltration of wave overtopping discharge into the crest, it is important to determine the filter velocity in the armour layer during this process. For that, this process has to be considered as a simplified appearance. The wave overtopping discharge is schematized as a layer of water which is situated on top of the crest without a horizontal velocity. The filter velocity of the infiltrating water depends on the gradient. The gradient is equal to the proportion between the layer thickness (Δh) of the infiltrating water and the infiltrated distance (Δx) across which resistance is encountered.

Forchheimer [6] formulated Equation 3.2-4 with which the relation between the filter velocity and the gradient is defined:

$$I = a \cdot u_f + b \cdot u_f \cdot \left| u_f \right| \qquad \textit{Equation 3.2-4}$$

in which

a	=coefficient of friction for laminar part	(s/m)
b	=coefficient of friction for turbulent part	(s^2/m^2)

The Reynolds number can now be rewritten as Equation 3.2-5 (in which U is equal to the velocity of the water in the pores and L is equal to the pore size).

$$\mathrm{Re} = \frac{u_p \cdot D_{15}}{\nu}$$ *Equation 3.2-5*

In which:

u_p	=velocity in the pores ($u_p = \frac{u_f}{n}$)	(m/s)
n	=porosity (≈35%=0.35)	(-)
v	=kinematic viscosity=$1 \cdot 10^{-6}$	(m^2/s)

Shih [18] proposed Equation 3.2-6 for coefficient 'a' (term for laminar contribution) and Equation 3.2-7 for coefficient 'b' (term for shape resistance and turbulence friction).

$$a = \alpha \frac{(1-n)^2}{n^3} \frac{\nu}{g \cdot D_{15}^2}$$ *Equation 3.2-6*

$$b = \beta \frac{1-n}{n^3} \frac{1}{g \cdot D_{15}}$$ *Equation 3.2-7*

in which:

$$\alpha = 1684 + 3.12 \cdot 10^{-3} \left(\frac{g}{\nu^2} \right)^{2/3} \cdot D_{15}^2$$ *Equation 3.2-8*

$$\beta = 1.72 + 1.57 \cdot e^{-5.10 \cdot 10^{-3} \left(\frac{g}{\nu^2} \right)^{1/3} D_{15}}$$ *Equation 3.2-9*

3.3. Scale model

The similarity criterions result in the final dimensions and material properties of the scale model.

3.3.1. Dimensions

The hydraulic similitude results in the following dimensions of the scale model coastal defence structure:

Crest freeboard	R_c=100mm
Slope	tan(α)=1:2 (α=tan(1/2)=26.6°)

With the following hydraulic conditions:

Water depth	d=650mm
Wave height	H_s=160mm ($H_s \approx H_{m0}$)
Wave steepness	s=1/30
Wave length	L=4800mm
Wave period	T_s=1.75s
Breaker parameter	ξ=2.74 ($\xi = \frac{\tan\alpha}{\sqrt{s_0}}$)

3.3.2. Materials

Armour layer

The hydraulic similitude results in the following material properties of the armour layer of the scale model coastal defence structure:

Grading=64-78mm;
M_{15}=0.41kg, M_{50}=0.56kg, M_{85}=0.75kg;
D_{n15}=53.7mm, D_{n50}=59.4mm, D_{n85}=65.7mm
D_{15}=63.9mm, D_{50}=70.7mm, D_{85}=78.2mm

Unfortunately no material with these properties was available in the laboratory. By means of a balance and a computer, this material had to be selected manually from material with a larger grading. This resulted in an even narrower grading with following properties:

Grading=66-76mm;
M_{15}=0.45kg, M_{50}=0.56kg, M_{85}=0.68kg;
D_{n15}=55mm, D_{n50}=60mm, D_{n85}=64mm
D_{15}=66mm, D_{50}=71mm, D_{85}=76mm

The specific density of this material is ρ_r=2655 kg/m^3.

Core

The Shore Protection Manual [20] recommends that the mass ratio of subsequent layers of quarry should be kept between 1/10 and 1/15. For the mass ratio equal to 1/10, this leads to the following material properties for the core in the scale model:

Grading=30-36mm;
M_{15}=0.041kg, M_{50}=0.056kg, M_{85}=0.075kg;
D_{n15}=24.9mm, D_{n50}=27.6mm, D_{n85}=30.5mm
D_{15}=29.6mm, D_{50}=32.9mm, D_{85}=36.3mm

Unfortunately also no material with these properties was available in the laboratory. This material had to be selected from other material, namely 'Yellow Sun extra split 20-40mm'. By sieving this material with a sieve mesh 30mm, the required material for the core could be approached. The specific density of the core material is ρ_r=2687 kg/m^3.

3.3.3. Infiltration

According to the porous flow method of Shih [18], described in 3.2.2, the material of the armour layer in the scale model results in a filter velocity of 0.136m/s and a Reynolds number of Re=2.57·10^4. The material of the core in the scale model results in a filter velocity of 0.087 m/s and a Reynolds number of Re=7.36·10^3. The complete calculations for infiltration into the armour layer and the core are given in Appendix III.

The Reynolds numbers of the armour layer and the core in the scale model are in the same order as the minimum criterion defined by Hughes (Re=O(10^4). This means that viscous forces can be excluded, moreover because certain remarks can be made in relation to this subject:

- The filter velocities are relatively large in comparison with the wave period (1.75s). The infiltrating water will be infiltrated deep enough before the next wave comes. In that way, viscous forces will not cause significant problems and the core will not get saturated.

- The infiltrating water regarded in these calculations has no horizontal velocity. However, during the experiments, this water does have horizontal velocity, which causes turbulence. Because of this, viscosity will be of less importance.

Based on the calculations and remarks described above, scale effects in the overtopping discharge as a result of viscous forces can be neglected.

3.3.4. Stability considerations

Armour layer

The method of van der Meer [21] can be used to check the correctness of the dynamic similarity method and to consider the stability of individual stones under sloping surface under wave attack:

$$D_{n50} = \frac{H_s}{\Delta \cdot c_{pl} \cdot P^{0.18} \cdot \left(\frac{S_d}{\sqrt{N}}\right)^{0.2} \cdot \xi^{-0.5}} = \frac{0.16}{1.65 \cdot 6.2 \cdot 0.5^{0.18} \cdot \left(\frac{2}{\sqrt{100}}\right)^{0.2} \cdot 2.74^{-0.5}} = 0.040\text{m}$$

The used rock diameter D_{n50}=0.060 m is sufficient to meet this requirement, so the stability of the breakwater in the scale model is guaranteed.

The maximum significant wave height under which the armour layer will meet the stability requirements can also be determined:

$$H_s = \Delta \cdot D_{n50} \cdot c_{pl} \cdot P^{0.18} \cdot \left(\frac{S_d}{\sqrt{N}}\right)^{0.2} \cdot \xi^{-0.5} = 1.65 \cdot 0.060 \cdot 6.2 \cdot 0.5^{0.18} \cdot \left(\frac{2}{\sqrt{100}}\right)^{0.2} \cdot 2.74^{-0.5}$$

$$= 0.237\text{m}$$

Filter stability requirements

Besides stability of individual stones under wave attack, the armour layer and core need to meet more stability requirements. Two relations for a geometrically closed granular filter will be considered.
The stability rule prevents movements of larger grains from the base layer (core). The space between the grains in the filter layer (armour later) is governed by the smaller grains (D_{15F}). The largest grains of the base layer (D_{85B}) get stuck in the pores of the filter and block the passage of all the other grains of the base layer. The stability rule can be written as $\frac{D_{15F}}{D_{85B}} \le 5$. For this scale model counts $\frac{D_{15F}}{D_{85B}} = \frac{0.066}{0.0363} = 1.82 \le 5$, so this situation meets the stability requirement.
In order to prevent pressure build-up, the permeability of a filter layer (armour layer) should be larger than the permeability of the base layer (core). Since the permeability is also governed by the smallest grains, this leads to the following rule: $\frac{D_{15F}}{D_{15B}} \ge 5$. For this scale model counts $\frac{D_{15F}}{D_{15B}} = \frac{0.066}{0.0296} = 2.23 \le 5$, so this situation does not meet the permeability requirement. This is mainly caused by the large grading of the base layer. The armour layer and the core are both remarkable permeable; there is no large gradient perpendicular to the interface. Therefore, this permeability rule is not a leading rule.

3.3.5. Final overview

The final material properties, hydraulic and physical conditions of the scale model are clarified in Appendix XII-1. Pictures of the scale model are showed in Appendix XIV-1 and Appendix XIV-2.

3.4. Laboratory equipment

3.4.1. Hydraulic instruments

Wave flume

The wave flume 'Lange Speurwerk Goot' in the Fluid Mechanics Laboratory of the Delft University of Technology was made available for the execution of the physical model experiments in this thesis. The flume has a length of approximately 40m, a width of 0.80m and a height of 0.80m. The wave flume can be filled and emptied with pumps valves on both sides of the flume.

Wave generator

The wave flume is equipped with a wave generator. This wave generator has Active Reflection Compensation (ARC) and a second order wave generation technique, which means that the second-order effects of the first higher and first lower harmonics of the wave field are taken into account in the wave generator motion.
The wave generator is controlled by the computer program 'DASYLab'. The user needs to create a steering file in which various parameters are defined: the water depth in the flume, the required wave height, the required wave length, the peak-enhancement factor, peak-width factor and duration of the spectrum (last 3 parameters only for JONSWAP-spectra).

3.4.2. Measurement instruments

Wave gauges

Two sets of three wave gauges are installed inside the wave flume. The first set is placed just in front of the breakwater and the other set is placed 15m in front of the breakwater. Changes in wave conditions during the propagation through the wave flume can be noticed in this way.
The differences in voltage between the two poles of the wave gauge are converted in the differences in water level. The water levels and corresponding voltages are established by several calibrations of the wave gauges. This calibration is executed by measuring the voltage for several known water levels.
The set of three wave gauges is necessary to calculate the significant wave height and significant wave period of the waves travelling to the structure. The wave gauges measure the differences in water level, but this is the interaction between incoming and reflected waves. Because the three wave gauges in a set are installed at a certain known distance from each other, a Matlab-code can distinguish the incoming and reflected wave. This results in the relevant incoming significant wave height (H_{m0}) and significant wave period ($T_{m-1,0}$).

Balance

The wave overtopping discharge is collected in the collecting tank. With the help of a submersible pump, this water is pumped to another tank outside the wave flume. This second tank is placed at a balance as a result of which the overtopping amount of water can be measured. Together with the overtopping time, which is measured with a stopwatch, the overtopping discharge in m^3/s can be calculated.

3.4.3. Measuring error

The measuring error depends on the accuracy of the instruments. In this research there are five parameters measured with instruments: the water depth, the wave height, the wave period, the overtopping volume and the overtopping time.

The water depth, wave height and wave period are measured with the wave gauges. The water depth is measured with the indicated voltage of the wave gauges in case of still water. This measured voltage is calibrated with a ruler frequently between the experiments. Therefore the error in the measured water depth is negligible. The wave height and wave period are measured during the experiments. For that reason, calibration of these measurements is very difficult. Variance in the wave height and the wave period has major influence on the wave overtopping discharge. But the final conclusion of the experiment results is based on the ratio between the overtopping discharges (reduction factor C_r) in different experiments with the same hydraulic conditions. Assuming that the possible error occurs in all the experiments with the same conditions, this error has no influence on the reduction factor. Therefore, the errors in the measured wave height and wave period are negligible.

The overtopping times and the overtopping volumes are measured manual with respectively a stopwatch and a balance. The stopwatch is started when the water level in the collecting tank has a certain level. The pump pumps the overtopping water to the tank outside the wave flume. When the required amount of overtopping water is collected and the water level in the collecting tank is the same as at the start of the test, the stopwatch is stopped. The measured time is the overtopping time. The overtopping volume is collected in the tank outside the flume during this overtopping time. This tank is placed at a balance, by which the weight (and the volume) can be measured.
Small errors can occur by the reading of the stopwatch and the balance, because both instruments had to be read manually at the same moment. In case of the overtopping time, the range of the error is approximately 0.5s. In case of the overtopping volume, the range of the error is approximately 0.3kg (=0.3l). The lowest overtopping time is approximately 80s and the corresponding highest overtopping volume is approximately 150l, which results in an average overtopping discharge of 1.875 l/s. With a maximum error, the overtopping time will be 79.5s and the overtopping volume will be 150.3, which results in an overtopping discharge of 1.89. Consequently the maximum error in the overtopping discharge is 0.015 l/s, which is 0.8% of the actual overtopping discharge. However, most experiments are executed with a higher duration, what makes the relative error in the overtopping discharge lower. But the maximum error in the overtopping discharge can be considered 0.8%.

3.5. Experiment setup

3.5.1. Varying parameters

Various influencing parameters could be varied to consider their influence on the spatial distribution of the overtopping discharge. Some of them, like wind and oblique waves, were impossible to investigate in this thesis, because the wave flume was not suitable to insert these parameters. Other parameters, like a berm, a toe or a slope, were very difficult and almost unfeasible to vary during the experiments. Consequently there was chosen to leave these parameters out of this thesis and only vary the practical and relevant parameters. The parameters whose influence is significant and crucial to investigate are: wave height, wave steepness, water depth, crest height and wave spectrum.

Wave height

Varying the wave height was not very difficult; it could be done by changing the wave height settings in the steering file for the wave generator.
Because of the ARC, the wave generator was only able to create waves up to a certain maximum wave height. For that reason, the significant wave height (H_s) in this research varied between 0.12m and 0.24m for regular waves and between 0.08m and 0.16m for irregular waves.

Wave steepness

Changing the wave steepness was not very difficult; it could be done by changing the wave period settings in the steering file for the wave generator.
The wave steepness is a combination of the wave height and the wave length (wave period). Therefore the settings of the wave height and the wave steepness had to be adjusted to each other.
The wave generator is only able to create wave steepnesses in a certain range, dependant of the wave height. In this thesis, the wave steepness varied between 1/20 – 1/50. In combination with the varying wave heights, this means that the significant wave period (T_s) varied between 1.3s and 2.5s and the wave length varied between 2.5m and 10m.
Also the influence of the wave steepness on the breaker parameter had to be taken into account. A varying breaker parameter leads to different types of breaking waves and different overtopping appearances.

Water depth and crest height

The water depth and the crest height are connected to each other. The height of the breakwater did not change, so the sum of the water depth and the crest height was always the same. These two parameters could be changed by adding or removing water with the pumps and the valves in the wave flume. The water depth during this research changed between 0.55m and 0.65m. Consequently the crest height changed between 0.10m and 0.20m

Regular waves and irregular waves

The wave generator was able to produce regular waves and irregular waves of a certain wave spectrum (JONSWAP-spectrum for instance). The JONSWAP (JOint North Sea WAve Project) spectrum is an empirical relationship that defines the distribution of energy with frequency within the ocean. This JONSWAP-spectrum is assumed to be especially suitable to imitate conditions of the North Sea. In these conditions, the stability of breakwaters or coastal morphology can be tested properly.
Nevertheless, most of the experiments in this research were performed with regular waves. The wave flume was not available long enough to perform all the

experiments with a JONSWAP-spectrum. Since the development of a JONSWAP-spectrum requires a certain amount of time (1800s), an experiment with regular waves takes less time than an experiment with a JONSWAP-spectrum. To investigate the spatial distribution of the overtopping discharge, many experiments were required and it was practically impossible to complete these experiments with irregular wave spectra.
An advantage of performing the experiments with regular waves is the overtopping discharge per wave. Most of the current wave overtopping regulations are based on the wave overtopping discharge per unit of time (l/s/m). This is a slightly vague indication; it is possible that overtopping waves appear once in a long time, this leads to a very large overtopping discharge per wave. Apart from the wave overtopping discharge per unit of time, the overtopping discharge per wave (l/m) is also a leading indication and will be used more and more in the future. This overtopping discharge per wave is easy to calculate from an experiment with regular waves.
However, it was certainly useful to perform some experiments with a JONSWAP spectrum. The results of these experiments can be compared with the results of the experiments with regular waves. If can be verified that the results are approximately the same, the conclusions of the result analysis counts for both wave spectra.

3.5.2. Experiment code

Experiment codes are used to clarify the large amount of various experiments. The experiment code is a combination of the relevant parameters in the experiment:

- type of experiment (T for total overtopping discharge, O for overtopping discharge directly behind the crest, I for overtopping discharge over impermeable backfill and P for overtopping discharge over permeable backfill)
- wave height (cm)
- wave steepness (noted as 1/s) (-)
- crest freeboard (cm)
- wave spectrum (R for regular waves and J for JONSWAP)
- length permeable or impermeable backfill (cm)

Example: I-18-30-10-R-20 is an experiment to measure the wave overtopping discharge behind an impermeable backfill with a length of 20cm. The experiment is executed with regular waves and H_s=0.18m, s=1/30 and R_c=0.10m.

3.6. Test programme

Four different types of wave overtopping discharges were measured in this research: total wave overtopping discharge, wave overtopping discharge directly behind the crest, wave overtopping discharge over impermeable backfill and wave overtopping discharge over permeable backfill.

3.6.1. Total wave overtopping discharge

To investigate the division of the total wave overtopping discharge in the infiltrating discharge into the crest and the overtopping discharge directly behind the crest, the total wave overtopping discharge had to be measured. Besides, the total wave overtopping discharge was used to determine the reliability of the scale model.
The collecting tank was placed on top of the crest. In this way, all the overtopping discharge was collected and measured at the balance.
Figure 9 gives an impression of this type of experiment. A picture of the setup for this experiment is given in Appendix XIV-3.

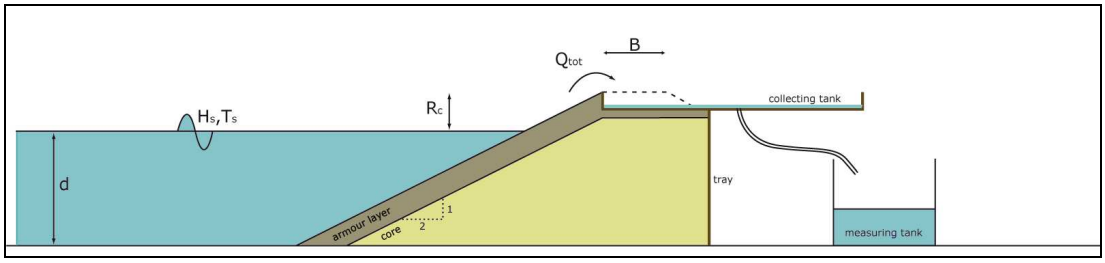

Figure 9 Total wave overtopping discharge

Wave height

Various tests were executed to investigate the influence of the wave height. The wave height varied between 0.13m and 0.22m, the wave steepness was 1/30 and the crest height was 0.10m.

Wave spectrum	Wave height (m)	Number of tests
Regular waves	0.13 – 0.22	10

Wave steepness

Various tests were executed to investigate the influence of the wave steepness. The wave steepness varied between 1/15 and 1/50, the wave height was 0.18m and the crest height was 0.10m.

Wave height (m)	Wave steepness	Number of tests
0.18	1/15 – 1/50	7

Wave steepness in combination with the wave height

Various tests were executed to investigate the influence of the wave height in combination with the wave steepness. The wave height varied between 0.16m and 0.20m, the wave steepness varied between 1/20 and 1/40 and the crest height was 0.10m.

Wave height (m)	Wave steepness	Number of tests
0.16	1/20 – 1/40	4
0.20	1/20 – 1/40	4

Crest height in combination with the wave height

Various tests were executed to investigate the influence of the crest height in combination with the wave height. The crest height varied between 0.075m and 0.15m, the wave height varied between 0.14m and 0.22m and the wave steepness was 1/30.

Wave height (m)	Crest height (m)	Number of tests
0.14	0.075	1
0.16	0.075 – 0.125	2
0.18	0.075 – 0.15	3
0.20	0.075 – 0.15	3
0.22	0.125 – 0.15	2

Wave spectrum

Various tests were executed with a JONSWAP-spectrum to investigate the reliability of the scale model. Besides, the influence of the different wave spectra was investigated. Therefore several experiments were executed with various parameters. The wave height varied between 0.08m and 0.18m, the wave steepness varied between 1/30 and 1/50 and the crest height varied between 0.10m and 0.20m.

Wave height (m)	Wave steepness	Crest height (m)	Number of tests
0.08 – 0.18	1/30 – 1/50	0.10 – 0.20	15

3.6.2. Wave overtopping discharge directly behind the crest

To determine the division of the total wave overtopping discharge in the infiltrating discharge into the crest and the overtopping discharge directly behind the crest, the overtopping discharge behind the crest of the coastal defence structure was investigated. By executing approximately the same experiment set as in the total wave overtopping discharge research, described in section 3.6.1, the division could be determined.
The collecting tank was shifted from the top of the crest to the back of the crest. In this way, the overtopping discharge directly behind the crest was collected and measured at the balance.
Figure 10 gives an impression of this experiment.

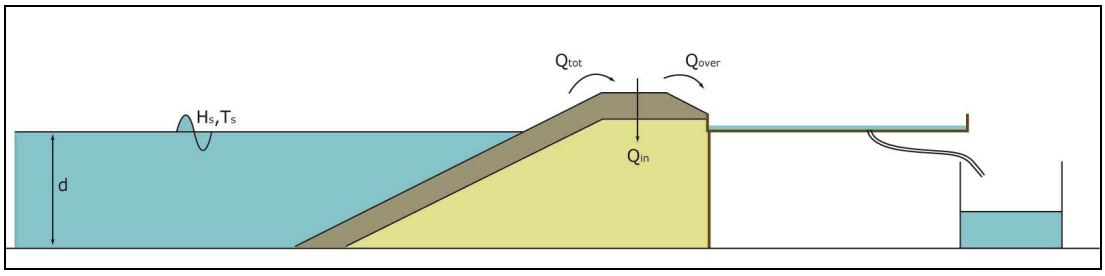

Figure 10 Wave overtopping discharge directly behind the crest

Wave height

Various tests were executed to investigate the influence of the wave height. The wave height varied between 0.15m and 0.22m, the wave steepness was 1/30 and the crest height was 0.10m.

Wave spectrum	Wave height (m)	Number of tests
Regular waves	0.15 – 0.22	8

Wave steepness

Various tests were executed to investigate the influence of the wave steepness. The wave steepness varied between 1/15 and 1/50, the wave height was 0.18m and the crest height was 0.10m.

Wave height (m)	Wave steepness	Number of tests
0.18	1/15 – 1/50	7

Wave steepness in combination with the wave height

Various tests were executed to investigate the influence of the wave height in combination with the wave steepness. The wave height varied between 0.16m and 0.20m, the wave steepness varied between 1/20 and 1/45 and the crest height was 0.10m.

Wave height (m)	Wave steepness	Number of tests
0.16	1/25 – 1/40	3
0.19	1/20 – 1/45	5
0.20	1/20 – 1/45	5

Crest height in combination with the wave steepness

Various tests were executed to investigate the influence of the crest height in combination with the wave steepness. The crest height was increased to 0.125m, the wave height was 0.22m and the wave steepness varied between 1/30 and 1/40.

Wave height (m)	Wave steepness	Number of tests
0.22	1/30 – 1/40	2

Wave spectrum

Various tests were executed with a JONSWAP-spectrum to investigate the influence of the different wave spectra. The wave height varied between 0.10m and 0.12m, the wave steepness varied between 1/30 and 1/40 and the crest height was 0.10m.

Wave spectrum	Wave height (m)	Wave steepness	Number of tests
JONSWAP	0.10	1/30	1
JONSWAP	0.12	1/30 – 1/40	2

3.6.3. Wave overtopping discharge over impermeable backfill

The spatial distribution of the wave overtopping discharge behind the crest depends on the type of material behind the crest. In case of an impermeable backfill, for example a roadway under a certain slope, the overtopping discharge flows over the roadway and can not infiltrate into the surface material. At every point behind the crest, the overtopping discharge directly behind the crest is separated in two parts: one part flows back to the breakwater under the influence of gravity and the other part passes the point and travels further away from the breakwater. The behaviour of the overtopping discharge as a function of the length of this impermeable backfill was investigated in this part of the research.

The scale model roadway was imitated by an impermeable board under a slope of 3% towards the crest. To investigate the spatial distribution of this overtopping discharge behind the crest, it was necessary to perform several tests, all with a different width of the roadway. For that reason, it was possible to close off the collecting tank (which is installed at the same place as in section 3.6.2) with watertight boards of a certain length. By increasing the length of the board

(roadway), the overtopping discharge behind the crest reduced. The discharge that flowed over the board was collected in the tank and measured at the balance.

Figure 11 gives an impression of this experiment.

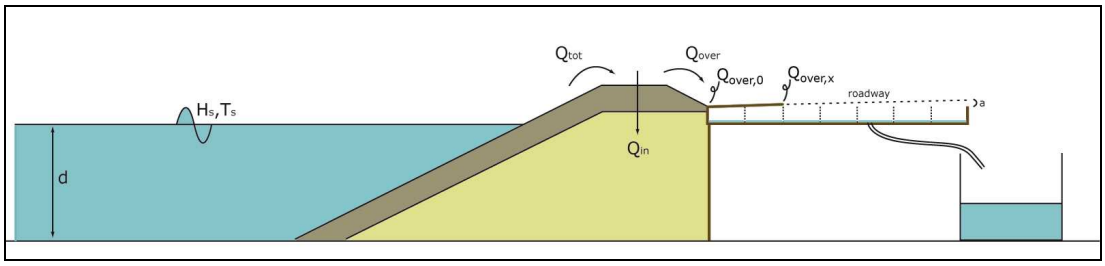

Figure 11 Spatial distribution of wave overtopping discharge behind the crest for a roadway (slope=3%) behind the crest

Wave height

Various tests were executed to investigate the influence of the wave height. The wave height varied between 0.17m and 0.22m, the wave steepness was 1/30 and the crest height was 0.10m.

Wave spectrum	Wave height (m)	Number of tests
Regular waves	0.17 – 0.22	6

Wave steepness

Various tests were executed to investigate the influence of the wave steepness. The wave steepness varied between 1/20 and 1/55, the wave height was 0.18m and the crest height was 0.10m.

Wave height (m)	Wave steepness	Number of tests
0.18	1/12 – 1/55	7

Wave steepness in combination with the wave height

Various tests were executed to investigate the influence of the wave height in combination with the wave steepness. The wave height varied between 0.16m and 0.20m, the wave steepness varied between 1/20 and 1/45 and the crest height was 0.10m.

Wave height (m)	Wave steepness	Number of tests
0.16	1/25 – 1/40	2
0.19	1/20 – 1/45	5
0.20	1/20 – 1/45	5

Crest height in combination with the wave steepness

Various tests were executed to investigate the influence of the crest height in combination with the wave steepness. The crest height was 0.125m, the wave height was 0.22m and the wave steepness varied between 1/30 and 1/40.

Wave height (m)	Wave steepness	Number of tests
0.22	1/30 – 1/40	2

Wave spectrum

Various tests were executed with a JONSWAP-spectrum to investigate the influence of the different wave spectra. The wave steepness varied between 1/30 and 1/40, the wave height was 0.12m and the crest height was 0.10m.

Wave spectrum	Wave steepness	Number of tests
JONSWAP	1/30 – 1/40	2

Board length

The amount of boards had to be enough to deliver appropriate and useful data. Too much boards should led to too much experiments, too much work and too much required time. Apart from the amount of boards also the lengths of the boards are important. Each length had to deliver a useful data point to consider the spatial overtopping distribution. The decision about the amount of boards and the board lengths was based on a loose prediction of the spatial distribution with existing theories.

All the experiments described above were executed for seven different lengths of the board. The board length varied between 0.05m and 0.60m.

Board length (m)	Experiments	Number of tests
0.05	Complete set	29
0.10	Complete set	29
0.15	Complete set	29
0.20	Complete set	29
0.30	Complete set	29
0.40	Not complete set	26
0.60	Not complete set	24

3.6.4. Wave overtopping discharge over permeable backfill

The spatial distribution of wave overtopping discharge behind the crest is different for impermeable and permeable backfill behind the crest. In case of permeable backfill the overtopping discharge will flow over the rock and is able to infiltrate into the backfill. At every point behind the crest, the overtopping discharge directly behind the crest is separated in two parts: one part infiltrates into the backfill (in the pores between the rocks) and the other part passes the point and travels further away from the breakwater. The behaviour of the overtopping discharge behind the crest for this permeable backfill was investigated in this part of the research.

For this part of the research a new collecting tank was constructed. The technical drawing of the collecting tank is given in Appendix XIII-1. This collecting tank had to be able to be divided into two parts by means of a replaceable watertight board: one rock filled part at the side of the breakwater and one empty part behind the board. There was a small gap between the breakwater and the collecting tank. The front of the collecting tank was constructed with wire netting. This resulted in a water level inside the rock filled part that was equal to the water level in the rest of the flume. A picture of this wire netting is given in Appendix XIV-4. A side view picture of the scale model in Appendix XIV-5 shows the small gap between the breakwater and the wire netting.
The rock filled part contained two layers armour rock on top and core material below. The replaceable watertight board prevented leaking of water from the rock filled part to the empty part. A picture of the watertight board, the rock filled part and the empty part is given in Appendix XIV-6.
The overtopping discharge flowed over the rock filled part and was separated into two parts. One part infiltrated into the rock filled part and flowed out of the

collecting tank through the wire netting (this prevented saturation of the rock filled part). The other part of the overtopping discharge flowed over the rock filled part and was collected in the collecting tank behind the watertight board and measured at the balance.

The behaviour of the overtopping discharge behind the crest as a function of the length of the permeable backfill was investigated in this part of the research. Figure 12 gives an impression of this experiment.

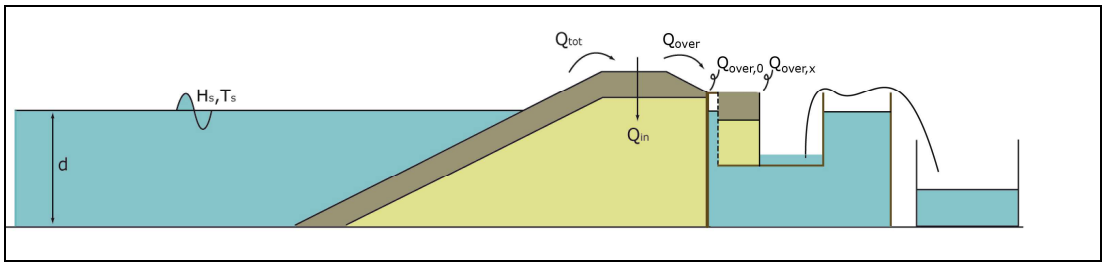

Figure 12 Spatial distribution of wave overtopping discharge behind the crest for a horizontal rockbed behind the crest

Wave height

Various tests were executed to investigate the influence of the wave height. The wave height varied between 0.20m and 0.23m, the wave steepness was 1/30 and the crest height was 0.10m.

Wave spectrum	Wave height	Number of tests
Regular waves	0.20m – 0.23m	3

Wave steepness in combination with the wave height

Various tests were executed to investigate the influence of the wave height in combination with the wave steepness. The wave height varied between 0.16m and 0.20m, the wave steepness varied between 1/35 and 1/55 and the crest height was 0.10m.

Wave height (m)	Wave steepness (-)	Number of tests
0.18	1/45 – 1/55	3
0.19	1/35 – 1/45	3
0.20	1/35 – 1/45	3

Crest height in combination with the wave steepness

Due to problems with the water reservoir in the laboratory, it was almost impossible to vary the water depth during the experiments. Therefore no experiments are executed with a varying crest height

Wave spectrum

Various tests were executed with a JONSWAP-spectrum to investigate the influence of the different wave spectra. The wave steepness varied between 1/30 and 1/40, the wave height was 0.12m and the crest height was 0.10m.

Wave spectrum	Wave height (m)	Wave steepness	Number of tests
JONSWAP	0.14	1/40 – 1/45	2
JONSWAP	0.15	1/40	1

Rock filled length

Same as for the experiments with an impermeable backfill behind the crest, described in section 3.6.3, the decision about the amount of rock filled parts and the lengths of the rock filled parts was based on loose predictions with existing methods.
All the experiments described above were executed for seven different lengths of the rock filled part. The rock filled part varied between 0.10m and 0.30m. Unfortunately it was physically impossible to place the watertight board in the first 10cm of the tank.

Length rock filled part (m)	Experiments	Number of tests
0.10	Complete set	12
0.125	Complete set	12
0.15	Complete set	12
0.175	Not complete set	9
0.20	Not complete set	9
0.25	Not complete set	6
0.30	Not complete set	5

4. Analysis of results

The analysis of the experiment results is divided in 5 section: total overtopping discharge (section 4.1), overtopping discharge directly behind the crest (section 4.2), overtopping discharge over impermeable backfill (section 4.3), overtopping discharge over permeable backfill (section 4.4) and overtopping discharge with irregular waves (section 4.5)

4.1. Total overtopping

To determine the reliability of the wave overtopping scale model, it is essential to compare the experiment results with other overtopping researches and theoretical methods. This will be done for the two different wave spectra: irregular waves and regular waves.
Appendix XIV-7 shows a picture of an experiment to measure the total overtopping discharge.
The physical process of the total wave overtopping discharge (Q_{tot}) is illustrated in Figure 13.

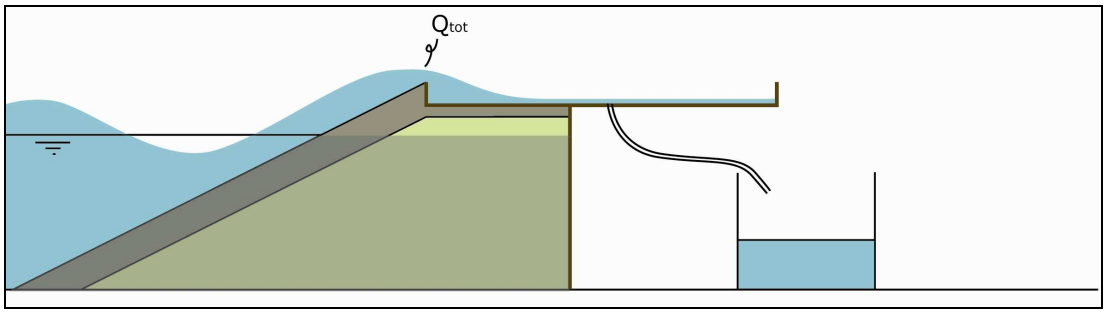

Figure 13 Physical process of total wave overtopping discharge

4.1.1. Irregular waves

There are 15 experiments executed with an irregular wave spectrum; a JONSWAP-spectrum. The JONSWAP (JOint North Sea WAve Project) spectrum is an empirical relationship that defines the distribution of energy with frequency within the ocean. This spectrum is based on the Pierson-Moskowitz spectrum[1]. The spectra observed during JONSWAP appear to have a sharper peak than the Pierson-Moskowitz spectrum. To account for this parameterisation of the observations, the scientists of JONSWAP chose to take the shape of the Pierson-Moskowitz spectrum and to enhance its peak with a peak-enhancement function.
The peak-enhancement function G(f) is defined in Equation 4.1-1:

$$G(f) = \gamma^{\exp\left[-\frac{1}{2}\left(\frac{f/f_{peak}-1}{\sigma}\right)^2\right]} \qquad \textit{Equation 4.1-1}$$

[1] The fully developed Pierson-Moskowitz spectrum is:

$$E_{PM}(f) = \alpha_{PM} g^2 (2\pi)^{-4} f^{-5} \exp\left[-\frac{5}{4}\left(\frac{f}{f_{PM}}\right)^{-4}\right]$$

This leads to the following description of a JONSWAP-spectrum defined in Equation 4.1-2:

$$E_{JONSWAP}(f) = \alpha g^2 (2\pi)^{-4} f^{-5} \exp\left[-\frac{5}{4}\left(\frac{f}{f_{peak}}\right)^{-4}\right] \gamma^{\exp\left[-\frac{1}{2}\left(\frac{f/f_{peak}-1}{\sigma}\right)^2\right]}$$

Equation 4.1-2

Figure 14 shows the Pierson-Moskowitz spectrum, the shape of the Pierson-Moskowitz spectrum and the shape of the JONSWAP spectrum.
The Pierson-Moskowitz spectrum represents a fully developed sea, where JONSWAP represents a fetch-limited spectrum.

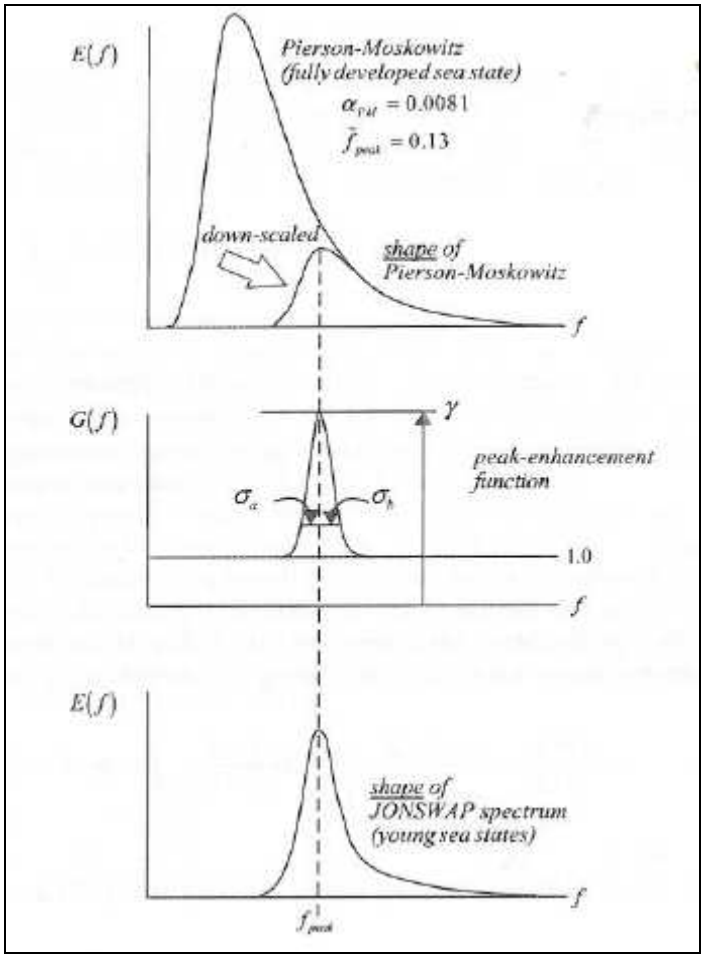

Figure 14 The Pierson-Moskowitz spectrum, the shape of the Pierson-Moskowitz spectrum and the shape of the JONSWAP spectrum

In JONSWAP, the scatter of the shape parameters was large, but the average values are: $\gamma = 3.3$, $\sigma_a = 0.07$ and $\sigma_b = 0.09$. These values are also applied in the experiments with JONSWAP-spectrum.
According to Dingemans [5], for a peak-enhancement factor $\gamma = 3.3$, the ratio between the peak period T_p and the mean energy period $T_{m-1,0}$ is 1.107 ($T_p / T_{m-1,0} = 1.107$).

The results of the 15 executed JONSWAP-experiments in this research are presented in Appendix IV-1.

The measured results are used to calculate the spectral wave period ($T_{m-1,0}$), the spectral wave height (H_{m0}), the wave length (L), the wave steepness (s) and the breaker parameter (ξ). The slope of the breakwater is 1:2 under all circumstances. The results of these calculations are presented in Table 4.

Experiment code	Spectral wave period Tm-1,0 (s)	Spectral wave height Hm0 (m)	Wave length L (m)	Wave steepness s (-)	Breaker parameter ξ (-)
T-8-30-10-J	1,11	0,085	1,928	4/91	2,38
T-9-30-10-J	1,13	0,096	1,991	1/21	2,28
T-10-30-10-J	1,31	0,105	2,679	3/77	2,53
T-12-30-20-J	1,36	0,125	2,867	1/23	2,39
T-13-30-20-J	1,40	0,136	3,061	2/45	2,37
T-14-30-20-J	1,47	0,130	3,385	1/26	2,55
T-15-30-20-J	1,54	0,140	3,682	3/79	2,57
T-16-30-20-J	1,59	0,148	3,947	3/80	2,58
T-17-30-20-J	1,60	0,153	3,992	1/26	2,55
T-18-30-20-J	1,66	0,159	4,313	1/27	2,60
T-14-50-20-J	2,03	0,139	6,450	2/93	3,40
T-15-50-20-J	2,08	0,147	6,740	1/46	3,39
T-16-50-20-J	2,22	0,158	7,710	1/49	3,49
T-15-40-20-J	1,77	0,144	4,894	1/34	2,92
T-16-40-20-J	2,07	0,154	6,681	2/87	3,29

Table 4 Calculations experiments for total wave overtopping

Table 4 shows that all experiments resulted in non-breaking waves (ξ_0>2). This means that the results should be compared with the wave overtopping formula of TAW [22] for non-breaking waves. This formula is defined in Equation 4.1-3.

$$\frac{Q}{\sqrt{g \cdot H_{m0}^3}} = 0.2 \exp\left(-2.6 \frac{R_c}{H_{m0} \cdot \gamma_f \cdot \gamma_\beta} \right)$$

Equation 4.1-3

in which

γ_f = influence factor for roughness elements (=0.55) (-)

γ_β = influence factor for the angel of wave attack (=1) (-)

According to TAW [22], the value for the roughness coefficient γ_f for two layers of armour rock is equal to 0.55. The influence factor for the angel of wave attack γ_β is equal to 1, because there are no oblique waves.

The reliability of Equation 4.1-3 is given by taking the coefficient 2.6 as a normally distributed stochastic function with a mean of 2.6 and a standard deviation σ=0.35. Using this standard deviation, the exceedance limits (μ+xσ) can also be drawn for μ plus a number of standard deviations (1.16 for the 5% under and upper exceedance limits and 1.48 for the 2.5% under and upper exceedance limits).

The dimensionless wave overtopping discharge is defined in Equation 4.1-4 and the dimensionless crest height is defined in Equation 4.1-5.

$$\frac{Q}{\sqrt{g \cdot H_{m0}^3}}$$ *Equation 4.1-4*

$$\frac{R_c}{H_{m0} \cdot \gamma_f \cdot \gamma_b}$$ *Equation 4.1-5*

This results in the dimensionless parameters given in Table 5.

Experiment code	Dimensionless crest height	Dimensionless wave overtopping
T-8-30-10-J	1,1792	5,7643E-04
T-9-30-10-J	1,0449	1,0852E-03
T-10-30-10-J	0,9559	1,6409E-03
T-12-30-20-J	1,5958	6,2464E-05
T-13-30-20-J	1,4686	1,0015E-04
T-14-30-20-J	1,5361	9,6748E-05
T-15-30-20-J	1,4331	1,8754E-04
T-16-30-20-J	1,3538	2,9833E-04
T-17-30-20-J	1,3082	3,7277E-04
T-18-30-20-J	1,2560	5,1466E-04
T-14-50-20-J	1,4378	3,7267E-04
T-15-50-20-J	1,3630	7,2071E-04
T-16-50-20-J	1,2627	9,6937E-04
T-15-40-20-J	1,3923	3,8076E-04
T-16-40-20-J	1,2992	7,0482E-04

Table 5 Dimensionless crest height and dimensionless wave overtopping

Figure 15 presents the dimensionless test results and the relation between the dimensionless overtopping discharge and the dimensionless crest height according to TAW [22], described in Equation 4.1-3. Furthermore the lower and upper 5% exceedance limits are illustrated in the figure.

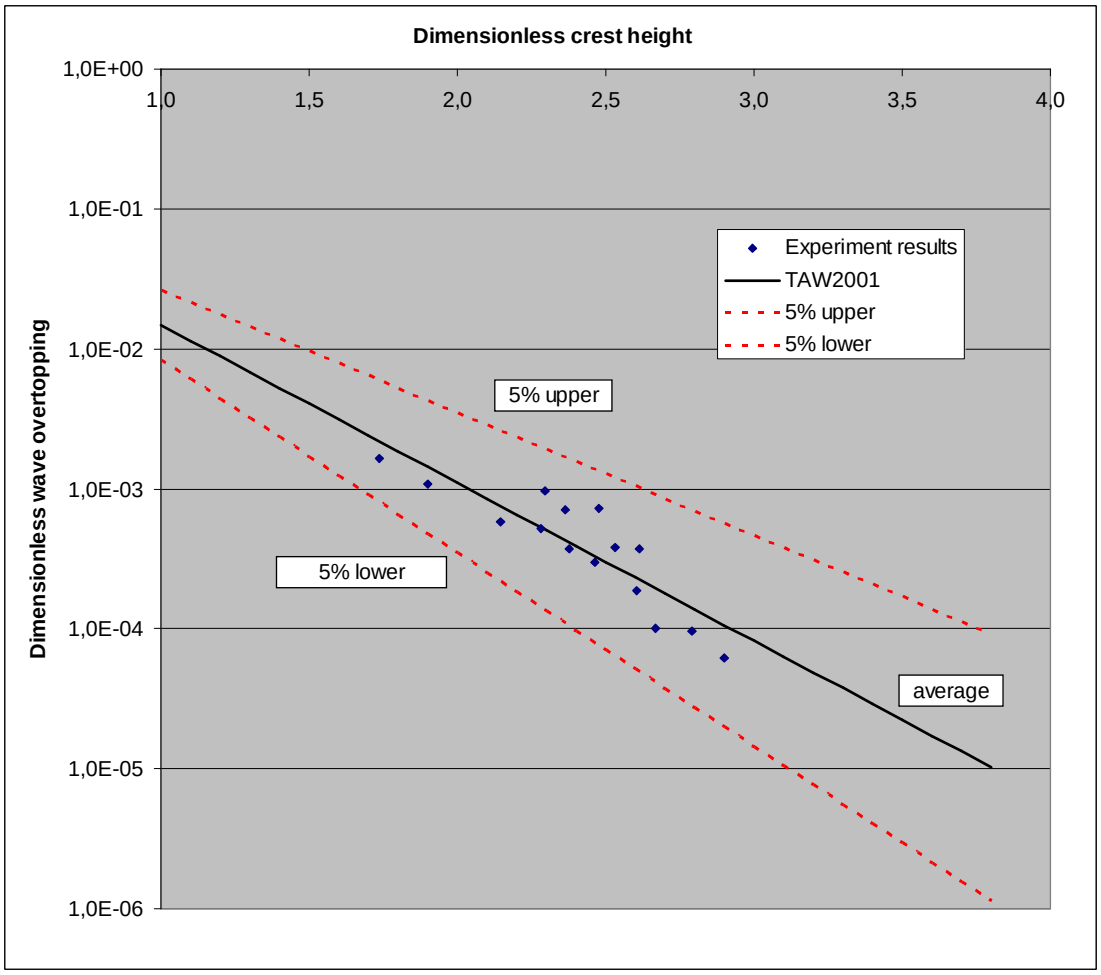

Figure 15 Relation between dimensionless crest height and dimensionless overtopping discharge according to TAW2002 compared with experiment results

Apparently the experiment results fit properly in the method of TAW [22].

4.1.2. Regular waves

Due to the limited period of time that the wave flume is available for this research, most of the experiments are not performed with irregular wave spectra, but with regular waves. In order to determine the reliability of the overtopping discharge for regular waves, 36 unique experiments with regular waves and different hydraulic parameters are performed and compared with theoretical methods. The results of these 36 experiments are presented in Appendix IV-2.
In contrast with the high quantity of overtopping theory for irregular wave spectra, fewer studies with regular waves have been performed and less theory is available about wave overtopping with regular waves. The experiments from the thesis of Schüttrumpf [17] delivers the most reliable and available data.

Schüttrumpf performed a lot of experiments for his thesis and varied several parameters during these experiments: the wave spectrum varied between regular waves and JONSWAP; the crest freeboard varied between 0cm and 15cm; the wave height varied between 0.065cm and 0.24cm; the wave period varied between 1.32s and 6.02s; the inner slope of the dike varied between 1:1 and 1:6 and the outer slope of the dike varied between 1:2 and 1:6. For all these different circumstances Schüttrumpf measured the overtopping discharge over the scale model dike.
The slopes of the dike were constructed of multiplex and can be considered as smooth slopes. Nevertheless, comparison of the experiments in this thesis (rough slope) with the experiments of Schüttrumpf is still possible by introducing the influence factor for roughness elements.
In order to make this comparison, the results of Schüttrumpf's 139 experiments are converted to a dimensionless overtopping discharge and a dimensionless crest height.
Schüttrumpf distinguishes three different types breaking waves: 'Sturzbrecher', 'Collapsing-brecher' and 'Reflexionsbrecher'. The trend in the dimensionless overtopping discharge differs for these three types of breaking waves. Most of the waves in this thesis are of the type 'Reflexionsbrecher' and will therefore only be compared with the experiments of Schüttrumpf with this same type of breaking waves.

Figure 16 shows the dimensionless presentation of the overtopping discharge and the crest height for the experiments of Schüttrumpf. The figure shows also the dimensionless presentation for the experiments of this thesis; the corresponding values are given in Appendix IV-2.

Apparently the results of this thesis are in accordance with the results of Schüttrumpf. The data points fit in the data cloud of Schüttrumpf's results or follow the trendline of Schüttrumpf's results.

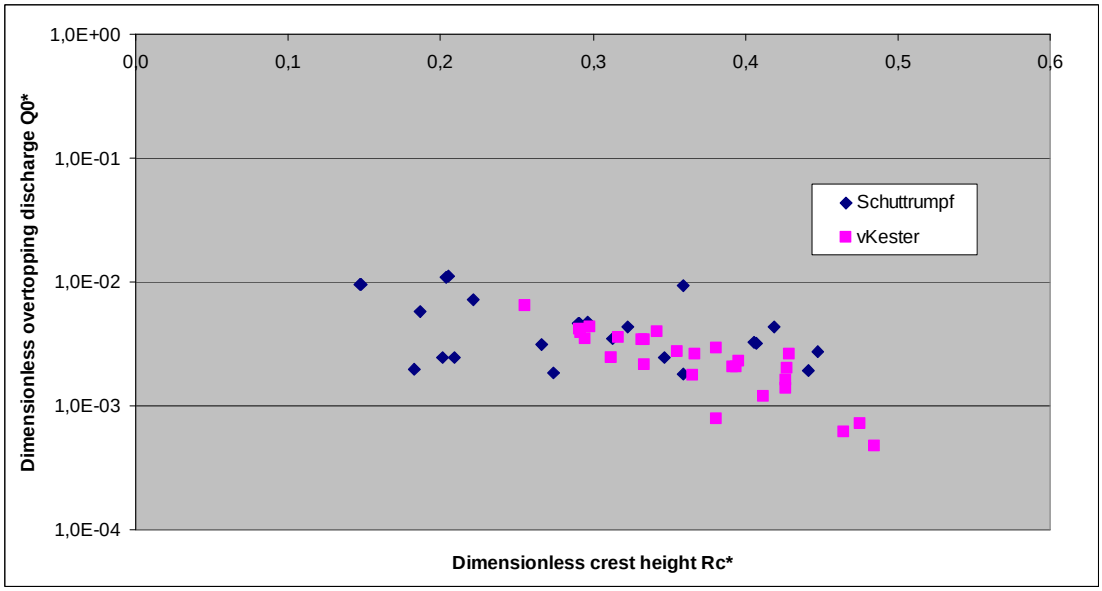

Figure 16 Comparison experiment results with Schüttrumpf by dimensionless presentation

4.1.3. Conclusion

The comparison of the total overtopping discharge experiment results with former studies and existing theories is necessary to determine the reliability of the scale model. In section 4.1.1 and section 4.1.2 is proved for respectively irregular wave spectra and regular waves that the results of the experiments fit properly with other studies and theories. This means that the dimensions and scale effects of the scale model are processed correctly and the scale model is constructed correctly.

For the continuation of this thesis this means that further experiment results are considered as acceptable and can be used to derive the relation for the spatial distribution of the wave overtopping discharge.

4.2. Wave overtopping discharge directly behind the crest

The total overtopping discharge at the crest of the breakwater (analysed in section 4.1) flows over the breakwater and is separated in two parts: one part infiltrates into the crest and the other part flows over the crest to behind the crest. One objective of this thesis is to investigate this division. Thereto data are required about the total overtopping discharge (Q_{tot}) and the overtopping discharge directly behind the crest (Q_{over}). The difference between these two discharges is the infiltrated discharge into the crest. The experiment results for the total overtopping discharge are presented in Appendix IV and the experiment results for the overtopping discharge directly behind the crest are presented in Appendix V.

The overtopping discharge directly behind the crest is measured by shifting the collecting tank from the top of the crest to the back of the crest. The discharge is measured for the same experiment set as in the total overtopping discharge experiments.
Pictures of experiments for measuring wave overtopping discharge directly behind the crest are given in Appendix XIV-8 and Appendix XIV-9.
The physical process of the wave overtopping discharge directly behind the crest is illustrated in Figure 17. Figure 17 shows the total wave overtopping discharge (Q_{tot}), the infiltrating discharge into the crest (arrows) and the overtopping discharge directly behind the crest (Q_{over}).

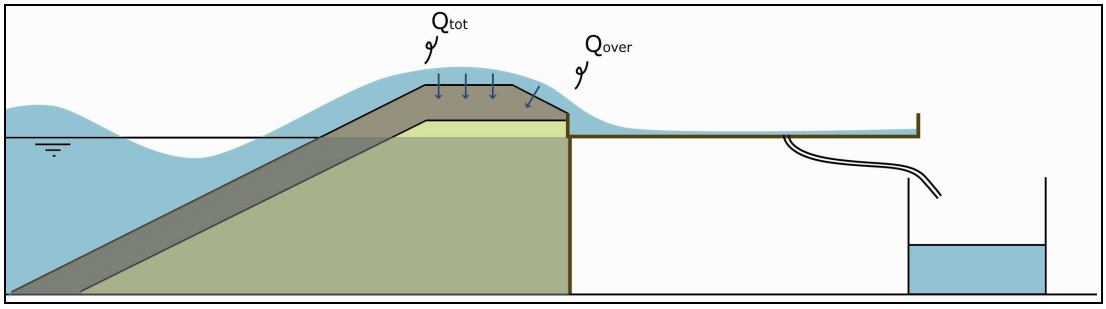

Figure 17 Physical process of wave overtopping discharge directly behind the crest

4.2.1. Correlation water depth and overtopping discharge

A peculiarity appeared during the experiments for the overtopping discharge directly behind the crest. In order to check the consistency of the experiments, some experiments were repeated frequently. Hereby was observed that the overtopping discharge depends on the duration of the experiment. By increasing the experiment duration, the overtopping discharge was decreasing.
This is caused by the correlation between the overtopping discharge and the water depth. In contrast with an ocean in reality, the wave flume in the laboratory does not have an unlimited water buffer. The overtopping amount of water is removed from the wave flume and collected in the tank at the scale to measure its weight. But this removed water influences the water depth inside the wave flume. The surface of water inside the wave flume is 40m*0.8m=32m^2. This means that for every removed litre of water, the water depth reduces with 0.031mm. For 150 litres (average extracted amount of water during the experiments) this results in a reduction of the water depth with 4.69mm. A reduced water depth results in a decreased overtopping discharge. So during an experiment, the overtopping discharge decreases.

This phenomenon disturbs the essence of this thesis. The target of this thesis is to measure the overtopping discharge for a constant water depth. The correlation between the water depth and the overtopping discharge must be excluded from the experiment results.

A method had to be developed to transform the actual measured overtopping discharge with a varying water depth into the required overtopping discharge with a constant water depth. This is a complex phenomenon and it is difficult to find a universal solution for this problem. Therefore an empirical method is developed that exclusively fits for the specific singular situation in this research.

To investigate the variation of the overtopping discharge, the overtopping volume and overtopping time is measured at various moments during six different experiments. The results of these measurements are presented in Appendix VI.

Figure 18 illustrates for each experiment the decrease of the overtopping discharge as a function of the water depth reduction.

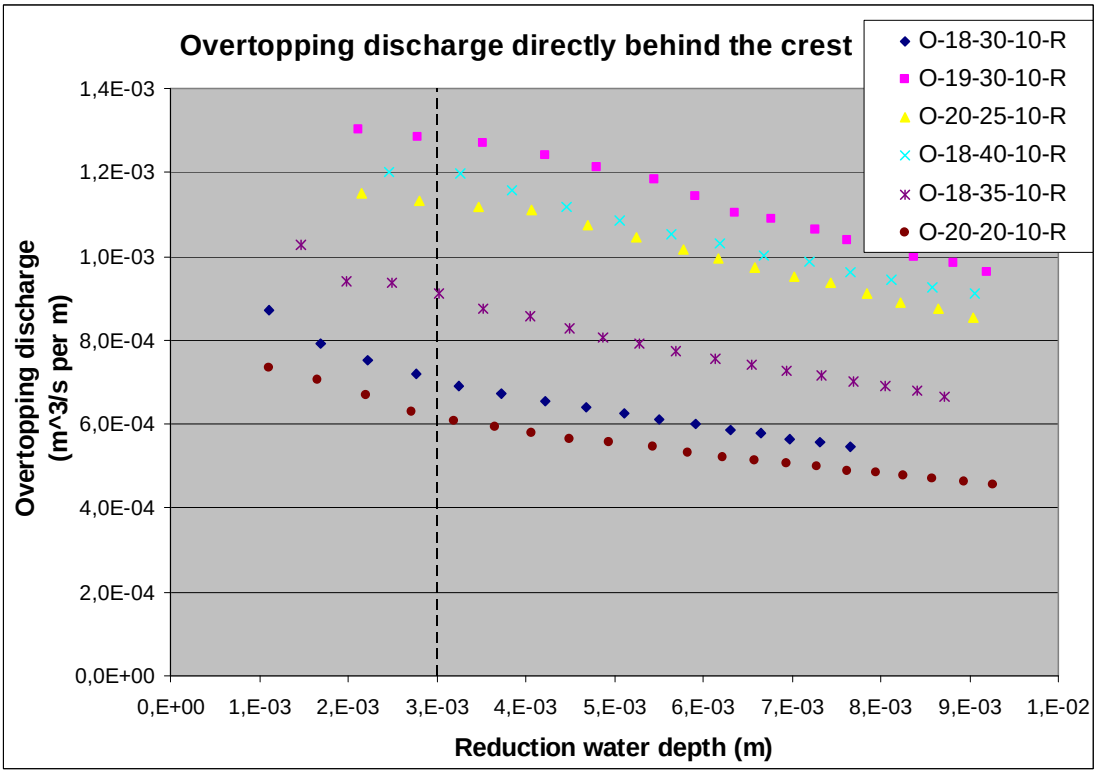

Figure 18 Overtopping discharge behind the crest as function of the water depth reduction

Obviously, during each experiment, the overtopping discharge decreases in time, but the exact progression is different. Naturally it depends on the initial overtopping discharge.
For that reason, the measured overtopping discharges are converted to a dimensionless factor in proportion to the first measured overtopping discharge (Q_x/Q_1). This results in dimensionless factors with a value between 0 and 1.

Additionally, Figure 18 shows also that the overtopping discharge varies greatly in the first period of the experiment, during the first measurements of the discharge. This can be explained by the time that the wave flume needs to tune the wave conditions inside the flume. The reflected waves need to be

compensated by the wave generator before constant wave conditions can be established. For that reason, the first period of the experiments, until a water depth reduction of 0.003m (left of the dashed line in Figure 18), will be excluded from this investigation.
The dimensionless factors for the six experiments are presented in Figure 19. The trendlines, the equations of the trendlines and the R-squared values of each trendline are added to the figure.
The values of the dimensionless factors are given in Appendix VI.

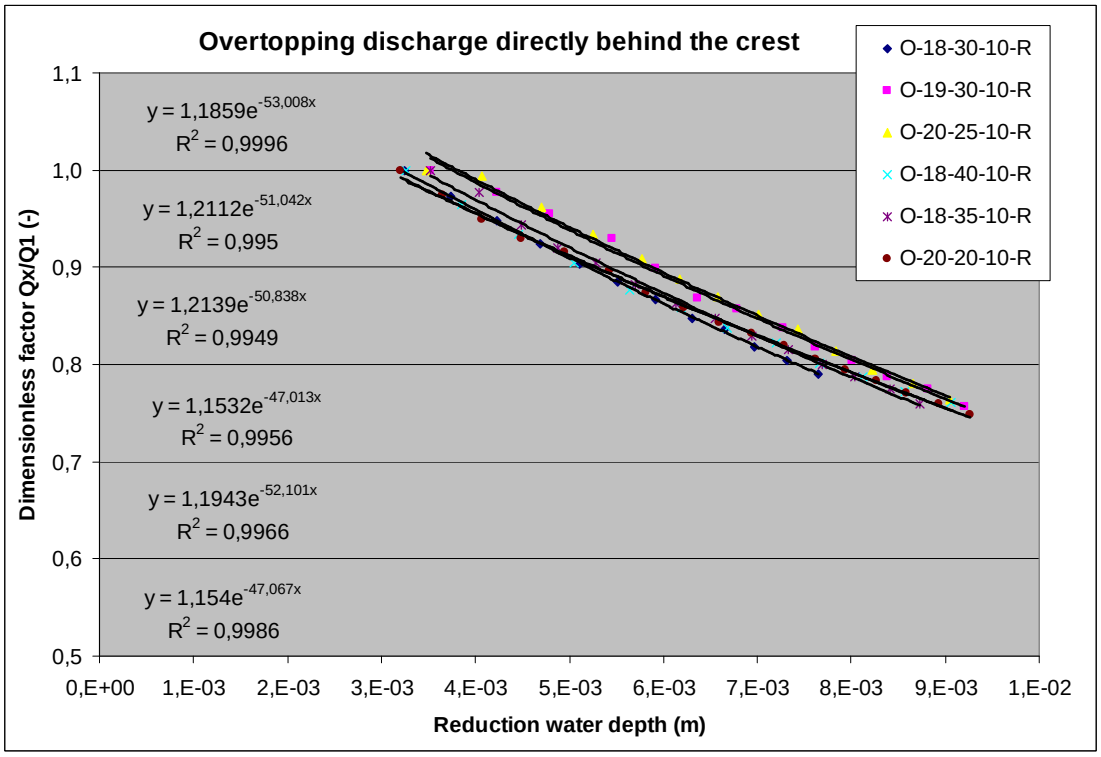

Figure 19 Dimensionless factors Qx/Q1

Due to the fact that the trendlines have an exponential form ($y=A\cdot e^{(Bx)}$), the parameters 'A' in the formulae are the dimensionless factors that correspond with the overtopping discharge without reduction of the water depth (x=0). To compare the progression of the decrease of all experiments with each other, it is necessary to set these parameters 'A' for each experiment equal to 1 and transform the other dimensionless factors as a factor of this parameter 'A'. In other words, all the dimensionless factors of an experiment are divided with the factor 'A' of that experiment. This results in compensation factors in a scale 0-1, presented in Figure 20. The values of the compensation factors are given in Appendix VI.

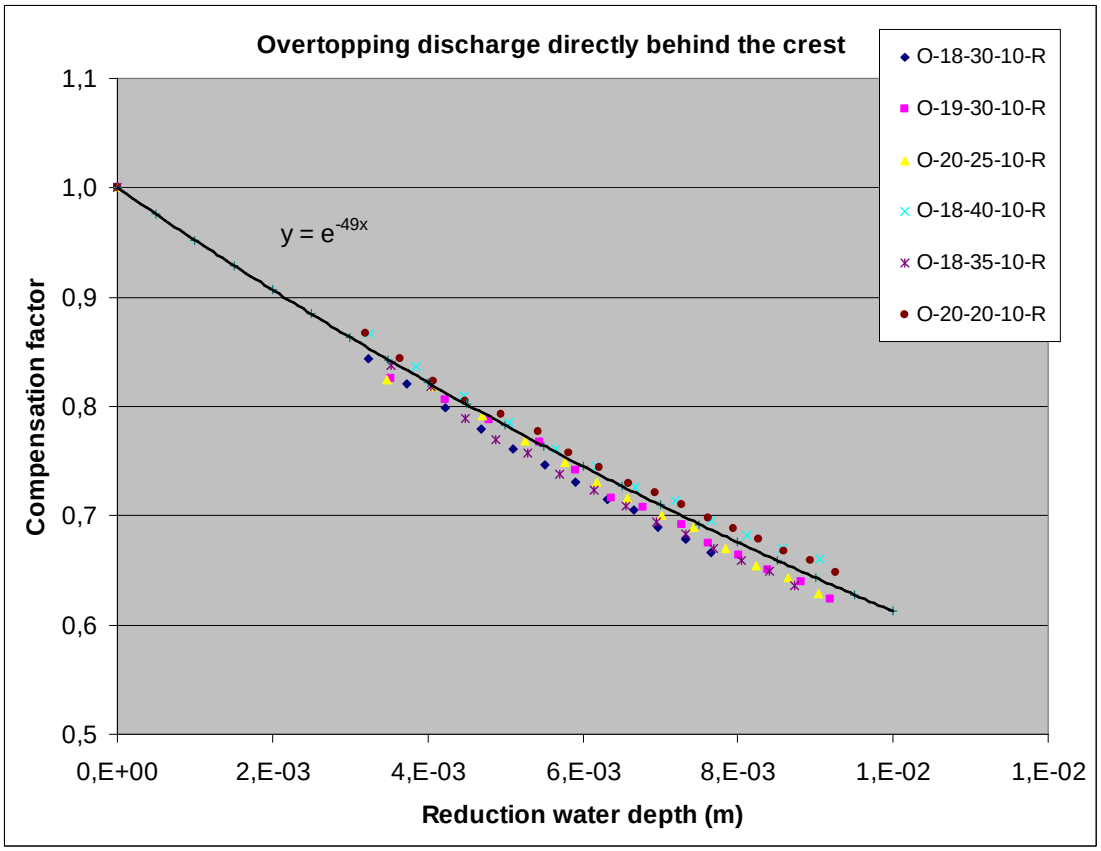

Figure 20 Compensation factors

Apparently, the regression of the decrease is approximately the same for each experiment and is more or less the same as the function $y=e^{-49x}$, where x is the water depth reduction. With this formula, every measured overtopping discharge directly behind the crest can be transformed into an overtopping discharge directly behind the crest without water depth reduction (constant water depth).

For example: the result of an experiment is an overtopping discharge directly behind the crest of 2 l/s and a water depth reduction of 0.008m. This means that the compensation factor for this experiment is $e^{-49*0.008}=0.678$. The actual overtopping discharge directly behind the crest for a constant water depth is in that case 2/0.678=2.96 l/s. This is the overtopping discharge directly behind the crest without water depth reduction (compensation factor = 1).

As mentioned before, this empirical method is only suitable for the specific singular situation of this thesis. It is only valid for transposing the measured overtopping discharge directly behind the crest to the overtopping discharge directly behind the crest for constant water depth in this thesis.

With this method, the measured overtopping discharges directly behind the crest can also be transposed in the required discharges with a certain water depth reduction to compare with other measurements.

4.2.2. Division total overtopping discharge

The total overtopping discharge flows over the crest of the breakwater and is divided in two components: the infiltrated discharge into the crest and the overtopping discharge directly behind the crest.

Steenaard [19] studied this division. The relation between the overtopping discharge directly behind the crest (Q_{over}) and the total overtopping discharge (Q_{tot}), according to Steenaard, is given in Equation 4.2-1.

$$\frac{Q_{over}}{Q_{tot}} = \frac{Q^*_{tot,S} - Q^*_d}{Q^*_{tot,S} + 7.0 \cdot 10^{-2}} \qquad \textit{Equation 4.2-1}$$

in which:

Q^*_d = threshold value for overtopping directly behind the crest ($\approx 8.1*10^{-3}$) (-)

B = crest width (=0.28) (m)

Table 6 gives the four required parameters for Equation 4.2-1: the total overtopping discharge (Q_{tot}), the equivalent overtopping discharge directly behind the crest ($Q_{e,over}$) (see section 4.2.1), the dimensionless overtopping discharge ($Q^*_{tot,S}$) and the relation $Q_{e,over}/Q_{tot}$.

Experiment code	Total overtopping discharge Qtot (m^3/s per m)	Equivalent overtopping discharge Qe,over (m^3/s per m)	Dimensionless total overtopping discharge Q*tot,S	Qe,over/Qtot
T/O-15-30-10-R-0	3,975E-04	9,114E-05	2,536E-03	0,23
T/O-16-30-10-R-0	1,029E-03	2,814E-04	5,534E-03	0,27
T/O-17-30-10-R-0	1,728E-03	6,644E-04	8,251E-03	0,38
T/O-18-30-10-R-0	1,714E-03	5,956E-04	8,464E-03	0,35
T/O-19-30-10-R-0	2,399E-03	1,331E-03	1,084E-02	0,55
T/O-20-30-10-R-0	4,066E-03	2,145E-03	1,618E-02	0,53
T/O-21-30-10-R-0	3,592E-03	2,048E-03	1,385E-02	0,57
T/O-18-20-10-R-0	1,719E-03	2,970E-04	7,816E-03	0,17
T/O-18-25-10-R-0	1,233E-03	3,996E-04	6,103E-03	0,32
T/O-18-35-10-R-0	1,543E-03	9,089E-04	7,802E-03	0,59
T/O-18-40-10-R-0	2,076E-03	1,164E-03	1,009E-02	0,56
T/O-18-45-10-R-0	2,576E-03	1,769E-03	1,248E-02	0,69
T/O-18-50-10-R-0	3,970E-03	3,068E-03	1,710E-02	0,77
T/O-16-25-10-R-0	5,222E-04	6,990E-05	3,184E-03	0,13
T/O-16-35-10-R-0	8,791E-04	3,403E-04	5,359E-03	0,39
T/O-20-20-10-R-0	2,093E-03	6,210E-04	8,905E-03	0,30
T/O-20-25-10-R-0	2,659E-03	1,204E-03	1,095E-02	0,45
T/O-20-35-10-R-0	3,937E-03	2,315E-03	1,582E-02	0,59
T/O-20-40-10-R-0	4,685E-03	3,406E-03	1,809E-02	0,73
T/O-22-30-13-R-0	2,653E-03	1,825E-03	9,373E-03	0,69

Table 6 Parameters required for method of Steenaard

The total overtopping discharge (Q_{tot}) and the overtopping discharge directly behind the crest (Q_{over}) are measured with different water depth reductions. To compare these two discharges, it is necessary to equal these reductions. Therefore, the overtopping discharge directly behind the crest is first transposed into the compensated overtopping discharge directly behind the crest, according to section 4.2.1. The compensated overtopping discharge directly behind the crest is the discharge for a constant water depth, without water depth reduction. Then this compensated overtopping discharge directly behind the crest is again transposed into the equivalent overtopping discharge directly behind the crest ($Q_{e,over}$); the overtopping discharge directly behind the crest with the same water depth reduction as in the equivalent total overtopping experiment.

Figure 21 shows the relation between $Q^*_{tot,S}$ and $Q_{e,over}/Q_{tot}$ according to Steenaard [19]. The trendline is also added to the figure.

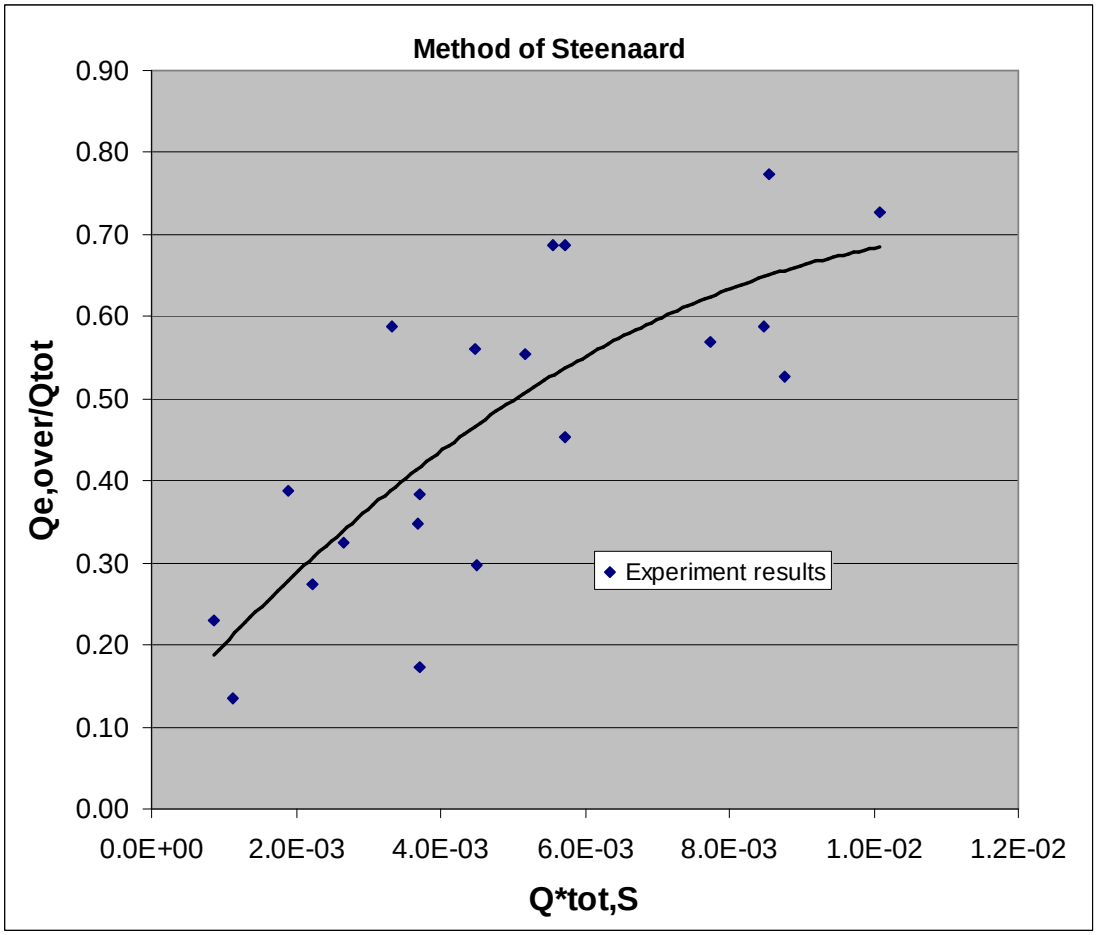

Figure 21 Relation between Q*tot,S and Qe,over/Qtot for the experiment results

Obviously, the spread in this relation is quite large; there is no proper relation between the two parameters. Apparently, the method of Steenaard is not applicable for this thesis. This can be caused by the lack of involved parameters in the relation defined in Equation 4.2-1. Steenaard only used the crest width and the overtopping discharges to formulate the dimensionless parameters; the wave height, wave length (wave steepness) and crest height were not used.
Data points in Figure 21 with a higher ratio value ($Q_{e,over}/Q_{tot}$) than the trendline are experiments with a relatively small wave steepness (large wave length). Consequently the data points with a lower ratio value than the trendline are experiments with a relatively large wave steepness (small wave length).

To introduce these missing parameters into the relation, a new dimensionless factor is established. This factor is defined in Equation 4.2-2.

$$H^* = \frac{H \cdot L}{B \cdot R_c}$$ *Equation 4.2-2*

in which:

H*	= dimensionless factor	(-)
H	= wave height	(m)
L	= wave length	(m)
B	= crest width	(m)
R_c	= crest height	(m)

Instead of the ratio between the measured overtopping discharges Q_{tot} and $Q_{e,over}$ used by Steenaard, in the following relation the ratio between the dimensionless overtopping discharges Q^*_{tot} and $Q^*_{e,over}$ is used. The dimensionless discharges are defined as $Q^*_{tot} = \frac{Q_{tot}}{\sqrt{g \cdot H_s^3}}$ and $Q^*_{e,over} = \frac{Q_{e,over}}{\sqrt{g \cdot H_s^3}}$.

The ratio between the dimensionless discharges and the dimensionless factor H* for the several experiments are presented in Table 7.

Experiment code	Q*e,over/ Q*tot	H*
T/O-15-30-10-R-0	0,222	33,938
T/O-16-30-10-R-0	0,280	40,260
T/O-17-30-10-R-0	0,386	46,160
T/O-18-30-10-R-0	0,346	49,545
T/O-19-30-10-R-0	0,535	54,807
T/O-20-30-10-R-0	0,522	62,452
T/O-21-30-10-R-0	0,584	64,857
T/O-18-20-10-R-0	0,171	34,299
T/O-18-25-10-R-0	0,309	40,641
T/O-18-35-10-R-0	0,586	56,296
T/O-18-40-10-R-0	0,583	63,001
T/O-18-45-10-R-0	0,693	75,037
T/O-18-50-10-R-0	0,755	91,035
T/O-16-25-10-R-0	0,131	32,341
T/O-16-35-10-R-0	0,383	43,202
T/O-20-20-10-R-0	0,298	39,843
T/O-20-25-10-R-0	0,462	49,868
T/O-20-35-10-R-0	0,618	69,052
T/O-20-40-10-R-0	0,724	84,353
T/O-22-30-13-R-0	0,682	59,050

Table 7 Overtopping ratio and dimensionless factor H*

Figure 22 illustrates the relation between these two factors. The trendline is also added to the figure.

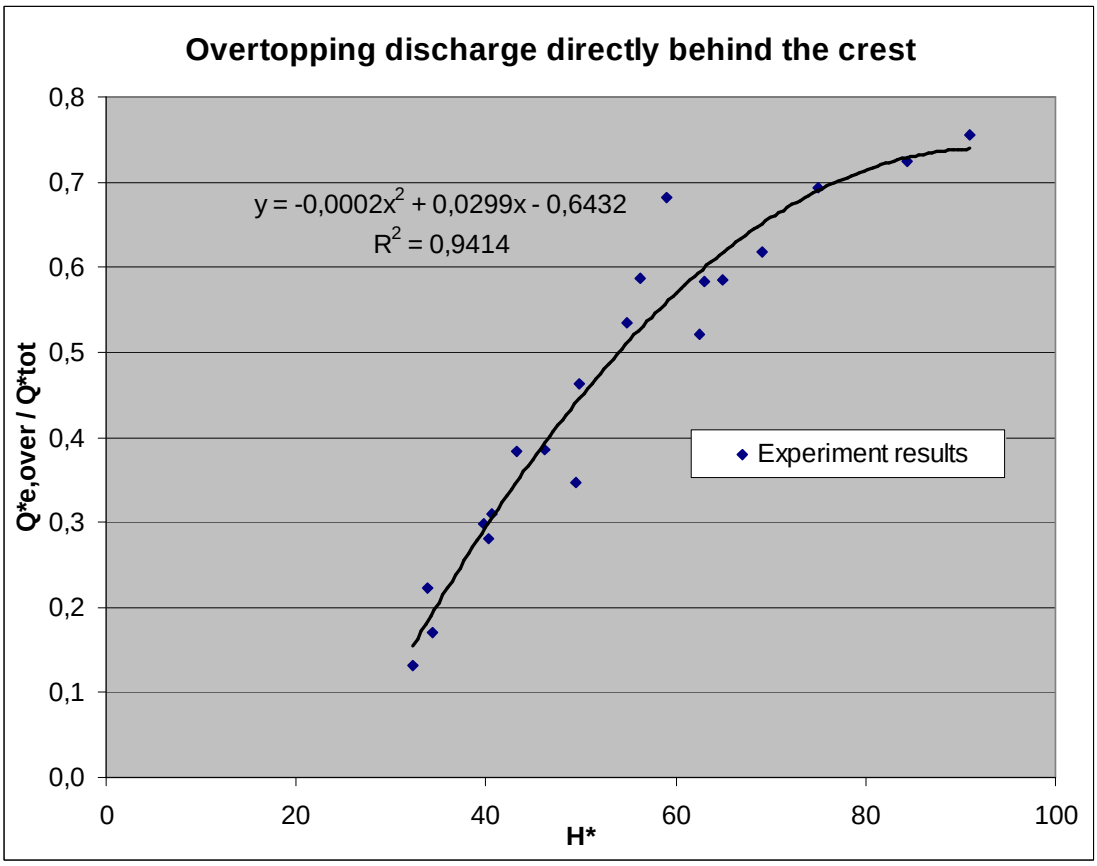

Figure 22 Relation between Q*e,over/Q*tot and H* plus trendline relation

Obviously this relation fits better than the relation defined by Steenaard. Next step is to determine a function for this relation based on the formulation used by Steenaard.

This formulation has to fulfil two important requirements:

- The ratio $Q^*_{e,over}/Q^*_{tot}$ approaches 1 for large values of H*
- The ratio $Q^*_{e,over}/Q^*_{tot}$ is equal to 0 for $H^* < H^*_d$

In which:
H^*_d = threshold value of H* for overtopping discharge directly behind the crest

The equation for the trendline in Figure 22 results in $H^*_d=26$.

This results in Equation 4.2-3:

Equation 4.2-3

$$\frac{Q^*_{e,over}}{Q^*_{tot}} = \begin{cases} \left(\frac{H^* - H^*_d}{H^* - 15}\right)^2 & \text{for } H^* \geq H^*_d \\ 0 & \text{for } H^* \leq H^*_d \end{cases}$$

Figure 23 shows the data points from the experiments (ratio dimensionless discharges as a function of the dimensionless factor H*). Also the relation defined in Equation 4.2-3 is added to the figure.

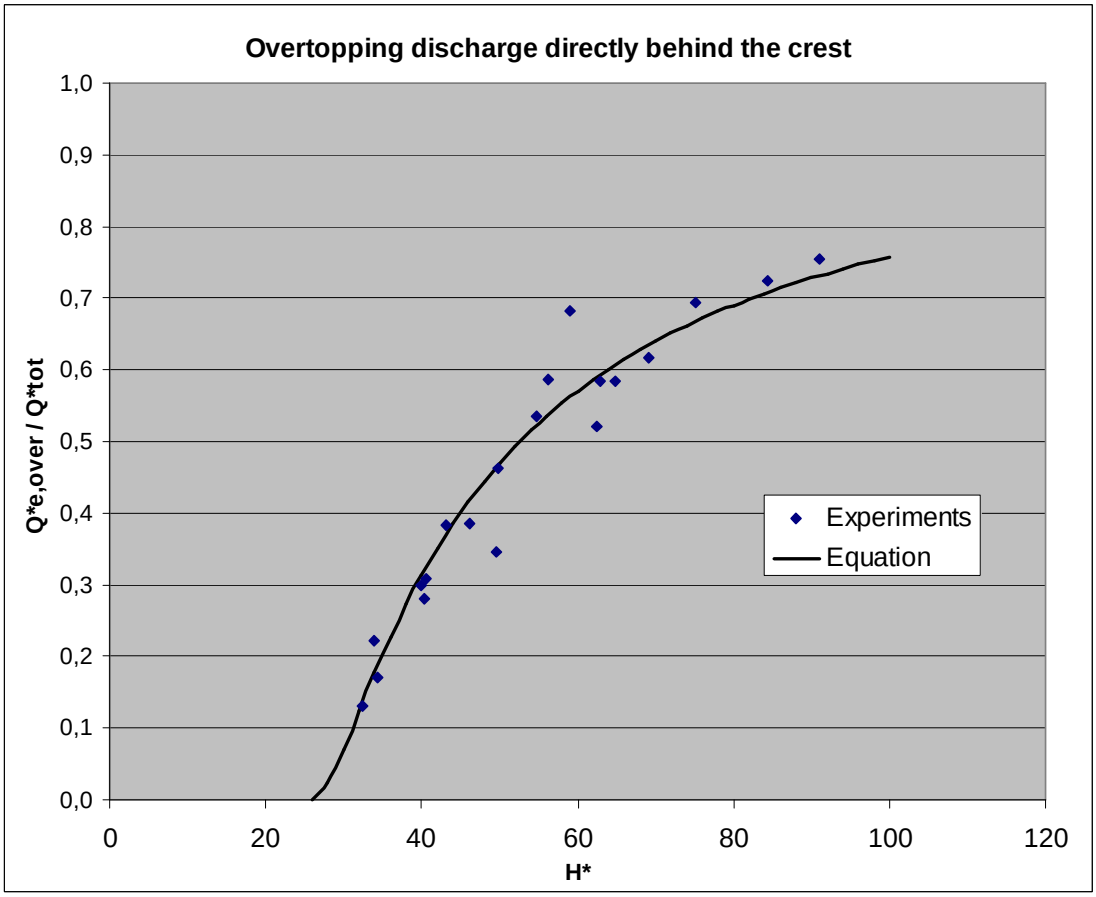

Figure 23 Relation between Q*e,over/Q*tot and H* plus Equation 4.2-3

Obviously, $Q^*_{e,over}/Q^*_{tot}$ approaches 1 only for extreme large values of H*. Actually, $Q^*_{e,over}/Q^*_{tot}$ can never reach 1, because there will always be some infiltrating discharge into the crest. Only for $R_c=0$ or B=0 there is no infiltrating discharge (and $Q^*_{e,over}/Q^*_{tot}=1$). This corresponds with the defined relation, because in that case H* is equal to infinity.

4.2.3. Conclusion

The method of Steenaard is not directly applicable to the experiment results of this thesis. This is caused by the influence of the wave height, wave length and crest height on the division of the overtopping discharge.

The method of Steenaard is transformed into Equation 4.2-4 by using the wave height, wave length and crest height.

Equation 4.2-4

$$\frac{Q^*_{e,over}}{Q^*_{tot}} = \begin{cases} \left(\frac{H^* - H^*_d}{H^* - 15}\right)^2 & \text{for } H^* \geq H^*_d \\ 0 & \text{for } H^* \leq H^*_d \end{cases}$$

with

$$H^* = \frac{H \cdot L}{B \cdot R_c} \quad \text{and} \quad H^*_d = 26$$

4.3. Wave overtopping discharge over impermeable backfill

4.3.1. Experiment results

For the execution of these experiments, the same collecting tank and the same arrangement as in the experiments for overtopping discharge directly behind the crest, described in section 4.2, was used. Only this time the top of the collecting tank could be closed off with a watertight board. This board was placed under a slope of 3% towards the breakwater. This causes separation of the overtopping discharge: one part of the discharge flows over the board into the collecting tank and the other part of the discharge flows back over the board to the breakwater under the influence of gravity. The behaviour of this division in relation to the length of the board leads to the spatial distribution of the overtopping discharge over impermeable backfill.
The same set of experiments was executed for seven different lengths of the board: 0.05m, 0.10m, 0.15m, 0.20m, 0.30m, 0.40m and 0.60m.
The varied hydraulic parameters during the experiments were: wave height, wave steepness, wave spectrum and water depth.

The various experiments and board lengths resulted in specific overtopping discharges. The experiment results are presented in Appendix VII.
The physical process of the wave overtopping discharge over impermeable backfill is illustrated in Figure 24. Figure 24 shows the total wave overtopping discharge (Q_{tot}), the overtopping discharge directly behind the crest (Q_{over}) and the division of the overtopping discharge over the impermeable backfill (the discharge that flows back to the breakwater (arrow) and the discharge that flows over the backfill into the collecting tank).

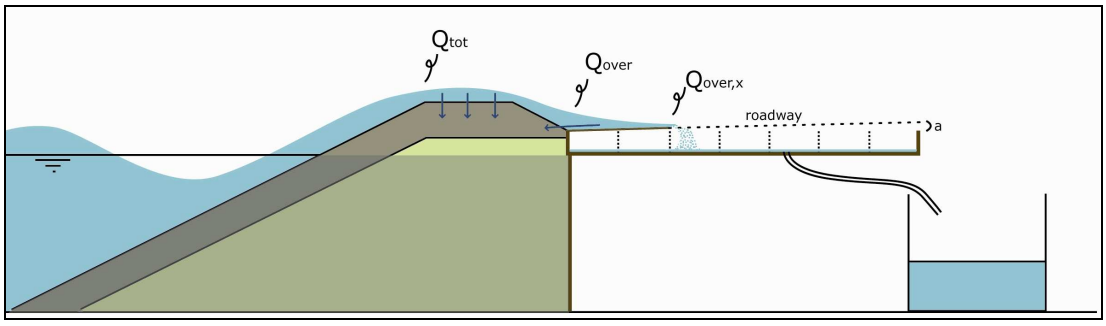

Figure 24 Physical process of wave overtopping discharge over impermeable backfill

4.3.2. Experiment analysis

A quick scan of the experimental results with regular waves shows that the overtopping discharge decreases for an increasing board length: the longer the board, the more discharge flows back to the breakwater, the less discharge flows over the board into the collecting tank. This is no surprise, but the difficulty is to transform these results into a generic method, which can be used to calculate the behaviour of the overtopping discharge as a function of the different parameters.
Therefore a dimensionless presentation of the results is necessary. Several manners can be applied to realize this. Former researches, like the method of Juul Jensen [10] and the method of Wallingford [9] can serve as an example.
As described in section 2.5.2, the method of Wallingford [9] computes a reduction factor for the overtopping discharge for a wide crested breakwater, see Equation 4.3-1.

Equation 4.3-1

$$C_r = 3.06 \cdot \exp\left(-1.5 \cdot {G_c}/{H_{m0}} \right)$$

This method computes the overtopping discharge behind a point x=G_c behind the breakwater, where the method of Juul Jensen (described in section 2.5.1) computes the cumulative overtopping discharge up to distance x behind the breakwater.
In this thesis the overtopping discharge behind a point x behind the breakwater (behind a certain length of the board) is measured. For that reason, the method of Wallingford will be more practical to apply for these measurements. This means that the reduction factor C_r will be presented as a function of the dimensionless distance x/H_s.

In the investigation to the spatial distribution relation, one small difference with the method of Wallingford will be applied: the dimensionless overtopping discharges will be used to calculate the reduction factor (C_r) in stead of the measured overtopping discharges used in the method of Wallingford. This is because the spatial distribution is measured in different experiments. Small differences in the wave height will be among these different experiments. However, these experiments need to be compared with each other to define the spatial relation. By using the dimensionless wave overtopping discharges, the differences in wave height between the experiments are excluded.
The dimensionless overtopping discharges can be calculated with $Q^*_{over,x} = \frac{Q_{over,x}}{\sqrt{g \cdot H^3_{m0}}}$, so the definition of reduction factor is $C_r = \frac{Q^*_{over,x}}{Q^*_{over}}$.

The total volume of extracted water is kept equal for each experiment with various board lengths. This means that the water depth reduction is equal for each execution of an experiment. For that reason, the measured overtopping discharges can be compared without influence of the water depth reductions. Only for x=0 (no board, so overtopping discharge directly behind the crest) the water depth reduction is different, but this is compensated by means of the method described in section 4.2.1.

The experiment results lead to the values for C_r and x/H_s as given in Appendix VIII-2 and Appendix VIII-3. Figure 25 shows the relation between these two dimensionless parameters.

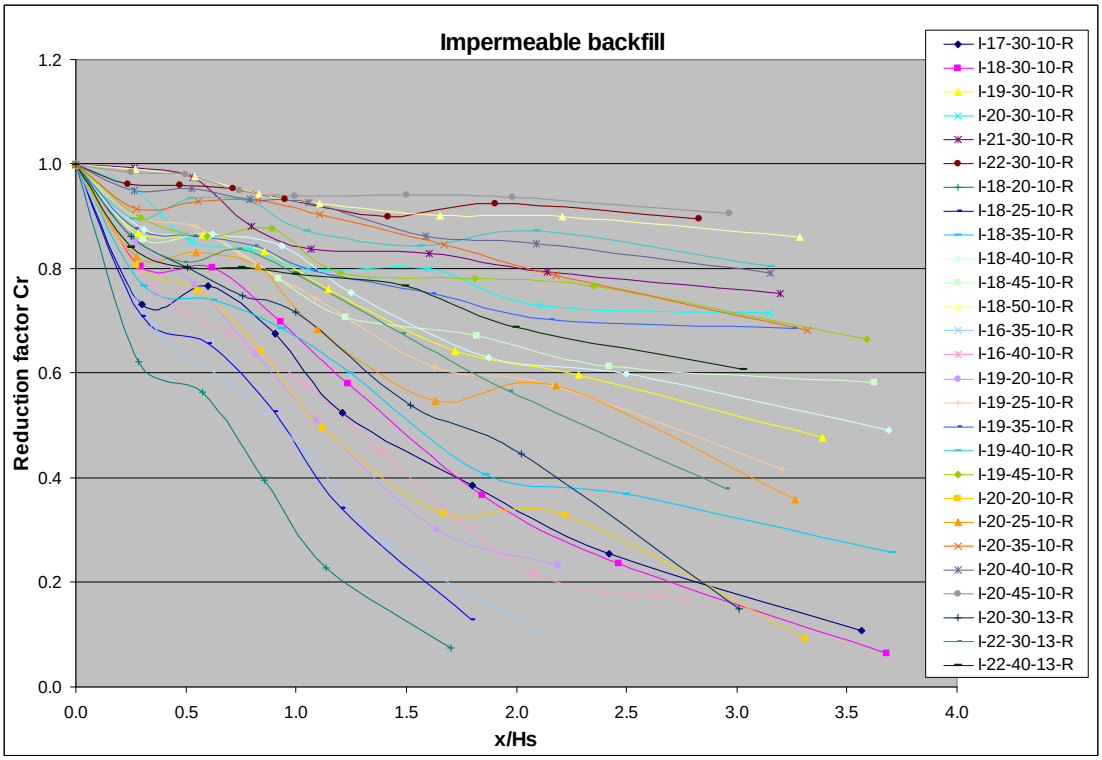

Figure 25 Relation between reduction factor Rc and dimensionless impermeable length x/Hs

Obviously there is completely no unique relation between R_c and x/H_s. There are considerable differences between the spatial distributions of the overtopping discharges for the various experiments.

Figure 26 shows the relation for experiments with the same wave height (H_s=0.161m) and different wave steepnesses.

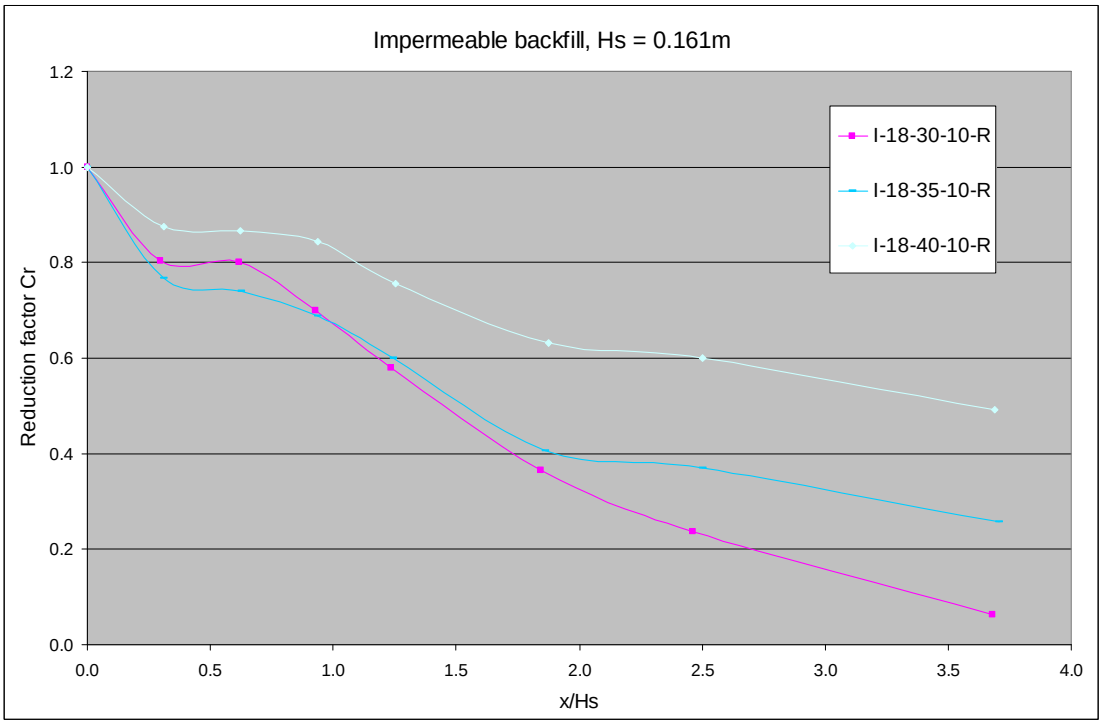

Figure 26 Relation between Cr and x/Hs for experiments with Hs=0.161m

These results suggest that the reduction of the overtopping discharge is inversely proportional to the wave steepness. A lower wave steepness (longer wave) leads to a higher reduction factor (higher overtopping discharge) at each point behind the breakwater.

Figure 27 shows the relation for experiments with the same wave steepness (s=1/33) and different wave heights.

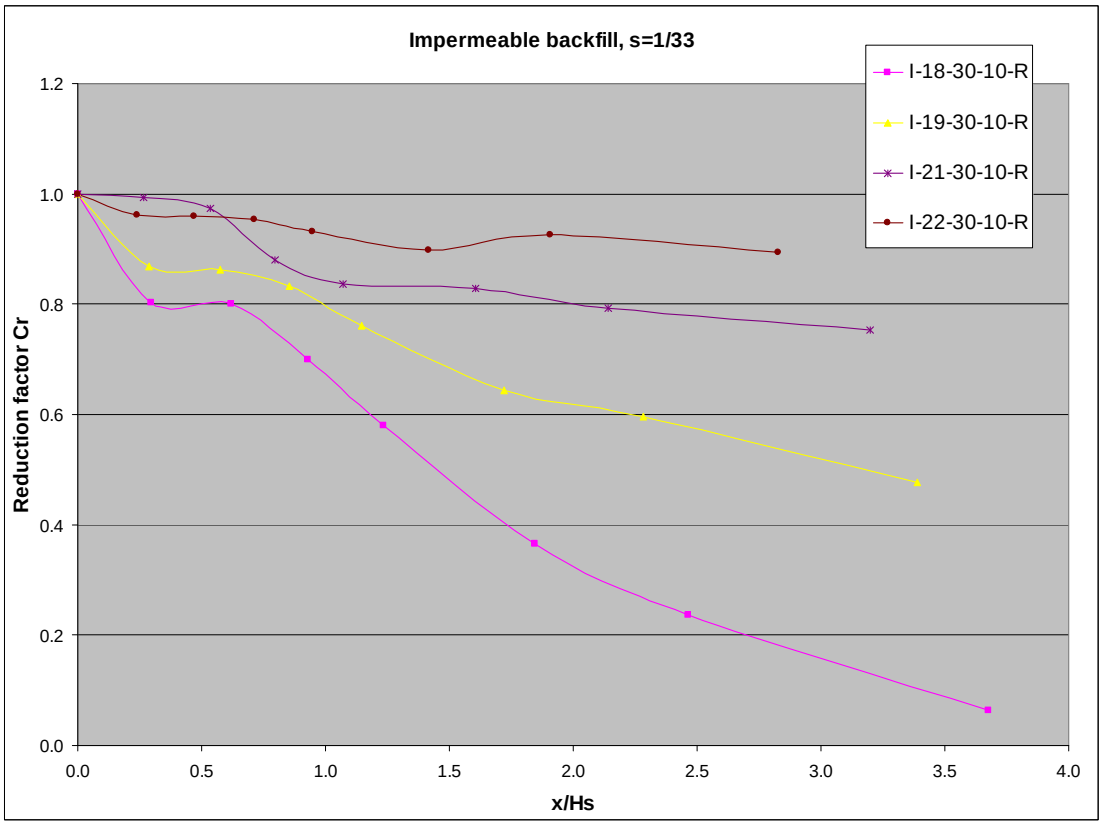

Figure 27 Relation between Cr and x/Hs for experiments with s=1/33

These results suggest that the reduction of the overtopping discharge is proportional to the wave height. A larger wave height leads to a higher reduction factor (higher overtopping discharge) at each point behind the breakwater.

These statements about the relations between the wave height, the wave steepness and the reduction factor leads to the introduction of a new parameter: the wave energy flux.

Holthuijsen [7] defines the time-averaged, wave induced energy (potential energy plus kinetic energy) per horizontal unit area is equal to Equation 4.3-2.

$$E = \frac{1}{2}\rho g a^2 = \frac{1}{8}\rho g H_s^2$$ *Equation 4.3-2*

In which:
ρ = specific density of the water (=1000) (kg/m^3)

The net time-averaged transport of energy in the wave direction (wave energy flux in W/m) is given as Equation 4.3-3.

$$P = E \cdot c_g$$ *Equation 4.3-3*

In deep water (as we assume in the experiments of this thesis) the group velocity can be defined as $c_g = \frac{L}{T} = \frac{g \cdot T}{2\pi}$.
So the wave energy flux can be defined as Equation 4.3-4.

$$P = \frac{1}{16 \cdot \pi} \rho g^2 H_s^2 \cdot T \qquad \textit{Equation 4.3-4}$$

This results in the values for the wave energy flux presented in Table 8.

Experiment code	Wave energy flux P (W/m)							
	x=0m	x=0,05m	x=0,10m	x=0,15m	x=0,20m	x=0,30m	x=0,40m	x=0,60m
I-17-30-10-R	93.0	94.5	95.5	94.9	93.8	95.3	94.0	97.6
I-18-30-10-R	94.0	101.6	93.8	93.9	94.6	95.0	94.9	95.3
I-19-30-10-R	111.4	111.9	111.6	113.5	111.9	111.5	112.8	115.3
I-20-30-10-R	131.8	131.1	135.7	134.4	134.1	130.5	135.0	136.3
I-21-30-10-R	133.8	136.4	134.6	135.5	134.1	133.9	133.8	134.9
I-22-30-10-R	170.7	179.7	179.4	175.2	176.4	177.9	175.6	181.6
I-18-20-10-R	85.2	88.9	88.5	89.3	90.1	90.2		
I-18-25-10-R	88.6	91.2	92.0	91.4	88.4	89.7		
I-18-35-10-R	97.8	100.7	98.9	99.3	99.7	100.4	99.0	101.4
I-18-40-10-R	103.1	106.2	106.1	105.1	104.7	104.7	104.8	108.3
I-18-45-10-R	116.2	118.6	120.8	115.6	115.5	117.8	120.0	119.1
I-18-50-10-R	148.8	156.6	156.5	151.3	151.4	152.2	151.7	154.4
I-18-55-10-R	120.5	120.9	121.6	120.5	120.4	120.2	120.2	124.1
I-16-35-10-R	71.5	72.9	72.1	72.5	72.9	73.4		
I-16-40-10-R	80.0	80.2	79.7	79.9	80.3	80.6	80.2	
I-19-20-10-R	97.5	100.5	100.5	100.0	99.3	99.4	99.0	
I-19-25-10-R	109.4	114.1	114.2	113.3	113.5	113.7	112.3	117.9
I-19-35-10-R	129.2	133.2	135.2	133.4	134.1	134.5	136.5	133.0
I-19-40-10-R	148.0	153.8	156.3	153.8	155.2	155.5	155.6	153.5
I-19-45-10-R	130.8	127.7	126.8	127.9	123.5	121.3	130.2	124.4
I-20-20-10-R	96.8	100.8	100.3	98.2	97.8	100.3	100.0	101.3
I-20-25-10-R	110.3	114.1	114.0	113.1	113.5	115.6	116.0	116.2
I-20-35-10-R	129.2	135.0	133.0	135.3	131.4	129.6	137.5	131.7
I-20-40-10-R	156.9	153.2	153.9	152.6	152.6	151.9	160.3	158.5
I-20-45-10-R	177.8	181.8	181.2	187.5	184.6	180.2	182.8	186.5
I-22-30-13-R	160.9	160.9	160.7	164.5	160.8	161.0	162.3	162.3
I-22-40-13-R	183.9	178.5	178.1	178.0	183.1	1832.3	182.8	176.6

Table 8 Wave energy flux P (W/m) for the impermeable overtopping experiment set

Certain experiments have approximately the same value for the wave energy flux. Figure 28 illustrates that the relation between the reduction factor C_r and x/H is also approximately the same for these experiments.

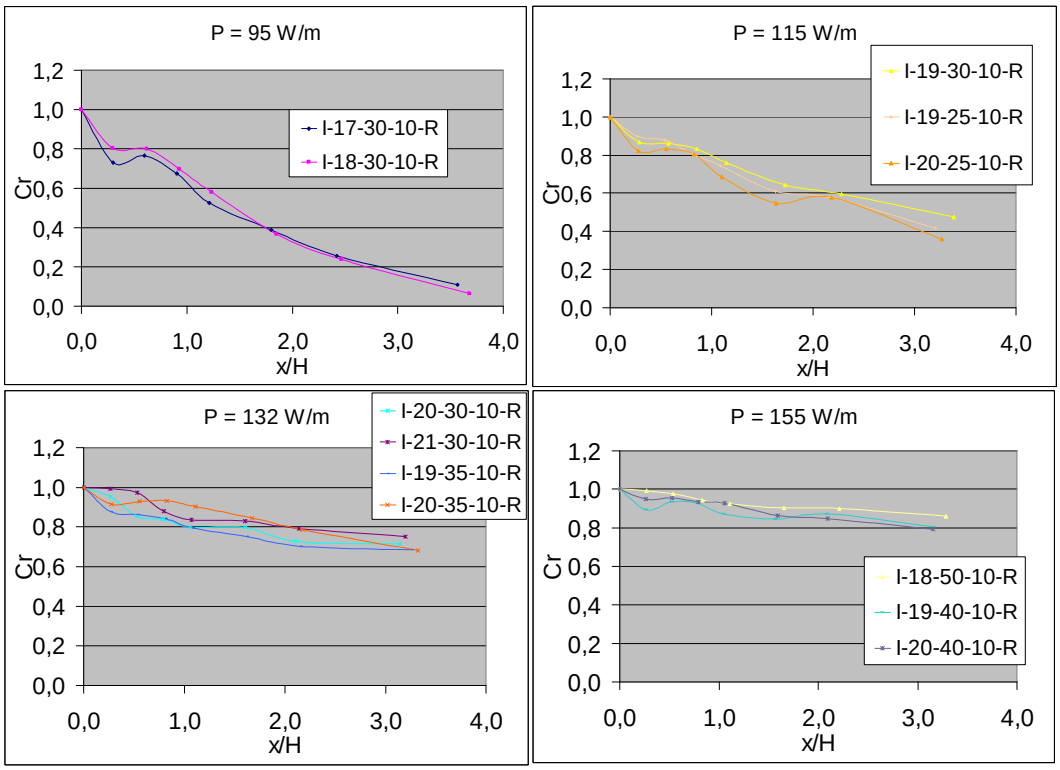

Figure 28 Relation between Cr and x/H for experiments with similar wave energy flux

Apparently, the decrease of the reduction factor as a function of x/H_s is higher for a lower value of the wave energy flux. In other words: the higher the wave energy flux of the incoming waves, the larger the overtopping discharge at a certain distance behind the crest.
This influence of the wave energy flux can be involved in the relation between C_r and x/H_s in order to create an appropriate relation for every combination of circumstances (various parameters).

To realize this, the dimensionless factor x/H_s has to be divided by a dimensionless presentation of the wave energy flux. For this purpose a new dimensionless parameter is introduced: H*T*.
This parameter is based on H0T0 (defined in Equation 4.3-5), which is usually used as the dynamic stability number in the hydraulic engineering.

$$H0T0 = \frac{H_s}{D_{n50}} \cdot T_s \sqrt{\frac{g}{D_{n50}}}$$

Equation 4.3-5

For this thesis the H0T0 is transformed into H*T* and represents the wave energy flux for a certain given crest height R_c, see Equation 4.3-6.

$$H*T* = \frac{H_s}{R_c} \cdot T_s \sqrt{\frac{g}{R_c}}$$

Equation 4.3-6

This results in a new dimensionless factor x* for the impermeable distance behind the crest. This factor is defined in Equation 4.3-7.

$$x^* = \frac{x}{H_s} \cdot \frac{1}{(H^*T^*)^n}$$ *Equation 4.3-7*

The value of the power 'n' depends on the specific circumstances of the experiment: the inside slope, the outside slope, the armour size, the slope of the impermeable backfill, wind etc. These parameters are not investigated in this research, so their influence can not be determined. Therefore the value of the power 'n' is only determined for the specific situation in this thesis.
The exact value of 'n' has to be determined by 'trial and error'. The most suitable value of 'n' will result in an appropriate relation between the reduction factor C_r and the dimensionless factor x*. For this value of 'n' the variation of the data points has to be minimized.

For n=6, the relation between C_r and x* is demonstrated in Figure 29. The values of x* for n=6 are given in Appendix VIII-4.

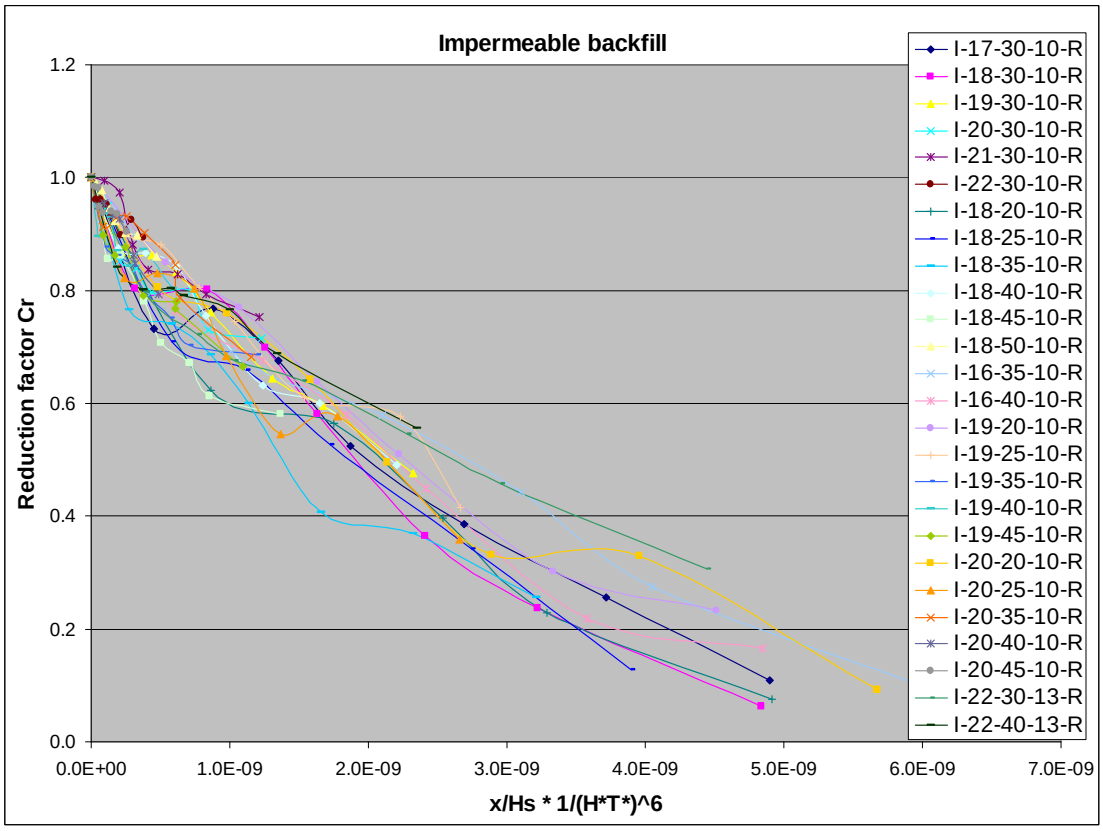

Figure 29 Relation between Cr and x* for n=6

Apparently, by introducing the dimensionless parameter $(H^*T^*)^6$, the influences of the various wave heights and various wave steepnesses are included appropriately and an appropriate relation between C_r and x* appears.

This change in relation is also demonstrated in Figure 30 and Figure 31, in which the same experiments as Figure 26 and Figure 27 are presented, this time including the dimensionless parameter $(H^*T^*)^6$. It is obvious that the relation does not depend on the wave height or wave steepness anymore.

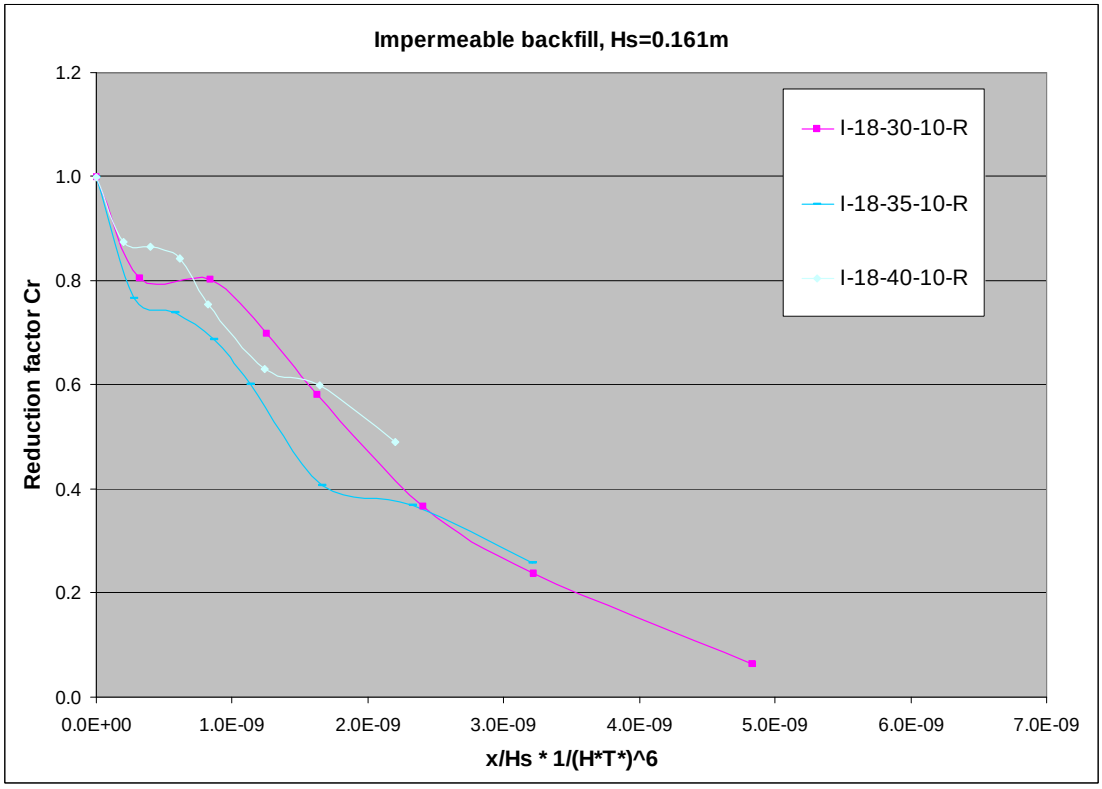

Figure 30 Relation between Cr and x* for experiments with Hs=0.161m

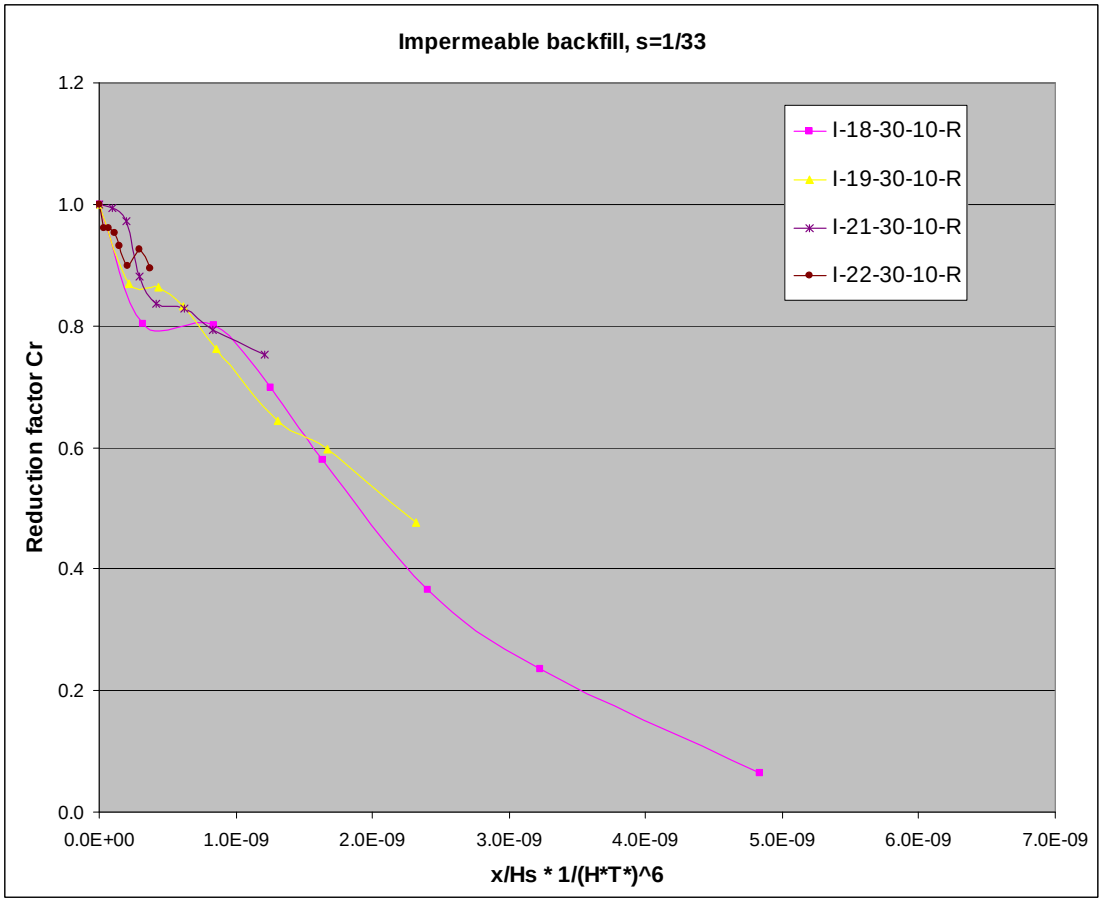

Figure 31 Relation between Cr and x* for experiments with s=1/33

Next step is to formulate an applicable equation for the relation between C_r and x*. With this equation it must be possible to make an analytical prediction for the overtopping discharge at a certain distance behind the crest with impermeable backfill behind the crest.

For this purpose all the data points of the various experiments are presented in Figure 32. Also the trendline for the data points is added to the figure.

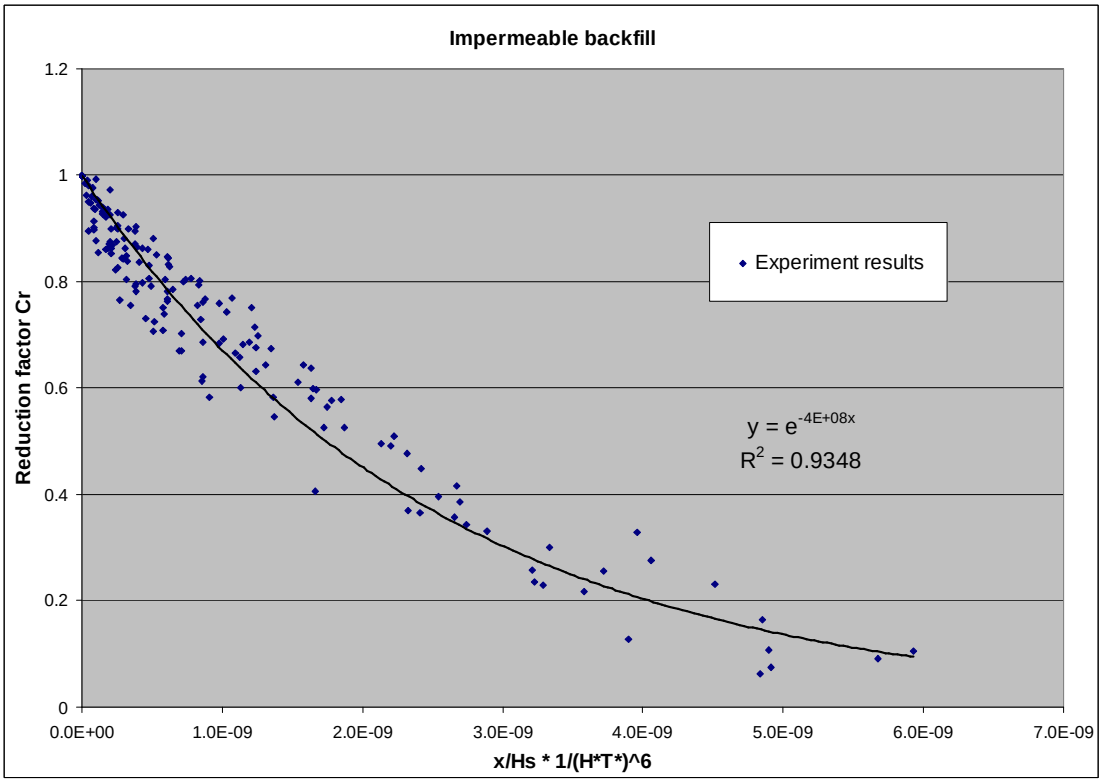

Figure 32 Relation between C_r and x* for n=6 for all data points

Evidently the equation for this trendline is given as $y = e^{-4 \cdot 10^8 \cdot x}$. This means that the relation between C_r and x* can be described as Equation 4.3-8.

Equation 4.3-8

$$\frac{Q^*_{over,x}}{Q^*_{over,0}} = e^{-4 \cdot 10^8 \cdot \left(\frac{x}{H_s} \cdot \frac{1}{\left(H*T*\right)^6} \right)}$$

Or

$$C_r = e^{-4 \cdot 10^8 \cdot x*}$$

with

$$C_r = \frac{Q^*_{over,x}}{Q^*_{over,0}}$$

$$x* = \frac{x}{H_s} \cdot \frac{1}{\left(H*T*\right)^6}$$

$$H*T* = \frac{H_s}{R_c} \cdot T_s \cdot \sqrt{\frac{g}{R_c}}$$

4.3.3. Reliability of experiments

The trendline in Figure 32 has a correlation coefficient R^2=0.9348, which is an indication for a good correlation between the experiment results and their predicted values (with the defined relation of Equation 4.3-8). The R-squared value is the square of the correlation coefficient between these parameters.

A method to determine the reliability of the relation is by means of the standard deviation. Therefore the variation of the measured overtopping discharges must be assumed as a normal distribution. The standard deviation may be thought of as the average difference of the experiment data points from the corresponding defined relation data points. A low standard deviation indicates that the experiment data points tend to be very close to the defined relation data points, whereas a high standard deviation indicates that the experiment data points are spread out over a large range of values.

The standard deviation of the experiment data points can be calculated with Equation 4.3-9.

$$\sigma = \sqrt{\frac{1}{N}\sum_{i=1}^{N}\left(C_{r,m} - C_{r,c}\right)^2} \qquad \textit{Equation 4.3-9}$$

In this situation the standard deviation σ of the measured correction factor is equal to 0.0545.

The empirical rule means that 95.45% of the values are within two standard deviations of the mean. In this case, it means that 95.45% of the experiment data points are within a range of 2σ=0.109 around the defined relation data points. Because the reduction factor is the ratio between the overtopping discharge at a certain point behind the crest ($Q_{over,x}$) and the overtopping discharge directly behind the crest ($Q_{over,0}$), the range of 0.109 means a range of 10.9% of the overtopping discharge directly behind the crest.

In other words: 95.45% of the measured reduction factors are within a range of 10.9% of the overtopping discharge directly behind the crest around the calculated reduction factors with the defined relation of Equation 4.3-8.

Figure 33 illustrates the variation of the measured data points with the corresponding calculated data points of the defined relation. The red lines are the range of 2σ around the line x=y (measured reduction factors = calculated reduction factors). Obviously, almost all the measured reduction factors are within this range of 2σ.

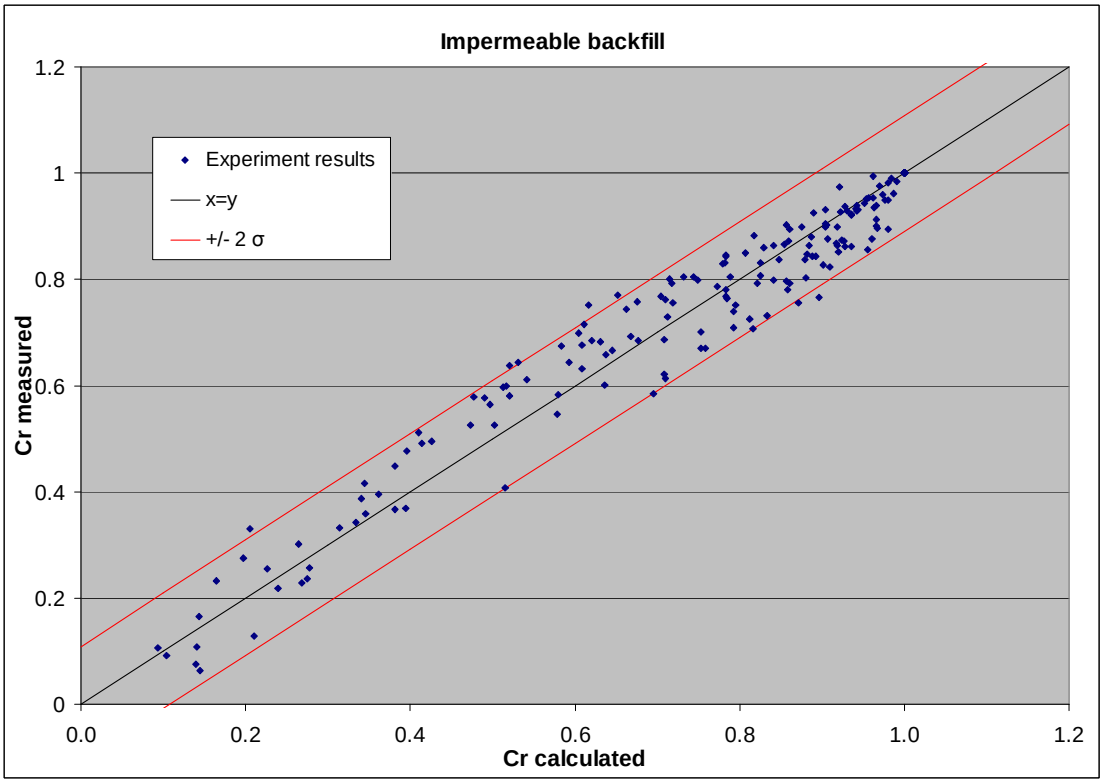

Figure 33 Calculated and measured reduction factor, including range of 2 σ

4.3.4. Probabilistic and deterministic design

The relation described in Equation 4.3-8 and illustrated in Figure 32 is based on the experiment results. This relation is the mean prediction (the trendline for the experiment results) and should be used for probabilistic design, prediction of measurements or comparison with measurements.

For deterministic calculations in design or safety assessment, the mean prediction of the reduction factor has to be increased. According to section 4.3.3, the deterministic design will be reliable for 95.45% if the reduction factor is increased with twice the standard deviation (2σ=0.109). This leads to Equation 4.3-10 for the relation for deterministic design or safety assessment.

Equation 4.3-10

$$\frac{Q^*_{over,x}}{Q^*_{over,0}} = 0.109 + e^{-4\cdot10^8 \cdot \left(\frac{x}{H_s} \cdot \frac{1}{(H^*T^*)^6} \right)}$$

However, the relation in Equation 4.3-10 is not asymptotic to 0, but is asymptotic to 0.109. Consequently, for reduction factors lower than 0.109, this relation will not give a solution for the safe distance behind the crest. Another relation that is asymptotic to 0 must be defined for the deterministic design.

Therefore, the reduction factors of the experiment results are increased with twice the standard deviation. The trendline for these increased reduction factors is illustrated in Figure 34 as the deterministic design relation.

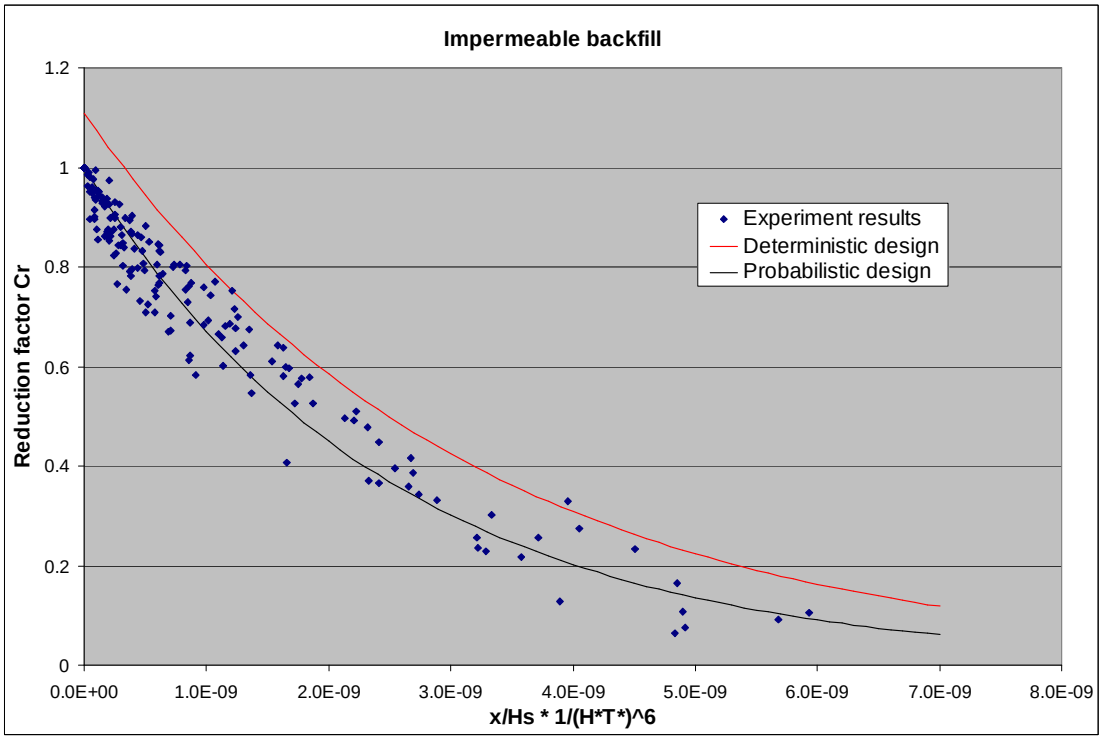

Figure 34 Probabilistic design relation and deterministic design relation for impermeable backfill

The corresponding deterministic design relation is given in Equation 4.3-11.

Equation 4.3-11

$$\frac{Q^*_{over,x}}{Q^*_{over,0}} = 1.109e^{-3.2\cdot10^8\cdot\left(\frac{x}{H_s}\cdot\frac{1}{(H^*T^*)^6}\right)}$$

This relation meets the required asymptotic characteristic and is asymptotic to 0 for large values of the dimensionless distance parameter.

For small values of the dimensionless distance parameter (values approaching 0), the reduction factor in Equation 4.3-11 is larger than 1. Naturally, this is physically impossible, because the overtopping discharge at a certain distance behind the crest can never be larger than the overtopping discharge directly behind the crest. Therefore, the deterministic design relation had to be cut off for the reduction factor equal to 1.
Figure 35 shows again the deterministic design relation of Figure 34, this time with the cut-off for C_r=1.

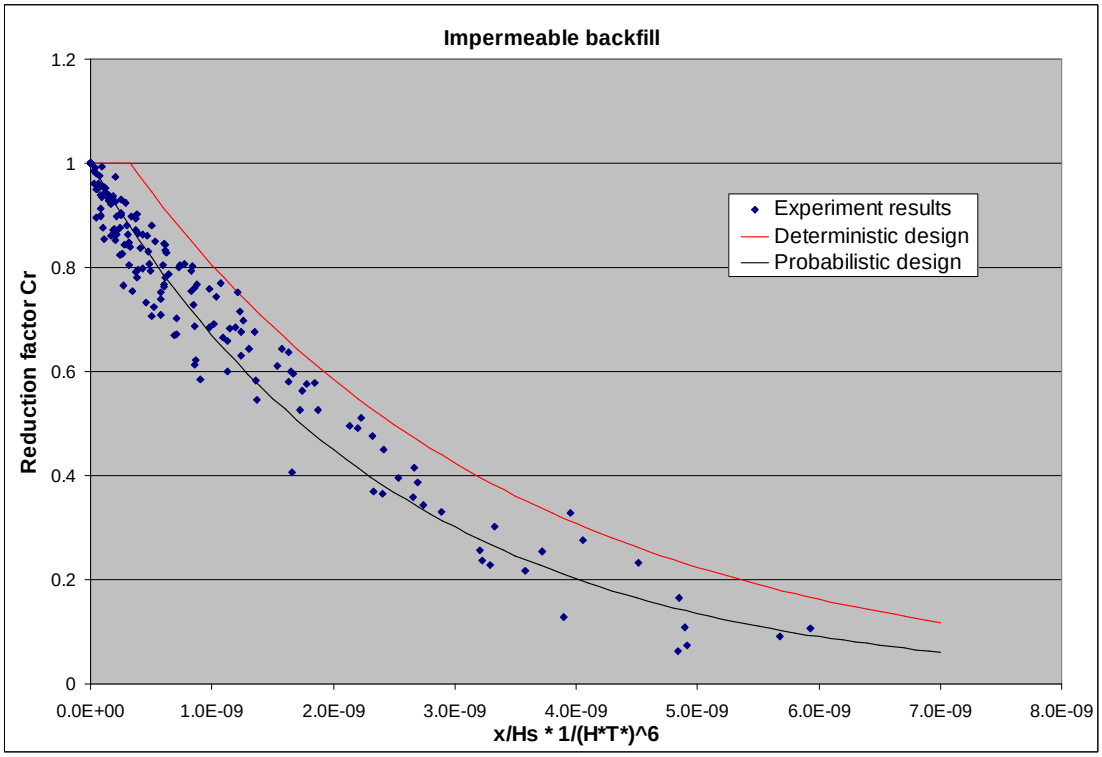

Figure 35 Probabilistic design relation and deterministic design relation with cut-off for impermeable backfill

The corresponding deterministic design relation is given in Equation 4.3-12.

Equation 4.3-12

$$\frac{Q^*_{over,x}}{Q^*_{over,0}} = 1.109e^{-3.2\cdot10^8\cdot\left(\frac{x}{H_s}\cdot\frac{1}{(H^*T^*)^6}\right)}$$

with $\frac{Q^*_{over,x}}{Q^*_{over,0}} \le 1$

4.3.5. Conclusion

Figure 36 illustrates the reduction factor C_r and the dimensionless distance x^* for the experiment results. Furthermore, the relation for probabilistic design and the relation for deterministic design or safety assessment are illustrated in Figure 36.

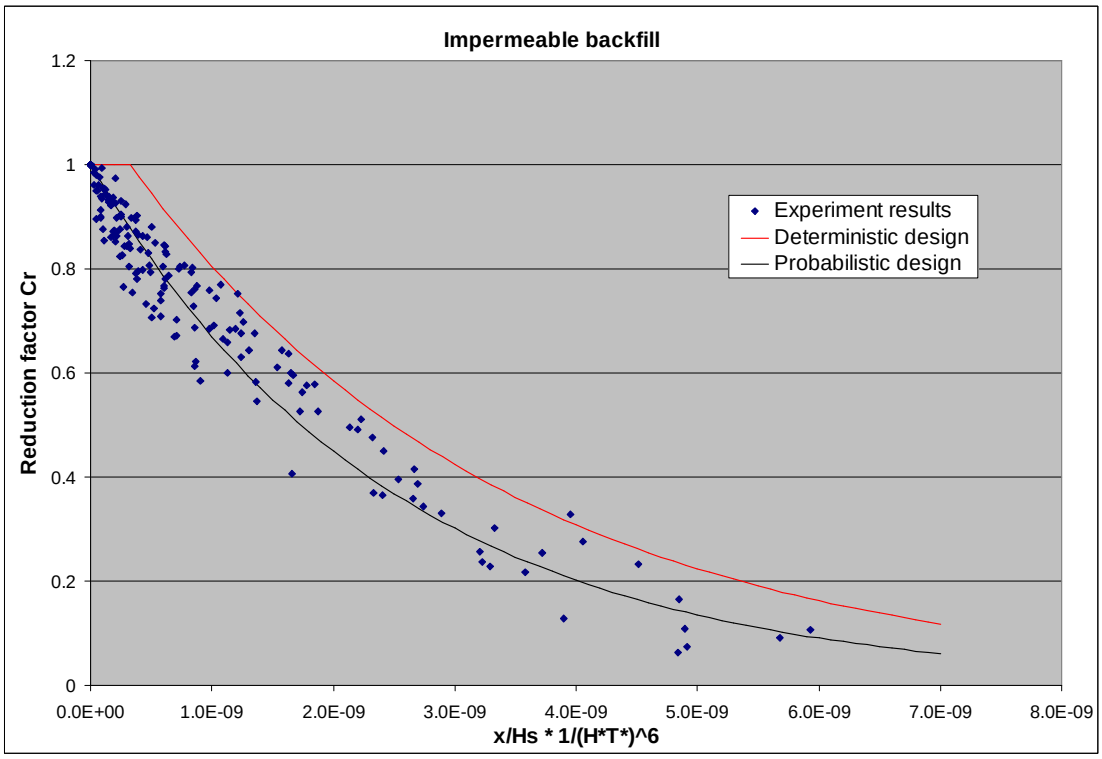

Figure 36 Relation between C_r and x* for n=6 and the deterministic relation

The corresponding relation for probabilistic design is defined in Equation 4.3-13. Consequently, the overtopping discharge at a certain location x behind the crest can be approached with Equation 4.3-13.

Equation 4.3-13

$$\frac{Q^*_{over,x}}{Q^*_{over,0}} = e^{-4.0 \cdot 10^8 \cdot \left(\frac{x}{H_s} \cdot \frac{1}{(H^*T^*)^6} \right)}$$

The corresponding relation for deterministic design or safety assessment is defined in Equation 4.3-14.
Consequently, the overtopping discharge at a certain point x behind the crest will not exceed a value calculated with Equation 4.3-14.

Equation 4.3-14

$$\frac{Q^*_{over,x}}{Q^*_{over,0}} = 1.109 e^{-3.2 \cdot 10^8 \cdot \left(\frac{x}{H_s} \cdot \frac{1}{(H^*T^*)^6} \right)}$$

with $\frac{Q^*_{over,x}}{Q^*_{over,0}} \leq 1$

4.4. Wave overtopping discharge over permeable backfill

4.4.1. Experiment results

For the execution of these experiments, a new collecting tank was constructed. The technical drawing of the collecting tank is given in Appendix XIII-1. This tank could be divided in two parts by means of a replaceable watertight board. The side of the breakwater was filled with rock, which resulted in the permeable backfill. The other side of the tank (behind the board) was empty. The rock filled part consists two layers of armour rock at the top and core material below. The front side of the tank was provided with wire netting. A picture of this wire netting is given in Appendix XIV-4. Because there was a small gap between the breakwater and the tank, water could flow inside and outside the tank through the wire netting. In this way, the water level inside the rock filled part of the tank was equal to the water level in the rest of the wave flume. The replaceable watertight board prevents leakage of water from the rock filled part to the empty part of the tank. A side view picture of the scale model in Appendix XIV-5 shows the small gap between the breakwater and the wire netting. A picture of the watertight board, the rock filled part and the empty part is given in Appendix XIV-6.

The two different parts of the tank lead to separation of the overtopping discharge directly behind the crest: one part of the discharge flows over the rock and the board into the empty part of the collecting tank and the other part of the discharge infiltrates into the rock and flows out of the collecting tank through the wire netting. The behaviour of this division in relation to the length of rock filled part results in the spatial distribution of the overtopping discharge.
The same set of experiments was executed for seven different lengths of the rock filled part: 0.10m, 0.125m, 0.15m, 0.175m, 0.20m, 0.25m and 0.30m. Unfortunately it was physical impossible to place the watertight board in the first 10cm of the tank. Therefore the behaviour of the overtopping discharge is unknown in this part.
The varied hydraulic parameters during the experiments were: wave height, wave steepness and wave spectrum. Due to problems with the water reservoir in the laboratory, it was almost impossible to vary the water depth during the experiments.

The various experiments and rock filled lengths resulted in specific overtopping discharges. The experiment results are presented in Appendix IX.
Pictures of experiments for measuring the wave overtopping discharge over permeable backfill are given in Appendix XIV-10 and Appendix XIV-11.

The physical process of the wave overtopping discharge over permeable backfill is illustrated in Figure 37. Figure 37 shows the total wave overtopping discharge (Q_{tot}), the overtopping discharge directly behind the crest (Q_{over}) and the division of the overtopping discharge over the permeable backfill (the discharge that infiltrates into the backfill and the discharge that flows over the backfill into the collecting tank). Figure 37 shows also that the infiltrated water in the backfill can flow through the wire netting back to the wave flume (arrows).

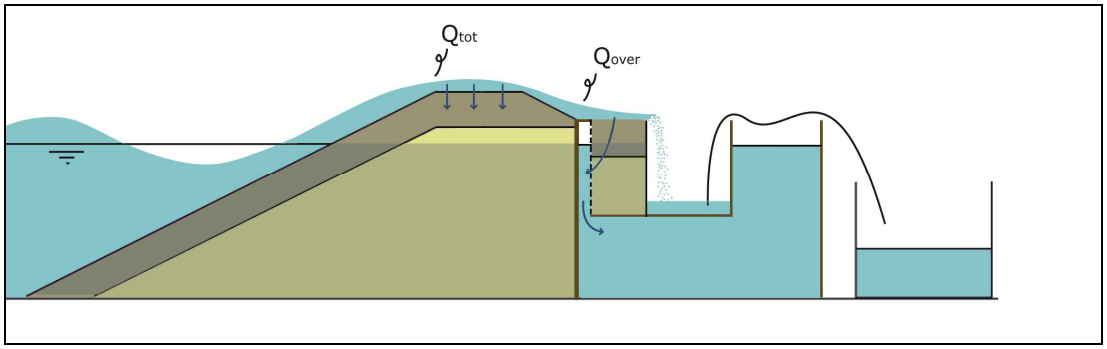

Figure 37 Physical process of wave overtopping discharge over permeable backfill

4.4.2. Experiment analysis

These experiments with permeable backfill behind the crest and regular waves require the same dimensionless presentation as the experiments with impermeable backfill behind the crest, described in section 4.3.2. This means that the reduction factor C_r can be described as the ratio between the dimensionless overtopping discharge at a certain point x behind the crest ($Q^*_{over,x}$) and the dimensionless overtopping discharge direct behind the crest ($Q^*_{over,0}$). This reduction factor is a function of the dimensionless permeable distance x*, see Equation 4.4-1.

$$C_r = \frac{Q^*_{over,x}}{Q^*_{over,0}} \text{ is a function of } x^* = \frac{x}{H_s} \cdot \frac{1}{\left(H^* T^*\right)^n} \qquad \textit{Equation 4.4-1}$$

For n=0 Equation 4.4-1 is reduced to a relation between C_r and x/H_s, like the method of Wallingford described in section 2.5.2. The values of C_r and x/H_s for these experiments are given in Appendix X-2 and Appendix X-3. Figure 38 shows the relation between these two dimensionless parameters.

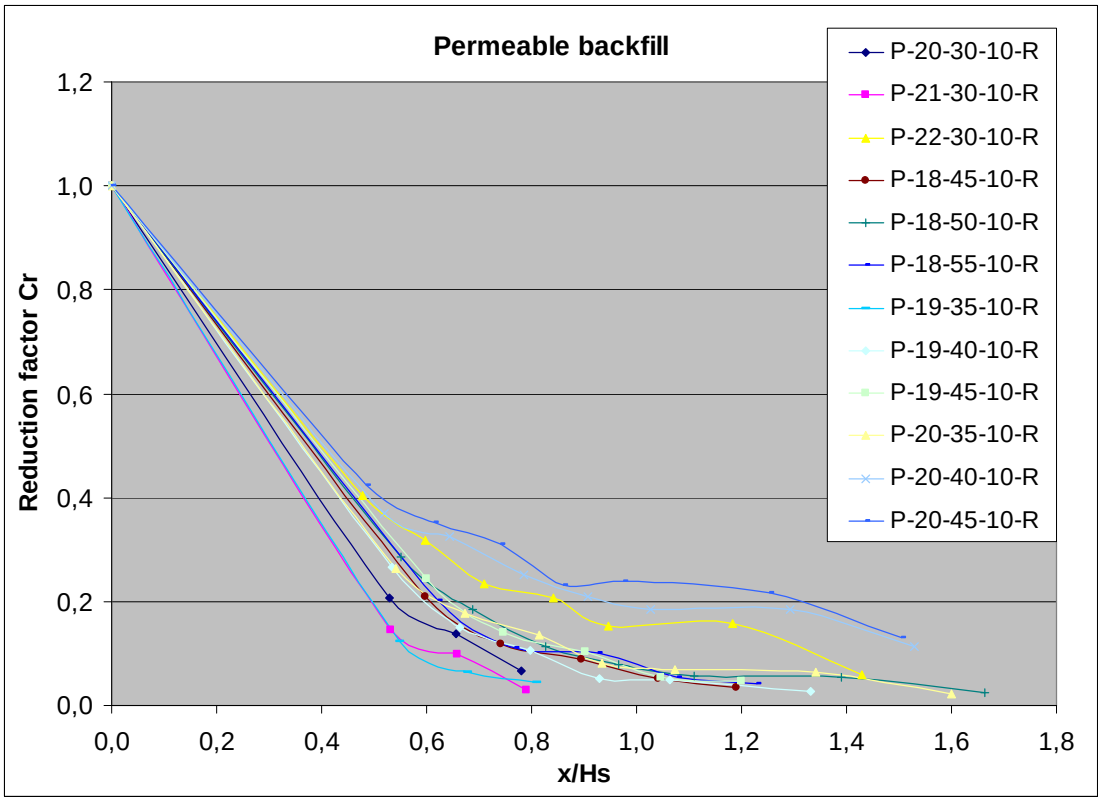

Figure 38 Relation between reduction factor Cr and dimensionless permeable length x/Hs

Obviously, the differences are smaller than for the experiments with impermeable backfill (Figure 25), but again there is no unique relation between R_c and x/H_s. There are considerable differences between the spatial distributions of the overtopping discharges for the various experiments.

Similar as in section 4.3.2, the wave energy flux for all experiment results is calculated. The values of the wave energy flux are given in Table 9.

Experiment code	Wave energy flux (W/m)							
	x=0m	x=0,10m	x=0,125m	x=0,15m	x=0,175m	x=0,20m	x=0,25m	x=0,30m
P - 20 - 30 - 10 - R	131,81	134,96	137,18	139,34				
P - 21 - 30 - 10 - R	133,80	136,56	139,75	139,28				
P - 22 - 30 - 10 - R	170,70	171,61	173,16	175,97	170,12	177,06	176,73	175,69
P - 18 - 45 - 10 - R	116,24	123,67	122,31	122,41	121,87	127,00		
P - 18 - 50 - 10 - R	148,80	150,14	150,82	150,37	150,40	147,72	148,12	149,05
P - 18 - 55 - 10 - R	120,55	125,49	128,67	127,62	128,24	128,90		
P - 19 - 35 - 10 - R	129,21	132,69	135,60	136,34				
P - 19 - 40 - 10 - R	147,97	147,98	149,08	148,68	148,40	148,63	147,89	
P - 19 - 45 - 10 - R	130,79	125,53	124,07	122,53	124,32	123,52		
P - 20 - 35 - 10 - R	129,16	139,45	140,54	138,61	142,89	141,75	141,80	143,17
P - 20 - 40 - 10 - R	156,86	159,59	163,57	156,99	160,19	162,67	161,18	165,84
P - 20 - 45 - 10 - R	177,83	195,50	191,31	190,14	190,12	193,03	184,57	181,62

Table 9 Wave energy flux (W/m) for the permeable overtopping experiment set

Certain experiments have approximately the same value for the wave energy flux. Figure 39 shows that the relation between the reduction factor C_r and x/H_s is also approximately the same for these experiments.

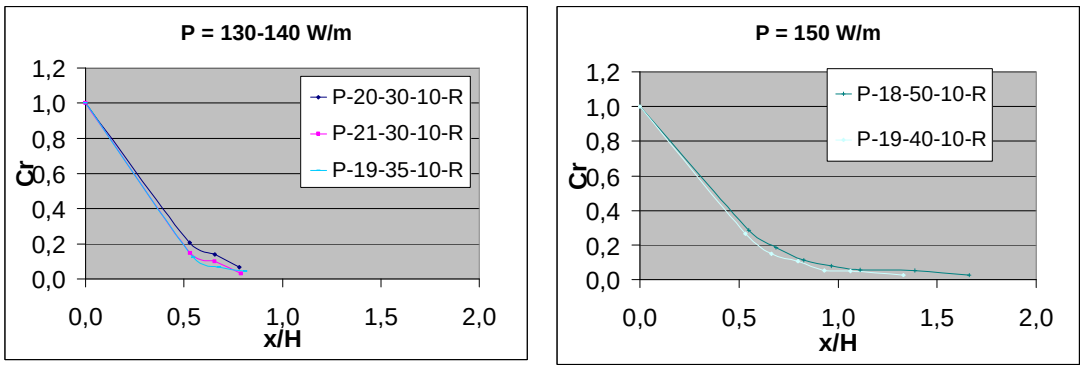

Figure 39 Relation between Cr and x/H for experiments with a similar wave energy flux

This figure shows, similar to the experiments with impermeable backfill behind the crest, that the decrease of the reduction factor as a function of x/H_s is higher for a lower value of the energy wave flux.
In the same way as in section 4.3.2, the dimensionless parameter H*T* is involved in the relation between C_r and x/H_s in order to create an appropriate relation for every combination of circumstances.

The dimensionless permeable length x* can be described as Equation 4.4-2.

$$\frac{x}{H_s} \cdot \frac{1}{(H*T*)^n} \qquad \textit{Equation 4.4-2}$$

The value of the power 'n' depends on the specific circumstances of the experiment: the inside slope, the outside slope, the armour size, the slope of the impermeable backfill, wind etc. These parameters are not investigated in this research, so their influence can not be determined. Therefore the value of the power 'n' is only determined for the specific situation in this thesis.
The exact value of 'n' has to be determined by 'trial and error'. The most suitable value of 'n' will result in an appropriate relation between the reduction factor C_r and the dimensionless factor x*. For this value of 'n' the variation of the data points has to be minimized.

For n=3, the relation between C_r and x/H_s is shown in Figure 40. The values of x* for n=3 are given in Appendix X-4.

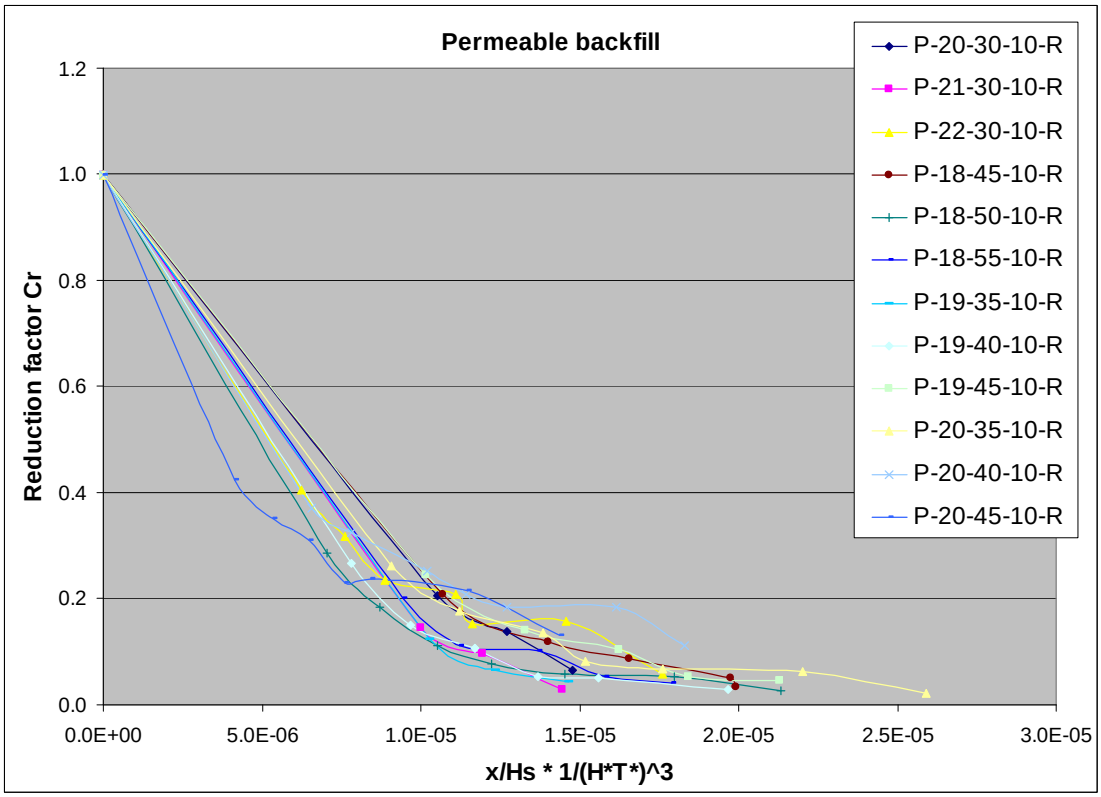

Figure 40 Relation between Cr and x* for n=3

By introducing the dimensionless factor $1/(H^*T^*)^3$, the influences of wave height and wave steepness are included appropriately and an appropriate relation between C_r and x* appears.

Apparently, the influence of the dimensionless energy factor H*T* is less for permeable backfill than for impermeable backfill (where n=6). This can be clarified by the infiltration into the backfill behind the crest. For impermeable backfill, there is no infiltration and the wave energy that causes the flow over the backfill is of major influence. For permeable backfill, there is infiltration and the wave energy that causes flow over the backfill is of minor influence in comparison with the infiltration.

Next step is to formulate an applicable equation for the relation between C_r and x*. With this equation it must be possible to make an analytical prediction for the overtopping discharge at a certain distance behind the crest with permeable backfill behind the crest.

For this purpose all the data points of the various experiments are presented in Figure 41. Also the trendline for the data points is added to the figure.

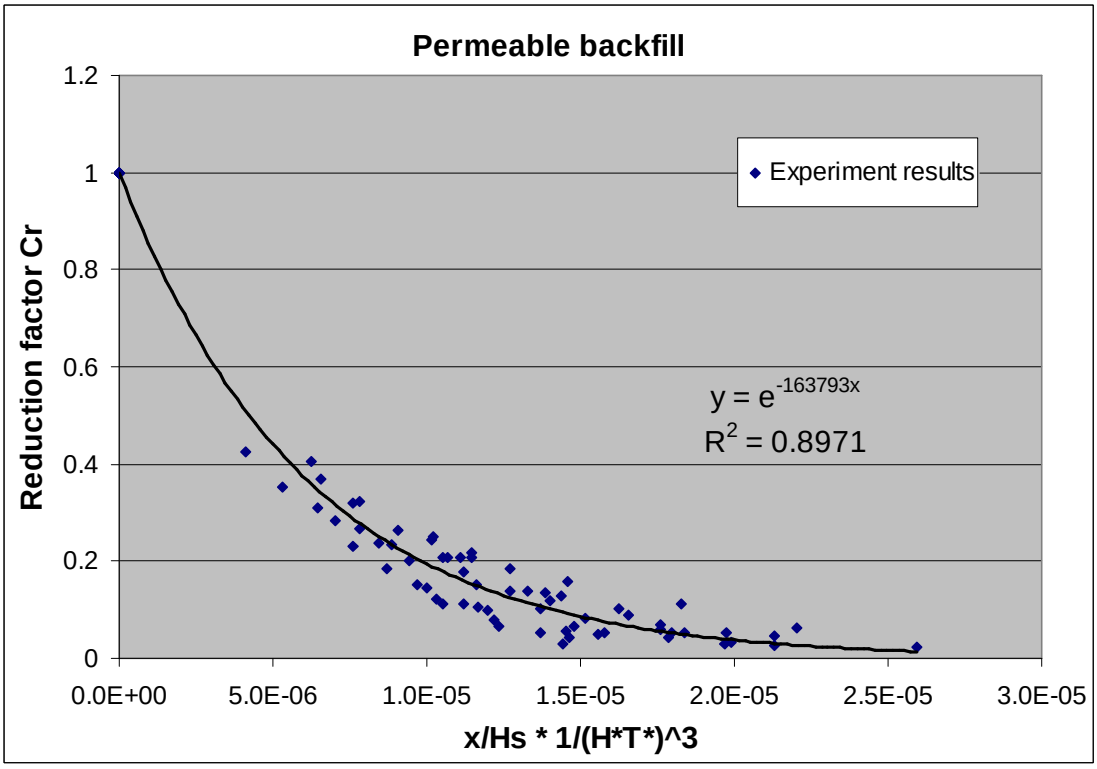

Figure 41 Relation between Cr and x* for n=3 for all data points

Evidently the equation for this trendline is given as $y = e^{-1.64 \cdot 10^5 \cdot x}$. This means that the relation between C_r and x* can be described as Equation 4.4-3.

Equation 4.4-3

$$\frac{Q^*_{over,x}}{Q^*_{over,0}} = e^{-1.64 \cdot 10^5 \cdot \left(\frac{x}{H_s} \cdot \frac{1}{\left(H^*T^*\right)^3} \right)}$$

Or

$$C_r = e^{-1.64 \cdot 10^5 \cdot x^*}$$

with

$$C_r = \frac{Q^*_{over,x}}{Q^*_{over,0}}$$

$$x^* = \frac{x}{H_s} \cdot \frac{1}{\left(H^*T^*\right)^3}$$

$$H^*T^* = \frac{H_s}{R_c} \cdot T_s \cdot \sqrt{\frac{g}{R_c}}$$

4.4.3. Reliability of experiments

The trendline in Figure 41 has a correlation coefficient R^2=0.8971, which shows more scatter than for the impermeable experiments, but still indicates a good correlation between the dimension parameters.

The standard deviation σ for this situation is equal to 0.0372. Same as in section 4.3.3, this means that 95.45% of the experiment data points are within a range of 2σ=0.0744 around the defined relation data points. So 95.45% of the measured reduction factors are within a range of 7.44% of the overtopping discharge directly behind the crest around the calculated reduction factors with the defined relation.

Figure 42 shows the variation of the measured data points with the corresponding calculated data points of the defined relation. The red lines are the range of 2σ around the line x=y (measured reduction factors = calculated reduction factors). Obviously, almost all the measured reduction factors are within this range of 2σ.

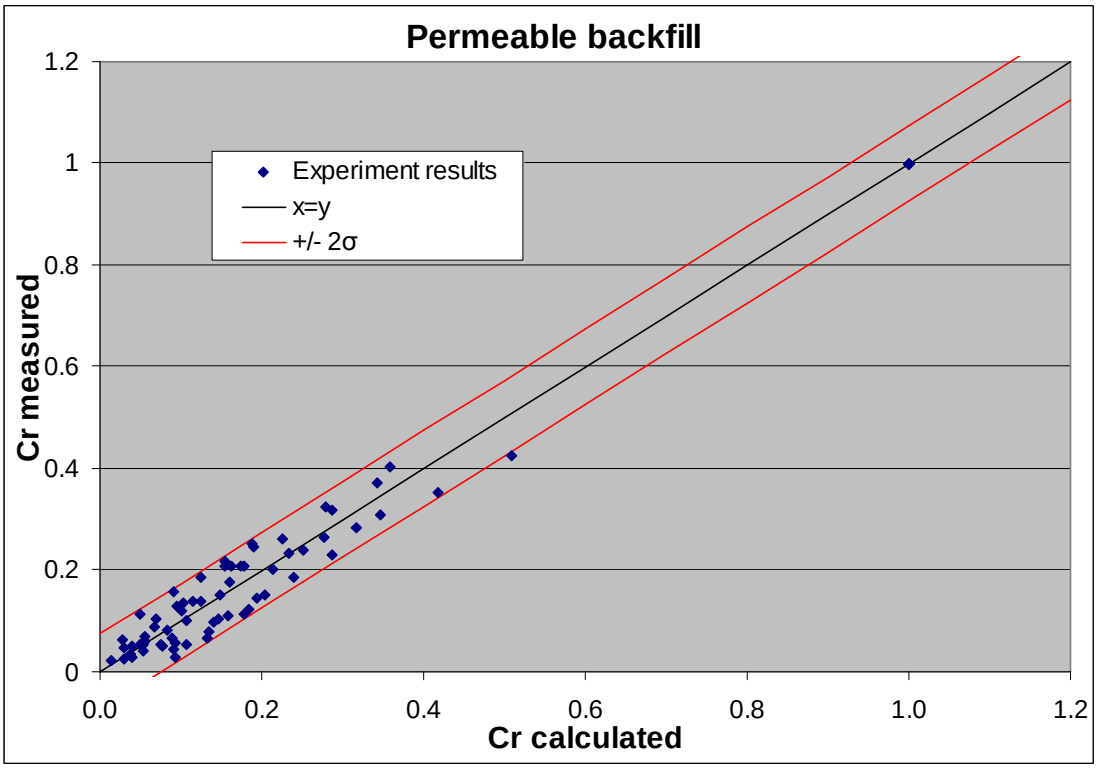

Figure 42 Calculated and measured reduction factor, including range of 2 σ

4.4.4. Probabilistic and deterministic design

The relation described in Equation 4.4-3 and illustrated in Figure 41 is based on the experiment results. This relation is the mean prediction (the trendline for the experiment results) and should be used for probabilistic design, prediction of measurements or comparison with measurements.

The relation for deterministic design or safety assessment is defined in the same way as described in section 4.3.4. According to section 4.4.3, the deterministic design will be reliable for 95.45% if the reduction factor is increased with twice the standard deviation (2σ=0.0744).
Same as in section 4.3.4, this relation must be asymptotic to 0 for large values of x^* and the reduction factor C_r can not be larger than 1 for small values of x^*. Therefore, the reduction factors of the experiment results are increased with twice the standard deviation. The trendline for these increased reduction factors leads to the relation for deterministic design. This relation will be cut off for C_r=1.

This results in the relation for deterministic design illustrated in Figure 43.

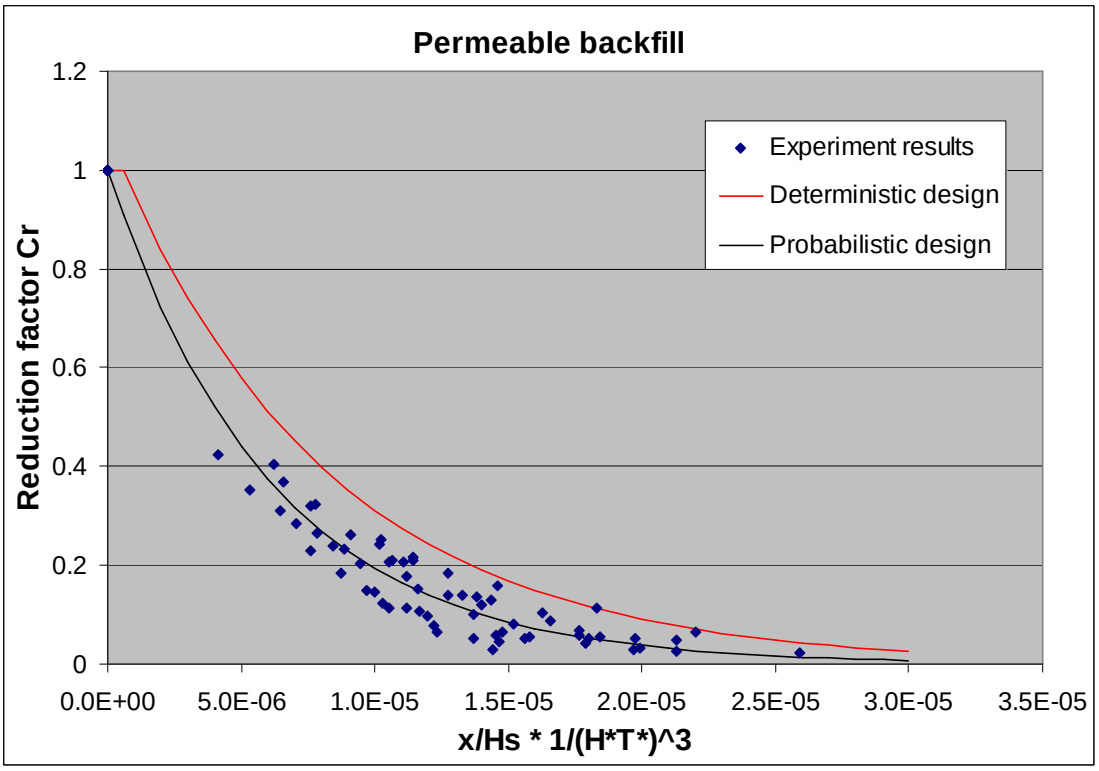

Figure 43 Probabilistic design relation and deterministic design relation with cut-off for permeable backfill

The corresponding deterministic design relation is given in Equation 4.3-12.

Equation 4.4-4

$$\frac{Q^*_{over,x}}{Q^*_{over,0}} = 1.0744e^{-1.24\cdot10^5\cdot\left(\frac{x}{H_s}\cdot\frac{1}{(H^*T^*)^3}\right)}$$

with $\frac{Q^*_{over,x}}{Q^*_{over,0}} \leq 1$

4.4.5. Conclusion

Figure 44 illustrates the reduction factor C_r and the dimensionless distance x^* for the experiment results. Furthermore, the relation for probabilistic design and the relation for deterministic design or safety assessment are illustrated in Figure 36.

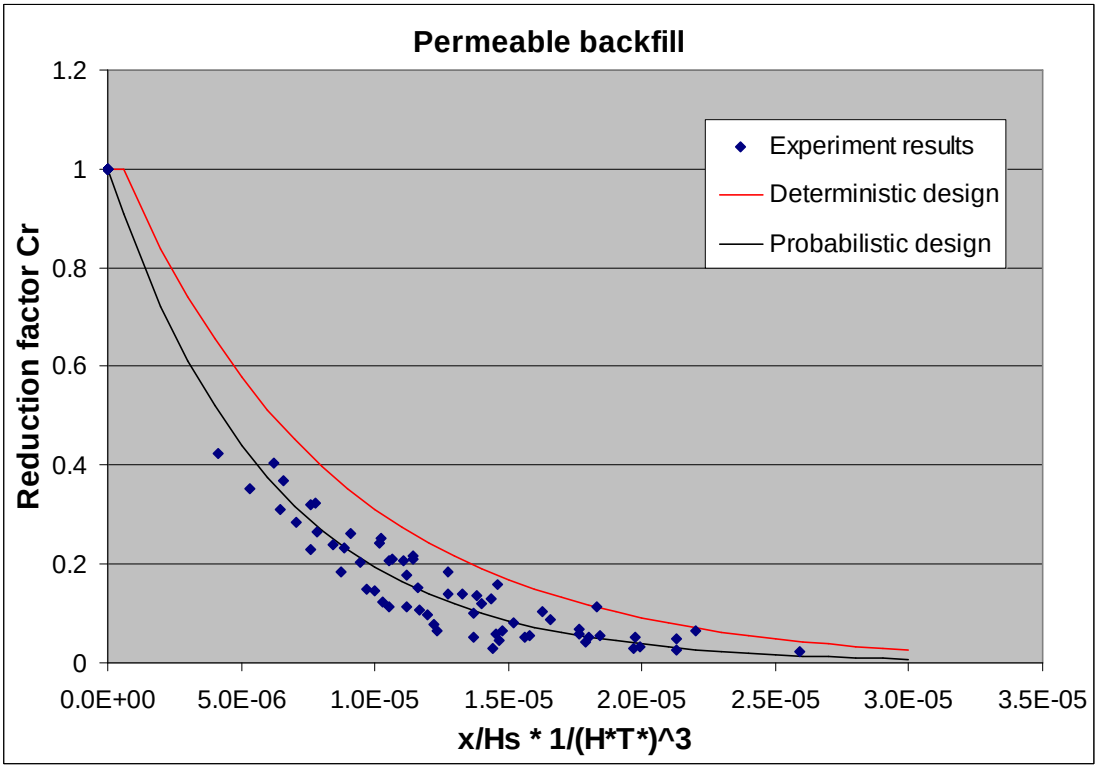

Figure 44 Relation between C_r and x* for n=3 and the deterministic relation

The corresponding relation for probabilistic design is defined in Equation 4.4-5. Consequently, the overtopping discharge at a certain location x behind the crest can be approached with Equation 4.4-5.

Equation 4.4-5

$$\frac{Q^*_{over,x}}{Q^*_{over,0}} = e^{-1.64 \cdot 10^5 \cdot \left(\frac{x}{H_s} \cdot \frac{1}{(H^*T^*)^3} \right)}$$

The corresponding relation for deterministic design or safety assessment is defined in Equation 4.4-5.
Consequently, the overtopping discharge at a certain point x behind the crest will not exceed a value calculated with Equation 4.4-5.

Equation 4.4-6

$$\frac{Q^*_{over,x}}{Q^*_{over,0}} = 1.0744 e^{-1.24 \cdot 10^5 \cdot \left(\frac{x}{H_s} \cdot \frac{1}{(H^*T^*)^3} \right)}$$

with $\frac{Q^*_{over,x}}{Q^*_{over,0}} \leq 1$

4.5. Irregular waves

The relations for the spatial distribution of wave overtopping behind the crest, defined in section 4.3 and section 4.4, are based on the results of experiments with regular waves. Due to the lack of time the wave flume was available, minor experiments with irregular wave spectra could be executed. The results of these experiments are not sufficient to define an appropriate relation for the spatial distribution of irregular waves.
However, the results of the experiments with irregular waves can be compared with the results of experiments with regular waves. The similarities and differences between those two can lead to a better insight into the spatial distribution of irregular wave overtopping.
The results of the experiments with irregular wave spectra for impermeable backfill behind the crest are presented in Appendix XI-1 and Appendix XI-2.
The results of experiments with regular waves for permeable backfill behind the crest can not be used, because the overtopping discharges directly behind the crest (x=0) are not investigated for the same experiment set. Therefore the reduction factor can not be determined.

4.5.1. Overtopping over impermeable backfill

The reduction of the wave overtopping discharge in relation to the distance behind the crest can be presented in the same way as for the regular waves in section 4.3. This means that the reduction factor, given as $C_r = \frac{Q^*_{over,x}}{Q^*_{over,0}}$ is presented as a function of the dimensionless distance behind the crest, defined as x/H_s ($=x/H_{m0}$). Figure 45 shows this relation for irregular waves in comparison with this relation for regular waves. The values for the reduction factor and the dimensionless distance are given in Appendix XI-3.

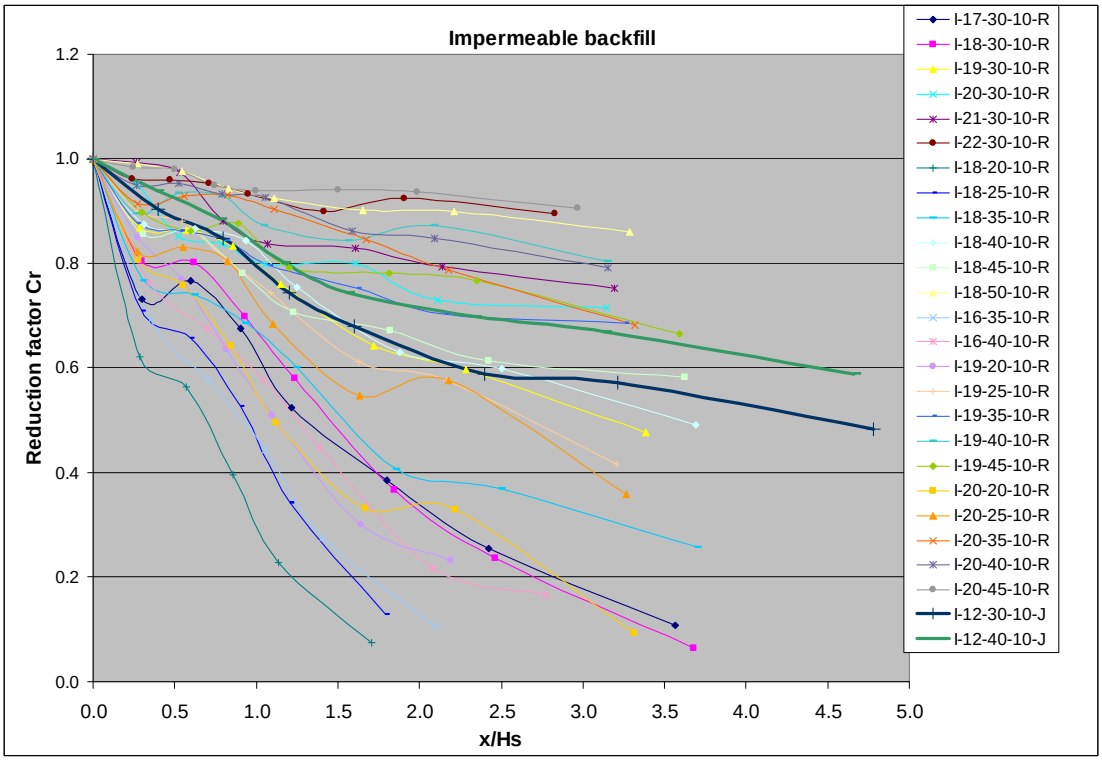

Figure 45 Relation between reduction factor Rc and dimensionless impermeable length x/H_{m0} for irregular waves in comparison with regular waves.

Obviously, the reduction of the overtopping discharge with irregular wave spectra is in the same order as for the experiments with regular waves. Nevertheless, this similarity changes when the dimensionless distance behind the crest is defined as $x^* = \frac{x}{H_{m0}} \cdot \frac{1}{(H^*T^*)^6}$ with $H^*T^* = \frac{H_{m0}}{R_c} \cdot T_{m-1,0} \cdot \sqrt{\frac{g}{R_c}}$.

This dimensionless distance is introduced to include the influence of the wave height and wave steepness in the reduction of overtopping discharge. This dimensionless factor x* causes a proper relation between the reduction factor C_r and x* for the experiments with regular waves.

Figure 46 shows the relation for irregular wave spectra between C_r and x* in comparison with this relation for regular waves. The values for C_r and x* for the irregular wave experiments are given in Appendix XI-3.

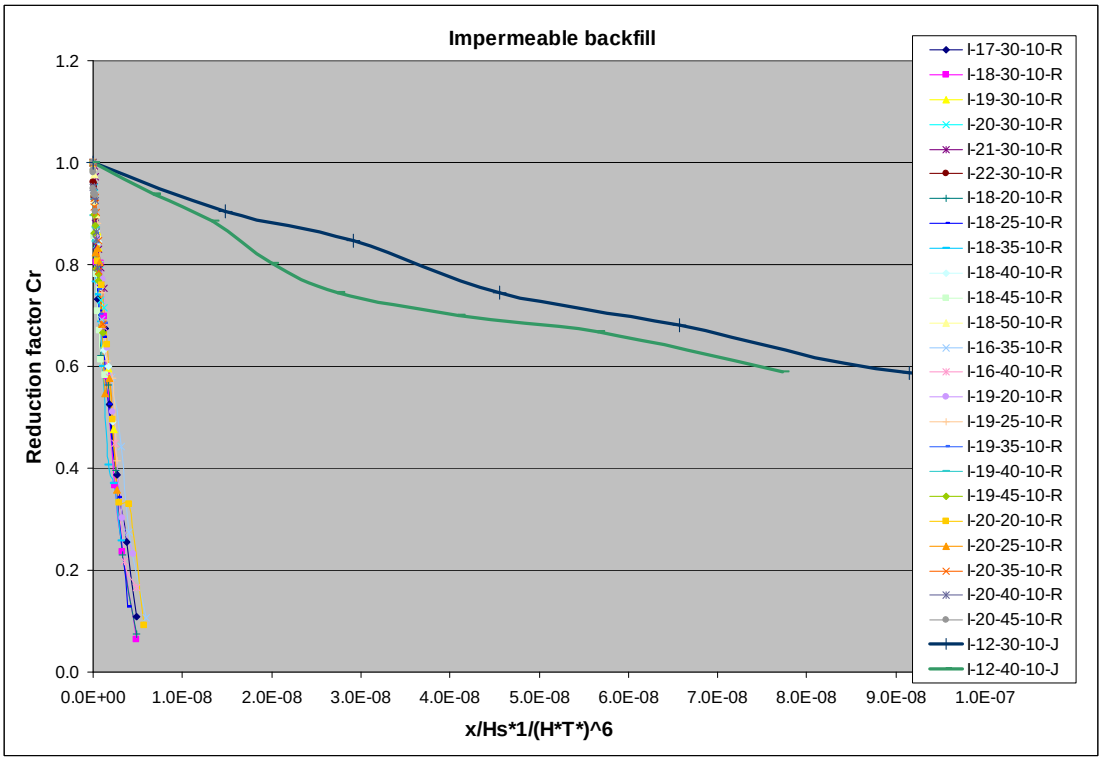

Figure 46 Relation between Cr and x* for n=6 for irregular wave spectra in comparison with the same relation for regular waves

Apparently, the dimensionless parameter x* causes large differences between the experiment results with regular waves and irregular wave spectra. It seems that the factor H*T* is smaller for the irregular wave spectra than for the regular waves. This results in a lower dimensionless distance x* for the regular waves than for the irregular wave spectra.
Actually, this is explicable by means of the spectral wave height. In case of irregular wave spectra, the wave overtopping discharge is primary caused by the larger waves in the spectrum. However, the spectral wave height (H_{m0}), used in the dimensionless factor H*T*, can be defined as approximately the average wave height of the one-third largest waves. By changing the spectral wave height H_{m0} into the average wave height of the one-thousandth largest waves $H_{1/1000}$, the influence of the larger waves in the spectrum is used for the relation.

The ratio between $H_{1/1000}$ and H_{m0} in shallow water is given by Battjes and Groenendijk [2]. One has to compute the dimensionless transitional wave height (H_{tr}/H_{rms}), which is used as input to Table 2 of Battjes and Groenendijk [2] to find the characteristic heights ($H_{1/1000}$)/(H_{rms}). Values of the transitional wave (H_{tr}), the root mean square wave height (H_{rms}) and the corresponding average wave height of the one-thousandth largest waves ($H_{1/1000}$) for the irregular wave spectra experiment results are given in Appendix XI-1 and Appendix XI-2.

This results in the relation illustrated in Figure 47. The thick black and brown lines are the results of the experiments with irregular waves. The values for x* with $H_{1/1000}$ for the irregular experiment results are given in Appendix XI-3.

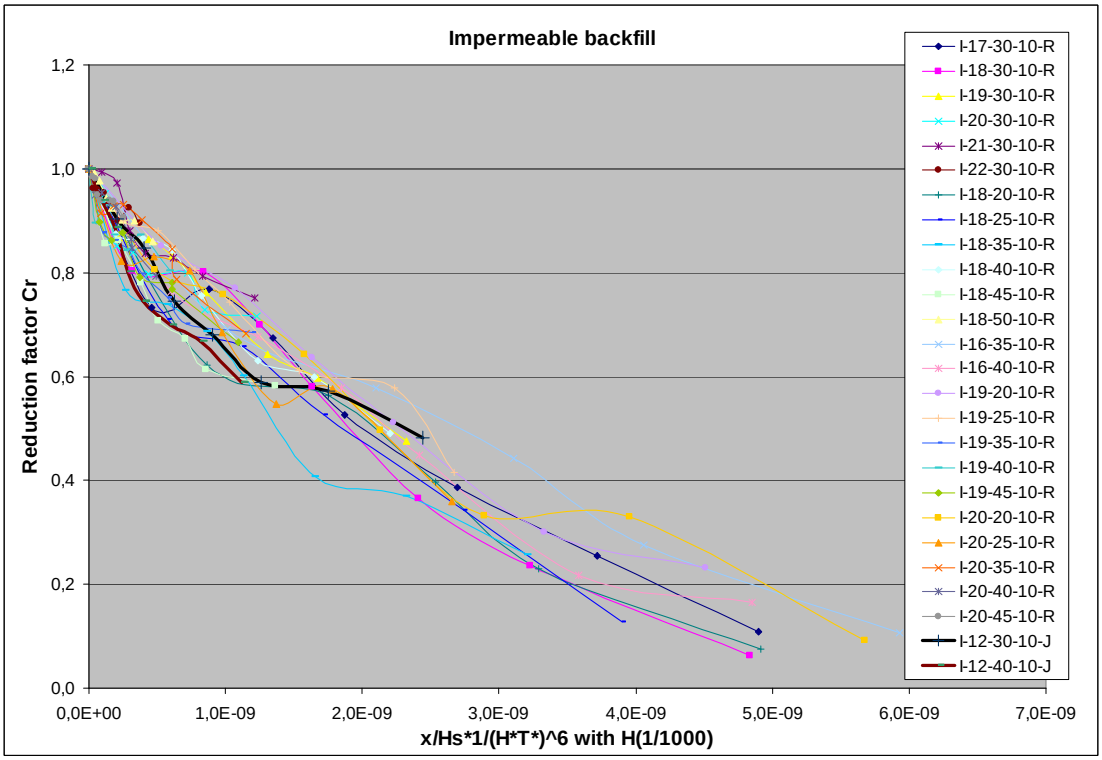

Figure 47 Relation between Cr and x* for n=6 and $H_{1/1000}$ for irregular waves in comparison with the same relation for regular waves

Obviously, by using $H_{1/1000}$, the relation defined in section 4.3 can also be applied to the experiments with irregular wave spectra. Nevertheless, the amount of experiments (2) is not sufficient to draw a general conclusion on this topic.

5. Application of conclusions

The conclusions described in section 4.3.3 and section 4.4.3 are based on the scale model experiment results, but because of their dimensionless presentation, they can also be applied to situations in reality. To illustrate this application, an example design will be made for the prototype described in section 3.1. This example will also be compared with existing methods. Besides, the overtopping volume per wave will be calculated for the given example.

5.1. Example prototype

The engineer wants to construct a building at a certain distance behind the crest. For both situations, permeable and impermeable backfill behind the crest, the distance behind the crest behind which the building can be safely constructed needs to be calculated.
According to EurOtop [13], the limit for building structure elements is equal to 1 l/s per m (=$1 \cdot 10^{-3}$ m^3/s per m)

5.1.1. Dimensions and conditions

The dimensions of the prototype are:

Crest freeboard	R_c=2m
Crest width	B=3.6m
Roughness factor	γ_f=0.55
Slope	tan(α)=1:2 (α=tan(1/2)=26.6°)
Material armour layer	grading=3-6 T; M_{15}=3.27 T, M_{50}=4.43 T, M_{85}=6.00 T D_{n15}=1.07m, D_{n50}=1.19m, D_{n85}=1.31m D_{15}=1.28m, D_{50}=1.41m, D_{85}=1.56m

For this example the following hydraulic conditions are applied:

Water depth	d=13m
Wave height	H_s=3.2m (regular waves)
Wave steepness	s=1/30
Wave length	L=96m ($L=H_s/s$)
Wave period	T_s=7.84 ($L = g \cdot T_s^2 / (2\pi)$)
Breaker parameter	ξ=2.74 ($\xi = \frac{\tan\alpha}{\sqrt{s_0}}$)

5.1.2. Total overtopping discharge

The Shore Protection Manual method for wave overtopping with regular waves, described in section 2.3.3, will be used to estimate the total wave overtopping.

The conditions and dimensions described in section 5.1.1 result in a total wave overtopping discharge Q equal to $1.07 \cdot 10^{-1}$ m^3/s per m (107 l/s per m)[1]. This overtopping discharge represents a dimensionless overtopping discharge Q^*_{tot} equal to $5.97 \cdot 10^{-3}$.

[1] This example corresponds with experiment T-16-30-10-R of the research. This experiment resulted in $1.029 \cdot 10^{-3}$ m^3/s per m. Overtopping discharge scaling factor $N_Q = \sqrt{(20^4} = 89.4$, so the total overtopping discharge in the scale model of $1.029 \cdot 10^{-3}$ m^3/s per m corresponds approximately with 0.9210^{-1} m^3/s per m (92.1 l/s per m) in the prototype.

5.1.3. Overtopping discharge directly behind the crest

The dimensionless parameter H*, described in section 4.2.2, is for these circumstances equal to 42.67. The threshold value H^*_d is equal to 26. The ratio between the dimensionless total wave overtopping discharge and the dimensionless wave overtopping discharge directly behind the crest can now be calculated with Equation 5.1-1.

Equation 5.1-1

$$\frac{Q^*_{over}}{Q^*_{tot}} = \begin{cases} \left(\frac{H^* - H^*_d}{H^* - 15} \right)^2 & \text{for } H^* \geq H^*_d \\ 0 & \text{for } H^* \leq H^*_d \end{cases}$$

This results in the ratio Q^*_{over}/ Q^*_{tot} equal to 0.363, so the overtopping discharge directly behind the crest Q_{over} is equal to $3.88 \cdot 10^{-2}$ m^3/s per m (38.8 l/s per m). This represent a dimensionless wave overtopping discharge directly behind the crest equal to $2.16 \cdot 10^{-3}$.

5.1.4. Spatial distribution for impermeable backfill

The reduction factor C_r is equal to the dimensionless overtopping discharge at a certain location behind the crest divided by the dimensionless overtopping discharge directly behind the crest. At the location of the building, this reduction factor must be equal to $1 \cdot 10^{-3}/3.88 \cdot 10^{-2}=0.026$.
Equation 5.1-2 is the deterministic design method to calculate the safe distance x behind the crest with impermeable backfill behind the crest. H*T* is in this example equal to 27.79.

Equation 5.1-2

$$\frac{Q^*_{over,x}}{Q^*_{over,0}} = 1.1 \cdot e^{-3.4 \cdot 10^8 \cdot \left(\frac{x}{H_s} \cdot \frac{1}{(H^*T^*)^6} \right)}$$

This results in a distance x=16.2m.

Consequently 16.2m behind the crest is the overtopping discharge reduced to 1 l/s per m and is it safe to construct a building

5.1.5. Spatial distribution for permeable backfill

The reduction factor C_r is equal to the dimensionless overtopping discharge at a certain location behind the crest divided by the dimensionless overtopping discharge directly behind the crest. At the location of the building, this reduction factor must be equal to $1 \cdot 10^{-3}/3.88 \cdot 10^{-2}=0.026$.
Equation 5.1-3 is the deterministic design method to calculate the safe distance x behind the crest with permeable backfill behind the crest. H*T* is in this example equal to 27.79.

Equation 5.1-3

$$\frac{Q^*_{over,x}}{Q^*_{over,0}} = e^{-1.3 \cdot 10^5 \cdot \left(\frac{x}{H_s} \cdot \frac{1}{(H^*T^*)^3} \right)}$$

This results in a distance x=1.93.

Consequently 1.93m behind the crest is the overtopping discharge reduced to 1 l/s per m and is it safe to construct a building

5.2. Comparison with existing methods

The safe distance for constructing the building behind the crest can also be calculated with other existing methods. The method of Steenaard, described in section 2.4, will be used to calculate the division of the overtopping discharge into the infiltrated discharge and the overtopping discharge directly behind the crest. The method for the spatial distribution of Juul Jensen, described in section 2.5.1, will be used to calculate the safe distance x behind the crest.
Again, the total wave overtopping discharge Q is equal to $1.07 \cdot 10^{-1}$ m^3/s per m (107 l/s per m). This overtopping discharge represents a dimensionless overtopping discharge equal to $5.97 \cdot 10^{-3}$.

5.2.1. Overtopping discharge directly behind the crest

According to Steenaard, the division of the total overtopping can be described as Equation 5.2-1.

$$\frac{Q_3}{Q_{tot}} = \begin{cases} \dfrac{Q^*_{tot} - Q^*_d}{Q^*_{tot} + 7.0 \cdot 10^{-2}} & \text{for } Q^*_{tot} \geq Q^*_d \\ 0 & \text{for } Q^*_{tot} \leq Q^*_d \end{cases} \qquad \textit{Equation 5.2-1}$$

For the conditions of this example, described in section 5.1.1, the dimensionless Q^*_{tot} is equal to $5.00 \cdot 10^{-3}$. Assuming threshold value Q^*_d is $8.1 * 10^{-3}$, the ratio Q_3/Q_{tpt} is equal to 0 ($Q^*_{tot} \leq Q^*_d$).
So according to Steenaard there will be no overtopping discharge directly behind the crest for these circumstances. This is incorrect; the method of Steenaard can not be applied for this example.

5.2.2. Spatial distribution behind the crest

As described in section 5.1.3, the overtopping discharge directly behind the crest Q_{over} in this example is equal to 3.88^{-2} m^3/s per m (38.8 l/s per m). This represent a dimensionless wave overtopping discharge directly behind the crest equal to $2.16 \cdot 10^{-3}$.
According to Jensen, the intensity overtopping discharge at a distance x behind the crest can be described as Equation 5.2-2.

$$q(x) = q_0 \cdot 10^{-(x/\beta)} \qquad \textit{Equation 5.2-2}$$

B* is the horizontal distance from the intersection of the SWL and the sea side slope to the rearmost extend of the crest, which is in this example equal to 9.6m. Constant β is for the type of breakwater in this example equal to 0.50· B*=4.8m.
Equation 5.2-3 can be used to calculate the overtopping intensity just behind the crest.

$$Q = q_0 \cdot \beta / \ln 10 \qquad \textit{Equation 5.2-3}$$

The overtopping discharge directly behind the crest Q is equal to 38.8 l/s per m, so q_0 is equal to 18.61 l/s/m per m. According to Equation 5.2-2, the overtopping discharge is reduced to the limit of 1 l/s for x equal to 7.6m.
Calculated with the results of this thesis, the safe length for overtopping over permeable backfill is much shorter (x=1.93m) and the safe length for overtopping discharge over impermeable backfill is much higher (x=16.2). Consequently, the safe distance behind the crest calculated with the method of Juul Jensen lies between these two values. The exact properties of the backfill behind the crest in the experiments of Juul Jensen are unknown, but apparently the backfill was semi-permeable and his method corresponds with the results of this thesis.

5.3. Overtopping volume per wave

Wave overtopping is a dynamic and irregular process and the mean overtopping discharge (Q in m^3/s per m) does not cover this aspect. Tests on the effects of overtopping on people suggest that information on mean discharges alone may not give reliable indicators of safety for some circumstances. Maximum individual volumes (in m^3 per m per wave) should be better indicators of hazard than average discharges. The volume of the largest overtopping event can vary significantly with wave condition and structure type, even for a given means discharge.
TAW2002 describes the overtopping volume per wave as an exceedance probability (P_v) of a certain volume (V) of water in an overtopping wave. This method is explained in section 2.3.5.

The results of this thesis are particularly suitable to calculate the maximum overtopping discharge per wave. The measured discharges in the experiments as well as the calculated discharges with the defined relation are given in mean overtopping discharges (m^3/s per m crest length). But because of the used regular waves, the wave periods of all the overtopping waves are known. By multiplying the mean overtopping discharge with the wave period of the specific waves, the overtopping discharge per wave is calculated.

In practice, the exceedance probability of certain maximum wave conditions in a certain irregular wave spectrum can be calculated. These wave conditions can be used in the relations defined in this thesis to calculate the overtopping volume for this specific wave at a certain point x behind the crest.

5.3.1. Example prototype

Based on the prototype described in section 5.1.1, the safe distance behind the crest for constructing a promenade can be calculated. This calculation is based on the overtopping discharge per wave. The maximum volume per wave for untrained people in pulsating flows along a promenade is equal to 0.75 m^3/m (750 l/m).
Assumed is that the probability of exceedance for the irregular wave spectrum in this example results in a maximum wave with H_s=3.6 and s=1/40. This leads to wave length L=144m, wave period T=9.6s and breaker parameter ξ=3.16.

Total overtopping discharge

The total wave overtopping for these conditions, according to the Shore Protection Manual (section 2.3.3), is equal to 0.217 m^3/s per m (217 l/s per m). For the defined maximum wave this is equal to 0.217·9.6 = 2.08 m^3/m (2080 l/m).

Overtopping discharge directly behind the crest

The dimensionless parameter H*, described in section 4.2.2, is for these conditions equal to 72. The threshold H^*_d is equal to 26. Equation 5.1-1 results in the ratio Q^*_{over}/ Q^*_{tot} equal to 0.65, so the overtopping discharge directly behind the crest Q_{over} is equal to 0.141 m^3/s per m (141 l/s per m). For the defined maximum wave this is equal to 0.141·9.6 = 1.36 m^3/m (1360 l/m).

Spatial distribution for impermeable backfill

The reduction factor C_r is equal to the dimensionless overtopping discharge at a certain location behind the crest divided by the dimensionless overtopping discharge directly behind the crest. At the location of the promenade, this reduction factor must be equal to 750/1360=0.551.

Equation 5.1-2 is the deterministic design method to calculate the safe distance x behind the crest with impermeable backfill behind the crest. H*T* is in this example equal to 38.3. This results in a distance x=23.1m

Consequently 23.1m behind the crest the wave overtopping discharge for the maximum defined wave is reduced to the safety limit of 750l/m and it is safe to construct the promenade.

Spatial distribution for permeable backfill

The reduction factor C_r is equal to the dimensionless overtopping discharge at a certain location behind the crest divided by the dimensionless overtopping discharge directly behind the crest. At the location of the promenade, this reduction factor must be equal to 750/1360=0.551.

Equation 5.1-3 is the deterministic design method to calculate the safe distance x behind the crest with permeable backfill behind the crest. H*T* is in this example equal to 38.3. This results in a distance x=0.93m.

Consequently 0.93m behind the crest the wave overtopping discharge for the maximum defined wave is reduced to the safety limit of 750l/m and it is safe to construct the promenade.

6. Conclusions and recommendations

6.1. Conclusions

The most important conclusions of this thesis are presented in this chapter. The determination of the distribution of the wave overtopping discharge for regular waves is divided in three parts: the distribution over the crest, the distribution behind the crest over impermeable backfill, the distribution behind the crest over permeable backfill. Additionally, the distribution behind the crest over impermeable backfill for irregular wave spectra is determined.

6.1.1. Overtopping discharge directly behind the crest

A method to determine the spatial distribution of the wave overtopping discharge over the crest is defined by Steenaard [19]. Steenaard's method is not applicable to the experimental results of this thesis. This is caused by the lack of a sufficient number of relevant parameters in this method. A variation of Steenaard's method is shown in Equation 6.1-1. This equation contains a division of the total wave overtopping discharge in the infiltrating discharge into the crest and the overtopping discharge directly behind the crest. Equation 6.1-1 introduces the influence of the wave height, wave length and crest height into Steenaard's method.

Equation 6.1-1

$$\frac{Q^*_{over}}{Q^*_{tot}} = \begin{cases} \left(\dfrac{H^* - H^*_d}{H^* - 15} \right)^2 & \text{for } H^* \geq H^*_d \\ 0 & \text{for } H^* \leq H^*_d \end{cases}$$

with

$$H^* = \frac{H \cdot L}{B \cdot R_c} \quad \text{and} \quad H^*_d = 26$$

H^*_d is the threshold value of H^* for overtopping discharge directly behind the crest. There is no overtopping discharge directly behind the crest for $H^* \leq H^*_d$.

6.1.2. Overtopping over impermeable backfill

The spatial distribution of the wave overtopping discharge behind the crest depends on the permeability of the backfill. For an impermeable backfill with a slope of 3% towards the breakwater, the overtopping discharge at every point behind the breakwater is divided in two parts: one part flows back over the impermeable backfill under the influence of gravity and the other part passes the point and travels further away from the breakwater.
The influence of the wave energy in the distribution of the wave overtopping discharge behind the crest is major. The overtopping discharge at a certain location x behind the crest can be estimated with Equation 6.1-2. This equation represents the mean line through all the data points and can therefore be used for a probabilistic design approach. The standard deviation of this line is 0.0545.

Equation 6.1-2

$$\frac{Q^*_{over,x}}{Q^*_{over,0}} = e^{-4.0 \cdot 10^8 \cdot \left(\frac{x}{H_s} \cdot \frac{1}{(H^* T^*)^6} \right)}$$

H*T* is a dimensionless presentation of the wave energy for a given crest height and is defined as $H*T* = \frac{H_s}{R_c} \cdot T_s \cdot \sqrt{\frac{g}{R_c}}$.

The maximum value of the overtopping discharge at a certain point x behind the crest can be calculated with Equation 6.1-3. This equation can be used for deterministic design or safety assessment and represent the upper 95.45% confidence limit of the data points.

Equation 6.1-3

$$\frac{Q^*_{over,x}}{Q^*_{over,0}} = 1.109e^{-3.2 \cdot 10^8 \cdot \left(\frac{x}{H_s} \cdot \frac{1}{(H*T*)^6} \right)}$$

with $\frac{Q^*_{over,x}}{Q^*_{over,0}} \leq 1$

6.1.3. Overtopping over permeable backfill

For a permeable backfill, the overtopping discharge at every point behind the breakwater is divided in two parts: one part infiltrates into the backfill and the other part passes the point and travels further away from the breakwater.
The influence of the wave energy in the distribution of wave overtopping discharge behind the crest is major, but less than for impermeable backfill. The overtopping discharge at a certain location x behind the crest can be estimated with Equation 6.1-4. This equation represents the mean line through all the data points and can therefore be used for a probabilistic design approach. The standard deviation of this line is 0.0372.

Equation 6.1-4

$$\frac{Q^*_{over,x}}{Q^*_{over,0}} = e^{-1.64 \cdot 10^5 \cdot \left(\frac{x}{H_s} \cdot \frac{1}{(H*T*)^3} \right)}$$

The maximum value of the overtopping discharge at a certain point x behind the crest can be calculated with Equation 6.1-5. This equation can be used for deterministic design or safety assessment and represent the upper 95.45% confidence limit of the data points.

Equation 6.1-5

$$\frac{Q^*_{over,x}}{Q^*_{over,0}} = 1.0744e^{-1.24 \cdot 10^5 \cdot \left(\frac{x}{H_s} \cdot \frac{1}{(H*T*)^3} \right)}$$

with $\frac{Q^*_{over,x}}{Q^*_{over,0}} \leq 1$

6.1.4. Irregular waves

The defined relation for wave overtopping discharge over an impermeable backfill behind the crest can also be applied for irregular wave spectra by using $H_{1/1000}$ in stead of H_s. This conclusion is only an indication, the amount of experiments (2) is not sufficient to draw a general conclusion on this topic.

6.2. Recommendations

The results of this thesis lead to a few recommendations.

6.2.1. Application of conclusions

The conclusions in this thesis are only applicable for a specific situation equal to the applied prototype and the tested conditions. The defined relations for the spatial distribution of the wave overtopping discharge are only valid for the defined limits of the relevant parameters used in this study. Expanding the validation of these relations by executing experiments outside the range of the varied parameters is useful to increase the appropriateness of the relations in practice.

6.2.2. Investigation influencing parameters

Various influencing parameters are have not been considered in this thesis. Their influence on the wave overtopping discharge must be investigated to define a universal method for calculating the overtopping discharge and its spatial distribution. The parameters that have not been varied are:

- Hydraulic conditions
  - Oblique waves
  - Wind
  - Storm duration
- Physical dimensions
  - Slope angle
  - Crest width
  - Presence of an underlayer
  - Bermed profiles
  - Toe structure
- Rock properties
  - Armour size
  - Core size

Additionally, some parameters have been taken into account in this thesis, but need more investigation to determine their exact influence on the wave overtopping discharge and its spatial distribution. The performed investigation in this thesis with the influence of these parameters is not sufficient to define a valid relation between these parameters and the overtopping discharge. These parameters are:

- Water depth / crest height
- Irregular wave spectrum
- Degree of backfill permeability

6.2.3. Practical recommendations for further investigation

Continuous system

The results of further investigations will be more reliable if a continuous pumping system is used in the scale model. The overtopping discharge should not be stored in a collecting tank outside the wave flume, but it should be measured and pumped back into the wave flume instantly and continuously.
Consequently, there will be no extracted overtopping water and no water depth reduction inside the wave flume. Because of that, only overtopping discharges with a constant water depth are measured and no correlation between the water depth reduction and the overtopping discharge will appear.

Experiment duration

The results of further investigation will be more reliable if the durations of the experiments are increased. The influences of measuring errors, leaking and other side effects will be reduced in this way. If the continuous system is used, the collecting tank is not a restricting factor anymore and it is not difficult to increase the experiment duration.

Impulse

For further investigation it will be useful to measure the impulse, layer thickness and velocity of the overtopping discharge flow. This can be done by using cameras and installing an impulse-gauge on top of the crest.

7. References

[1] D'ANGREMOND *et al.* [2008] Breakwaters and Closure Dams 2nd edition. *VSSD, Delft*

[2] BATTJES, J.A.; GROENENDIJK, H.W. [2000] Wave height distribution shallow Foreshores. Coastal Engineering, Vol 40, No.3, pp.161-182.

[3] BRADBURY, A.P. *et al* [1988] A hydraulic performance of breakwater crown walls. *Report no. SR146, Hydraulic Research, Wallingford, UK*

[4] CIRIA;CUR;CETMEF [2007] The Rock Manual. The use of rock in hydraulic engineering (2nd edition). *C683, CIRIA, London*

[5] DINGEMANS, M. [1987] Verification of numerical wave propagation models with laboratory measurements, HISWA verification in the directional wave basin. *Technical report H228, Part 1B, Appendices A-G, Delft Hydraulics, Delft*

[6] FORCHHEIMER, P. [1901] Wasserbewegung durch bodem. *Zeischrift Verein Deutscher Ingenieure, Vol 45, pp 1782-1788*

[7] HOLTHUIJSEN, L.H. [2006] Waves in Oceanic and Coastal Waters. *Delft University of Technology, UNESCO-IHE, Delft*

[8] HUGHES, S.A. [1993] Physical Models and Laboratory Techniques in Coastal Engineering. *Coastal Engineering Research Center, Waterways Experiment Station, USA.*

[9] HYDRAULIC RESEARCH WALLINGFORD [1999] Wave overtopping of sea-walls, design and assessment manual. *Hydraulic Research, Wallingford R&D, Report W178*

[10] JUUL JENSEN, O. [1984] A Monograph on Rubble Mound Breakwaters. *Danish Hydraulic Institute, Hørsholm*

[11] LYKKE ANDERSEN, T.; BURCHARTH H.F. [2006] Hydraulic Response on Rubble Mound Breakwaters. *Aalborg University, Aalborg*

[12] OWEN, M.W. [1980] Design for seawalls allowing for wave overtopping. *Report EX924, Hydraulics Research, Wallingford*

[13] PULLEN, T. *et al.* [2007] Wave Overtopping of Sea Defences and Related Structures: Assessment Manual. *EurOtop*

[14] SAVILLE, T.; CALDWELL, J.M. [1953] Experimental Study of Wave Overtopping on Shore Structures. *International Association of Hydraulic Research, Minneapolis*

[15] SAVILLE, T. [1955] Laboratory Data on Wave Runup and Overtopping on Shore Structures. *TM-64, U.S. Army Corps of Engineers, Beach Erosion Board, Washington D.C.*

[16] SAVILLE, T. [1958b] Large-Scale Model Tests of Wave Runup and Overtopping, Lake Okeechobee Levee Sections. *U.S. Army Corps of Engineers, Beach Erosion Board, Washington D.C.*

[17] SCHÜTTRUMPF, H.F.R. [2001] Wellenüberlaufströmung bei Seedeichen – experimentelle und theoretische untersuchungen-. *Technischen Universität Carolo-Wilhelmina, Braunschweig*

[18] SHIH, R.W.K [1990] Permeability characteristics of rubble material – new formulae. *International Conference on Coastal Engineering, ASCE, New York (1990), pp1499-1512*

[19] STEENAARD, J. [2002] Verdeling van overslaand water over een golfbreker. *Delft University of Technology, Faculty of Civil Engineering and Geosciences, Delft*

[20] U.S. ARMY ENGINEER WATERWAYS EXPERIMENT STATION [1984] Shore Protection Manual (4th edition*). Government Printing Office, Washington D.C.*

[21] VAN DER MEER, J.W. [1988b] Rock slopes and gravel beaches under wave attack. *PhD thesis, Delft University of Technology, Delft*

[22] VAN DER MEER, J.W. [2002] Technical report: Wave Run-up and Wave Overtopping at Dikes. *Technical Advisory Committee on Flood Defences, Delft*

[23] WARNOCK, J.E. [1950] Hydraulic similitude. *Engineering Hydraulics, pp 136-176, New York.*

Appendices

I

Figures Shore Protection Manual

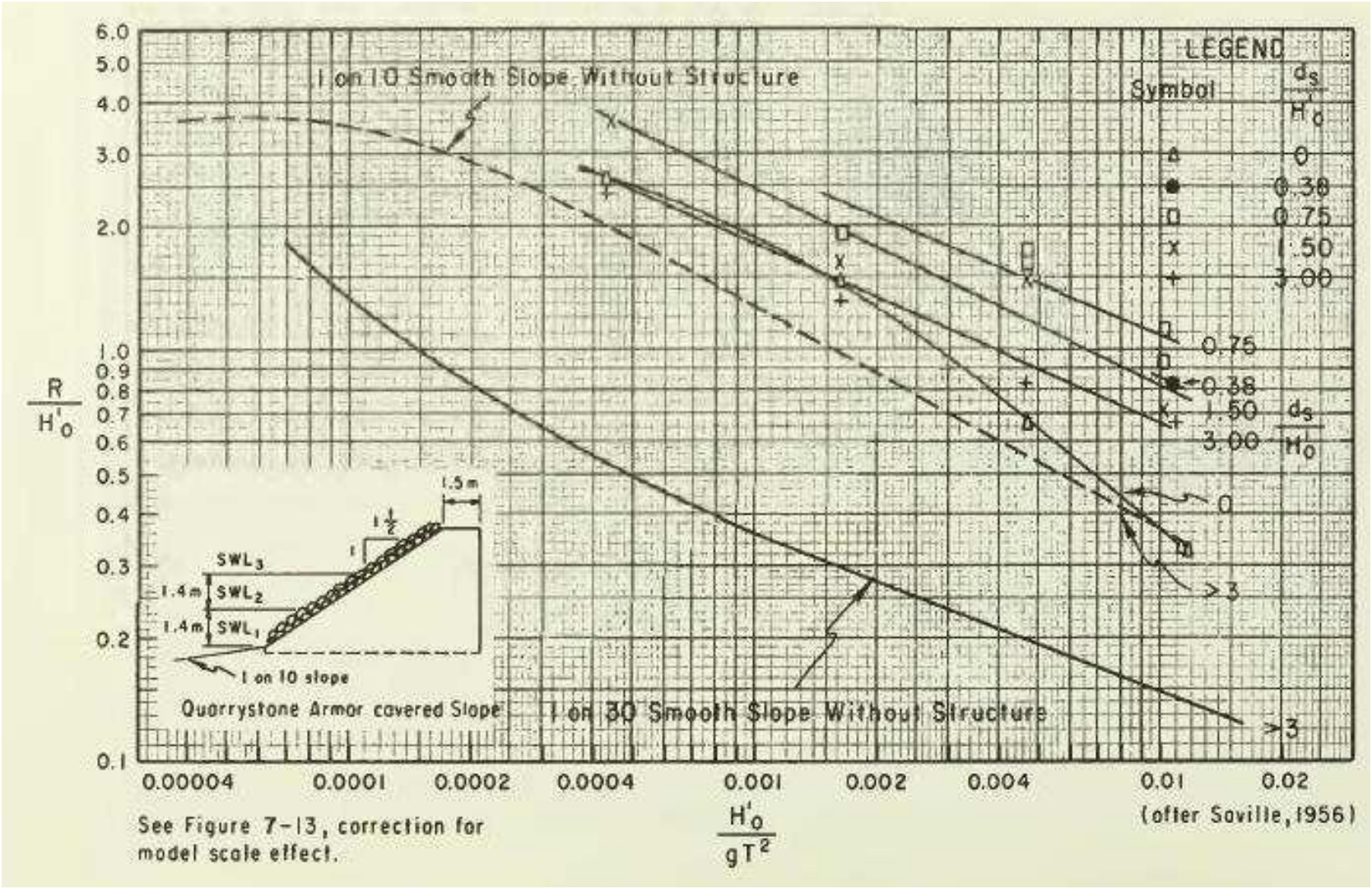

Appendix I-1 Wave run-up versus H'0/(g·T²) according to the Shore Protection Manual.

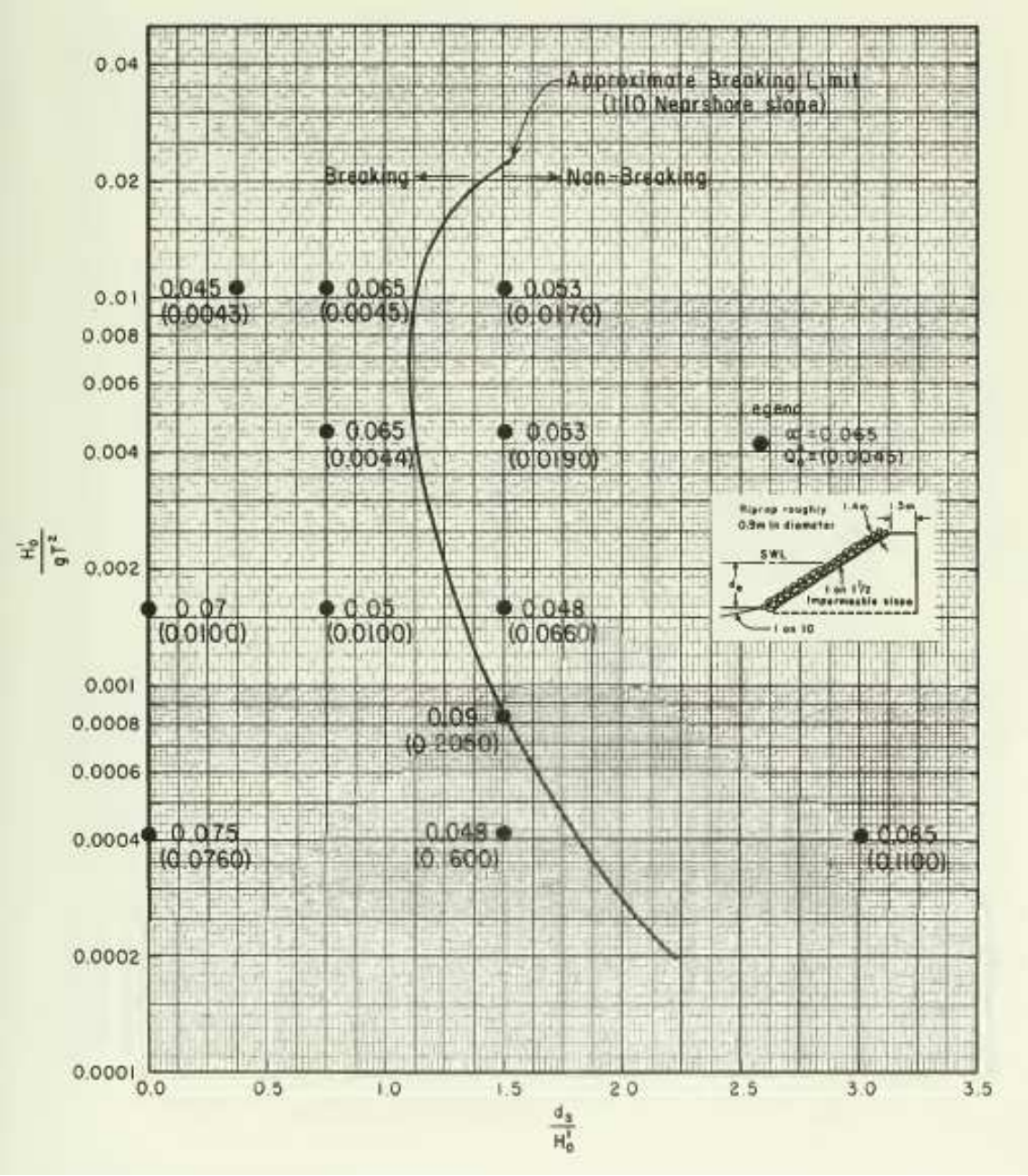

Appendix I-2 Overtopping parameters α and Q^*_0 according to the Shore Protection Manual.

II

Scaling process

Scale factors

Correspondence between prototype and model parameters is denoted by the scale ratio or simply the scale. The scale ratio is the ratio of a parameter in the prototype to the value of the same parameter in the model. Symbolically, this is represented as in Equation II-6.

$$N_X = \frac{X_p}{X_m} = \frac{\text{Value of X in Prototype}}{\text{Value of X in Model}} \qquad \textit{Equation II-6}$$

where N_X is the prototype-to-model scale ratio of the parameter X, and the subscripts 'p' and 'm' represent prototype and model, respectively.

Hydraulic similitude

The scale model can be less reliable by means of a scale effect. Scale effects occur when negligible forces in the prototype have considerable influence in the model.

Experience indicates that almost any major problem can be simplified into the interplay of two major forces. This allows the similitude criteria to be developed theoretically. Several well known criteria for fluid flow model investigations have been developed based on the assumption that two forces dominate the flow while the other forces are minor.
Inertial forces are always present in flow problems, so inertia needs to be balanced by one of the other forces. Some of these forces are expressed in terms of their physical units in Equation II-7, Equation II-8 and Equation II-9:

$$\hat{F}_i = \text{mass}\times\text{acceleration} = \left(\rho \cdot \mathrm{L}^3\right)\left(V^2 / L\right) = \rho \cdot L^2 \cdot V^2 \qquad \textit{Equation II-7}$$

$$\hat{F}_g = \text{mass}\times\text{gravitational acceleration} = \rho \cdot L^3 \cdot g \qquad \textit{Equation II-8}$$

$$\hat{F}_\mu = \text{viscosity}\times\frac{\text{velocity}}{\text{distance}}\times\text{area} = \mu\left(\mathrm{V/L}\right)L^2 = \mu \cdot V \cdot L \qquad \textit{Equation II-9}$$

The ratio of the inertial force to any other force provides the relative influence of the two forces in the flow situation. Requiring that the force ratio be the same in the model as in the prototype leads to a similitude criterion for each of the force ratios.

Froude Criterion

A parameter that expresses the relative influence of inertial and gravity forces in a hydraulic flow is given by the square root of the ratio of inertial to gravity forces:

$$\sqrt{\frac{\text{inertial force}}{\text{gravity force}}} = \sqrt{\frac{\rho \cdot L^2 \cdot V^2}{\rho \cdot L^3 \cdot g}} = \frac{V}{\sqrt{g \cdot L}}$$

This is called the Froude number.
Requiring that the Froude Number be the same in the model as in the prototype leads to:

$$\left(\frac{V}{\sqrt{g \cdot L}}\right)_p = \left(\frac{V}{\sqrt{g \cdot L}}\right)_m$$

$$\frac{V_p}{V_m} = \sqrt{\left(\frac{g_p}{g_m}\right)\left(\frac{L_p}{L_m}\right)}$$

This is expressed in terms of scale ratios, and rearranging in Equation II-10.

$$\frac{N_V}{\sqrt{N_g \cdot N_L}} = 1 \qquad \textit{Equation II-10}$$

The gravity scale ratio is equal to unity, so this expression leads to $N_V = \sqrt{N_L}$

This corresponds with the kinematic similarity requirement $N_T = \sqrt{N_L}$.

$\frac{N_V}{\sqrt{N_g \cdot N_L}} = 1$ is the Froude model criterion for modelling flows in which inertial forces are balanced primarily by the gravitational forces, which happens to the most flows with a free surface. The majority of hydraulic models in coastal engineering are scaled according to the Froude model law. Consequently, it is usually the most important criterion to be considered when designing a coastal scale model.

Reynolds Criterion

When viscous forces dominate a hydraulic flow, the important parameter is the ratio of inertial to viscous forces given by the Reynolds number:

$$\frac{\text{inertial force}}{\text{viscous force}} = \frac{\rho \cdot L^2 \cdot V^2}{\mu \cdot V \cdot L} = \frac{\rho \cdot L \cdot V}{\mu}$$

Similitude is achieved when Reynolds number is the same in the model as in the prototype:

$$\left(\frac{\rho \cdot L \cdot V}{\mu}\right)_p = \left(\frac{\rho \cdot L \cdot V}{\mu}\right)_m \text{ or } \left(\frac{V_p}{V_m}\right)\left(\frac{L_p}{L_m}\right)\left(\frac{\rho_p}{\rho_m}\right) = \frac{\mu_p}{\mu_m}$$

In terms of scale ratios, the Reynolds model criterion is given in Equation II-11.

$$\frac{N_V N_L N_\rho}{N_\mu} = 1 \qquad \textit{Equation II-11}$$

The Reynolds scale law is intended for modelling flows where the viscous forces predominate.

The fluid density scale ratio and dynamic viscosity scale ratio are equal to unity, so this expression leads to $N_V \cdot N_L = 1$. Earlier, the Froude criterion led to $N_V = \sqrt{N_L}$, so the Froude criterion does not correspond with the Reynolds criterion. This means that gravity and viscous forces can not be processed in the same scale model. If gravity is important, viscous forces have to be reduced to a minimum.

Strouhal Criterion

Internal forces in fluid flows can be caused by two types of acceleration. Convective accelerations are accelerations due to different fluid velocities at different locations in the flow field, and they are represented mathematically by terms such as $u\left(\partial u/\partial x\right)$ or $v\left(\partial u/\partial y\right)$. Temporal (or local) accelerations are changes in flow velocity at a point that occur in time. They represent the unsteadiness of the flow, and can be expressed mathematically by terms such as $\partial u/\partial t$ or $\partial v/\partial t$. In terms of their physical units the inertial forces due to acceleration can be expressed as:

Temporal inertial force = $\left(\rho \cdot L^3\right)\left(V/t\right)$

Convective inertial force = $\left(\rho \cdot L^3\right)\left(V^2/L\right)$

The relative importance of the temporal inertial force to the convective inertial force is given as

$$\frac{\text{temporal inertial force}}{\text{convective inertial force}} = \frac{\left(\rho \cdot L^3\right)\left(V/t\right)}{\left(\rho \cdot L^3\right)\left(V^2/L\right)} = \frac{L}{V \cdot t}$$

which is referred as the Strouhal Number.

If we attempt to create a criterion of similitude by requiring the Strouhal number to be the same in the model as in the prototype, we get

$$\left(\frac{L}{V \cdot t}\right)_p = \left(\frac{L}{V \cdot t}\right)_m \text{ or } \left(\frac{L_p}{L_m}\right) = \left(\frac{V_p}{V_m}\right)\left(\frac{t_p}{t_m}\right)$$

In terms of scale ratios, this results in Equation II-12:

$$\frac{N_L}{N_V \cdot N_t} = 1 \qquad \textit{Equation II-12}$$

This simply states that the velocity scale ratio is equal to the length scale ratio divided by the time scale ratio. This is the same definition for velocity scale that arises from considerations of the fundamental dimensions of velocity.

Conclusion
According to Warnock [24], for practically all coastal engineering problems, the forces associated with surface tension and elastic compression are relatively small, and thus, can be safely neglected. This leaves selection of an appropriate hydrodynamic scaling law to an evaluation of whether gravity or viscous forces are dominant in the phenomenon. The Froude and Reynolds number are important because similarity of one of these numbers, combined with geometric similarity, provides necessary conditions for hydrodynamic similitude in an overwhelming majority of coastal models. Reynolds similitude is seldom invoked for most models of coastal processes, instead it is recognized that gravity forces predominate in free surface flows; and consequently, most models are designed using the Froude criterion. Nevertheless, efforts must be made to reduce the effect of viscosity in the model, otherwise the dissimilar viscous effects will constitute a scale effect.

Requirements of similitude

Geometric similarity
Geometrically similar models are also known as geometrically undistorted models. Geometrically undistorted models are models in which the vertical and horizontal scales are the same, and they represent the true geometric reproduction of the prototype.

"Geometric similarity exists between two objects or systems if the ratios of all corresponding linear dimensions are equal. This relationship is independent of motion of any kind and involves only similarity in form Warnock [24]"

The limiting dimension of the wave flume is its height. The height of the wave flume is 850mm and the height of the coastal defence structure in the prototype is 15000mm (11000mm water depth and 4000mm crest freeboard). The ratio between the prototype and the model is 15000/850=17.65. To incorporate safety space and space for the overtopping wave inside the flume, a handy scale ratio N=20 is chosen for the geometric similarity.

In that case, the main dimensions of the model coastal defence structure are:
Crest freeboard R_c=100mm
Slope tan(α)=1:2 (length of the front slope is 1500mm)

Because the vertical scale and horizontal scale in a geometrically undistorted model are the same, the water depth scale (N_d), the wave height scale (N_H) and the wave length scale (N_L) are the same as the scale factor N=20. The wave steepness and breaker parameter are dimensionless parameters, so the ratio of the parameters between prototype and model should be invariant.
This leads to the following hydraulic conditions in the model:
Water depth d=650mm
Wave height Hs=160mm
Wave steepness s=1/30
Wave length L=4800mm
Breaker parameter ξ=2.74

Kinematic similarity
Kinematic similarity indicates a similarity of motion between particles in model and prototype. Kinematic similarity is achieved when the ratio between the components of all vectorial motions for the prototype and model is the same for all particles at all times. In a geometrically similar model, kinematic similarity gives particles paths that are geometrically similar to the prototype.

This kinematic similarity is needed to calculate the wave length in the scale model.

The wave length of gravity waves is given as $L = \frac{g \cdot T^2}{2\pi}$ in which:

The scale relationship between the length and wave period scales is found from the prototype-to-model ratio of wavelength:

$$\frac{\left[L = \frac{g \cdot T^2}{2\pi} \right]_p}{\left[L = \frac{g \cdot T^2}{2\pi} \right]_m} \text{ or } \frac{L_p}{L_m} = \left(\frac{g_p}{g_m} \right) \cdot \left(\frac{T_p}{T_m} \right)^2$$

The relation is written in terms of scale factors as $N_L = N_g \cdot N_T^2$.

The gravity scale ratio in the above expression is, for all practical purpose, equal to unity. The wavelength scale is the same as the generic length scale, so we see that kinematic similarity in gravity wave motion requires the Froude criterion $N_T = \sqrt{N_L}$. For this scale model this results in $N_T = \sqrt{N_L} = \sqrt{20} = 4.47$. The relationship given above constitutes a criterion of similitude because it is constrained by the mathematical relationship for wave motion.
This leads to a wave period in the scale model of T_s=7.84/4.47=1.75s.

Dynamic similarity
The forces exerted by the wave motion on an object or boundary may not be in similitude in the model unless additional requirements are met related to the prototype and model fluid properties. These additional requirements stem from the necessity of maintaining dynamic similarity.

"Dynamic similarity between two geometrically and kinematically similar systems requires that the ratios of all vectorial forces in the two systems be the same Warnock [1950]"

This definition means that there must be constant prototype-to-model ratios of all masses and forces acting on the system.
The requirement for dynamic similarity arises from Newton's second law that equates the vector sum of the external forces acting on an element to the element's mass reaction to those forces: $m\frac{dV}{dt} = \sum_n F_n$
In fluid mechanics problems, the inertial force is equal to the sum of the gravitational force, viscous force, surface tension force, elastic compression force and pressure force.
Overall dynamic similarity requires that the ratio of the internal forces between prototype and model be equal to the ratio of the sum of all the active forces.
Perfect similitude requires that all force ratios between prototype and model also be equal.

Dynamic similarity is needed to determine the scale factor for the stability of the breakwater under wave attack. The scale factor for the armour stone mass (N_{Ms}) depends on the scale factor for the wave height (N_H=20).
The mass of armour stones is the specific density of the material multiplied by the volume of the stone ($W_s=\rho_s \cdot V_s$). The scale ratio of the mass is given as:

$$N_{M_s} = \frac{(M_s)_p}{(M_s)_m} = \frac{(\rho_s)_p}{(\rho_s)_m} \cdot \frac{(V_s)_p}{(V_s)_m} = N_{\rho_s} \cdot N_{V_s}$$

Because the specific densities of the materials in the model and prototype are almost equal, we assume $N_{\rho s}$=1. We also note that in a geometrically similar model, the volume scale is simply the length scale cubed ($N_{Vs}=(N_L)^3$). Making these substitutions yields for this scale model: $N_{M_s} = \frac{(M_s)_p}{(M_s)_m} = N_L^3 = 20^3 = 8000$

III

Infiltration calculations

Infiltration into the armour layer
The armour layer of the scale model is constructed of material with the following dimensions:

grading=66-76mm;
M_{15}=0.45kg, M_{50}=0.56kg, M_{85}=0.68kg;
D_{n15}=55mm, D_{n50}=60mm, D_{n85}=64mm
D_{15}=66mm, D_{50}=71mm, D_{85}=76mm

Hereby it is more important that the infiltration requirements are obeyed than that the scale factor between prototype and scale model is exactly correct. After all, the prototype is just an assumed situation and is certainly not a standard for every coastal defence structure.

Based on the equations in section 3.2.2, this leads to the following calculation to determine the Reynolds number of this scale model armour layer.

$$\alpha = 1684 + 3.12 \cdot 10^{-3} \left(\frac{g}{\nu^2} \right)^{2/3} \cdot D_{15}^2 = 1684 + 3.12 \cdot 10^{-3} \left(\frac{9.81}{\left(1 \cdot 10^{-6}\right)^2} \right)^{2/3} \cdot 0.066^2 = 7912.094$$

$$\beta = 1.72 + 1.57 \cdot e^{-5.10 \cdot 10^{-3} \left(\frac{g}{\nu^2} \right)^{1/3} D_{15}} = \beta = 1.72 + 1.57 \cdot e^{-5.10 \cdot 10^{-3} \left(\frac{9.81}{\left(1 \cdot 10^{-6}\right)^2} \right)^{1/3} 0.066} = 1.721$$

$$a = \alpha \frac{(1-n)^2}{n^3} \frac{\nu}{g \cdot D_{15}^2} = 7912.094 \frac{(1-0.35)^2}{0.35^3} \frac{1 \cdot 10^{-6}}{9.81 \cdot 0.066^2} = 1.825$$

$$b = \beta \frac{1-n}{n^3} \frac{1}{g \cdot D_{15}} = 1.721 \frac{1-0.35}{0.35^3} \frac{1}{9.81 \cdot 0.066} = 40.305$$

If we assume hydrostatic pressures, the pressure gradient is equal to 1. This results in:

$$I = a \cdot u_f + b \cdot u_f \cdot \left| u_f \right| \rightarrow 1 = 1.825 \cdot u_f + 40.305 \cdot u_f \cdot \left| u_f \right| \rightarrow u_f = 0.136 \text{m/s}$$

and $u_p = \frac{u_f}{n} = \frac{0.134}{0.35} = 0.384 \text{m/s}$.

This results in the following Reynolds number:

$$\text{Re} = \frac{u_p \cdot D_{15}}{\nu} = \frac{0.384 \cdot 0.066}{1 \cdot 10^{-6}} = 2.57 \cdot 10^4$$

Infiltration into the core

The core of the scale model is constructed of material with the following dimensions:
Grading=30-36mm;

M_{15}=0.041kg, M_{50}=0.056kg, M_{85}=0.075kg;
D_{n15}=0.0249m=24.9mm, D_{n50}=0.0276m=27.6mm, D_{n85}=0.0305m=30.5mm
D_{15}=0.0296m=29.6mm, D_{50}=0.0329m=32.9mm, D_{85}=0.0363m=36.3mm

Based on the equations in section 3.2.2, this leads to the following calculation to determine the Reynolds number of this scale model core.

$$\alpha = 1684 + 3.12 \cdot 10^{-3} \left(\frac{g}{\nu^2} \right)^{2/3} \cdot D_{15}^2 = 1684 + 3.12 \cdot 10^{-3} \left(\frac{9.81}{\left(1 \cdot 10^{-6}\right)^2} \right)^{2/3} \cdot 0.0296^2 = 2936.71$$

$$\beta = 1.72 + 1.57 \cdot e^{-5.10 \cdot 10^{-3} \left(\frac{g}{\nu^2} \right)^{1/3} D_{15}} = \beta = 1.72 + 1.57 \cdot e^{-5.10 \cdot 10^{-3} \left(\frac{9.81}{\left(1 \cdot 10^{-6}\right)^2} \right)^{1/3} 0.0296} = 1.786$$

$$a = \alpha \frac{(1-n)^2}{n^3} \frac{\nu}{g \cdot D_{15}^2} = 2936.71 \frac{(1-0.35)^2}{0.35^3} \frac{1 \cdot 10^{-6}}{9.81 \cdot 0.0296^2} = 3.367$$

$$b = \beta \frac{1-n}{n^3} \frac{1}{g \cdot D_{15}} = 1.786 \frac{1-0.35}{0.35^3} \frac{1}{9.81 \cdot 0.0296} = 93.249$$

If we assume hydrostatic pressures, the pressure gradient is equal to 1. This results in:

$$I = a \cdot u_f + b \cdot u_f \cdot \left| u_f \right| \rightarrow 1 = 3.367 \cdot u_f + 93.247 \cdot u_f \cdot \left| u_f \right| \rightarrow u_f = 0.087 \text{m/s}$$

and $u_p = \frac{u_f}{n} = \frac{0.125}{0.35} = 0.249 \text{m/s}$.

This results in the following Reynolds number:

$$\text{Re} = \frac{u_p \cdot D_{15}}{\nu} = \frac{0.249 \cdot 0.0296}{1 \cdot 10^{-6}} = 7363$$

IV

Experiment results;
Total wave overtopping discharge

Experiment results									
Experiment code	water depth d (m)	wave height gauge 1 Hm0 (m)	wave height gauge 2 Hm0 (m)	peak period gauge 1 Tp (s)	peak period gauge 2 Tp (s)	overtopping volume V (l)	overtopping time t (s)	total overtopping discharge Q (l/s)	total overtopping discharge Qtot (m^3/s per m)
T - 8 - 30 - 10 - J	0,65	0,086	0,085	1,23	1,23	64,2	1800	0,036	4,458E-05
T - 9 - 30 - 10 - J	0,65	0,096	0,096	1,31	1,25	144,9	1800	0,081	1,006E-04
T - 10 - 30 - 10 - J	0,65	0,105	0,105	1,39	1,45	250,4	1800	0,139	1,739E-04
T - 12 - 30 - 20 - J	0,55	0,125	0,125	1,53	1,50	12,5	1800	0,007	8,681E-06
T - 13 - 30 - 20 - J	0,55	0,135	0,136	1,56	1,55	22,7	1800	0,013	1,576E-05
T - 14 - 30 - 20 - J	0,55	0,130	0,130	1,63	1,63	20,5	1800	0,011	1,424E-05
T - 15 - 30 - 20 - J	0,55	0,139	0,140	1,73	1,70	44,1	1800	0,025	3,063E-05
T - 16 - 30 - 20 - J	0,55	0,147	0,148	1,76	1,76	76,4	1800	0,042	5,306E-05
T - 17 - 30 - 20 - J	0,55	0,152	0,153	1,78	1,77	100,5	1800	0,056	6,979E-05
T - 18 - 30 - 20 - J	0,55	0,158	0,159	1,88	1,84	147,5	1800	0,082	1,024E-04
T - 14 - 50 - 20 - J	0,55	0,140	0,139	2,25	2,25	87,2	1800	0,048	6,056E-05
T - 15 - 50 - 20 - J	0,55	0,148	0,147	2,16	2,30	182,7	1800	0,102	1,269E-04
T - 16 - 50 - 20 - J	0,55	0,157	0,158	2,46	2,46	275,6	1800	0,153	1,914E-04
T - 15 - 40 - 20 - J	0,55	0,144	0,144	2,05	1,96	93,5	1800	0,052	6,493E-05
T - 16 - 40 - 20 - J	0,55	0,154	0,154	2,07	2,29	192,0	1800	0,107	1,333E-04

Appendix IV-1 Experiment results for total wave overtopping with JONSWAP wave spectra

Experiment results										
Experiment code	water depth d (m)	wave height gauge 1 Hm0 (m)	wave height gauge 2 Hm0 (m)	peak period Tp (s)	overtopping volume V (l)	overtopping time t (s)	total overtopping discharge Q (l/s)	total overtopping discharge Qtot (m^3/s per m)	dimensionless crest height Rc* (-)	dimensionless overtopping discharge Q* (-)
T - 13 - 30 - 10 - R	0,65	0,128	0,127	1,59	25,9	358	0,072	9,043E-05	0,5139	1,620E-04
T - 14 - 30 - 10 - R	0,65	0,141	0,139	1,64	111,0	293	0,379	4,735E-04	0,4753	7,486E-04
T - 15 - 30 - 10 - R	0,65	0,137	0,136	1,70	79,5	250	0,318	3,975E-04	0,4646	6,222E-04
T - 16 - 30 - 10 - R	0,65	0,153	0,152	1,75	158,0	192	0,823	1,029E-03	0,4263	1,396E-03
T - 17 - 30 - 10 - R	0,65	0,165	0,165	1,82	141,0	102	1,382	1,728E-03	0,3940	2,083E-03
T - 18 - 30 - 10 - R	0,65	0,163	0,161	1,85	161,8	118	1,371	1,714E-03	0,3919	2,078E-03
T - 19 - 30 - 10 - R	0,65	0,178	0,171	1,92	187,1	97,5	1,919	2,399E-03	0,3666	2,641E-03
T - 20 - 30 - 10 - R	0,65	0,197	0,186	1,97	230,0	70,7	3,253	4,066E-03	0,3425	4,009E-03
T - 21 - 30 - 10 - R	0,65	0,188	0,190	2,00	250,9	87,3	2,874	3,592E-03	0,3338	3,416E-03
T - 22 - 30 - 10 - R	0,65	0,214	0,214	2,11	197,0	45	4,378	5,472E-03	0,2981	4,379E-03
T - 18 - 15 - 10 - R	0,65	0,171	0,169	1,32	174,7	194,4	0,899	1,123E-03	0,5360	1,818E-03
T - 18 - 20 - 10 - R	0,65	0,174	0,170	1,52	213,9	155,5	1,376	1,719E-03	0,4640	2,401E-03
T - 18 - 25 - 10 - R	0,65	0,163	0,161	1,70	176,9	179,4	0,986	1,233E-03	0,4269	1,629E-03
T - 18 - 35 - 10 - R	0,65	0,156	0,159	2,00	174,2	141,1	1,235	1,543E-03	0,3654	1,758E-03
T - 18 - 40 - 10 - R	0,65	0,159	0,163	2,16	183,0	110,2	1,661	2,076E-03	0,3339	2,133E-03
T - 18 - 45 - 10 - R	0,65	0,165	0,163	2,31	214,5	104,1	2,061	2,576E-03	0,3119	2,469E-03
T - 18 - 50 - 10 - R	0,65	0,181	0,176	2,35	176,6	55,6	3,176	3,970E-03	0,2948	3,460E-03
T - 16 - 20 - 10 - R	0,65	0,140	0,139	1,43	71,7	252	0,285	3,557E-04	0,5461	6,471E-04
T - 16 - 25 - 10 - R	0,65	0,145	0,140	1,61	98,6	236	0,418	5,222E-04	0,4831	8,374E-04
T - 16 - 35 - 10 - R	0,65	0,144	0,140	1,89	134,4	191,1	0,703	8,791E-04	0,4115	1,201E-03
T - 16 - 40 - 10 - R	0,65	0,140	0,142	2,03	128,7	255,6	0,504	6,294E-04	0,3810	7,912E-04
T - 20 - 20 - 10 - R	0,65	0,179	0,178	1,61	131,1	78,3	1,674	2,093E-03	0,4286	2,640E-03
T - 20 - 25 - 10 - R	0,65	0,182	0,182	1,79	159,3	74,9	2,127	2,659E-03	0,3813	2,951E-03
T - 20 - 35 - 10 - R	0,65	0,184	0,185	2,14	214,8	68,2	3,150	3,937E-03	0,3164	3,598E-03
T - 20 - 40 - 10 - R	0,65	0,193	0,190	2,29	232,0	61,9	3,748	4,685E-03	0,2917	3,895E-03
T - 14 - 30 - 7,5 - R	0,675	0,142	0,140	1,64	143,3	101,4	1,413	1,767E-03	0,3552	2,772E-03
T - 16 - 30 - 7,5 - R	0,675	0,143	0,143	1,74	167,3	89,3	1,873	2,342E-03	0,3321	3,409E-03
T - 16 - 30 - 12,5 - R	0,625	0,158	0,158	1,75	13,8	292,4	0,047	5,899E-05	0,5228	7,707E-05
T - 18 - 30 - 7,5 - R	0,675	0,160	0,159	1,88	232,8	85,3	2,729	3,411E-03	0,2910	4,118E-03
T - 18 - 30 - 12,5 - R	0,625	0,173	0,171	1,85	89,5	175,9	0,509	6,360E-04	0,4757	7,270E-04
T - 18 - 30 - 15 - R	0,600	0,178	0,175	1,85	32,8	283,1	0,116	1,448E-04	0,5648	1,621E-04
T - 20 - 30 - 7,5 - R	0,675	0,191	0,183	2,00	202,1	39,1	5,169	6,461E-03	0,2553	6,388E-03
T - 20 - 30 - 12,5 - R	0,625	0,198	0,193	1,94	112,1	66,8	1,678	2,098E-03	0,4272	2,028E-03
T - 20 - 30 - 15 - R	0,600	0,197	0,197	1,96	94,2	231,7	0,407	5,082E-04	0,5015	4,751E-04
T - 22 - 30 - 12,5 - R	0,625	0,215	0,201	2,05	207,8	97,9	2,123	2,653E-03	0,3954	2,322E-03
T - 22 - 30 - 15 - R	0,600	0,205	0,193	2,05	73,5	175,9	0,418	5,223E-04	0,4844	4,765E-04

Appendix IV-2 Experiment results for total wave overtopping with regular waves

V

Experiment results;
Overtopping discharge directly behind the crest

Experiment results									
Experiment code	water depth d (m)	wave height gauge 1 Hm0 (m)	wave height gauge 2 Hm0 (m)	peak period gauge 1 Tp (s)	peak period gauge 2 Tp (s)	overtopping volume V (l)	overtopping time t (s)	overtopping discharge (l/s)	overtopping discharge Qover,0 (m^3/s per m)
O - 10 - 30 - 10 - J - 0	0,65	0,106	0,105	1,39	1,43	44,8	1800	0,025	3,111E-05
O - 12 - 30 - 10 - J - 0	0,65	0,126	0,125	1,53	1,55	180,1	1800	0,100	1,251E-04
O - 12 - 40 - 10 - J - 0	0,65	0,128	0,127	1,71	1,71	297,3	1800	0,165	2,065E-04

Appendix V-1 Experiment results for wave overtopping discharge directly behind the crest with JONSWAP wave spectra

Experiment code	Measured						Calculated				
	wave height gauge 1 Hs (m)	wave height gauge 2 Hs (m)	wave period T (s)	total extracted volume (l)	Over-topping volume V (l)	Over-topping time t (s)	wave length L (m)	wave steepness s (-)	breaker parameter ξ (-)	Overtopping discharge (l/s)	Overtopping discharge Qover,0 (m^3/s per m)
O - 15 - 30 - 10 - R - 0	0,139	0,139	1,68	42,5	33,3	409,97	4,41	1/32	2,82	0,081	1,015E-04
O - 16 - 30 - 10 - R - 0	0,150	0,150	1,76	120,5	110,9	446,25	4,84	3/97	2,84	0,249	3,106E-04
O - 17 - 30 - 10 - R - 0	0,164	0,164	1,80	158,1	142,8	251,96	5,06	1/31	2,77	0,567	7,084E-04
O - 18 - 30 - 10 - R - 0	0,164	0,162	1,88	168,4	153,8	301,50	5,52	1/34	2,92	0,510	6,376E-04
O - 19 - 30 - 10 - R - 0	0,183	0,175	1,90	168,4	137,8	117,40	5,64	1/32	2,84	1,174	1,467E-03
O - 20 - 30 - 10 - R - 0	0,196	0,187	1,96	214,8	192,2	104,15	6,00	1/32	2,83	1,845	2,307E-03
O - 21 - 30 - 10 - R - 0	0,185	0,187	2,00	182,7	152,1	82,31	6,25	2/67	2,89	1,848	2,310E-03
O - 22 - 30 - 10 - R - 0	0,219	0,207	2,08	264,7	243,4	69,62	6,75	3/98	2,86	3,496	4,370E-03
O - 18 - 20 - 10 - R - 0	0,172	0,171	1,52	98,8	89,3	303,12	3,61	1/21	2,30	0,295	3,683E-04
O - 18 - 25 - 10 - R - 0	0,166	0,166	1,68	115,7	102,9	271,97	4,41	2/53	2,58	0,378	4,729E-04
O - 18 - 35 - 10 - R - 0	0,158	0,159	2,02	187,6	156,4	201,63	6,37	1/40	3,16	0,776	9,696E-04
O - 18 - 40 - 10 - R - 0	0,159	0,159	2,14	209,7	158,0	167,16	7,15	1/45	3,36	0,945	1,182E-03
O - 18 - 45 - 10 - R - 0	0,165	0,162	2,31	161,4	121,3	74,16	8,33	1/51	3,58	1,636	2,045E-03
O - 18 - 50 - 10 - R - 0	0,182	0,179	2,42	245,4	200,3	87,53	9,14	1/51	3,57	2,288	2,860E-03
O - 18 - 55 - 10 - R - 0	0,162	0,159	2,50	180,5	146,4	92,47	9,76	1/61	3,92	1,583	1,979E-03
O - 16 - 25 - 10 - R - 0	0,143	0,142	1,62	41,2	32,0	443,68	4,10	1/29	2,69	0,072	9,016E-05
O - 16 - 35 - 10 - R - 0	0,143	0,141	1,88	130,7	119,8	424,59	5,52	1/39	3,13	0,282	3,527E-04
O - 16 - 40 - 10 - R - 0	0,143	0,144	2,02	126,7	111,5	276,00	6,37	1/44	3,33	0,404	5,050E-04
O - 19 - 20 - 10 - R - 0	0,180	0,181	1,55	145,8	132,2	290,37	3,75	3/62	2,27	0,455	5,691E-04
O - 19 - 25 - 10 - R - 0	0,185	0,181	1,74	171,0	154,8	170,78	4,73	1/26	2,55	0,906	1,133E-03
O - 19 - 35 - 10 - R - 0	0,190	0,181	2,05	195,3	187,4	100,91	6,56	1/36	3,01	1,857	2,321E-03
O - 19 - 40 - 10 - R - 0	0,189	0,187	2,20	233,7	197,5	92,78	7,56	1/40	3,17	2,129	2,661E-03
O - 19 - 45 - 10 - R - 0	0,174	0,171	2,35	180,9	155,6	75,25	8,62	1/51	3,56	2,068	2,585E-03
O - 20 - 20 - 10 - R - 0	0,178	0,177	1,61	147,5	130,8	248,46	4,05	1/23	2,39	0,526	6,581E-04
O - 20 - 25 - 10 - R - 0	0,181	0,179	1,79	167,4	134,0	134,22	5,00	1/28	2,64	0,998	1,248E-03
O - 20 - 35 - 10 - R - 0	0,182	0,179	2,11	208,7	171,6	89,06	6,95	1/39	3,12	1,927	2,408E-03
O - 20 - 40 - 10 - R - 0	0,194	0,190	2,26	225,6	200,2	71,22	7,97	1/42	3,24	2,811	3,514E-03
O - 20 - 45 - 10 - R - 0	0,202	0,199	2,35	233,5	212,7	54,94	8,62	2/87	3,29	3,871	4,839E-03
O - 22 - 30 - 12,5 - R - 0	0,217	0,202	2,05	179,9	157,7	100,00	6,56	2/65	2,85	1,577	1,971E-03
O - 22 - 40 - 12,5 - R - 0	0,203	0,200	2,40	193,5	167,0	84,51	8,99	1/45	3,35	1,976	2,470E-03

Appendix V-2 Experiment results for wave overtopping discharge directly behind the crest with regular waves

VI

Experiment results;
Correlation water depth and overtopping discharge

Correlation water depth and overtopping discharge, experiment O-18-30-10-R											
INPUT		**OUTPUT**									
Data		*Data*		*Overtopping volume (l)*	*Overtopping time (s)*	*Overtopping discharge (l/s)*	*Overtopping discharge (m^3/s)*	*Reduction water depth Δd (m)*	*Corrected water depth d*(m)*	*Dimensionless factor Qx/Q1*	*Compensation factor (0-1)*
Stuurfile	T007	wave height gauge 1(m)	0,167	17,8	0,0			0,0000		1,186	1,000
Wave height (m)	0,18	wave height gauge 2(m)	0,165	35,7	20,6	0,871	8,710E-04	0,0011	0,6489		
Wave period (s)	1,86	wave period gauge 1(s)	1,88	54,2	46,0	0,791	7,910E-04	0,0017	0,6483		
Water depth (m)	0,65	wave period gauge 2(s)	1,88	71,2	70,9	0,753	7,533E-04	0,0022	0,6478		
				88,8	98,9	0,718	7,182E-04	0,0028	0,6472		
		wave length (m)	5,52	103,7	124,1	0,692	6,921E-04	0,0032	0,6468	1,000	0,843
		wave steepness (-)	2/67	119,4	150,9	0,673	6,735E-04	0,0037	0,6463	0,973	0,821
		tan(a)	0,5	135,1	178,9	0,656	6,557E-04	0,0042	0,6458	0,947	0,799
		breaker parameter (-)	2,89	150,1	206,7	0,640	6,399E-04	0,0047	0,6453	0,925	0,780
				163,5	233,1	0,625	6,252E-04	0,0051	0,6449	0,903	0,762
				176,3	258,6	0,613	6,130E-04	0,0055	0,6445	0,886	0,747
				189,2	285,7	0,600	5,999E-04	0,0059	0,6441	0,867	0,731
				201,9	313,8	0,587	5,866E-04	0,0063	0,6437	0,848	0,715
				213,0	337,1	0,579	5,791E-04	0,0067	0,6433	0,837	0,706
				223,0	362,5	0,566	5,660E-04	0,0070	0,6430	0,818	0,690
		Matlab file	O007_2	234,2	388,6	0,557	5,568E-04	0,0073	0,6427	0,804	0,678
		Dasylab file	O_00003	244,9	414,9	0,547	5,473E-04	0,0077	0,6423	0,791	0,667

Appendix VI-1 Correlation between the water depth and the overtopping discharge for experiment O-18-30-10-R

Correlation water depth and overtopping discharge, experiment O-19-30-10-R											
INPUT		**OUTPUT**									
Data		*Data*		*Overtopping volume (l)*	*Overtopping time (s)*	*Overtopping discharge (l/s)*	*Overtopping discharge (m^3/s)*	*Reduction water depth Δd (m)*	*Corrected water depth d*(m)*	*Dimensionless factor Qx/Q1*	*Compensation factor (0-1)*
Stuurfile	T008	wave height gauge 1(m)	0,183	35,1	0,0			0,0000		1,211	1,000
Wave height (m)	0,19	wave height gauge 2(m)	0,176	67,6	25,0	1,301	1,301E-03	0,0021	0,6479		
Wave period (s)	1,91	wave period gauge 1(s)	1,92	89,3	42,2	1,283	1,283E-03	0,0028	0,6472		
Water depth (m)	0,65	wave period gauge 2(s)	1,92	112,7	61,1	1,270	1,270E-03	0,0035	0,6465	1,000	0,826
				135,1	80,6	1,241	1,241E-03	0,0042	0,6458	0,977	0,806
		wave length (m)	5,76	153,5	97,6	1,213	1,213E-03	0,0048	0,6452	0,954	0,788
		wave steepness (-)	3/98	174,4	117,9	1,181	1,181E-03	0,0055	0,6446	0,930	0,768
		tan(a)	0,5	189,1	134,8	1,142	1,142E-03	0,0059	0,6441	0,899	0,742
		breaker parameter (-)	2,86	203,7	152,9	1,103	1,103E-03	0,0064	0,6436	0,868	0,717
				216,8	167,0	1,088	1,088E-03	0,0068	0,6432	0,857	0,707
				232,7	185,5	1,065	1,065E-03	0,0073	0,6427	0,838	0,692
				243,9	201,0	1,039	1,039E-03	0,0076	0,6424	0,818	0,675
				256,1	216,5	1,021	1,021E-03	0,0080	0,6420	0,804	0,663
				268,3	233,1	1,000	1,000E-03	0,0084	0,6416	0,787	0,650
		Matlab file	O008_2	282,1	251,1	0,984	9,839E-04	0,0088	0,6412	0,774	0,639
		Dasylab file	O_00006	294,4	269,9	0,961	9,608E-04	0,0092	0,6408	0,756	0,624

Appendix VI-2 Correlation between the water depth and the overtopping discharge for experiment O-19-30-10-R

Correlation water depth and overtopping discharge, experiment O-20-25-10-R											
INPUT		**OUTPUT**									
Data		*Data*		*Overtopping volume (l)*	*Overtopping time (s)*	*Overtopping discharge (l/s)*	*Overtopping discharge (m^3/s)*	*Reduction water depth Δd (m)*	*Corrected water depth d*(m)*	*Dimensionless factor Qx/Q1*	*Compensation factor (0-1)*
Stuurfile	T035	wave height gauge 1(m)	0,183	41,4	0,0			0,0000		1,214	1,000
Wave height (m)	0,2	wave height gauge 2(m)	0,182	68,7	23,7	1,151	1,151E-03	0,0021	0,6479		
Wave period (s)	1,79	wave period gauge 1(s)	1,80	89,7	42,6	1,134	1,134E-03	0,0028	0,6472		
Water depth (m)	0,65	wave period gauge 2(s)	1,80	111,1	62,3	1,119	1,119E-03	0,0035	0,6465	1,000	0,824
				130,0	79,7	1,112	1,112E-03	0,0041	0,6459	0,993	0,818
		wave length (m)	5,06	150,4	101,3	1,076	1,076E-03	0,0047	0,6453	0,961	0,792
		wave steepness (-)	1/28	168,2	121,4	1,045	1,045E-03	0,0053	0,6447	0,933	0,769
		tan(a)	0,5	184,8	140,9	1,018	1,018E-03	0,0058	0,6442	0,909	0,749
		breaker parameter (-)	2,64	197,6	157,3	0,993	9,932E-04	0,0062	0,6438	0,887	0,731
				210,4	173,6	0,974	9,736E-04	0,0066	0,6434	0,870	0,717
				224,6	192,3	0,952	9,525E-04	0,0070	0,6430	0,851	0,701
				237,7	209,7	0,936	9,363E-04	0,0074	0,6426	0,837	0,689
				250,9	229,9	0,911	9,111E-04	0,0078	0,6422	0,814	0,671
				263,3	249,7	0,889	8,888E-04	0,0082	0,6418	0,794	0,654
		Matlab file	O035_2	276,9	269,5	0,874	8,739E-04	0,0087	0,6413	0,781	0,643
		Dasylab file	O_00007	289,3	289,9	0,855	8,550E-04	0,0090	0,6410	0,764	0,629

Appendix VI-3 Correlation between the water depth and the overtopping discharge for experiment O-20-25-10-R

Correlation water depth and overtopping discharge, experiment O-18-40-10-R											
INPUT		**OUTPUT**									
Data		*Data*		*Overtopping volume (l)*	*Overtopping time (s)*	*Overtopping discharge (l/s)*	*Overtopping discharge (m^3/s)*	*Reduction water depth Δd (m)*	*Corrected water depth d*(m)*	*Dimensionless factor Qx/Q1*	*Compensation factor (0-1)*
Stuurfile	T027	wave height gauge 1(m)	0,163	56,6	0,0			0,0000		1,153	1,000
Wave height (m)	0,18	wave height gauge 2(m)	0,163	78,7	18,4	1,202	1,202E-03	0,0025	0,6475		
Wave period (s)	2,15	wave period gauge 1(s)	2,14	104,3	39,8	1,198	1,198E-03	0,0033	0,6467	1,000	0,867
Water depth (m)	0,65	wave period gauge 2(s)	2,14	123,3	57,7	1,157	1,157E-03	0,0039	0,6461	0,965	0,837
				142,7	76,9	1,119	1,119E-03	0,0045	0,6455	0,934	0,810
		wave length (m)	7,15	161,8	97,0	1,085	1,085E-03	0,0051	0,6449	0,905	0,785
		wave steepness (-)	1/44	180,6	117,9	1,052	1,052E-03	0,0056	0,6444	0,877	0,761
		tan(a)	0,5	198,0	137,4	1,029	1,029E-03	0,0062	0,6438	0,859	0,745
		breaker parameter (-)	3,31	213,8	156,7	1,003	1,003E-03	0,0067	0,6433	0,837	0,726
				230,2	176,1	0,986	9,861E-04	0,0072	0,6428	0,823	0,713
				245,1	196,2	0,961	9,607E-04	0,0077	0,6423	0,802	0,695
				259,8	215,5	0,943	9,431E-04	0,0081	0,6419	0,787	0,682
		Matlab file	O027_2	274,5	235,4	0,926	9,256E-04	0,0086	0,6414	0,772	0,670
		Dasylab file	O_00008	290,0	255,9	0,912	9,121E-04	0,0091	0,6409	0,761	0,660

Appendix VI-4 Correlation between the water depth and the overtopping discharge for experiment O-18-40-10-R

Correlation water depth and overtopping discharge, experiment O-18-35-10-R											
INPUT		**OUTPUT**									
Data		*Data*		*Overtopping volume (l)*	*Overtopping time (s)*	*Overtopping discharge (l/s)*	*Overtopping discharge (m^3/s)*	*Reduction water depth Δd (m)*	*Corrected water depth d*(m)*	*Dimensionless factor Qx/Q1*	*Compensation factor (0-1)*
Stuurfile	T026	wave height gauge 1(m)	0,161	27,4	0,0			0,0000		1,194	1,000
Wave height (m)	0,18	wave height gauge 2(m)	0,162	47,0	19,1	1,026	1,026E-03	0,0015	0,6485		
Wave period (s)	2,01	wave period gauge 1(s)	2,02	63,5	38,3	0,942	9,418E-04	0,0020	0,6480		
Water depth (m)	0,65	wave period gauge 2(s)	2,02	80,1	56,3	0,936	9,361E-04	0,0025	0,6475		
				96,9	76,3	0,911	9,112E-04	0,0030	0,6470		
		wave length (m)	6,37	112,8	97,4	0,877	8,769E-04	0,0035	0,6465	1,000	0,837
		wave steepness (-)	1/39	129,4	119,0	0,857	8,574E-04	0,0040	0,6460	0,978	0,819
		tan(a)	0,5	143,7	140,6	0,827	8,269E-04	0,0045	0,6455	0,943	0,790
		breaker parameter (-)	3,13	156,0	159,5	0,806	8,065E-04	0,0049	0,6451	0,920	0,770
				169,2	178,8	0,793	7,931E-04	0,0053	0,6447	0,904	0,757
				182,4	200,4	0,773	7,733E-04	0,0057	0,6443	0,882	0,738
				196,4	223,2	0,757	7,571E-04	0,0061	0,6439	0,863	0,723
				209,6	245,3	0,743	7,429E-04	0,0066	0,6435	0,847	0,709
				222,3	268,1	0,727	7,269E-04	0,0069	0,6431	0,829	0,694
				234,6	289,7	0,715	7,152E-04	0,0073	0,6427	0,816	0,683
				246,1	311,6	0,702	7,019E-04	0,0077	0,6423	0,800	0,670
				257,4	333,2	0,690	6,902E-04	0,0080	0,6420	0,787	0,659
		Matlab file	O026_2	269,1	355,7	0,680	6,795E-04	0,0084	0,6416	0,775	0,649
		Dasylab file	O_00010	279,2	378,0	0,666	6,661E-04	0,0087	0,6413	0,760	0,636

Appendix VI-5 Correlation between the water depth and the overtopping discharge for experiment O-18-35-10-R

Correlation water depth and overtopping discharge, experiment O-20-20-10-R											
INPUT		**OUTPUT**									
Data		*Data*		*Overtopping volume (l)*	*Overtopping time (s)*	*Overtopping discharge (l/s)*	*Overtopping discharge (m^3/s)*	*Reduction water depth Δd (m)*	*Corrected water depth d*(m)*	*Dimensionless factor Qx/Q1*	*Compensation factor (0-1)*
Stuurfile	T034	wave height gauge 1(m)	0,182	18,2	0,0			0,0000		1,154	1,000
Wave height (m)	0,20	wave height gauge 2(m)	0,182	35,8	24,0	0,734	7,339E-04	0,0011	0,6489		
Wave period (s)	1,60	wave period gauge 1(s)	1,62	53,3	49,8	0,705	7,052E-04	0,0017	0,6483		
Water depth (m)	0,65	wave period gauge 2(s)	1,62	70,4	78,1	0,668	6,684E-04	0,0022	0,6478		
				87,2	109,6	0,630	6,296E-04	0,0027	0,6473		
		wave length (m)	4,10	102,4	138,4	0,608	6,084E-04	0,0032	0,6468	1,000	0,867
		wave steepness (-)	2/45	116,9	166,5	0,593	5,927E-04	0,0037	0,6463	0,974	0,844
		tan(a)	0,5	130,4	194,2	0,578	5,778E-04	0,0041	0,6459	0,950	0,823
		breaker parameter (-)	2,38	143,7	221,9	0,566	5,655E-04	0,0045	0,6455	0,929	0,805
				158,2	251,4	0,557	5,569E-04	0,0049	0,6451	0,915	0,793
				173,7	285,0	0,546	5,457E-04	0,0054	0,6446	0,897	0,777
				186,3	316,3	0,531	5,315E-04	0,0058	0,6442	0,873	0,757
				199,1	346,5	0,522	5,222E-04	0,0062	0,6438	0,858	0,744
				210,8	375,7	0,513	5,126E-04	0,0066	0,6434	0,843	0,730
				222,0	402,6	0,506	5,063E-04	0,0069	0,6431	0,832	0,721
				233,0	431,0	0,498	4,984E-04	0,0073	0,6427	0,819	0,710
				243,8	460,5	0,490	4,899E-04	0,0076	0,6424	0,805	0,698
				254,1	488,2	0,483	4,832E-04	0,0079	0,6421	0,794	0,688
				264,4	516,5	0,477	4,767E-04	0,0083	0,6417	0,783	0,679
				274,8	547,1	0,469	4,691E-04	0,0086	0,6414	0,771	0,668
		Matlab file	O034_2	285,9	578,8	0,463	4,625E-04	0,0089	0,6411	0,760	0,659
		Dasylab file	O_00011	296,4	611,5	0,455	4,550E-04	0,0093	0,6407	0,748	0,648

Appendix VI-6 Correlation between the water depth and the overtopping discharge for experiment O-20-20-10-R

VII

Experiment results;
Overtopping discharge over impermeable backfill

Experiment code	Measured						Calculated				
	wave height gauge 1 Hs (m)	wave height gauge 2 Hs (m)	wave period T (s)	total extracted volume (l)	Over-topping volume V (l)	Over-topping time t (s)	wave length L (m)	wave steepness s (-)	breaker parameter ξ (-)	Equivalent overtopping discharge Qe,over (m^3/s per m)	Equivalent dimensionless overtopping discharge Q*e,over
O - 17 - 30 - 10 - R - 0	0,164	0,164	1,80	158,1	142,8	251,96	5,06	1/31	2,77	7,564E-04	3,628E-03
O - 18 - 30 - 10 - R - 0	0,164	0,162	1,88	168,4	153,8	301,50	5,52	1/34	2,92	6,924E-04	3,403E-03
O - 19 - 30 - 10 - R - 0	0,183	0,175	1,90	168,4	137,8	117,40	5,64	1/32	2,84	1,440E-03	6,279E-03
O - 20 - 30 - 10 - R - 0	0,196	0,187	1,96	214,8	192,2	104,15	6,00	1/32	2,83	2,461E-03	9,683E-03
O - 21 - 30 - 10 - R - 0	0,185	0,187	2,00	182,7	152,1	82,31	6,25	2/67	2,89	2,317E-03	9,154E-03
O - 22 - 30 - 10 - R - 0	0,219	0,207	2,08	264,7	243,4	69,62	6,75	3/98	2,86	4,326E-03	1,466E-02
O - 18 - 20 - 10 - R - 0	0,172	0,171	1,52	98,8	89,3	303,12	3,61	1/21	2,30	3,623E-04	1,634E-03
O - 18 - 25 - 10 - R - 0	0,166	0,166	1,68	115,7	102,9	271,97	4,41	2/53	2,58	4,750E-04	2,242E-03
O - 18 - 35 - 10 - R - 0	0,158	0,159	2,02	187,6	156,4	201,63	6,37	1/40	3,16	9,791E-04	4,928E-03
O - 18 - 40 - 10 - R - 0	0,159	0,159	2,14	209,7	158,0	167,16	7,15	1/45	3,36	1,243E-03	6,282E-03
O - 18 - 45 - 10 - R - 0	0,165	0,162	2,31	161,4	121,3	74,16	8,33	1/51	3,58	2,018E-03	9,868E-03
O - 18 - 50 - 10 - R - 0	0,182	0,179	2,42	245,4	200,3	87,53	9,14	1/51	3,57	2,862E-03	1,204E-02
O - 18 - 55 - 10 - R - 0	0,162	0,159	2,50	180,5	146,4	92,47	9,76	1/61	3,92	1,968E-03	9,939E-03
O - 16 - 35 - 10 - R - 0	0,143	0,141	1,88	130,7	119,8	424,59	5,52	1/39	3,13	3,636E-04	2,194E-03
O - 16 - 40 - 10 - R - 0	0,143	0,144	2,02	126,7	111,5	276,00	6,37	1/44	3,33	5,140E-04	3,008E-03
O - 19 - 20 - 10 - R - 0	0,180	0,181	1,55	145,8	132,2	290,37	3,75	3/62	2,27	5,979E-04	2,473E-03
O - 19 - 25 - 10 - R - 0	0,185	0,181	1,74	171,0	154,8	170,78	4,73	1/26	2,55	1,141E-03	4,723E-03
O - 19 - 35 - 10 - R - 0	0,190	0,181	2,05	195,3	187,4	100,91	6,56	1/36	3,01	2,458E-03	1,016E-02
O - 19 - 40 - 10 - R - 0	0,189	0,187	2,20	233,7	197,5	92,78	7,56	1/40	3,17	2,651E-03	1,043E-02
O - 19 - 45 - 10 - R - 0	0,174	0,171	2,35	180,9	155,6	75,25	8,62	1/51	3,56	2,607E-03	1,182E-02
O - 20 - 20 - 10 - R - 0	0,178	0,177	1,61	147,5	130,8	248,46	4,05	1/23	2,39	6,898E-04	2,952E-03
O - 20 - 25 - 10 - R - 0	0,181	0,179	1,79	167,4	134,0	134,22	5,00	1/28	2,64	1,218E-03	5,115E-03
O - 20 - 35 - 10 - R - 0	0,182	0,179	2,11	208,7	171,6	89,06	6,95	1/39	3,12	2,489E-03	1,051E-02
O - 20 - 40 - 10 - R - 0	0,194	0,190	2,26	225,6	200,2	71,22	7,97	1/42	3,24	3,515E-03	1,351E-02
O - 20 - 45 - 10 - R - 0	0,202	0,199	2,35	233,5	212,7	54,94	8,62	2/87	3,29	4,571E-03	1,646E-02
O - 22 - 30 - 12,5 - R - 0	0,217	0,202	2,05	179,9	157,7	100,00	6,56	2/65	2,85	1,995E-03	6,989E-03
O - 22 - 40 - 12,5 - R - 0	0,203	0,200	2,40	193,5	167,0	84,51	8,99	1/45	3,35	2,535E-03	9,045E-03

Appendix VII-1 Experiment results: Impermeable backfill, x=0m

Experiment code	Measured						Calculated				
	wave height gauge 1 Hs (m)	wave height gauge 2 Hs (m)	wave period T (s)	total extracted volume (l)	Over-topping volume V (l)	Over-topping time t (s)	wave length L (m)	wave steepness s (-)	breaker parameter ξ (-)	Overtopping discharge Qover,x (m^3/s per m)	Dimensionless overtopping discharge Q*over,x
I - 17 - 30 - 10 - R - 5	0,166	0,166	1,80	121,2	109,8	245,03	5,06	2/61	2,76	5,601E-04	2,654E-03
I - 18 - 30 - 10 - R - 5	0,165	0,168	1,88	122,7	106,2	225,19	5,52	1/33	2,87	5,895E-04	2,734E-03
I - 19 - 30 - 10 - R - 5	0,181	0,174	1,92	180,8	151,6	152,25	5,76	1/33	2,87	1,245E-03	5,453E-03
I - 20 - 30 - 10 - R - 5	0,198	0,187	1,95	174,7	157,3	84,03	5,94	3/95	2,81	2,340E-03	9,212E-03
I - 21 - 30 - 10 - R - 5	0,188	0,189	2,00	167,8	147,4	78,88	6,25	1/33	2,88	2,336E-03	9,094E-03
I - 22 - 30 - 10 - R - 5	0,223	0,211	2,11	269,7	251,7	73,56	6,95	1/33	2,87	4,277E-03	1,410E-02
I - 18 - 20 - 10 - R - 5	0,175	0,175	1,52	108,4	96,3	517,68	3,61	3/62	2,27	2,325E-04	1,016E-03
I - 18 - 25 - 10 - R - 5	0,167	0,166	1,72	112,7	101,7	375,97	4,62	1/28	2,63	3,381E-04	1,591E-03
I - 18 - 35 - 10 - R - 5	0,160	0,161	2,02	181,9	154,4	251,75	6,37	2/79	3,14	7,666E-04	3,775E-03
I - 18 - 40 - 10 - R - 5	0,161	0,161	2,14	172,1	128,2	144,18	7,15	2/89	3,33	1,111E-03	5,494E-03
I - 18 - 45 - 10 - R - 5	0,168	0,165	2,27	169,6	129,4	91,19	8,05	1/49	3,49	1,774E-03	8,437E-03
I - 18 - 50 - 10 - R - 5	0,187	0,185	2,40	219,9	184,7	77,89	8,99	1/49	3,49	2,964E-03	1,193E-02
I - 18 - 55 - 10 - R - 5	0,163	0,159	2,50	194,2	153,9	108,28	9,76	1/61	3,92	1,777E-03	8,954E-03
I - 16 - 35 - 10 - R - 5	0,145	0,142	1,88	109,6	100,3	491,03	5,52	1/39	3,11	2,553E-04	1,518E-03
I - 16 - 40 - 10 - R - 5	0,143	0,144	2,02	111,3	99,6	316,56	6,37	1/44	3,33	3,933E-04	2,297E-03
I - 19 - 20 - 10 - R - 5	0,183	0,184	1,55	112,6	101,0	242,72	3,75	3/61	2,26	5,201E-04	2,104E-03
I - 19 - 25 - 10 - R - 5	0,188	0,185	1,75	177,8	161,3	191,29	4,78	1/26	2,55	1,054E-03	4,246E-03
I - 19 - 35 - 10 - R - 5	0,193	0,184	2,05	181,8	163,9	92,94	6,56	2/71	2,98	2,204E-03	8,901E-03
I - 19 - 40 - 10 - R - 5	0,192	0,190	2,22	268,6	200,4	103,24	7,69	2/81	3,18	2,426E-03	9,336E-03
I - 19 - 45 - 10 - R - 5	0,173	0,169	2,35	194,5	167,0	90,87	8,62	1/51	3,58	2,297E-03	1,060E-02
I - 20 - 20 - 10 - R - 5	0,181	0,181	1,61	119,7	105,3	229,62	4,05	3/67	2,37	5,732E-04	2,380E-03
I - 20 - 25 - 10 - R - 5	0,184	0,182	1,79	186,8	154,9	188,31	5,00	2/55	2,62	1,028E-03	4,211E-03
I - 20 - 35 - 10 - R - 5	0,184	0,182	2,14	206,4	171,6	92,23	7,15	2/79	3,14	2,326E-03	9,600E-03
I - 20 - 40 - 10 - R - 5	0,193	0,190	2,22	271,9	240,6	90,44	7,69	2/81	3,18	3,325E-03	1,283E-02
I - 20 - 45 - 10 - R - 5	0,204	0,201	2,35	263,4	253,6	69,28	8,62	1/43	3,27	4,576E-03	1,621E-02
I - 22 - 30 - 12,5 - R - 5	0,217	0,202	2,05	166,5	147,1	121,57	6,56	2/65	2,85	1,513E-03	5,300E-03
I - 22 - 40 - 12,5 - R - 5	0,203	0,199	2,35	184,7	150,0	88,47	8,62	1/43	3,29	2,119E-03	7,612E-03

Appendix VII-2 Experiment results: Impermeable backfill, x=0.05m

Experiment code	Measured						Calculated				
	wave height gauge 1 Hs (m)	wave height gauge 2 Hs (m)	wave period T (s)	total extracted volume (l)	Over-topping volume V (l)	Over-topping time t (s)	wave length L (m)	wave steepness s (-)	breaker parameter ξ (-)	Overtopping discharge Qover,x (m^3/s per m)	Dimensionless overtopping discharge Q*over,x
I - 17 - 30 - 10 - R - 10	0,166	0,167	1,80	124,6	112,6	237,66	5,06	3/91	2,76	5,922E-04	2,783E-03
I - 18 - 30 - 10 - R - 10	0,164	0,161	1,88	126,4	110,6	249,62	5,52	1/34	2,92	5,538E-04	2,727E-03
I - 19 - 30 - 10 - R - 10	0,181	0,174	1,92	171,2	147,3	149,09	5,76	1/33	2,87	1,235E-03	5,420E-03
I - 20 - 30 - 10 - R - 10	0,200	0,190	1,96	211,8	165,2	96,32	6,00	2/63	2,81	2,144E-03	8,254E-03
I - 21 - 30 - 10 - R - 10	0,186	0,187	2,00	178,8	157,0	86,63	6,25	1/33	2,89	2,265E-03	8,910E-03
I - 22 - 30 - 10 - R - 10	0,224	0,212	2,08	270,9	255,1	73,96	6,75	1/32	2,82	4,311E-03	1,408E-02
I - 18 - 20 - 10 - R - 10	0,173	0,174	1,52	110,5	97,9	582,46	3,61	3/62	2,27	2,101E-04	9,208E-04
I - 18 - 25 - 10 - R - 10	0,167	0,167	1,72	115,1	104,4	413,35	4,62	3/83	2,63	3,157E-04	1,475E-03
I - 18 - 35 - 10 - R - 10	0,158	0,160	2,02	177,4	150,6	257,78	6,37	1/40	3,16	7,303E-04	3,645E-03
I - 18 - 40 - 10 - R - 10	0,161	0,161	2,14	160,5	117,1	133,10	7,15	2/89	3,33	1,100E-03	5,439E-03
I - 18 - 45 - 10 - R - 10	0,169	0,166	2,29	148,5	124,7	86,43	8,19	1/49	3,51	1,803E-03	8,514E-03
I - 18 - 50 - 10 - R - 10	0,187	0,185	2,40	224,1	202,7	86,75	8,99	1/49	3,49	2,921E-03	1,176E-02
I - 18 - 55 - 10 - R - 10	0,163	0,159	2,50	168,8	148,0	101,37	9,76	1/61	3,91	1,825E-03	9,158E-03
I - 16 - 35 - 10 - R - 10	0,143	0,142	1,88	108,6	97,1	573,18	5,52	1/39	3,12	2,118E-04	1,269E-03
I - 16 - 40 - 10 - R - 10	0,143	0,144	2,02	108,2	96,9	349,38	6,37	2/89	3,33	3,467E-04	2,035E-03
I - 19 - 20 - 10 - R - 10	0,183	0,184	1,55	119,2	107,2	284,63	3,75	3/61	2,26	4,708E-04	1,904E-03
I - 19 - 25 - 10 - R - 10	0,189	0,185	1,75	176,4	161,4	195,16	4,78	1/26	2,54	1,034E-03	4,162E-03
I - 19 - 35 - 10 - R - 10	0,193	0,186	2,05	183,5	155,7	88,75	6,56	2/71	2,97	2,193E-03	8,755E-03
I - 19 - 40 - 10 - R - 10	0,193	0,192	2,22	234,3	212,3	103,47	7,69	1/40	3,17	2,565E-03	9,752E-03
I - 19 - 45 - 10 - R - 10	0,172	0,168	2,35	187,7	157,1	89,46	8,62	1/51	3,58	2,195E-03	1,019E-02
I - 20 - 20 - 10 - R - 10	0,180	0,180	1,61	115,9	100,4	233,57	4,05	2/45	2,37	5,373E-04	2,239E-03
I - 20 - 25 - 10 - R - 10	0,183	0,182	1,79	181,9	150,0	180,69	5,00	2/55	2,62	1,038E-03	4,253E-03
I - 20 - 35 - 10 - R - 10	0,183	0,180	2,14	197,7	166,1	88,72	7,15	1/40	3,15	2,340E-03	9,770E-03
I - 20 - 40 - 10 - R - 10	0,193	0,190	2,22	266,6	234,4	87,47	7,69	2/81	3,18	3,350E-03	1,289E-02
I - 20 - 45 - 10 - R - 10	0,203	0,201	2,35	277,2	267,2	73,44	8,62	1/43	3,28	4,548E-03	1,615E-02
I - 22 - 30 - 12,5 - R - 10	0,218	0,202	2,05	171,0	149,6	136,34	6,56	2/65	2,85	1,372E-03	4,811E-03
I - 22 - 40 - 12,5 - R - 10	0,203	0,199	2,35	194,7	152,8	94,74	8,62	2/87	3,29	2,016E-03	7,254E-03

Appendix VII-3 Experiment results: Impermeable backfill, x=0.10m

Experiment code	Measured						Calculated				
	wave height gauge 1 Hs (m)	wave height gauge 2 Hs (m)	wave period T (s)	total extracted volume (l)	Over-topping volume V (l)	Over-topping time t (s)	wave length L (m)	wave steepness s (-)	breaker parameter ξ (-)	Overtopping discharge Qover,x (m^3/s per m)	Dimensionless overtopping discharge Q*over,x
I - 17 - 30 - 10 - R - 15	0,165	0,166	1,80	122,1	111,0	267,57	5,06	2/61	2,76	5,186E-04	2,449E-03
I - 18 - 30 - 10 - R - 15	0,164	0,161	1,88	127,1	113,8	294,41	5,52	1/34	2,92	4,832E-04	2,377E-03
I - 19 - 30 - 10 - R - 15	0,181	0,176	1,92	165,7	142,4	147,66	5,76	1/33	2,86	1,205E-03	5,225E-03
I - 20 - 30 - 10 - R - 15	0,198	0,189	1,96	196,4	163,5	97,63	6,00	3/95	2,81	2,093E-03	8,117E-03
I - 21 - 30 - 10 - R - 15	0,186	0,188	2,00	193,7	165,3	100,29	6,25	1/33	2,88	2,060E-03	8,063E-03
I - 22 - 30 - 10 - R - 15	0,222	0,210	2,07	257,0	236,6	70,07	6,69	1/32	2,82	4,221E-03	1,398E-02
I - 18 - 20 - 10 - R - 15	0,174	0,175	1,52	110,8	101,9	856,97	3,61	2/41	2,27	1,486E-04	6,470E-04
I - 18 - 25 - 10 - R - 15	0,167	0,167	1,72	104,2	95,4	474,22	4,62	3/83	2,63	2,515E-04	1,181E-03
I - 18 - 35 - 10 - R - 15	0,159	0,160	2,02	171,7	153,9	282,84	6,37	1/40	3,15	6,802E-04	3,385E-03
I - 18 - 40 - 10 - R - 15	0,160	0,160	2,14	144,7	107,5	126,28	7,15	2/89	3,34	1,064E-03	5,301E-03
I - 18 - 45 - 10 - R - 15	0,166	0,163	2,26	191,5	128,5	100,75	7,97	1/49	3,49	1,594E-03	7,704E-03
I - 18 - 50 - 10 - R - 15	0,183	0,181	2,42	215,5	182,9	83,56	9,14	1/51	3,56	2,736E-03	1,137E-02
I - 18 - 55 - 10 - R - 15	0,162	0,159	2,50	177,1	154,0	118,31	9,76	1/61	3,92	1,627E-03	8,219E-03
I - 16 - 35 - 10 - R - 15	0,144	0,142	1,88	107,1	97,1	745,25	5,52	1/39	3,12	1,629E-04	9,727E-04
I - 16 - 40 - 10 - R - 15	0,143	0,144	2,02	102,7	92,3	388,22	6,37	2/89	3,33	2,972E-04	1,742E-03
I - 19 - 20 - 10 - R - 15	0,182	0,184	1,55	121,0	110,9	357,25	3,75	2/41	2,26	3,880E-04	1,576E-03
I - 19 - 25 - 10 - R - 15	0,188	0,184	1,75	165,0	151,2	201,09	4,78	1/26	2,55	9,399E-04	3,805E-03
I - 19 - 35 - 10 - R - 15	0,193	0,184	2,05	159,5	144,4	85,06	6,56	2/71	2,98	2,122E-03	8,559E-03
I - 19 - 40 - 10 - R - 15	0,192	0,190	2,22	216,5	197,4	98,03	7,69	2/81	3,18	2,517E-03	9,685E-03
I - 19 - 45 - 10 - R - 15	0,172	0,169	2,35	169,8	160,2	89,19	8,62	1/51	3,58	2,245E-03	1,036E-02
I - 20 - 20 - 10 - R - 15	0,178	0,179	1,61	119,3	91,3	254,59	4,05	3/68	2,38	4,483E-04	1,898E-03
I - 20 - 25 - 10 - R - 15	0,183	0,182	1,79	177,2	151,0	189,16	5,00	2/55	2,62	9,978E-04	4,115E-03
I - 20 - 35 - 10 - R - 15	0,185	0,182	2,14	179,9	163,8	86,22	7,15	2/79	3,14	2,375E-03	9,785E-03
I - 20 - 40 - 10 - R - 15	0,192	0,189	2,22	233,2	208,7	80,09	7,69	2/81	3,19	3,257E-03	1,261E-02
I - 20 - 45 - 10 - R - 15	0,205	0,202	2,40	267,6	253,3	71,25	8,99	2/89	3,34	4,444E-03	1,563E-02
I - 22 - 30 - 12,5 - R - 15	0,218	0,204	2,07	164,3	147,7	142,38	6,69	1/33	2,87	1,297E-03	4,502E-03
I - 22 - 40 - 12,5 - R - 15	0,203	0,199	2,35	182,7	153,0	94,78	8,62	2/87	3,29	2,018E-03	7,261E-03

Appendix VII-4 Experiment results: Impermeable backfill, x=0.15m

Experiment code	Measured						Calculated				
	wave height gauge 1 Hs (m)	wave height gauge 2 Hs (m)	wave period T (s)	total extracted volume (l)	Over-topping volume V (l)	Over-topping time t (s)	wave length L (m)	wave steepness s (-)	breaker parameter ξ (-)	Overtopping discharge Qover,x (m^3/s per m)	Dimensionless overtopping discharge Q*over,x
I - 17 - 30 - 10 - R - 20	0,164	0,165	1,80	123,2	111,4	348,12	5,06	3/92	2,77	4,000E-04	1,905E-03
I - 18 - 30 - 10 - R - 20	0,164	0,162	1,88	119,4	108,1	334,94	5,52	1/34	2,92	4,034E-04	1,974E-03
I - 19 - 30 - 10 - R - 20	0,181	0,174	1,92	163,4	141,6	162,18	5,76	1/33	2,87	1,091E-03	4,781E-03
I - 20 - 30 - 10 - R - 20	0,199	0,189	1,96	185,1	165,7	104,15	6,00	3/95	2,82	1,989E-03	7,725E-03
I - 21 - 30 - 10 - R - 20	0,185	0,187	2,00	196,8	173,0	111,35	6,25	2/67	2,89	1,942E-03	7,660E-03
I - 22 - 30 - 10 - R - 20	0,223	0,211	2,07	278,8	260,0	78,35	6,69	3/95	2,82	4,148E-03	1,366E-02
I - 18 - 20 - 10 - R - 20	0,175	0,176	1,52	107,2	97,3	1408,06	3,61	2/41	2,26	8,638E-05	3,736E-04
I - 18 - 25 - 10 - R - 20	0,166	0,166	1,68	106,3	96,0	738,81	4,41	2/53	2,58	1,624E-04	7,686E-04
I - 18 - 35 - 10 - R - 20	0,159	0,161	2,02	175,4	155,2	325,53	6,37	1/40	3,15	5,960E-04	2,957E-03
I - 18 - 40 - 10 - R - 20	0,160	0,160	2,14	157,9	123,9	163,06	7,15	1/45	3,34	9,498E-04	4,744E-03
I - 18 - 45 - 10 - R - 20	0,166	0,163	2,27	184,1	132,2	114,81	8,05	2/99	3,51	1,439E-03	6,982E-03
I - 18 - 50 - 10 - R - 20	0,183	0,181	2,42	229,1	201,5	94,06	9,14	1/51	3,56	2,678E-03	1,112E-02
I - 18 - 55 - 10 - R - 20	0,163	0,159	2,50	187,6	165,1	139,00	9,76	1/62	3,92	1,485E-03	7,506E-03
I - 16 - 35 - 10 - R - 20	0,144	0,142	1,88	96,2	85,9	1056,72	5,52	1/39	3,11	1,016E-04	6,042E-04
I - 16 - 40 - 10 - R - 20	0,144	0,144	2,02	108,7	97,4	525,94	6,37	1/44	3,32	2,315E-04	1,351E-03
I - 19 - 20 - 10 - R - 20	0,182	0,183	1,55	112,4	101,2	408,69	3,75	2/41	2,26	3,095E-04	1,263E-03
I - 19 - 25 - 10 - R - 20	0,188	0,184	1,75	168,8	154,1	221,72	4,78	1/26	2,55	8,688E-04	3,513E-03
I - 19 - 35 - 10 - R - 20	0,193	0,185	2,05	183,5	143,3	88,97	6,56	2/71	2,98	2,013E-03	8,088E-03
I - 19 - 40 - 10 - R - 20	0,191	0,191	2,22	226,7	192,3	101,10	7,69	1/40	3,17	2,378E-03	9,090E-03
I - 19 - 45 - 10 - R - 20	0,171	0,166	2,33	195,0	171,4	107,71	8,48	1/51	3,57	1,989E-03	9,358E-03
I - 20 - 20 - 10 - R - 20	0,178	0,178	1,61	126,5	96,7	350,57	4,05	4/91	2,38	3,448E-04	1,464E-03
I - 20 - 25 - 10 - R - 20	0,183	0,182	1,79	173,8	146,8	215,72	5,00	2/55	2,62	8,506E-04	3,499E-03
I - 20 - 35 - 10 - R - 20	0,183	0,180	2,11	185,6	166,9	91,66	6,95	2/77	3,10	2,276E-03	9,488E-03
I - 20 - 40 - 10 - R - 20	0,192	0,189	2,22	245,4	223,6	86,46	7,69	2/81	3,19	3,233E-03	1,251E-02
I - 20 - 45 - 10 - R - 20	0,204	0,201	2,38	273,3	259,8	74,31	8,84	1/44	3,31	4,370E-03	1,545E-02
I - 22 - 30 - 12,5 - R - 20	0,218	0,202	2,05	170,2	150,4	155,00	6,56	2/65	2,85	1,213E-03	4,252E-03
I - 22 - 40 - 12,5 - R - 20	0,203	0,200	2,38	178,8	154,0	95,78	8,84	1/44	3,32	2,010E-03	7,149E-03

Appendix VII-5 Experiment results: Impermeable backfill, x=0.20m

Experiment code	Measured						Calculated				
	wave height gauge 1 Hs (m)	wave height gauge 2 Hs (m)	wave period T (s)	total extracted volume (l)	Over-topping volume V (l)	Over-topping time t (s)	wave length L (m)	wave steepness s (-)	breaker parameter ξ (-)	Overtopping discharge Qover,x (m^3/s per m)	Dimensionless overtopping discharge Q*over,x
I - 17 - 30 - 10 - R - 30	0,166	0,167	1,79	109,0	98,6	412,09	5,00	1/30	2,74	2,991E-04	1,402E-03
I - 18 - 30 - 10 - R - 30	0,165	0,162	1,88	109,9	98,7	483,19	5,52	1/34	2,91	2,553E-04	1,245E-03
I - 19 - 30 - 10 - R - 30	0,181	0,174	1,92	177,3	154,6	210,28	5,76	1/33	2,87	9,190E-04	4,038E-03
I - 20 - 30 - 10 - R - 30	0,196	0,187	1,95	173,8	150,8	96,21	5,94	1/32	2,82	1,959E-03	7,737E-03
I - 21 - 30 - 10 - R - 30	0,185	0,187	2,00	171,8	148,4	96,53	6,25	2/67	2,89	1,922E-03	7,588E-03
I - 22 - 30 - 10 - R - 30	0,224	0,212	2,07	296,2	272,4	84,57	6,69	2/63	2,81	4,026E-03	1,318E-02
I - 18 - 20 - 10 - R - 30	0,175	0,176	1,52	41,6	37,2	1649,03	3,61	2/41	2,26	2,820E-05	1,219E-04
I - 18 - 25 - 10 - R - 30	0,168	0,167	1,68	59,5	49,3	1007,82	4,41	3/79	2,57	6,115E-05	2,860E-04
I - 18 - 35 - 10 - R - 30	0,159	0,161	2,02	185,3	152,7	469,75	6,37	2/79	3,14	4,063E-04	2,006E-03
I - 18 - 40 - 10 - R - 30	0,160	0,160	2,14	161,2	129,6	204,16	7,15	1/45	3,34	7,935E-04	3,964E-03
I - 18 - 45 - 10 - R - 30	0,167	0,165	2,27	192,5	141,2	127,37	8,05	1/49	3,49	1,386E-03	6,621E-03
I - 18 - 50 - 10 - R - 30	0,183	0,181	2,42	229,4	203,6	96,90	9,14	1/50	3,55	2,626E-03	1,087E-02
I - 18 - 55 - 10 - R - 30	0,162	0,158	2,50	175,0	154,8	135,91	9,76	1/62	3,92	1,424E-03	7,205E-03
I - 16 - 35 - 10 - R - 30	0,145	0,143	1,88	33,5	30,9	984,03	5,52	2/77	3,11	3,925E-05	2,321E-04
I - 16 - 40 - 10 - R - 30	0,144	0,144	2,02	75,8	65,7	730,10	6,37	1/44	3,32	1,125E-04	6,548E-04
I - 19 - 20 - 10 - R - 30	0,182	0,183	1,55	113,2	102,0	697,83	3,75	2/41	2,26	1,827E-04	7,451E-04
I - 19 - 25 - 10 - R - 30	0,188	0,184	1,75	175,4	155,0	271,22	4,78	1/26	2,55	7,144E-04	2,885E-03
I - 19 - 35 - 10 - R - 30	0,193	0,185	2,05	184,1	156,6	102,81	6,56	2/71	2,98	1,904E-03	7,633E-03
I - 19 - 40 - 10 - R - 30	0,191	0,191	2,22	212,3	192,1	104,09	7,69	1/40	3,17	2,307E-03	8,804E-03
I - 19 - 45 - 10 - R - 30	0,170	0,166	2,31	178,5	156,6	100,44	8,33	1/50	3,55	1,949E-03	9,231E-03
I - 20 - 20 - 10 - R - 30	0,179	0,180	1,62	106,2	96,5	516,25	4,10	4/91	2,39	2,337E-04	9,782E-04
I - 20 - 25 - 10 - R - 30	0,183	0,184	1,79	169,0	145,7	264,34	5,00	1/27	2,61	6,890E-04	2,794E-03
I - 20 - 35 - 10 - R - 30	0,181	0,179	2,11	175,8	154,1	91,22	6,95	1/39	3,11	2,112E-03	8,894E-03
I - 20 - 40 - 10 - R - 30	0,192	0,189	2,22	250,8	227,2	94,63	7,69	1/41	3,19	3,001E-03	1,166E-02
I - 20 - 45 - 10 - R - 30	0,202	0,200	2,35	251,9	233,7	67,31	8,62	1/43	3,28	4,340E-03	1,548E-02
I - 22 - 30 - 12,5 - R - 30	0,218	0,203	2,05	158,3	144,0	173,69	6,56	3/97	2,85	1,036E-03	3,630E-03
I - 22 - 40 - 12,5 - R - 30	0,204	0,201	2,38	179,1	155,3	99,62	8,84	1/44	3,32	1,949E-03	6,927E-03

Appendix VII-6 Experiment results: Impermeable backfill, x=0.30m

Experiment code	Measured						Calculated				
	wave height gauge 1 Hs (m)	wave height gauge 2 Hs (m)	wave period T (s)	total extracted volume (l)	Over-topping volume V (l)	Over-topping time t (s)	wave length L (m)	wave steepness s (-)	breaker parameter ξ (-)	Overtopping discharge Qover,x (m^3/s per m)	Dimensionless overtopping discharge Q*over,x
I - 17 - 30 - 10 - R - 40	0,164	0,165	1,80	112,1	100,8	646,90	5,06	3/92	2,77	1,948E-04	9,266E-04
I - 18 - 30 - 10 - R - 40	0,165	0,162	1,88	113,3	100,8	764,87	5,52	1/34	2,91	1,647E-04	8,039E-04
I - 19 - 30 - 10 - R - 40	0,180	0,175	1,92	199,0	176,5	256,63	5,76	1/33	2,87	8,597E-04	3,744E-03
I - 20 - 30 - 10 - R - 40	0,199	0,190	1,96	185,4	148,8	101,85	6,00	3/95	2,81	1,826E-03	7,060E-03
I - 21 - 30 - 10 - R - 40	0,185	0,187	2,00	182,2	153,4	104,34	6,25	2/67	2,89	1,838E-03	7,262E-03
I - 22 - 30 - 10 - R - 40	0,222	0,210	2,08	275,3	254,2	77,75	6,75	1/32	2,84	4,087E-03	1,356E-02
I - 18 - 20 - 10 - R - 40											
I - 18 - 25 - 10 - R - 40											
I - 18 - 35 - 10 - R - 40	0,159	0,160	2,02	180,2	158,8	544,19	6,37	1/40	3,16	3,648E-04	1,820E-03
I - 18 - 40 - 10 - R - 40	0,159	0,160	2,14	155,9	127,1	210,72	7,15	1/45	3,34	7,540E-04	3,764E-03
I - 18 - 45 - 10 - R - 40	0,167	0,165	2,30	209,1	154,0	151,47	8,26	1/50	3,54	1,271E-03	6,050E-03
I - 18 - 50 - 10 - R - 40	0,183	0,181	2,42	223,0	195,0	93,38	9,14	1/51	3,55	2,610E-03	1,083E-02
I - 18 - 55 - 10 - R - 40	0,162	0,158	2,50	178,4	154,2	146,40	9,76	1/62	3,92	1,317E-03	6,663E-03
I - 16 - 35 - 10 - R - 40											
I - 16 - 40 - 10 - R - 40	0,143	0,144	2,02	61,1	50,9	748,35	6,37	1/44	3,33	8,502E-05	4,966E-04
I - 19 - 20 - 10 - R - 40	0,182	0,183	1,55	109,4	98,2	874,88	3,75	2/41	2,27	1,403E-04	5,740E-04
I - 19 - 25 - 10 - R - 40	0,188	0,185	1,72	162,9	151,0	278,57	4,62	1/25	2,50	6,776E-04	2,726E-03
I - 19 - 35 - 10 - R - 40	0,194	0,186	2,07	214,5	168,0	117,69	6,69	1/36	3,00	1,784E-03	7,127E-03
I - 19 - 40 - 10 - R - 40	0,193	0,191	2,22	225,3	201,5	105,69	7,69	1/40	3,17	2,383E-03	9,093E-03
I - 19 - 45 - 10 - R - 40	0,174	0,170	2,35	190,6	164,8	103,29	8,62	1/51	3,56	1,994E-03	9,075E-03
I - 20 - 20 - 10 - R - 40	0,180	0,180	1,61	106,6	95,8	514,47	4,05	2/45	2,37	2,328E-04	9,722E-04
I - 20 - 25 - 10 - R - 40	0,184	0,183	1,80	173,7	149,8	258,12	5,06	2/55	2,63	7,254E-04	2,947E-03
I - 20 - 35 - 10 - R - 40	0,186	0,184	2,13	191,5	155,9	95,60	7,08	2/77	3,11	2,038E-03	8,269E-03
I - 20 - 40 - 10 - R - 40	0,194	0,191	2,29	278,7	241,9	100,82	8,19	1/43	3,27	2,999E-03	1,145E-02
I - 20 - 45 - 10 - R - 40	0,204	0,202	2,35	265,6	249,7	71,44	8,62	1/43	3,27	4,369E-03	1,542E-02
I - 22 - 30 - 12,5 - R - 40	0,216	0,203	2,05	173,7	152,9	219,06	6,56	3/97	2,84	8,725E-04	3,038E-03
I - 22 - 40 - 12,5 - R - 40	0,203	0,200	2,38	192,6	166,5	119,19	8,84	1/44	3,32	1,746E-03	6,220E-03

Appendix VII-7 Experiment results: Impermeable backfill, x=0.40m

Experiment code	Measured						Calculated				
	wave height gauge 1 Hs (m)	wave height gauge 2 Hs (m)	wave period T (s)	total extracted volume (l)	Over-topping volume V (l)	Over-topping time t (s)	wave length L (m)	wave steepness s (-)	breaker parameter ξ (-)	Overtopping discharge Qover,x (m^3/s per m)	Dimensionless overtopping discharge Q*over,x
I - 17 - 30 - 10 - R - 60	0,167	0,168	1,80	82,4	70,0	1031,24	5,06	1/30	2,74	8,485E-05	3,925E-04
I - 18 - 30 - 10 - R - 60	0,166	0,163	1,87	60,2	49,8	1393,60	5,46	2/67	2,89	4,467E-05	2,165E-04
I - 19 - 30 - 10 - R - 60	0,182	0,177	1,92	181,7	164,1	293,63	5,76	2/65	2,85	6,986E-04	2,992E-03
I - 20 - 30 - 10 - R - 60	0,201	0,191	1,96	169,2	149,4	103,56	6,00	2/63	2,81	1,803E-03	6,922E-03
I - 21 - 30 - 10 - R - 60	0,186	0,188	2,00	175,6	154,7	110,29	6,25	1/33	2,88	1,753E-03	6,886E-03
I - 22 - 30 - 10 - R - 60	0,223	0,212	2,11	286,0	265,8	82,84	6,95	1/33	2,86	4,011E-03	1,311E-02
I - 18 - 20 - 10 - R - 60											
I - 18 - 25 - 10 - R - 60											
I - 18 - 35 - 10 - R - 60	0,160	0,162	2,02	144,5	129,9	628,72	6,37	2/79	3,14	2,583E-04	1,266E-03
I - 18 - 40 - 10 - R - 60	0,162	0,163	2,14	155,2	128,2	252,84	7,15	1/44	3,32	6,338E-04	3,087E-03
I - 18 - 45 - 10 - R - 60	0,168	0,166	2,27	196,7	153,5	158,38	8,05	2/97	3,49	1,211E-03	5,743E-03
I - 18 - 50 - 10 - R - 60	0,185	0,183	2,42	223,2	181,4	89,62	9,14	1/50	3,54	2,530E-03	1,036E-02
I - 18 - 55 - 10 - R - 60	0,165	0,160	2,52	205,5	149,7	160,30	9,91	1/62	3,93	1,167E-03	5,802E-03
I - 16 - 35 - 10 - R - 60											
I - 16 - 40 - 10 - R - 60											
I - 19 - 20 - 10 - R - 60											
I - 19 - 25 - 10 - R - 60	0,190	0,187	1,76	164,1	149,4	375,47	4,84	1/26	2,54	4,974E-04	1,963E-03
I - 19 - 35 - 10 - R - 60	0,193	0,184	2,05	170,8	150,7	109,40	6,56	2/71	2,99	1,722E-03	6,961E-03
I - 19 - 40 - 10 - R - 60	0,192	0,190	2,22	211,4	186,1	106,91	7,69	2/81	3,18	2,176E-03	8,384E-03
I - 19 - 45 - 10 - R - 60	0,172	0,167	2,33	198,8	155,0	115,15	8,48	1/51	3,56	1,683E-03	7,870E-03
I - 20 - 20 - 10 - R - 60	0,182	0,181	1,61	54,1	44,7	848,40	4,05	3/67	2,36	6,586E-05	2,725E-04
I - 20 - 25 - 10 - R - 60	0,183	0,184	1,80	175,1	154,1	426,84	5,06	2/55	2,62	4,513E-04	1,831E-03
I - 20 - 35 - 10 - R - 60	0,183	0,181	2,11	216,5	160,8	116,65	6,95	2/77	3,10	1,723E-03	7,170E-03
I - 20 - 40 - 10 - R - 60	0,193	0,190	2,29	270,8	229,0	102,97	8,19	1/43	3,28	2,780E-03	1,071E-02
I - 20 - 45 - 10 - R - 60	0,206	0,202	2,38	280,6	266,1	78,35	8,84	1/44	3,31	4,245E-03	1,490E-02
I - 22 - 30 - 12,5 - R - 60	0,216	0,203	2,05	159,8	143,3	305,25	6,56	3/97	2,84	5,868E-04	2,043E-03
I - 22 - 40 - 12,5 - R - 60	0,201	0,198	2,35	175,2	141,4	127,12	8,62	2/87	3,30	1,390E-03	5,035E-03

Appendix VII-8 Experiment results: Impermeable backfill, x=0.60m

VIII

Impermeable backfill; Dimensionless parameters

Impermeable length x (m)	Dimensionless overtopping discharge								
	I-17-30-10-R	I-18-30-10-R	I-19-30-10-R	I-20-30-10-R	I-21-30-10-R	I-22-30-10-R	I-18-20-10-R	I-18-25-10-R	I-18-35-10-R
0,000	3,628E-03	3,403E-03	6,279E-03	9,683E-03	9,154E-03	1,466E-02	1,634E-03	2,242E-03	4,928E-03
0,050	2,654E-03	2,734E-03	5,453E-03	9,212E-03	9,094E-03	1,410E-02	1,016E-03	1,591E-03	3,775E-03
0,100	2,783E-03	2,727E-03	5,420E-03	8,254E-03	8,910E-03	1,408E-02	9,208E-04	1,475E-03	3,645E-03
0,150	2,449E-03	2,377E-03	5,225E-03	8,117E-03	8,063E-03	1,398E-02	6,470E-04	1,181E-03	3,385E-03
0,200	1,905E-03	1,974E-03	4,781E-03	7,725E-03	7,660E-03	1,366E-02	3,736E-04	7,686E-04	2,957E-03
0,300	1,402E-03	1,245E-03	4,038E-03	7,737E-03	7,588E-03	1,318E-02	1,219E-04	2,860E-04	2,006E-03
0,400	9,266E-04	8,039E-04	3,744E-03	7,060E-03	7,262E-03	1,356E-02			1,820E-03
0,600	3,925E-04	2,165E-04	2,992E-03	6,922E-03	6,886E-03	1,311E-02			1,266E-03

Impermeable length x (m)	Dimensionless overtopping discharge								
	I-18-40-10-R	I-18-45-10-R	I-18-50-10-R	I-18-55-10-R	I-16-35-10-R	I-16-40-10-R	I-19-20-10-R	I-19-25-10-R	I-19-35-10-R
0,000	6,282E-03	9,868E-03	1,204E-02	9,939E-03	2,194E-03	3,008E-03	2,473E-03	4,723E-03	1,016E-02
0,050	5,494E-03	8,437E-03	1,193E-02	8,954E-03	1,518E-03	2,297E-03	2,104E-03	4,246E-03	8,901E-03
0,100	5,439E-03	8,514E-03	1,176E-02	9,158E-03	1,269E-03	2,035E-03	1,904E-03	4,162E-03	8,755E-03
0,150	5,301E-03	7,704E-03	1,137E-02	8,219E-03	9,727E-04	1,742E-03	1,576E-03	3,805E-03	8,559E-03
0,200	4,744E-03	6,982E-03	1,112E-02	7,506E-03	6,042E-04	1,351E-03	1,263E-03	3,513E-03	8,088E-03
0,300	3,964E-03	6,621E-03	1,087E-02	7,205E-03	2,321E-04	6,548E-04	7,451E-04	2,885E-03	7,633E-03
0,400	3,764E-03	6,050E-03	1,083E-02	6,663E-03		4,966E-04	5,740E-04	2,726E-03	7,127E-03
0,600	3,087E-03	5,743E-03	1,036E-02	5,802E-03				1,963E-03	6,961E-03

Impermeable length x (m)	Dimensionless overtopping discharge								
	I-19-40-10-R	I-19-45-10-R	I-20-20-10-R	I-20-25-10-R	I-20-35-10-R	I-20-40-10-R	I-20-45-10-R	I-20-40-13-R	I-20-45-13-R
0,000	1,043E-02	1,182E-02	2,952E-03	5,115E-03	1,051E-02	1,351E-02	1,646E-02	6,989E-03	9,045E-03
0,050	9,336E-03	1,060E-02	2,380E-03	4,211E-03	9,600E-03	1,283E-02	1,621E-02	5,300E-03	7,612E-03
0,100	9,752E-03	1,019E-02	2,239E-03	4,253E-03	9,770E-03	1,289E-02	1,615E-02	4,811E-03	7,254E-03
0,150	9,685E-03	1,036E-02	1,898E-03	4,115E-03	9,785E-03	1,261E-02	1,563E-02	4,502E-03	7,261E-03
0,200	9,090E-03	9,358E-03	1,464E-03	3,499E-03	9,488E-03	1,251E-02	1,545E-02	4,252E-03	7,149E-03
0,300	8,804E-03	9,231E-03	9,782E-04	2,794E-03	8,894E-03	1,166E-02	1,548E-02	3,630E-03	6,927E-03
0,400	9,093E-03	9,075E-03	9,722E-04	2,947E-03	8,269E-03	1,145E-02	1,542E-02	3,038E-03	6,220E-03
0,600	8,384E-03	7,870E-03	2,725E-04	1,831E-03	7,170E-03	1,071E-02	1,490E-02	2,043E-03	5,035E-03

Appendix VIII-1 Dimensionless overtopping discharges over impermeable backfill

Impermeable length x (m)	Reduction factor Cr of dimensionless overtopping discharge								
	I-17-30-10-R	I-18-30-10-R	I-19-30-10-R	I-20-30-10-R	I-21-30-10-R	I-22-30-10-R	I-18-20-10-R	I-18-25-10-R	I-18-35-10-R
0,000	1,000	1,000	1,000	1,000	1,000	1,000	1,000	1,000	1,000
0,050	0,732	0,803	0,869	0,951	0,993	0,961	0,622	0,709	0,766
0,100	0,767	0,801	0,863	0,852	0,973	0,960	0,564	0,658	0,740
0,150	0,675	0,699	0,832	0,838	0,881	0,953	0,396	0,527	0,687
0,200	0,525	0,580	0,761	0,798	0,837	0,932	0,229	0,343	0,600
0,300	0,386	0,366	0,643	0,799	0,829	0,899	0,075	0,128	0,407
0,400	0,255	0,236	0,596	0,729	0,793	0,925			0,369
0,600	0,108	0,064	0,477	0,715	0,752	0,894			0,257

Impermeable length x (m)	Reduction factor Cr of dimensionless overtopping discharge								
	I-18-40-10-R	I-18-45-10-R	I-18-50-10-R	I-18-55-10-R	I-16-35-10-R	I-16-40-10-R	I-19-20-10-R	I-19-25-10-R	I-19-35-10-R
0,000	1,000	1,000	1,000	1,000	1,000	1,000	1,000	1,000	1,000
0,050	0,875	0,855	0,991	0,901	0,692	0,764	0,851	0,899	0,877
0,100	0,866	0,863	0,977	0,921	0,578	0,676	0,770	0,881	0,862
0,150	0,844	0,781	0,944	0,827	0,443	0,579	0,637	0,806	0,843
0,200	0,755	0,708	0,924	0,755	0,275	0,449	0,511	0,744	0,796
0,300	0,631	0,671	0,902	0,725	0,106	0,218	0,301	0,611	0,752
0,400	0,599	0,613	0,899	0,670		0,165	0,232	0,577	0,702
0,600	0,491	0,582	0,860	0,584				0,416	0,685

Impermeable length x (m)	Reduction factor Cr of dimensionless overtopping discharge								
	I-19-40-10-R	I-19-45-10-R	I-20-20-10-R	I-20-25-10-R	I-20-35-10-R	I-20-40-10-R	I-20-45-10-R	I-20-40-13-R	I-20-45-13-R
0,000	1,000	1,000	1,000	1,000	1,000	1,000	1,000	1,000	1,000
0,050	0,895	0,897	0,806	0,823	0,913	0,950	0,985	0,758	0,842
0,100	0,935	0,862	0,759	0,831	0,929	0,954	0,981	0,688	0,802
0,150	0,929	0,876	0,643	0,804	0,931	0,933	0,949	0,644	0,803
0,200	0,872	0,792	0,496	0,684	0,903	0,926	0,939	0,608	0,790
0,300	0,844	0,781	0,331	0,546	0,846	0,863	0,940	0,519	0,766
0,400	0,872	0,768	0,329	0,576	0,787	0,848	0,936	0,435	0,688
0,600	0,804	0,666	0,092	0,358	0,682	0,793	0,905	0,292	0,557

Appendix VIII-2 Reduction factor Cr of dimensionless overtopping discharges over impermeable backfill

Impermeable length x (m)	Dimensionless impermeable distance x/Hs								
	I-17-30-10-R	I-18-30-10-R	I-19-30-10-R	I-20-30-10-R	I-21-30-10-R	I-22-30-10-R	I-18-20-10-R	I-18-25-10-R	I-18-35-10-R
0,000	0,000	0,000	0,000	0,000	0,000	0,000	0,000	0,000	0,000
0,050	0,302	0,298	0,287	0,267	0,265	0,237	0,286	0,301	0,310
0,100	0,601	0,620	0,574	0,526	0,533	0,471	0,573	0,598	0,625
0,150	0,904	0,929	0,854	0,793	0,797	0,713	0,856	0,900	0,936
0,200	1,212	1,234	1,146	1,058	1,069	0,948	1,137	1,207	1,245
0,300	1,799	1,846	1,723	1,604	1,604	1,416	1,704	1,796	1,862
0,400	2,422	2,464	2,284	2,109	2,140	1,905			2,500
0,600	3,566	3,678	3,388	3,149	3,197	2,830			3,706

Impermeable length x (m)	Dimensionless impermeable distance x/Hs								
	I-18-40-10-R	I-18-45-10-R	I-18-50-10-R	I-18-55-10-R	I-16-35-10-R	I-16-40-10-R	I-19-20-10-R	I-19-25-10-R	I-19-35-10-R
0,000	0,000	0,000	0,000	0,000	0,000	0,000	0,000	0,000	0,000
0,050	0,311	0,303	0,271	0,315	0,351	0,347	0,272	0,271	0,271
0,100	0,621	0,602	0,542	0,627	0,706	0,696	0,543	0,542	0,539
0,150	0,937	0,918	0,830	0,945	1,057	1,044	0,817	0,816	0,814
0,200	1,251	1,227	1,106	1,261	1,405	1,388	1,093	1,087	1,082
0,300	1,877	1,822	1,655	1,893	2,100	2,078	1,639	1,628	1,621
0,400	2,501	2,423	2,210	2,524		2,777	2,190	2,166	2,156
0,600	3,690	3,625	3,287	3,741				3,208	3,259

Impermeable length x (m)	Dimensionless impermeable distance x/Hs								
	I-19-40-10-R	I-19-45-10-R	I-20-20-10-R	I-20-25-10-R	I-20-35-10-R	I-20-40-10-R	I-20-45-10-R	I-20-40-13-R	I-20-45-13-R
0,000	0,000	0,000	0,000	0,000	0,000	0,000	0,000	0,000	0,000
0,050	0,263	0,297	0,276	0,274	0,275	0,263	0,249	0,247	0,251
0,100	0,522	0,596	0,554	0,548	0,555	0,526	0,498	0,494	0,503
0,150	0,788	0,890	0,840	0,826	0,825	0,792	0,743	0,736	0,754
0,200	1,047	1,202	1,123	1,099	1,109	1,055	0,994	0,988	0,998
0,300	1,568	1,811	1,668	1,633	1,675	1,587	1,499	1,481	1,496
0,400	2,091	2,351	2,221	2,180	2,178	2,092	1,985	1,967	1,997
0,600	3,157	3,592	3,310	3,268	3,323	3,156	2,966	2,951	3,029

Appendix VIII-3 Dimensionless permeable distance x/H

Impermeable length x (m)	Dimensionless impermeable distance x/Hs * 1/(H*T*)^6								
	I-17-30-10-R	I-18-30-10-R	I-19-30-10-R	I-20-30-10-R	I-21-30-10-R	I-22-30-10-R	I-18-20-10-R	I-18-25-10-R	I-18-35-10-R
0,000	0,000E+00	0,000E+00	0,000E+00	0,000E+00	0,000E+00	0,000E+00	0,000E+00	0,000E+00	0,000E+00
0,050	4,563E-10	3,178E-10	2,149E-10	1,189E-10	9,692E-11	3,232E-11	8,626E-10	5,795E-10	2,733E-10
0,100	8,779E-10	8,409E-10	4,331E-10	2,078E-10	2,033E-10	6,738E-11	1,748E-09	1,124E-09	5,824E-10
0,150	1,348E-09	1,256E-09	6,131E-10	3,221E-10	2,979E-10	1,112E-10	2,541E-09	1,723E-09	8,621E-10
0,200	1,871E-09	1,633E-09	8,590E-10	4,331E-10	4,119E-10	1,446E-10	3,289E-09	2,743E-09	1,133E-09
0,300	2,693E-09	2,408E-09	1,306E-09	7,233E-10	6,214E-10	2,106E-10	4,916E-09	3,897E-09	1,660E-09
0,400	3,718E-09	3,225E-09	1,672E-09	8,469E-10	8,310E-10	2,907E-10			2,326E-09
0,600	4,896E-09	4,835E-09	2,321E-09	1,229E-09	1,211E-09	3,736E-10			3,210E-09

Impermeable length x (m)	Dimensionless impermeable distance x/Hs * 1/(H*T*)^6								
	I-18-40-10-R	I-18-45-10-R	I-18-50-10-R	I-18-55-10-R	I-16-35-10-R	I-16-40-10-R	I-19-20-10-R	I-19-25-10-R	I-19-35-10-R
0,000	0,000E+00	0,000E+00	0,000E+00	0,000E+00	0,000E+00	0,000E+00	0,000E+00	0,000E+00	0,000E+00
0,050	1,968E-10	1,154E-10	3,795E-11	8,477E-11	1,012E-09	6,060E-10	5,345E-10	2,534E-10	9,910E-11
0,100	3,945E-10	2,115E-10	7,605E-11	1,661E-10	2,104E-09	1,239E-09	1,068E-09	5,050E-10	1,880E-10
0,150	6,122E-10	3,829E-10	1,256E-10	2,570E-10	3,105E-09	1,848E-09	1,634E-09	7,779E-10	2,957E-10
0,200	8,267E-10	5,060E-10	1,673E-10	3,439E-10	4,055E-09	2,415E-09	2,226E-09	1,031E-09	3,870E-10
0,300	1,240E-09	7,074E-10	2,462E-10	5,184E-10	5,932E-09	3,580E-09	3,333E-09	1,536E-09	5,749E-10
0,400	1,650E-09	8,567E-10	3,318E-10	6,912E-10		4,850E-09	4,510E-09	2,233E-09	7,110E-10
0,600	2,204E-09	1,364E-09	4,685E-10	9,085E-10				2,669E-09	1,196E-09

Impermeable length x (m)	Dimensionless impermeable distance x/Hs * 1/(H*T*)^6								
	I-19-40-10-R	I-19-45-10-R	I-20-20-10-R	I-20-25-10-R	I-20-35-10-R	I-20-40-10-R	I-20-45-10-R	I-20-40-13-R	I-20-45-13-R
0,000	0,000E+00	0,000E+00	0,000E+00	0,000E+00	0,000E+00	0,000E+00	0,000E+00	0,000E+00	0,000E+00
0,050	4,904E-11	8,154E-11	4,806E-10	2,389E-10	8,485E-11	4,975E-11	2,370E-11	3,810E-10	1,884E-10
0,100	9,284E-11	1,673E-10	9,792E-10	4,792E-10	1,790E-10	9,801E-11	4,795E-11	7,652E-10	3,798E-10
0,150	1,472E-10	2,438E-10	1,580E-09	7,399E-10	2,525E-10	1,513E-10	6,056E-11	1,033E-09	5,701E-10
0,200	1,904E-10	3,751E-10	2,135E-09	9,748E-10	3,868E-10	2,017E-10	8,715E-11	1,527E-09	6,674E-10
0,300	2,832E-10	6,116E-10	2,891E-09	1,370E-09	6,089E-10	3,077E-10	1,467E-10	2,282E-09	9,984E-10
0,400	3,774E-10	6,100E-10	3,957E-09	1,781E-09	6,439E-10	3,145E-10	1,861E-10	2,960E-09	1,343E-09
0,600	5,924E-10	1,096E-09	5,676E-09	2,656E-09	1,151E-09	4,907E-10	2,523E-10	4,440E-09	2,348E-09

Appendix VIII-4 Dimensionless impermeable distance x/Hs * 1/(H*T*)^6

IX

Experiment results;
Overtopping discharge over permeable backfill

Experiment code	Measured						Calculated				
	wave height gauge 1 Hs (m)	wave height gauge 2 Hs (m)	wave period T (s)	total extracted volume (l)	Over-topping volume V (l)	Over-topping time t (s)	wave length L (m)	wave steepness s (-)	breaker parameter ξ (-)	Equivalent overtopping discharge Qe,over (m^3/s per m)	Equivalent dimensionless overtopping discharge Q*e,over
O - 20 - 30 - 10 - R - 0	0,196	0,187	1,96	214,8	192,2	104,15	6,00	1/32	2,83	2,547E-03	1,002E-02
O - 21 - 30 - 10 - R - 0	0,185	0,187	2,00	182,7	152,1	82,31	6,25	2/67	2,89	2,428E-03	9,594E-03
O - 22 - 30 - 10 - R - 0	0,219	0,207	2,08	264,7	243,4	69,62	6,75	3/98	2,86	5,209E-03	1,765E-02
O - 18 - 45 - 10 - R - 0	0,165	0,162	2,31	161,4	121,3	74,16	8,33	1/51	3,58	2,081E-03	1,018E-02
O - 18 - 50 - 10 - R - 0	0,182	0,179	2,42	245,4	200,3	87,53	9,14	1/51	3,57	3,310E-03	1,393E-02
O - 18 - 55 - 10 - R - 0	0,162	0,159	2,50	180,5	146,4	92,47	9,76	1/61	3,92	2,074E-03	1,047E-02
O - 19 - 35 - 10 - R - 0	0,190	0,181	2,05	195,3	187,4	100,91	6,56	1/36	3,01	2,488E-03	1,028E-02
O - 19 - 40 - 10 - R - 0	0,189	0,187	2,20	233,7	197,5	92,78	7,56	1/40	3,17	3,025E-03	1,190E-02
O - 19 - 45 - 10 - R - 0	0,174	0,171	2,35	180,9	155,6	75,25	8,62	1/51	3,56	2,710E-03	1,229E-02
O - 20 - 35 - 10 - R - 0	0,182	0,179	2,11	208,7	171,6	89,06	6,95	1/39	3,12	2,635E-03	1,113E-02
O - 20 - 40 - 10 - R - 0	0,194	0,190	2,26	225,6	200,2	71,22	7,97	1/42	3,24	3,945E-03	1,516E-02
O - 20 - 45 - 10 - R - 0	0,202	0,199	2,35	233,5	212,7	54,94	8,62	2/87	3,29	5,499E-03	1,981E-02

Appendix IX-1 Experiment results: Permeable backfill, x=0m

Experiment code	Measured						Calculated				
	wave height gauge 1 Hs (m)	wave height gauge 2 Hs (m)	wave period T (s)	total extracted volume (l)	Over-topping volume V (l)	Over-topping time t (s)	wave length L (m)	wave steepness s (-)	breaker parameter ξ (-)	Overtopping discharge Qover,x (m^3/s per m)	Dimensionless overtopping discharge Q*over,x
P - 20 - 30 - 10 - R - 10	0,200	0,189	1,97	167,0	152,3	355,90	6,06	1/32	2,83	5,349E-04	2,076E-03
P - 21 - 30 - 10 - R - 10	0,184	0,188	2,02	169,6	149,0	525,80	6,37	1/34	2,91	3,542E-04	1,388E-03
P - 22 - 30 - 10 - R - 10	0,223	0,209	2,05	174,1	149,9	87,61	6,56	3/94	2,80	2,139E-03	7,142E-03
P - 18 - 45 - 10 - R - 10	0,170	0,167	2,31	171,0	155,2	426,65	8,33	1/50	3,53	4,547E-04	2,123E-03
P - 18 - 50 - 10 - R - 10	0,184	0,182	2,38	169,6	147,2	191,30	8,84	1/49	3,49	9,618E-04	3,971E-03
P - 18 - 55 - 10 - R - 10	0,165	0,161	2,54	176,3	155,5	455,06	10,07	1/63	3,96	4,271E-04	2,118E-03
P - 19 - 35 - 10 - R - 10	0,191	0,183	2,08	170,5	153,6	622,18	6,75	1/37	3,04	3,086E-04	1,263E-03
P - 19 - 40 - 10 - R - 10	0,189	0,187	2,20	165,7	148,0	230,22	7,56	1/40	3,17	8,036E-04	3,162E-03
P - 19 - 45 - 10 - R - 10	0,171	0,167	2,36	173,2	153,3	299,59	8,70	1/52	3,61	6,396E-04	3,001E-03
P - 20 - 35 - 10 - R - 10	0,186	0,184	2,14	175,1	151,3	260,80	7,15	1/39	3,11	7,252E-04	2,922E-03
P - 20 - 40 - 10 - R - 10	0,196	0,192	2,26	199,5	155,2	131,17	7,97	2/83	3,22	1,479E-03	5,611E-03
P - 20 - 45 - 10 - R - 10	0,209	0,206	2,40	176,7	140,0	70,86	8,99	2/87	3,30	2,470E-03	8,417E-03

Appendix IX-2 Experiment results: Permeable backfill, x=0.10m

Experiment code	Measured						Calculated				
	wave height gauge 1 Hs (m)	wave height gauge 2 Hs (m)	wave period T (s)	total extracted volume (l)	Over-topping volume V (l)	Over-topping time t (s)	wave length L (m)	wave steepness s (-)	breaker parameter ξ (-)	Overtopping discharge Qover,x (m^3/s per m)	Dimensionless overtopping discharge Q*over,x
P - 20 - 30 - 10 - R - 12,5	0,201	0,191	1,97	161,8	145,6	502,86	6,06	1/32	2,82	3,619E-04	1,387E-03
P - 21 - 30 - 10 - R - 12,5	0,187	0,190	2,02	177,9	162,3	831,27	6,37	2/67	2,89	2,441E-04	9,402E-04
P - 22 - 30 - 10 - R - 12,5	0,223	0,209	2,07	194,6	152,7	113,33	6,69	1/32	2,83	1,684E-03	5,627E-03
P - 18 - 45 - 10 - R - 12,5	0,171	0,169	2,25	164,9	152,6	729,68	7,90	1/47	3,42	2,614E-04	1,207E-03
P - 18 - 50 - 10 - R - 12,5	0,184	0,182	2,38	164,6	147,7	295,46	8,84	2/97	3,49	6,249E-04	2,571E-03
P - 18 - 55 - 10 - R - 12,5	0,167	0,163	2,54	166,1	150,3	782,11	10,07	1/62	3,93	2,402E-04	1,169E-03
P - 19 - 35 - 10 - R - 12,5	0,192	0,185	2,08	164,2	148,0	1118,88	6,75	2/73	3,03	1,653E-04	6,660E-04
P - 19 - 40 - 10 - R - 12,5	0,189	0,189	2,19	170,4	155,6	424,36	7,49	1/40	3,15	4,583E-04	1,787E-03
P - 19 - 45 - 10 - R - 12,5	0,172	0,167	2,31	163,8	144,9	492,45	8,33	1/50	3,53	3,678E-04	1,713E-03
P - 20 - 35 - 10 - R - 12,5	0,187	0,186	2,13	168,6	152,0	385,21	7,08	1/38	3,09	4,932E-04	1,969E-03
P - 20 - 40 - 10 - R - 12,5	0,197	0,194	2,26	175,7	155,2	146,96	7,97	1/41	3,20	1,320E-03	4,916E-03
P - 20 - 45 - 10 - R - 12,5	0,205	0,203	2,42	196,4	153,8	96,05	9,14	1/45	3,35	2,002E-03	6,977E-03

Appendix IX-3 Experiment results: Permeable backfill, x=0.125m

Experiment code	Measured						Calculated				
	wave height gauge 1 Hs (m)	wave height gauge 2 Hs (m)	wave period T (s)	total extracted volume (l)	Over-topping volume V (l)	Over-topping time t (s)	wave length L (m)	wave steepness s (-)	breaker parameter ξ (-)	Overtopping discharge Qover,x (m^3/s per m)	Dimensionless overtopping discharge Q*over,x
P - 20 - 30 - 10 - R - 15	0,202	0,192	1,97	151,5	135,4	969,45	6,06	2/63	2,81	1,746E-04	6,615E-04
P - 21 - 30 - 10 - R - 15	0,186	0,190	2,02	60,8	48,7	825,27	6,37	2/67	2,90	7,376E-05	2,849E-04
P - 22 - 30 - 10 - R - 15	0,226	0,211	2,06	174,2	153,4	152,52	6,63	3/94	2,80	1,257E-03	4,135E-03
P - 18 - 45 - 10 - R - 15	0,170	0,167	2,28	151,9	138,9	906,08	8,12	2/97	3,48	1,916E-04	8,928E-04
P - 18 - 50 - 10 - R - 15	0,184	0,182	2,38	166,1	152,3	502,52	8,84	1/49	3,49	3,788E-04	1,562E-03
P - 18 - 55 - 10 - R - 15	0,167	0,162	2,54	145,3	131,6	757,71	10,07	1/62	3,94	2,171E-04	1,063E-03
P - 19 - 35 - 10 - R - 15	0,193	0,185	2,08	135,3	120,4	1327,71	6,75	2/73	3,02	1,134E-04	4,547E-04
P - 19 - 40 - 10 - R - 15	0,189	0,188	2,19	160,2	144,4	561,80	7,49	1/40	3,15	3,213E-04	1,255E-03
P - 19 - 45 - 10 - R - 15	0,171	0,166	2,32	164,5	149,5	696,09	8,40	1/51	3,56	2,685E-04	1,266E-03
P - 20 - 35 - 10 - R - 15	0,186	0,184	2,13	154,0	137,6	460,96	7,08	2/77	3,10	3,731E-04	1,505E-03
P - 20 - 40 - 10 - R - 15	0,194	0,191	2,25	182,4	158,7	198,82	7,90	2/83	3,22	9,978E-04	3,819E-03
P - 20 - 45 - 10 - R - 15	0,204	0,203	2,42	176,6	150,9	107,83	9,14	1/45	3,36	1,749E-03	6,125E-03

Appendix IX-4 Experiment results: Permeable backfill, x=0.15m

Experiment code	Measured						Calculated				
	wave height gauge 1 Hs (m)	wave height gauge 2 Hs (m)	wave period T (s)	total extracted volume (l)	Over-topping volume V (l)	Over-topping time t (s)	wave length L (m)	wave steepness s (-)	breaker parameter ξ (-)	Overtopping discharge Qover,x (m^3/s per m)	Dimensionless overtopping discharge Q*over,x
P - 20 - 30 - 10 - R - 17,5											
P - 21 - 30 - 10 - R - 17,5											
P - 22 - 30 - 10 - R - 17,5	0,222	0,208	2,06	178,9	156,4	179,87	6,63	1/32	2,82	1,087E-03	3,666E-03
P - 18 - 45 - 10 - R - 17,5	0,171	0,168	2,25	105,1	89,8	994,79	7,90	1/47	3,43	1,128E-04	5,223E-04
P - 18 - 50 - 10 - R - 17,5	0,183	0,181	2,39	155,7	140,5	663,24	8,92	1/49	3,51	2,648E-04	1,095E-03
P - 18 - 55 - 10 - R - 17,5	0,167	0,162	2,54	114,1	102,1	1110,96	10,07	1/62	3,94	1,149E-04	5,605E-04
P - 19 - 35 - 10 - R - 17,5											
P - 19 - 40 - 10 - R - 17,5	0,189	0,188	2,19	160,4	146,5	1141,93	7,49	1/40	3,15	1,604E-04	6,275E-04
P - 19 - 45 - 10 - R - 17,5	0,172	0,167	2,32	155,7	141,4	1242,11	8,40	1/50	3,54	1,423E-04	6,639E-04
P - 20 - 35 - 10 - R - 17,5	0,189	0,187	2,13	161,4	148,3	807,67	7,08	1/38	3,08	2,295E-04	9,048E-04
P - 20 - 40 - 10 - R - 17,5	0,197	0,193	2,25	170,9	151,6	225,24	7,90	1/41	3,20	8,413E-04	3,172E-03
P - 20 - 45 - 10 - R - 17,5	0,206	0,203	2,40	197,4	155,0	147,62	8,99	1/44	3,32	1,312E-03	4,568E-03

Appendix IX-5 Experiment results: Permeable backfill, x=0.175m

Experiment code	Measured						Calculated				
	wave height gauge 1 Hs (m)	wave height gauge 2 Hs (m)	wave period T (s)	total extracted volume (l)	Over-topping volume V (l)	Over-topping time t (s)	wave length L (m)	wave steepness s (-)	breaker parameter ξ (-)	Overtopping discharge Qover,x (m^3/s per m)	Dimensionless overtopping discharge Q*over,x
P - 20 - 30 - 10 - R - 20											
P - 21 - 30 - 10 - R - 20											
P - 22 - 30 - 10 - R - 20	0,225	0,211	2,07	174,5	146,3	224,42	6,69	3/95	2,81	8,149E-04	2,677E-03
P - 18 - 45 - 10 - R - 20	0,171	0,168	2,35	104,0	91,2	1543,20	8,62	1/51	3,58	7,387E-05	3,425E-04
P - 18 - 50 - 10 - R - 20	0,182	0,180	2,38	149,0	132,8	870,41	8,84	1/49	3,50	1,907E-04	7,970E-04
P - 18 - 55 - 10 - R - 20	0,167	0,163	2,54	110,7	98,1	1363,02	10,07	1/62	3,93	8,997E-05	4,372E-04
P - 19 - 35 - 10 - R - 20											
P - 19 - 40 - 10 - R - 20	0,189	0,188	2,19	153,3	139,2	1135,24	7,49	1/40	3,15	1,533E-04	5,990E-04
P - 19 - 45 - 10 - R - 20	0,172	0,167	2,32	153,4	140,9	1425,09	8,40	1/50	3,55	1,236E-04	5,794E-04
P - 20 - 35 - 10 - R - 20	0,188	0,186	2,13	160,0	146,5	949,09	7,08	1/38	3,08	1,929E-04	7,652E-04
P - 20 - 40 - 10 - R - 20	0,198	0,195	2,24	167,1	146,3	241,83	7,83	1/40	3,17	7,562E-04	2,809E-03
P - 20 - 45 - 10 - R - 20	0,208	0,205	2,40	181,3	156,1	142,11	8,99	1/44	3,31	1,373E-03	4,724E-03

Appendix IX-6 Experiment results: Permeable backfill, x=0.20m

Experiment code	Measured						Calculated				
	wave height gauge 1 Hs (m)	wave height gauge 2 Hs (m)	wave period T (s)	total extracted volume (l)	Over-topping volume V (l)	Over-topping time t (s)	wave length L (m)	wave steepness s (-)	breaker parameter ξ (-)	Overtopping discharge Qover,x (m^3/s per m)	Dimensionless overtopping discharge Q*over,x
P - 20 - 30 - 10 - R - 25											
P - 21 - 30 - 10 - R - 25											
P - 22 - 30 - 10 - R - 25	0,225	0,211	2,07	177,4	156,7	231,80	6,69	3/95	2,81	8,450E-04	2,780E-03
P - 18 - 45 - 10 - R - 25											
P - 18 - 50 - 10 - R - 25	0,182	0,180	2,39	162,2	147,5	1043,08	8,92	2/99	3,52	1,768E-04	7,395E-04
P - 18 - 55 - 10 - R - 25											
P - 19 - 35 - 10 - R - 25											
P - 19 - 40 - 10 - R - 25	0,189	0,188	2,19	159,3	130,5	1908,00	7,49	1/40	3,16	8,550E-05	3,354E-04
P - 19 - 45 - 10 - R - 25											
P - 20 - 35 - 10 - R - 25	0,188	0,186	2,13	159,2	146,9	1035,18	7,08	1/38	3,08	1,774E-04	7,033E-04
P - 20 - 40 - 10 - R - 25	0,197	0,193	2,25	164,4	147,8	248,11	7,90	1/41	3,20	7,446E-04	2,795E-03
P - 20 - 45 - 10 - R - 25	0,202	0,200	2,42	189,7	153,1	160,08	9,14	1/46	3,38	1,195E-03	4,281E-03

Appendix IX-7 Experiment results: Permeable backfill, x=0.25m

Experiment code	Measured						Calculated				
	wave height gauge 1 Hs (m)	wave height gauge 2 Hs (m)	wave period T (s)	total extracted volume (l)	Over-topping volume V (l)	Over-topping time t (s)	wave length L (m)	wave steepness s (-)	breaker parameter ξ (-)	Overtopping discharge Qover,x (m^3/s per m)	Dimensionless overtopping discharge Q*over,x
P - 20 - 30 - 10 - R - 30											
P - 21 - 30 - 10 - R - 30											
P - 22 - 30 - 10 - R - 30	0,221	0,210	2,08	175,9	155,8	620,87	6,75	1/32	2,84	3,137E-04	1,040E-03
P - 18 - 45 - 10 - R - 30											
P - 18 - 50 - 10 - R - 30	0,183	0,180	2,39	113,3	99,3	1439,27	8,92	2/99	3,51	8,624E-05	3,591E-04
P - 18 - 55 - 10 - R - 30											
P - 19 - 35 - 10 - R - 30											
P - 19 - 40 - 10 - R - 30											
P - 19 - 45 - 10 - R - 30											
P - 20 - 35 - 10 - R - 30	0,189	0,187	2,13	78,5	64,2	1264,43	7,08	1/38	3,07	6,347E-05	2,498E-04
P - 20 - 40 - 10 - R - 30	0,200	0,196	2,25	171,8	157,9	425,46	7,90	1/40	3,17	4,639E-04	1,704E-03
P - 20 - 45 - 10 - R - 30	0,201	0,199	2,39	166,5	147,2	256,27	8,92	1/45	3,35	7,180E-04	2,578E-03

Appendix IX-8 Experiment results: Permeable backfill, x=0.30m

X

Permeable backfill; Dimensionless parameters

Permeable length x (m)	Dimensionless overtopping discharge					
	P-20-30-10-R	P-21-30-10-R	P-22-30-10-R	P-18-45-10-R	P-18-50-10-R	P-18-55-10-R
0,000	1,002E-02	9,594E-03	1,765E-02	1,018E-02	1,393E-02	1,047E-02
0,100	2,076E-03	1,388E-03	7,142E-03	2,123E-03	3,971E-03	2,118E-03
0,125	1,387E-03	9,402E-04	5,627E-03	1,207E-03	2,571E-03	1,169E-03
0,150	6,615E-04	2,849E-04	4,135E-03	8,928E-04	1,562E-03	1,063E-03
0,175			3,666E-03	5,223E-04	1,095E-03	5,605E-04
0,200			2,677E-03	3,425E-04	7,970E-04	4,372E-04
0,250			2,780E-03		7,395E-04	
0,300			1,040E-03		3,591E-04	

Permeable length x (m)	Dimensionless overtopping discharge					
	P-19-35-10-R	P-19-40-10-R	P-19-45-10-R	P-20-35-10-R	P-20-40-10-R	P-20-45-10-R
0,000	1,028E-02	1,190E-02	1,229E-02	1,113E-02	1,516E-02	1,981E-02
0,100	1,263E-03	3,162E-03	3,001E-03	2,922E-03	5,611E-03	8,417E-03
0,125	6,660E-04	1,787E-03	1,713E-03	1,969E-03	4,916E-03	6,977E-03
0,150	4,547E-04	1,255E-03	1,266E-03	1,505E-03	3,819E-03	6,125E-03
0,175		6,275E-04	6,639E-04	9,048E-04	3,172E-03	4,568E-03
0,200		5,990E-04	5,794E-04	7,652E-04	2,809E-03	4,724E-03
0,250		3,354E-04		7,033E-04	2,795E-03	4,281E-03
0,300				2,498E-04	1,704E-03	2,578E-03

Appendix X-1 Dimensionless overtopping discharge over permeable backfill

Permeable length x (m)	Reduction factor Cr for dimensionless overtopping discharge					
	P-20-30-10-R	P-21-30-10-R	P-22-30-10-R	P-18-45-10-R	P-18-50-10-R	P-18-55-10-R
0,000	1,000	1,000	1,000	1,000	1,000	1,000
0,100	0,207	0,145	0,405	0,209	0,285	0,202
0,125	0,138	0,098	0,319	0,119	0,185	0,112
0,150	0,066	0,030	0,234	0,088	0,112	0,102
0,175			0,208	0,051	0,079	0,054
0,200			0,152	0,034	0,057	0,042
0,250			0,157		0,053	
0,300			0,059		0,026	

Permeable length x (m)	Reduction factor Cr for dimensionless overtopping discharge					
	P-19-35-10-R	P-19-40-10-R	P-19-45-10-R	P-20-35-10-R	P-20-40-10-R	P-20-45-10-R
0,000	1,000	1,000	1,000	1,000	1,000	1,000
0,100	0,123	0,266	0,244	0,263	0,370	0,425
0,125	0,065	0,150	0,139	0,177	0,324	0,352
0,150	0,044	0,105	0,103	0,135	0,252	0,309
0,175		0,053	0,054	0,081	0,209	0,231
0,200		0,050	0,047	0,069	0,185	0,239
0,250		0,028		0,063	0,184	0,216
0,300				0,022	0,112	0,130

Appendix X-2 Reduction factor Cr of dimensionless overtopping discharge over impermeable backfill

Permeable length x (m)	Dimensionless permeable distance x/Hs					
	P-20-30-10-R	P-21-30-10-R	P-22-30-10-R	P-18-45-10-R	P-18-50-10-R	P-18-55-10-R
0,000	0,000	0,000	0,000	0,000	0,000	0,000
0,100	0,529	0,532	0,478	0,598	0,551	0,623
0,125	0,655	0,658	0,598	0,742	0,687	0,768
0,150	0,780	0,790	0,710	0,896	0,826	0,926
0,175			0,843	1,040	0,965	1,078
0,200			0,946	1,190	1,111	1,228
0,250			1,184		1,390	
0,300			1,428		1,662	

Permeable length x (m)	Dimensionless permeable distance x/Hs					
	P-19-35-10-R	P-19-40-10-R	P-19-45-10-R	P-20-35-10-R	P-20-40-10-R	P-20-45-10-R
0,000	0,000	0,000	0,000	0,000	0,000	0,000
0,100	0,548	0,534	0,600	0,542	0,521	0,485
0,125	0,677	0,663	0,746	0,673	0,643	0,615
0,150	0,811	0,797	0,903	0,814	0,786	0,740
0,175		0,930	1,046	0,935	0,907	0,860
0,200		1,062	1,199	1,073	1,027	0,976
0,250		1,331		1,341	1,292	1,253
0,300				1,601	1,529	1,506

Appendix X-3 Dimensionless permeable distance x/H

Permeable length x (m)	Dimensionless permeable distance x/Hs * 1/(H*T*)^3					
	P-20-30-10-R	P-21-30-10-R	P-22-30-10-R	P-18-45-10-R	P-18-50-10-R	P-18-55-10-R
0,000	0,000E+00	0,000E+00	0,000E+00	0,000E+00	0,000E+00	0,000E+00
0,100	1,051E-05	1,001E-05	6,249E-06	1,068E-05	7,032E-06	9,431E-06
0,125	1,272E-05	1,195E-05	7,597E-06	1,401E-05	8,711E-06	1,121E-05
0,150	1,479E-05	1,444E-05	8,871E-06	1,656E-05	1,052E-05	1,368E-05
0,175			1,107E-05	1,976E-05	1,221E-05	1,581E-05
0,200			1,163E-05	1,991E-05	1,453E-05	1,788E-05
0,250			1,459E-05		1,799E-05	
0,300			1,763E-05		2,132E-05	

Permeable length x (m)	Dimensionless permeable distance x/Hs * 1/(H*T*)^3					
	P-19-35-10-R	P-19-40-10-R	P-19-45-10-R	P-20-35-10-R	P-20-40-10-R	P-20-45-10-R
0,000	0,000E+00	0,000E+00	0,000E+00	0,000E+00	0,000E+00	0,000E+00
0,100	1,030E-05	7,830E-06	1,014E-05	9,065E-06	6,554E-06	4,113E-06
0,125	1,233E-05	9,689E-06	1,326E-05	1,121E-05	7,799E-06	5,324E-06
0,150	1,464E-05	1,169E-05	1,625E-05	1,383E-05	1,021E-05	6,468E-06
0,175		1,369E-05	1,841E-05	1,518E-05	1,143E-05	7,610E-06
0,200		1,559E-05	2,132E-05	1,763E-05	1,273E-05	8,438E-06
0,250		1,969E-05		2,202E-05	1,614E-05	1,144E-05
0,300				2,592E-05	1,829E-05	1,436E-05

Appendix X-4 Dimensionless impermeable distance $x/Hs * 1/(H*T*)^3$

XI

Experiment results;
Irregular wave spectra

Experiment code	Measured						Calculated						Battjes-Groenendijk		
	spectral wave height gauge 1 Hm-1,0 (m)	spectral wave height gauge 2 Hm-1,0 (m)	peak wave period Tp (s)	total extracted volume (l)	Over-topping volume V (l)	Over-topping time t (s)	spectral wave period Tm-1,0 (s)	wave length L (m)	wave steepness s (-)	breaker parameter ξ (-)	Overtopping discharge Qover,x (m^3/s per m)	Dimensionless overtopping discharge Q*over,x	transitional wave height Htr (m)	rms wave height Hrms (m)	1/1000 largest waves H1/1000 (m)
O - 12 - 30 - 10 - J - 0	0,126	0,125	1,55	180,1	180,1	1800,00	1,40	3,06	2/49	2,48	1,251E-04	9,044E-04	0,228	0,089	0,230
I - 12 - 30 - 10 - J - 5	0,127	0,126	1,54	164,0	164,0	1800,00	1,39	3,02	1/24	2,45	1,139E-04	8,169E-04	0,228	0,089	0,232
I - 12 - 30 - 10 - J - 10	0,126	0,125	1,55	153,1	153,1	1800,00	1,40	3,06	2/49	2,47	1,063E-04	7,662E-04	0,228	0,089	0,231
I - 12 - 30 - 10 - J - 15	0,126	0,125	1,54	134,4	134,4	1800,00	1,39	3,02	1/24	2,46	9,333E-05	6,731E-04	0,228	0,089	0,231
I - 12 - 30 - 10 - J - 20	0,126	0,125	1,52	122,8	122,8	1800,00	1,37	2,94	2/47	2,42	8,528E-05	6,149E-04	0,228	0,089	0,231
I - 12 - 30 - 10 - J - 30	0,129	0,125	1,54	106,1	106,1	1800,00	1,39	3,02	1/24	2,46	7,368E-05	5,317E-04	0,228	0,089	0,231
I - 12 - 30 - 10 - J - 40	0,125	0,124	1,54	102,2	102,2	1800,00	1,39	3,02	3/73	2,46	7,097E-05	5,168E-04	0,228	0,088	0,229
I - 12 - 30 - 10 - J - 60	0,127	0,126	1,54	87,6	87,6	1800,00	1,39	3,02	1/24	2,45	6,083E-05	4,364E-04	0,228	0,089	0,232

Appendix XI-1 Experiment results for I-12-30-10-J for all shelf lengths

Experiment code	Measured						Calculated						Battjes-Groenendijk		
	spectral wave height gauge 1 Hm-1,0 (m)	spectral wave height gauge 2 Hm-1,0 (m)	peak wave period Tp (s)	total extracted volume (l)	Over-topping volume V (l)	Over-topping time t (s)	spectral wave period Tm-1,0 (s)	wave length L (m)	wave steepness s (-)	breaker parameter ξ (-)	Overtopping discharge Qover,x (m^3/s per m)	Dimensionless overtopping discharge Q*over,x	transitional wave height Htr (m)	rms wave height Hrms (m)	1/1000 largest waves H1/1000 (m)
O - 12 - 40 - 10 - J - 0	0,128	0,127	1,71	297,3	297,3	1800,00	1,54	3,73	3/88	2,71	2,065E-04	1,454E-03	0,228	0,091	0,233
I - 12 - 40 - 10 - J - 5	0,129	0,128	1,71	283,2	283,2	1800,00	1,54	3,73	1/29	2,69	1,967E-04	1,365E-03	0,228	0,091	0,235
I - 12 - 40 - 10 - J - 10	0,129	0,129	1,71	268,0	268,0	1800,00	1,54	3,73	1/29	2,69	1,861E-04	1,288E-03	0,228	0,092	0,236
I - 12 - 40 - 10 - J - 15	0,129	0,129	1,71	242,6	242,6	1800,00	1,54	3,73	1/29	2,69	1,685E-04	1,166E-03	0,228	0,092	0,236
I - 12 - 40 - 10 - J - 20	0,129	0,128	1,71	224,0	224,0	1800,00	1,54	3,73	1/29	2,70	1,556E-04	1,083E-03	0,228	0,091	0,235
I - 12 - 40 - 10 - J - 30	0,129	0,128	1,71	210,7	210,7	1800,00	1,54	3,73	1/29	2,69	1,463E-04	1,017E-03	0,228	0,091	0,235
I - 12 - 40 - 10 - J - 40	0,129	0,128	1,71	199,8	199,8	1800,00	1,54	3,73	1/29	2,70	1,388E-04	9,719E-04	0,228	0,091	0,234
I - 12 - 40 - 10 - J - 60	0,130	0,129	1,72	178,4	178,4	1800,00	1,55	3,77	3/88	2,71	1,239E-04	8,567E-04	0,228	0,092	0,236

Appendix XI-2 Experiment results for I-12-30-10-J for all shelf lengths

Impermeable length x (m)	Dimensionless overtopping discharge		Reduction factor		Dimensionless impermeable distance x/Hm0		Dimensionless impermeable distance x* (with Hm0)		Dimensionless impermeable distance x* (with H(1/1000))	
	I-12-30-10-J	I-12-40-10-J	I-12-30-10-J	I-12-40-10-J	I-12-30-10-J	I-12-40-10-J	I-12-30-10-J	I-12-40-10-J	I-12-30-10-J	I-12-40-10-J
0,000	9,044E-04	1,454E-03	1,000E+00	1,000E+00	0,000	0,000	0,000E+00	0,000E+00	0,000E+00	0,000E+00
0,050	8,169E-04	1,365E-03	9,032E-01	9,386E-01	0,398	0,389	1,482E-08	6,775E-09	2,034E-10	9,788E-11
0,100	7,662E-04	1,288E-03	8,471E-01	8,859E-01	0,799	0,777	2,914E-08	1,339E-08	4,004E-10	1,933E-10
0,150	6,731E-04	1,166E-03	7,443E-01	8,016E-01	1,199	1,166	4,561E-08	2,004E-08	6,270E-10	2,893E-10
0,200	6,149E-04	1,083E-03	6,799E-01	7,446E-01	1,598	1,561	6,570E-08	2,747E-08	9,032E-10	3,972E-10
0,300	5,317E-04	1,017E-03	5,879E-01	6,993E-01	2,398	2,339	9,148E-08	4,092E-08	1,258E-09	5,914E-10
0,400	5,168E-04	9,719E-04	5,714E-01	6,684E-01	3,217	3,135	1,271E-07	5,662E-08	1,752E-09	8,201E-10
0,600	4,364E-04	8,567E-04	4,826E-01	5,892E-01	4,778	4,662	1,780E-07	7,723E-08	2,444E-09	1,115E-09

Appendix XI-3 Dimensionless overtopping discharge, reduction factor C_r, dimensionless distance parameter x/H_{m0}, dimensionless distance parameter x* with H_{m0} and dimensionless distance parameter x* with $H_{1/100}$ for the experiment I-12-30-10-J and I-12-40-10-J

XII

Final overview of the scale model

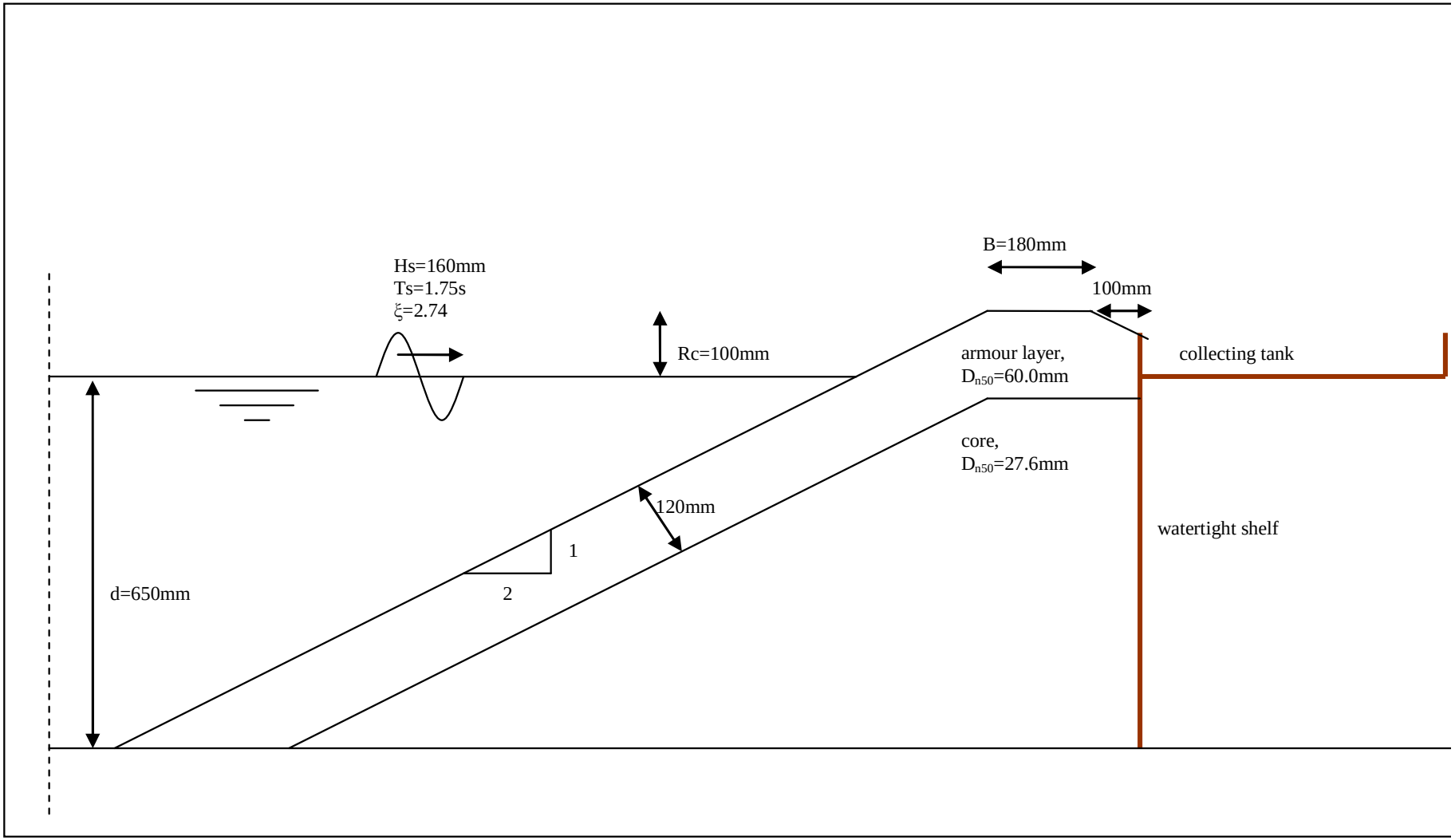

Appendix XII-1 Intersection scale model breakwater with material properties, physical dimensions and hydraulic conditions

XIV

Technical drawing collecting tank

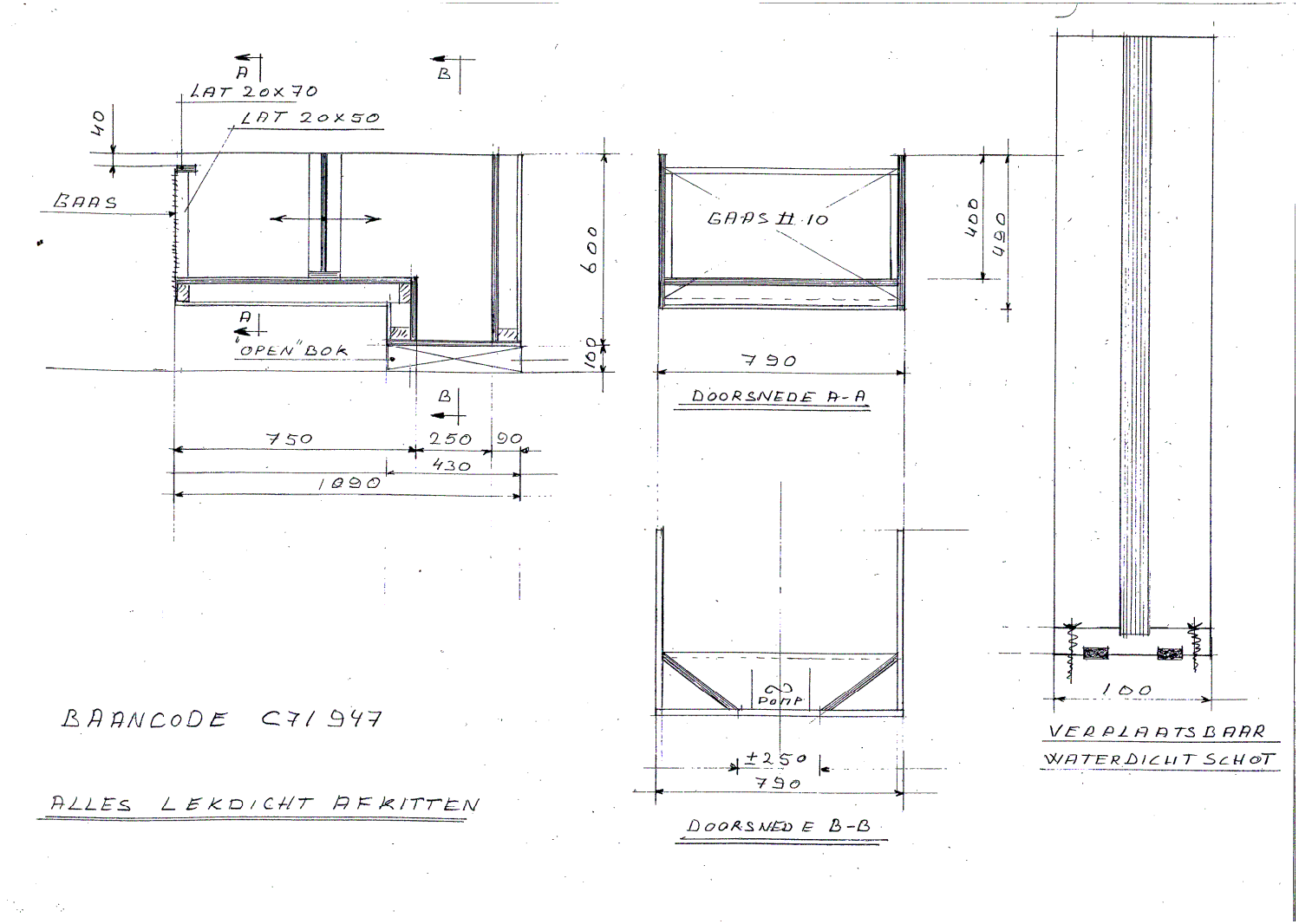

Appendix XIII-1 Technical drawing of collecting tank for experiments with permeable backfill

XIV

Pictures

Appendix XIV-1 Scale model

Appendix XIV-2 Scale model

Appendix XIV-3 Setup total overtopping experiment

Appendix XIV-4 Wire netting

Appendix XIV-5 Side view picture of scale model

Appendix XIV-6 Watertight board, rock filled part and empty part

Appendix XIV-7 Experiment total wave overtopping discharge

Appendix XIV-8 Experiment wave overtopping discharge directly behind the crest

Appendix XIV-9 Experiment wave overtopping discharge directly behind the crest

Appendix XIV-10 Experiment overtopping discharge over permeable backfill

Appendix XIV-11 Experiment overtopping discharge over permeable backfill